TESIS DE LA UNIVERSIDAD DE ZARAGOZA

2024

100

Ruth González Gómez

Generation and development of immunotargeted tools for the noninvasive diagnosis of ancreatic ductal adenocarcinoma

Director/es
Jiménez Schuhmacher, Alberto

EXTRACTO

http://zaguan.unizar.es/collection/Tesis

ISSN 2254-7606

Prensas de la Universidad
Universidad Zaragoza

El presente documento es un extracto de la tesis original depositada en el Archivo Universitario.

En cumplimiento del artículo 14.6 del Real Decreto 99/2011, de 28 de enero, por el que se regulan las enseñanzas oficiales de doctorado, los autores que puedan verse afectados por alguna de las excepciones contempladas en la normativa citada deberán solicitar explícitamente la no publicación del contenido íntegro de su tesis doctoral en el repositorio de la Universidad de Zaragoza.
Las situaciones excepcionales contempladas son:

- Que la tesis se haya desarrollado en los términos de un convenio de confidencialidad con una o más empresas o instituciones.
- Que la tesis recoja resultados susceptibles de ser patentados.
- Alguna otra circunstancia legal que impida su difusión completa en abierto.

Universidad de Zaragoza
Servicio de Publicaciones

ISSN 2254-7606

Universidad Zaragoza
1542

Tesis Doctoral [Extracto]

GENERATION AND DEVELOPMENT OF IMMUNOTARGETED TOOLS FOR THE NONINVASIVE DIAGNOSIS OF ANCREATIC DUCTAL ADENOCARCINOMA

Autor

Ruth González Gómez

Director/es

Jiménez Schuhmacher, Alberto

UNIVERSIDAD DE ZARAGOZA
Escuela de Doctorado

Programa de Doctorado en Bioquímica y Biología Molecular

2022

Repositorio de la Universidad de Zaragoza – Zaguan http://zaguan.unizar.es

Universidad Zaragoza
1542

Tesis Doctoral

GENERATION AND DEVELOPMENT OF IMMUNOTARGETED TOOLS FOR THE NON-INVASIVE DIAGNOSIS OF PANCREATIC DUCTAL ADENOCARCINOMA

Autor

Ruth González Gómez

Director/es

Alberto Jiménez Schuhmacher

UNIVERSIDAD DE ZARAGOZA
Bioquímica y Biología Molecular

2021

UNIVERSIDAD DE ZARAGOZA
Programa de Doctorado en Bioquímica y Biología Molecular

TESIS DOCTORAL

GENERATION AND DEVELOPMENT OF IMMUNOTARGETED TOOLS FOR THE NON-INVASIVE DIAGNOSIS OF PANCREATIC DUCTAL ADENOCARCINOMA

Memoria presentada por RUTH GONZÁLEZ GÓMEZ
para optar al grado de doctor por la Universidad de Zaragoza
Zaragoza, 2021

D. ALBERTO JIMÉNEZ SCHUHMACHER, Doctor en Biología Molecular por la Universidad Autónoma de Madrid. Investigador ARAID, responsable del Grupo de Oncología Molecular del Instituto de Investigación Sanitaria Aragón.

HACE CONSTAR:

Que Dña. Ruth González Gómez ha realizado bajo mi dirección el trabajo de tesis doctoral: **"Generation and development of immunotargeted tools for the non-invasive diagnosis of pancreatic ductal adenocarcinoma"** y corresponde fielmente a los resultados obtenidos.

Una vez redactada la presente memoria, ha sido revisada por mí y posee la calidad científica necesaria para ser presentada y aspirar al grado de Doctor por la Universidad de Zaragoza.

La doctoranda ha alcanzado la madurez científica necesaria para llevar a cabo una extraordinaria labor científica de forma independiente.

Y para que conste, en cumplimiento de las disposiciones vigentes, expido el presente informe favorable.

Zaragoza, a 11 de noviembre de 2021.

El desarrollo y ejecución de esta Tesis Doctoral se han enmarcado dentro del proyecto: “Virtual biopsy: Development of non-invasive immunotargeted imaging agents for the diagnosis of pancreatic ductal adenocarcinoma”, financiado por el Instituto de Ciencias de la Salud Carlos III de Madrid (PI18/01665). Así como los contratos concedidos a Da. Ruth González Gómez procedentes de la DGA y Garantía Juvenil del Servicio Público de Empleo Estatal (PEJ2018-03855).

“La vida no es fácil para ninguno de nosotros. Debemos tener perseverancia y, sobre todo, confianza en nosotros mismos. Debemos creer que estamos dotados para algo y que esto debe ser alcanzado”

Marie Curie

Por todos los fallos que hemos cometido y nos han llevado a ser lo que somos hoy en día. Por no darnos por vencidos nunca y luchar por nuestros sueños.

AKCNOWLEDGEMENTS

Creo que esta es la parte que más me ha costado escribir de toda la tesis… Así que intentaré mostrar absolutamente todo lo que he sentido en estos más de 4 años de sufrimiento, porque ha sido mucho, pero sobre de todo de satisfacción y felicidad. Nunca pensé que acabaría en Zaragoza haciendo el doctorado, pero la verdad es que esta ciudad me ha ganado el corazón, supongo que lo bonita que es hace mucho, pero sobre todo ha sido el cariño con el que me ha acogido, que, aunque los maños tengáis fama de cabezones, que lo sois, tenéis un corazón enorme.

Lo primero quiero agradecer a las casualidades de la vida, que por allá en primavera del 2017 en la sala de cultivos del CNIO, acabásemos hablando Alberto, Álvaro y yo de por qué no hacer el doctorado en Zaragoza, que Alberto iba a empezar su grupo en verano. Y así fue, así que gracias Alberto por confiar en mí y dejarme ser la primera doctoranda de tu grupo, eso nadie me lo va a poder quitar nunca, y aún muy a tu pesar siendo madrileña e hija única. En estos cuatro años nuestra relación ha pasado por todo tipo de sentimientos, pero siento que he crecido muchísimo tanto a nivel personal como científico y sin ti no hubiese sido igual; para nada soy la persona que entró en 2017 en el laboratorio.

Y los siguientes tenéis que ser vosotros, mis OMIGOS, mis chicos del grupo de Oncología Molecular. Y es que para mí no sois compañeros de trabajo, sois muchísimo más. Ay, Edu, fuiste el primero que conocí, recuerdo que pensé que hablabas muchísimo, y lo sigo pensando y me encanta. Hemos pasado los dos por muchísimo, y la verdad es que sin ti no sé si hubiese sido capaz de pasar por todo lo que hemos pasado y todo lo científico que hemos conseguido, que no es poco. Noe, me alegro infinitamente de tener la relación que tenemos, tú y yo sí que hemos pasado por absolutamente de todo juntas, y al final eso nos ha llevado a unirnos y a valorarnos como nos merecemos. Rocío, mira que has llegado hace poquísimo y que rápido te has ganado nuestro cariño, eres pura alegría y amabilidad, así que por favor no cambies nunca y sigue uniéndonos solo como tú sabes. Y por último Irene, que eres la que menos tiempo llevas con nosotros, aunque ahora hagamos un cambio generacional en el laboratorio esto

que tenemos entre todos va a ser difícil de superar, y todavía nos queda tiempo por disfrutar juntas.

Y además de mi grupo, ahí están los ciberos. Y no puedo empezar por otra persona que no sea Samantha, me da igual con h que sin ella, fuiste de las primeras personas que conocí de la planta A y cómo agradezco que haya sido así, has sido mi paño de lágrimas, mi fuente de alegría, mi ayuda en cada momento, me has demostrado ser amiga por encima de todo, gracias. A todas las personas que están y las que han volado a otros sitios, y que incluso han vuelto, Pilar, Natalia, Iris, Pedro, Edu, Sofía, gracias por tantos momentos en los laboratorios, en el office, en cualquier sitio dentro y fuera del CIBA.

Y mis chicas del Servet, Bea y Pilar, que, aunque no estén en el CIBA es como si lo estuvierais, mil gracias por todas las ayudas que me habéis ofrecido en este tiempo, con la cantidad de tiempo y risas que hemos pasado en el animalario. Y la última de este grupo es Patricia, la verdad es que no sé cómo expresarte lo agradecida que estoy, a pesar de que cada vez que nos veamos te de las gracias porque es que siempre me estás ayudando. Por si aún no disfrutaba suficiente de la ciencia, tú me has hecho no querer parar de aprender, eres para mí un gran referente como científica y persona.

A todas esas personas de los SCTs del CIBA que han aguantado mis constantes preguntas y pedidas de experimentos sin parar. César, Marck, Javier, … qué gusto da que siempre estéis dispuestos a ayudar.

Carol, a pesar de la distancia que hemos tenido después de todos los años de universidad juntas siempre has estado ahí. Tus constantes whatsapps para preguntarme qué tal iban mis nanobodies y mis ratoncetes. Siempre estás ahí amiga.

Por supuesto, a mi familia, esa que siempre está ahí ante cualquier adversidad. Me fui de Madrid, aunque bien cerquita, pero siempre se echa de menos estar en casa; mamá y papá gracias por confiar en mí desde siempre, por animarme y decirme que valgo para esto, que se me da muy bien y que puedo con todo, y sobre todo por quererme igual o más incluso en la distancia. Abuela, aunque no

te enteres de nada de lo que estoy haciendo tú siempre me estrás preguntado, pero por encima de todo siempre estás cuidando de mí. Y por todas las personas que no están y que sé que siempre me apoyan desde allá donde estén.

Y como no, tenías que ser el último, gracias Jairo. No tengo palabras para describirte todo lo agradecida que le estoy a la vida porque ahí en cada momento. Dejaste todo por venirte conmigo a Zaragoza por cumplir mi sueño de hacer el doctorado, y es que no podría haberlo hecho sin ti. Has aguantado mis quejas, mis derrotas, mis alegrías porque me salieran los experimentos, mis lloreras porque esto es muy duro, y me has ayudado con esas partes científicas que se me escapan y que tú siempre me solucionas. Durante estos años has sido mi mayor apoyo, pero sobre todo has sido mi hogar, allá donde estemos siempre lo serás.

Gracias a todos los que habéis formado parte de esta etapa tan importante para mí y que nunca olvidaré. Además, hemos pasado incluso por una pandemia todos juntos, lo que eso no una… De verdad, GRACIAS.

INDEX

INDEX

ABBREVIATIONS

LIST OF ABBREVIATIONS

[^{18}F] FDG	2-deoxy-[^{18}F] fluoro-D-glucose
^{18}F	Fluorine
^{24}I	Iodine
^{44}Sc	Scandium
^{53}Mn	Manganese
^{64}Cu	Copper
^{68}Ga	Gallium
^{76}Br	Bromine
^{86}Y	Yttrium
^{89}Zr	Zirconium
Ab	Antibody
ABC	ATP-binding cassette
ABCC	ATP-binding cassette subfamily C
ABCC1	ATP-binding cassette subfamily C Member 1
ABCC3	ATP-binding cassette subfamily C Member 3
ADC	apparent diffusion coefficient
ADP	adenosine diphosphate
ALDH	aldehyde dehydrogenase
AML	acute myeloid leukemia
ATF4	Activating transcription factor
ATM	Ataxia telangiectasia mutated
ATP	Adenosine triphosphate
ATR	Ataxia telangiectasia and Rad3-related
BFP	Blue fluorescent protein

BR-PDAC	Borderline pancreatic ductal adenocarcinoma
BRAF	Serine/threonine-protein kinase B-raf
BRCA	Breast cancer protein
BSA	Bovine serum albumin
BTK	Bruton tyrosine kinase
C	Constant
C	Connector
CA19-9	Carbohydrate-antigen 19-9
CAF	Cancer-associated fibroblasts
cAMP	Cyclic adenosine monophosphate
CAR	Chimeric antigen receptor
CAR	Chimeric Antigen Receptor
CDKN2a	Cyclin-dependent kinase inhibitor 2A
cDNA	Complementary DNA
CDR	Complementarity-determining regions
CDR	Complementary-determining region
cFNA	Cell-free nucleic acid
CFTR	Cystic fibrosis transmembrane conductance regulator
CFU	Colony forming unit
cGMP	Cyclic guanosine monophosphate
CH	Constant heavy
CHA	Common hepatic artery
CL	Constant light
Cm	Chloramphenicol
CP	Chronic pancreatitis
CSC	Cancer stem cell

CT	Celiac trunk
CT	Computed tomography
CTC	Circulating tumor cells
CTLA-4 / CD152	Cytotoxic T-lymphocyte-associated protein 4 / cluster differentiation 152
Cys, C	Cysteine
D	Aspartic Acid
Db	Diabody
dCTP	Deoxycytidine
DDR	DNA damage repair
DHEAS	*D*ehydroepiandrosterone
DOTA	1,4,7,10-tetraazacyclododecane-1,4,7,10-tetraacetic acid
DWI	Diffusion-weighted images
E. coli	*Escherichia coli*
$E_2$17ßG	7ßestradiol 17-ß-D-glucuronide
ECM	Extracellular matrix
EDTA	Ethylenediaminetetraacetic acid
EGFR	Epidermal growth factor receptor
ELDA	Extreme limiting dilutions assay
EMT	Epithelial to mesenchymal transition
EpCAM	Epithelial cell adhesion molecule
ERK	Extracellular signal-regulated kinase
EUS	Endoscopic ultrasound
F(ab`)$_2$	Fab dimer
Fab	Antibody-binding domain

Fab	Fragment antigen-binding
FACS	fluorescent-activated cell sorting
FAK	Focal adhesion kinase
FAO	Fatty acid oxidation
FBS	Fetal bovine serum
Fc	Effector domain
Fc	Fragment crystallizable
FR	Framework regions
FR	Framework region
G	Glycine
GA	Nab-paclitaxel plus gemcitabine
GEM	Genetically engineered models
GFP	Green fluorescent protein
GSH	Glutathione
GSSG	Glutathione disulfide
GTPase	Guanosine triphosphatase
H	Heavy
H	Heavy
HA	Hyaluronic acid
HCAb	Heavy chain antibody
HCAb	Heavy-chain antibody
hESC	Human embryonic stem cells
HIF1α	Hypoxia-inducible factor 1 alpha
His	Histidine
IgG	Immunoglobulin G
IPMN	Intraductal papillary mucinous neoplasm

IPTG	Isopropyl β-D-1-thiogalactopyranoside
IPTG	Isopropylthio-β-D-galactoside
IVC	Inferior vena cava
K-RAS	Kristen rat sarcoma viral oncogene homologue
KO	Knock-out
L	Light
L	Light
LA-PDAC	Locally advanced pancreatic ductal adenocarcinoma
LB	Luria Broth
LTC_4	Leukotriene
MACS	magnetic-activated cell sorting
MAPK	Mitogen-activated protein kinase
MCN	Mucinous cystic neoplasm
MDCT	Multiphase multi-detector row computed tomography
MEK	Mitogen-activated kinase
MetSC	Metastatic stem cells
MFCP	Mass-forming chronic pancreatitis
mFOLFIRINOX	Modified 5-fluorouracil/leucovorin, irinotecan and oxaliplatin
Mg	Magnesium
microRNA	miRNA
MRCP	Magnetic resonance cholangiopancreatography
MRI	Magnetic resonance imaging
MRP	Multidrug resistance-related proteins
MUC1	Mucin 1
Nb	Nanobody

NBF	Nucleotide-binding fold
NCNN	National Comprehensive Cancer Network
ncRNA	non-codingRNA
NOTA	1,4,7-triazacyclononane-1,4,7-triacetic acid
NRG1	Neuregulin-1
NT	Non-targeting
O/N	Overnight
OCT-3/4 / POU5F1	Octamer-binding transcription factor ¾ / POU domain class 5 transcription factor 1
OD	Optical density
OS	Overall survival
OXPHOS	Oxidative phosphorylation
P	Phosphate
P/S	Penicillin / Streptomycin
p16	Cyclin-dependent inhibitor p16
PanIN	Pancreatic intraepithelial neoplasia
PanNEN	Pancreatic neuroendocrine neoplasm
PARP	Poly (ADP-ribose) polymerase
PBMC	Peripheral blood mononuclear cell
PBS	Phosphate buffer saline
PCG1-α	Transcription coactivator peroxisome proliferator-activator 1 alpha
PD-1	Programmed death 1
PD-L1	Programmed death ligand 1
PDAC	Pancreatic Ductal Adenocarcinoma

PDX	Patient-derived xenograft
PEGPH20	Pegvorhyaluronidase-α
PET	Positron emission tomography
PGA	Phosphoglyceric acid
PI3K	Phosphoinositide-3 kinase
PKB / AKT	Proteinase kinase b
PMEA	P-Methoxyethylamphetamine
PP	Pancreatic Polypeptide
PSC	Pancreatic stellate cell
PV	Portal vein
R	Regulator
Rb	Retinoblastoma
ROS	Reactive oxygen species
RT	Room temperature
scFv	Single-chain variable fragment
sgRNA	Small guide RNA
SMA	Superior mesenteric artery
SMAD4 / DPC4	Mothers against decapentaplegic homolog 4 or Deleted in Pancreatic Cancer 4
SMV	Superior mesenteric vein
SOC	Standard of care
SOC	Super optimal broth
SOX2	SRY-related HMG-box 2
SP	Secreted passenger
STAT3	Signal transducer and activator of transcription 3
TCA	Trycarboxilic Acid Cycle

TCA	Tricarboxylic acid cycle
TES	Tris-EDTA-Sucrose
TGF β	Transformant growth factor beta
TMD	Transmembrane domains
TNF	Tumoral necrosis factor
TP53	Tumor protein 53
TRK	Tropomyosin receptor kinase
TRNT	Targeted radionuclide therapy
UTR	Untranslated region
UV	Ultraviolet
V	Variable
VH	Variable heavy
VHH	Variable domain of camelid heavy chain-only
VL	Variable light
WT	Wild type

SUMMARY / RESUMEN

SUMMARY

Pancreatic cancer is the 12th leading type of cancer worldwide but the 7th in causing deaths[1]. The incidence and mortality of pancreatic cancer correlate with increasing age, tobacco and alcohol consumption, diabetes, and obesity globlally[2]. There have been advances in the knowledge of risk factors and biomarkers. However, there is a need to improve diagnosis techniques. Pancreatic ductal adenocarcinoma (PDAC) is a highly malignant tumor characterized by rapid local progression and potential to metastasize. In addition, the diagnosis is typically at the late stages of the disease, and tumoral cells are resistant to current treatments; due to this, PDAC represents one of the cancers with the lowest survivability[3]. The standard of care (SOC) for advanced-PDAC tumors consists of the combination of gemcitabine and abraxane. Gemcitabine's effectiveness failed in the translation to clinics, probably due to the poor tumor penetration because of the hypo-vascularized and dense stroma.

Additionally, within weeks of treatment, tumors develop gemcitabine chemoresistance[4]. Combining gemcitabine with other agents as abraxane improves PDAC treatment. However, tumor cells become resistant and can relapse at prolonged times[5].

ATP-binding cassette (ABC) transporters constitute one of the largest families of transmembrane proteins; they are involved in the movement of several xenobiotics, drugs, lipids, and metabolic products between the cytoplasm and the extracellular space[6]. Especially, the ABCC subfamily, also known as multidrug resistance protein (MRP), addresses the highest number of proteins implicated in drug transport. ABC transporters, and more specifically MRP proteins, have been found to be overexpressed in several cancers, suggesting them as biomarkers[7]. Even more, these transporters have been related to the resistance to chemotherapeutic agents in the treatment of PDAC patients[8]. ABCC3 has been recently shown to be overexpressed in PDAC, and it has been associated with increased proliferation in cells and tumors[9]. Our studies have gone deep into the functional role of ABCC3 in PDAC as a possible drug transporter of gemcitabine and its probable relationship with stemness characteristics in this type of tumor.

We hypothesized that ABCC3 is overexpressed in PDAC tumors to confer resistance to gemcitabine. Our first objective was to determine the implication of ABCC3 in proliferation and chemoresistance in PDAC. We corroborated that the lack of ABCC3 reduces proliferation *in vitro* and *in vivo*. Additionally, we demonstrated that ABCC3 is implicated in gemcitabine resistance in PDAC.

One of the major challenges in approaching PDAC treatment is the resistance of cancer stem cells (CSCs). These cells constitute a subpopulation of cells with characteristics of self-renewal, differentiation, and abilities to participate in the initiation, progression, and metastasis of tumors[10]. CSCs have been described to express several proteins to favor their abilities, such as aldehyde dehydrogenase (ALDH) or ABC transporters, and they contribute to self-renewal capacity and chemoresistance[11].

ABCC3 has been related to stemness in other tumor types, including brain or breast cancers[12,13]. Once we have demonstrated the implication of ABCC3 in chemoresistance, we wanted to search for a relationship between ABCC3 transporter and stemness in PDAC. We could observe that CSCs are the subpopulation that expresses ABCC3, which could explain, at least in part, their resistance to chemotherapeutic agents.

PDAC CSCs are distinguished for favoring mitochondrial over glycolytic metabolism. The oxidative metabolic reactions lead to an increase in enzymes related to this metabolism and an increase in the reactive oxygen species (ROS) levels[14]. Glutathione (GSH) is a well-known antioxidant in cells, and it has been reported to be a substrate of different ABC transporters, including ABCC3[15]. We hypothesize that CSCs could modulate ROS levels in an ABCC3 dependent manner regulating the intracellular transport of GSH. We corroborated that CSCs use oxidative phosphorylation (OXPHOS) as the main route of obtaining adenosine triphosphate (ATP). Furthermore, we could observe that ABCC3 is one of the transporters of GSH and that it is implicated in antioxidant pathways.

Antibodies and fragment-derived antibodies have been explored in their use in the diagnosis and therapy of different diseases. The "third-generation" of antibodies (Abs) are represented by single variable antibodies (VHH) or

nanobodies (Nbs). Nbs consist of the antigen-binding region derived from heavy-chain antibodies (HcAbs) found in camelids. Nbs conserve the antigen-binding potential, but there are smaller in size (12-15 kDa), which reduces their half-life in the bloodstream (0.5-1 h)[16].

Immuno-positron emission tomography (immuno-PET) is an imaging technique that combines the specificity of Abs or fragment-derived Abs with the selectivity of PET. It is a novel option to improve diagnostic imaging for a concise detection and quantification of the target[17]. To generate innovative immuno-PET tools to identify ABCC3 in patients, we planned a second objective consisting of the generation of Nbs that recognize ABCC3. These Nbs will also have multiple applications for the diagnosis and therapy of PDAC. Furthermore, the role of ABCC3 in cancer is still unclear, partially due to the lack of specific Abs for detecting ABCC3 protein. Hence, the generation and validation of ABCC3 Nbs could impact cancer research.

To obtain anti-ABCC3 Nbs, we generated a Nb library. First, we immunized camels with ABCC3-overexpressing cells. After the immunization, we obtained VHH regions from camels and generated an *E. coli* display library of Nbs with a complexity of 10^8 clones. To identify and select Nbs that target ABCC3, we used two different selection methods: cell surface selection and cell sorting selection.

We identified two Nbs that were validated in detecting ABCC3 *in vitro* and *in vivo* using preclinical models and patient-derived samples of PDAC. These Nbs did not result in toxicity in mouse models and could be efficient molecular probes to diagnose PDAC by immuno-PET. In addition to their potential as diagnostic tools, the Nbs were tested as therapeutic tools. Interestingly, these Nbs decrease proliferation in ABCC3-expressing cells and reduce chemoresistance to gemcitabine in PDAC cells.

ABCC3 has been demonstrated to be expressed in CSCs and contribute to maintaining their mitochondrial metabolism by participating in GSH transport. Finally, by cell sorting selection of Nbs, we obtained two Nbs that recognize ABCC3 *in vitro* and *in vivo* that can be used as diagnostic tools, including

immuno-PET. These Nbs could also have therapeutic potential by reducing the proliferation and chemoresistance to gemcitabine in ABCC3 expressing cells.

In summary, our results point to ABCC3 as a possible biomarker of PDAC tumors that could provide information about their prognosis and treatment response. Additionally, we have generated valuable Nbs that could impact the diagnosis and treatment of PDAC.

RESUMEN

El cáncer de páncreas ocupa el puesto 12 en la incidencia de distintos tipos de cáncer globalmente, pero constituye la 7ª causa de muertes por cáncer[1]. La incidencia y mortalidad del cáncer de páncreas está relacionada con el envejecimiento, el tabaco y el consumo de alcohol, la diabetes y la obesidad[2]. Ha habido avances en el conocimiento de factores de riesgos y en biomarcadores, pero sigue existiendo la necesidad de mejora de las técnicas diagnósticas. El adenocarcinoma pancreático ductal (PDAC) es un tumor altamente maligno caracterizado por una rápida progresión local y con gran potencial para metastatizar. Además, el diagnóstico normalmente se produce en estadios avanzados de la enfermedad, y las células tumorales son resistentes a los tratamientos actuales, todo esto hace que el PDAC represente uno de los cánceres con la más baja probabilidad de supervivencia[3]. El tratamiento estándar (SOC) para tumores avanzados de PDAC consiste en la combinación de gemcitabina y abraxane. La efectividad de la gemcitabina no resultó suficiente en su traslado a ensayos clínicos, probablemente debido a la poca penetración en el tumor debido a la baja vascularización y el denso estroma del tumor. Además, tras semanas de tratamiento los tumores de los pacientes desarrollan resistencia a gemcitabina[4]. La combinación de gemcitabina con otros agentes como abraxane mejora el tratamiento de pacientes de PDAC, aun así, las células tumores se vuelven resistentes y aparecen recidivas a lo largo del tiempo[5].

Los transportadores ATP-binding cassete (ABC) constituyen una de las familias más amplias de proteínas transmembrana, están implicados en el movimiento de diferentes xenobióticos, compuestos, lípidos y productos metabólicos entre el citoplasma y el espacio extracelular[6]. Especialmente, la subfamilia ABCC, también conocida como proteína de resistencia a compuestos (MRP), aborda el mayor número de proteínas implicadas en el transporte de compuestos. Los transportadores ABC, y más específicamente las proteínas MRP, se han encontrado sobreexpresados en diversos tipos de cáncer, y han sido propuestos como biomarcadores de los mismos[7]. Incluso, estos transportadores han sido relacionados con la resistencia a agentes quimioterapéuticos en el tratamiento de pacientes de PDAC[8]. ABCC3 ha sido recientemente mostrado como una de

las proteínas sobreexpresadas en PDAC, y ha sido relacionada con un incremento de la proliferación de células y tumores[9]. Nuestros estudios han consistido en profundizar en las funciones de ABCC3 en PDAC con un posible transportador de gemcitabina y su posible relación con la capacidad stemness de este tipo de cáncer.

Nuestra hipótesis era que ABCC3 está sobreexpresado en tumores PDAC y confiere resistencia a tratamientos con gemcitabina. Nuestro primer objetivo fue determinar la implicación de ABCC3 en proliferación y resistencia en PDAC. Corroboramos que la falta de ABCC3 reduce la proliferación in vitro e in vivo y que es uno de los responsables de la resistencia a gemcitabina en PDAC.

Uno de los principales retos en el abordaje del tratamiento de PDAC es la resistencia de las “cancer stem cells” (CSCs). Estas células constituyen una subpoblación de células con características de auto-regeneración, diferenciación, y habilidades que participan en el inicio, la progresión y la metástasis de tumores[10]. Las CSCs han sido caracterizadas por la expresión de proteínas que favorecen sus habilidades especiales, como la aldehído deshidrogenasa (ALDH) o los transportadores ABC, que contribuyen a su capacidad de auto-regeneración y quimioresistencia[11].

ABCC3 se ha relacionado con “stemness” en otros tipos de cáncer, como cerebro o mama[12,13]. Una vez que demostramos la implicación de ABCC3 en quimioresistencia, quisimos investigar la relación del transportador ABCC3 y “stemness” en PDAC. Pudimos observar que las CSCs son la subpoblación que expresa ABCC3, y que esto podría estar relacionado, en parte, con su capacidad para ser resistentes a agentes quimioterapéuticos.

Las CSCs de PDAC se caracterizan por favorecer el metabolismo mitocondrial en lugar del glicolítico. Estas metabolismo oxidativo conlleva un incremento de las enzimas relacionadas con este metabolismo, y un incremento de niveles de especies reactivas de oxígeno (ROS)[14]. El glutatión (GSH) es un conocido antioxidante en las células, y se ha descrito como sustrato de diferentes transportadores ABC, incluido ABCC3[15]. Nuestra hipótesis fue que las CSCs podrían regular los niveles de ROS mediante la participación de ABCC3 en el

transporte intracelular de GSH para mantener un equilibrio y evitar los altos niveles de ROS. Corroboramos que las CSCs utilizan la fosforilación oxidativa (OXPHOS) como la principal ruta de obtención de adenosín trifosfato (ATP). Es más, pudimos observar que ABCC3 es uno de los transportadores de GSH y que está implicado en rutas antioxidantes.

Los anticuerpos y fragmentos derivados de anticuerpos han sido utilizados para su uso en diagnóstico y terapia en diferentes enfermedades. Los nanoanticuerpos (Nbs) son derivados de la región de unión a antígeno de anticuerpos de cadena pesada (HcAbs) presentes en camélidos. Los Nbs conserva el potencial de unión a antígenos pero presentan un tamaño menor (12-15 kDa), lo que reduce su tiempo de vida medio en el torrente sanguíneo (0.5-1 h)[16].

La inmuno-tomografía por emisión de positrones (PET) es una técnica de imagen que combina la especificidad de los Abs o fragmentos derivados de Abs con la selectividad del PET. Es una novedosa opción para mejorar el diagnóstico por imagen para una detección concisa y la cuantificación de la diana[17]. Nuestro segundo objetivo fue generar Nbs que reconocen ABCC3 para su uso en técnicas rutinarias de laboratorio, diagnóstico y terapia de PDAC. Asimismo, el papel de ABCC3 no está determinado, probablemente debido a la falta de anticuerpos específicos en la detección de la proteína ABCC3. Por ello, la generación y validación de anticuerpos frente a ABCC3 podría impactar en la investigación contra el cáncer.

Por ello, generamos una librería de Nbs. Primero, inmunizamos dromedarios con células que sobreexpresan ABCC3. Después de la inmunización, obtuvimos las regiones VHH producidas por los dromedarios y generamos un método de selección de Nbs en *E. coli* con una complejidad de 10^8 clones. Para identificar y seleccionar los Nbs que reconocen ABCC3 usamos dos métodos de selección diferentes: selección en superficie celular y “cell sorting”.

Finalmente, identificamos dos Nbs que fueron validados para la detección de ABCC3 *in vitro* e *in vivo* de PDAC utilizando modelos preclínicos y muestras derivadas de pacientes. Estos Nbs no resultaron tóxicos en modelos de ratón y

podrían ser eficientes como sondas moleculares para su uso en el diagnóstico de PDAC mediante inmuno-PET. Además de su potencial como herramientas de diagnóstico, los Nbs se testaron como herramientas terapéuticas. Así los Nbs fueron capaces de disminuir la proliferación en células que expresan ABCC3 y redujeron la resistencia a gemcitabina en células de PDAC.

Los resultados de este trabajo sugieren ABCC3 como un posible biomarcador de tumores de PDAC, dando información sobre su respuesta a tratamientos. Hemos demostrado que ABCC3 se expresa en las CSCs y que contribuye a mantener su metabolismo mitocondrial mediante su participación en el transporte de GSH. Finalmente, mediante la selección de Nbs por “cell sorting”, se generaron dos Nbs que reconocen ABCC3 *in vitro* e *in vivo* y que pueden ser usados como herramientas de diagnóstico, incluido el inmuno-PET. Estos Nbs podrían tener también potencial terapéutico al reducir la proliferación y resistencia a gemcitabina en células que expresan ABCC3.

En resumen, nuestros resultados sugieren ABCC3 como un posible biomarcador de tumores de PDAC que podría dar información acerca del pronóstico y respuesta a tratamiento. Además, hemos generado Nbs que podrían ser utilizados en el diagnóstico y el tratamiento de pacientes de PDAC.

REFERENCES

1. *Pancreas*.; 2020. https://gco.iarc.fr/today. Accessed October 21, 2021.
2. Enhanced Reader. moz-extension://45f875a8-6053-bb49-8ae3-c81ebe7900d0/enhanced-reader.html?openApp&pdf=http%3A%2F%2Feknygos.lsmuni.lt%2Fspringer%2F360%2F1-117.pdf. Accessed October 18, 2021.
3. Winter K, Talar-Wojnarowska R, Dąbrowski A, et al. Diagnostic and therapeutic recommendations in pancreatic ductal adenocarcinoma. Recommendations of the working group of the Polish Pancreatic Club. *Przeglad Gastroenterologiczny*. 2019;14(1):1-18. doi:10.5114/pg.2019.83422
4. Amrutkar M, Gladhaug IP. Pancreatic cancer chemoresistance to gemcitabine. *Cancers*. 2017;9(11). doi:10.3390/cancers9110157
5. De Vita F, Ventriglia J, Febbraro A, et al. NAB-paclitaxel and gemcitabine in metastatic pancreatic ductal adenocarcinoma (PDAC): From clinical trials to clinical practice. *BMC Cancer*. 2016;16(1). doi:10.1186/s12885-016-2671-9
6. Fletcher JI, Haber M, Henderson MJ, Norris MD. ABC transporters in cancer: More than just drug efflux pumps. *Nature Reviews Cancer*. 2010;10(2):147-156. doi:10.1038/nrc2789
7. Szakács G, Paterson JK, Ludwig JA, Booth-Genthe C, Gottesman MM. Targeting multidrug resistance in cancer. *Nature Reviews Drug Discovery*. 2006;5(3):219-234. doi:10.1038/nrd1984
8. Teodori E, Dei S, Martelli C, Scapecchi S, Gualtieri F. The Functions and Structure of ABC Transporters: Implications for the Design of New Inhibitors of Pgp and MRP1 to Control Multidrug Resistance (MDR). *Current Drug Targets*. 2006;7(7):893-909. doi:10.2174/138945006777709520
9. Adamska A, Domenichini A, Capone E, et al. Pharmacological inhibition of ABCC3 slows tumour progression in animal models of pancreatic cancer. *Journal of Experimental and Clinical Cancer Research*. 2019;38(1):312. doi:10.1186/s13046-019-1308-7
10. Bomken S, Fišer K, Heidenreich O, Vormoor J. Understanding the cancer stem cell. *British Journal of Cancer*. 2010;103(4):439-445. doi:10.1038/sj.bjc.6605821
11. Meacham CE, Morrison SJ. Tumour heterogeneity and cancer cell plasticity. *Nature*. 2013;501(7467):328-337. doi:10.1038/nature12624
12. Balaji SA, Udupa N, Chamallamudi MR, Gupta V, Rangarajan A. Role of the drug transporter ABCC3 in breast cancer chemoresistance. *PLoS ONE*. 2016;11(5). doi:10.1371/journal.pone.0155013
13. Pessina S, Cantini G, Kapetis D, et al. The multidrug-resistance transporter Abcc3

protects NK cells from chemotherapy in a murine model of malignant glioma. *OncoImmunology*. 2016;5(5). doi:10.1080/2162402X.2015.1108513

14. Sancho P, Burgos-Ramos E, Tavera A, et al. MYC/PGC-1α balance determines the metabolic phenotype and plasticity of pancreatic cancer stem cells. *Cell Metabolism*. 2015;22(4):590-605. doi:10.1016/j.cmet.2015.08.015

15. Begicevic RR, Falasca M. ABC transporters in cancer stem cells: Beyond chemoresistance. *International Journal of Molecular Sciences*. 2017;18(11). doi:10.3390/ijms18112362

16. Sroga P, Safronetz D, Stein DR. Nanobodies: A new approach for the diagnosis and treatment of viral infectious diseases. *Future Virology*. 2020;15(3):195-205. doi:10.2217/fvl-2019-0167

17. van Dongen GAMS, Visser GWM, Lub-de Hooge MN, de Vries EG, Perk LR. Immuno-PET: A Navigator in Monoclonal Antibody Development and Applications. *The Oncologist*. 2007;12(12):1379-1389. doi:10.1634/theoncologist.12-12-1379

INTRODUCTION / INTRODUCCIÓN

INTRODUCTION

1. Pancreas

The pancreas is an organ derived from the endoderm; it is located in the abdomen near the spleen and adjacent to the stomach and intestines. It is connected to the intestines with the pancreatic duct to eliminate secretions to the intestinal lumen.

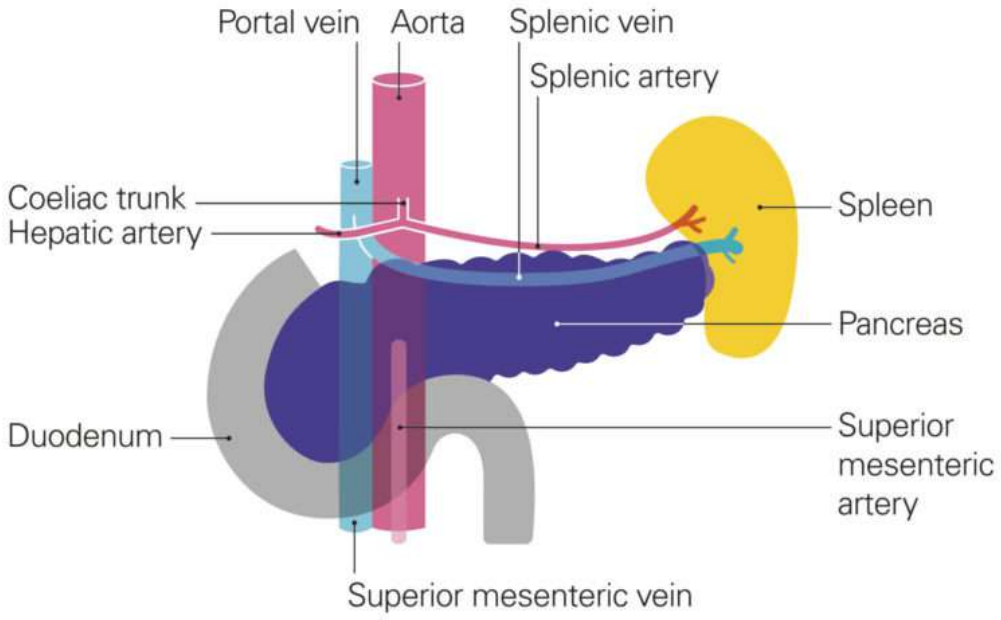

Figure Intro. 1. Blood vessels implicated in the pancreas. Image taken from Pancreatic Cancer UK.

Two main parts of the pancreas can be identified and have different functions, the endocrine and exocrine pancreas. The endocrine pancreas is the principal regulator of metabolic and glucose homeostasis in the body. This compartment is organized in shaped patches called islets or islands of Langerhans; each islet is composed of four types of cells, α-, β-, δ-, γ- and PP-cells (figure Intro. 2). In response to signals, these cells produce and secrete different hormones like glucagon, insulin, somatostatin, ghrelin, and pancreatic polypeptide (PP), respectively[1].

The other compartment, the exocrine pancreas, helps in the digestion of proteins, lipids, and carbohydrates. This tissue is formed by acinar and centroacinar cells connected by ductal cells that form the epithelial lining of the branched tubes

(figure Intro. 2). Acinar cells conform acini; this structure is organized by polarized cells around a lumen; the apical part of these cells is in contact with the centroacinar cells. The function of the exocrine pancreas is to secrete zymogens, which are inactive forms of digestive enzymes, to the duodenum. These zymogens are activated in acidic media. Thus, ductal cells are responsible for alkaline microenvironment maintenance to avoid activation in the pancreas. The epithelium formed by ductal cells ends in the pancreatic duct, representing the principal transport of pancreatic juice, and is connected to the bile duct. Another important tissue is the stroma; stromal cells are composed of endothelial cells and quiescent fibroblasts. This stroma represents less than 1% of the normal pancreas. Their main function is to maintain the intercellular structure of the organ by regulating the correct function of the epithelium. There is a continuous communication between the stroma and the epithelium to coordinate homeostasis[2].

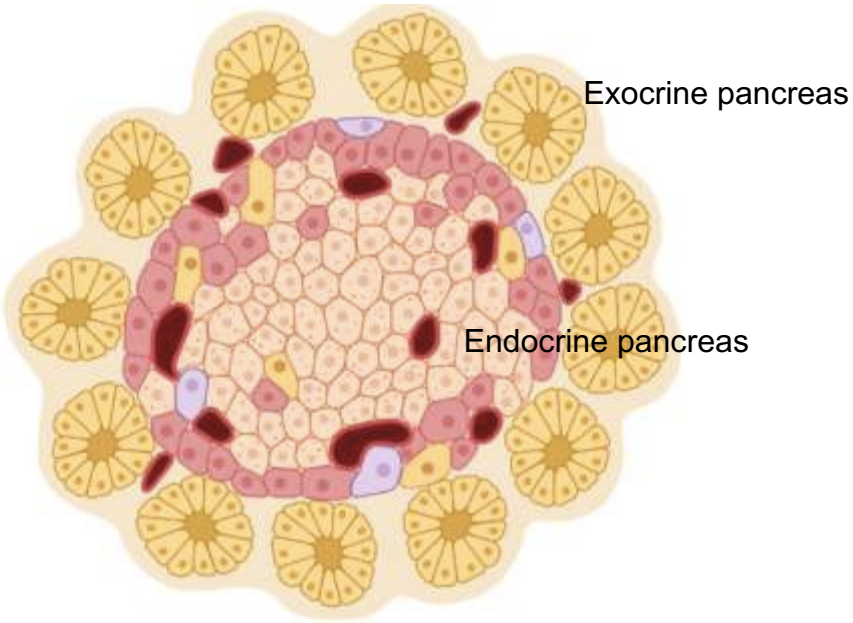

Figure Intro. 2. Pancreas compartmentalization. A) Exocrine and endocrine pancreas. *Image generated with Biorender.*

Pancreas is vascularized by splenic, gastroduodenal, and mesenteric superior arteries, which send various branches into the different parts of the pancreas. The head and uncinate processes are supplied by the superior and inferior pancreaticoduodenal arteries; they are branches of the gastroduodenal and

superior mesenteric arteries, respectively. The body and tail are supplied by the splenic, gastroduodenal, and superior mesenteric arteries. For draining deoxygenated blood, the anterior superior pancreaticoduodenal vein goes to the superior mesenteric vein, and the posterior variant empties into the hepatic portal vein. The pancreatic veins from de body and tail empty into the splenic vein (figure Intro. 1)[3,4].

2. Pancreatic cancer

Pancreatic cancer is about the 8th most frequent cancer globally but one of the cancer types with the highest mortality rate[5]. The number of new cases and deaths rounds 460,000, being more frequent in men than women, 55% and 45% respectively[6]. The overall survival time is 4.6 months and the median 5 years survival of patients is only around 5%.

Surgical strategies are not commonly applied because tumor is normally adhered to or invades adjacent vascular structures, and resection is not an option; even patients who undergo surgery, in 80% of the cases, will have metastasis or relapses[7].

This poor prognosis, lethality, and increasing incidence make it essential to understand the mechanism of appearance, development, resistance to chemotherapy and radiotherapy, and metastasis of pancreatic ductal adenocarcinoma (PDAC).

I. Pancreatic cancer classification

There are two main types of pancreatic cancer; pancreatic neuroendocrine neoplasm (PanNENs), which are a rare disease with a wide heterogeneity and behaviour[8], and PDAC, constituting more than 90% of all pancreatic tumors, including endocrine and exocrine tumors[9].

Three potential precursors lesions are considered in developing PDAC, pancreatic intraepithelial neoplasias (PanINs), mucinous cystic neoplasms (MCN), and intraductal papillary mucinous neoplasms (IPMNs). The majority of PDAC come from a progression of PanINs, supported by the activated pancreatic

stellate cells (PSCs) contained in the tumor microenvironment and immune cells[10]. Independently, PDAC can proceed from acinar and centroacinar cells via PanIN progression and other mucinous precursors or from duct cells via non-mucinous tubular lesions[11].

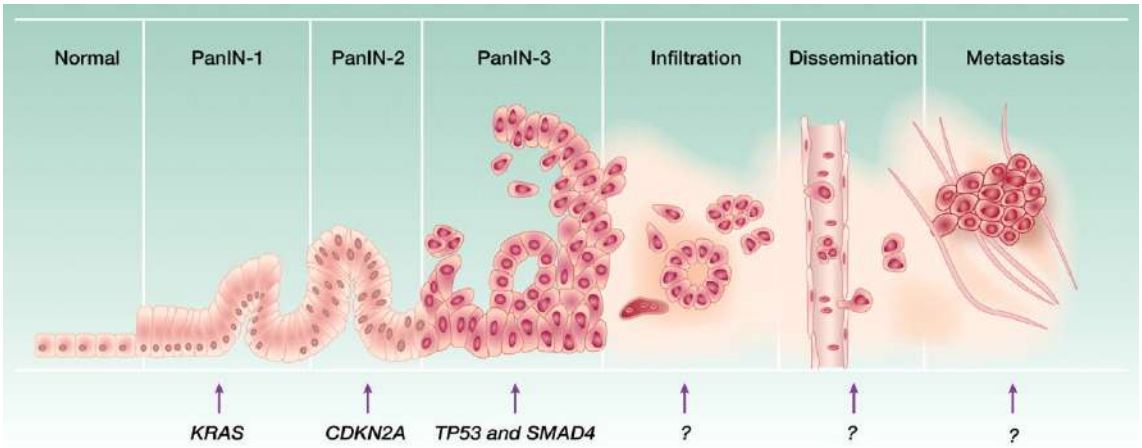

Figure Intro. 3. PDAC development and classification. Image adapted from American Association for Cancer Research (AACR)

PanINs are lesions in the intralobular pancreatic ducts; they are usually < 5 mm and are asymptomatic in patients. Various point mutations occur in the progression from normal tissue to PDAC; although these mutations are very well known for decades (figure Intro. 3), it is still unclear at which stage they occur. Three grades of PanINs can be differentiated:

a. PanIN-1 or low-grade PanINs:

In this first step, early mutations originate activation of oncogenes or telomere shortening constitutively, but the pancreatic architecture is not affected.

Kristen rat sarcoma viral oncogene homolog (*K-RAS*) suffers an amino acid substitution from Glycine (G) to Aspartic Acid (D), Valine (V), or Cysteine (C) in codon 12, which makes a constitutively active GTPase located in the cytosol[12]. K-RAS mutation is the most frequently found in PDAC tumors, around 95% of cases[13]… Oncogenic K-RAS activates downstream effectors, including mitogen-activated protein kinase (MAPK) and/or phosphoinositide-3 Kinase (PI3K) pathways, affecting proliferation, initiation, and tumor development[14].

Telomere shortening also happens in the early stages of PDAC progression; by this cutback, there is no prevention of fusions between the ends of chromosomes, which promotes neoplastic progression in cells[15,16].

Two subtypes can be classified:

- PanIN-1A or flat lesions.
- PanIN-1B or papillary lesions.

b. PanIN-2 or intermediate-grade PanINs.

In this second step of progression begins the inactivation of tumor suppression genes, as well as cyclin-dependent kinase inhibitor 2A (CDKN2A) or cyclin-dependent inhibitor p16 (p16). CDKN2A gene encodes p16 tumor suppressor protein. p16 triggers retinoblastoma (Rb) protein phosphorylation inhibiting proliferation. Its inactivation leads to G1 phase of the cell cycle progression and consequently increases proliferation[17,18].

Histologically PanIn-2 differentiate from PanIn-1, showing modifications in the structure and cytology, as nuclear crowding or pleomorphism.

c. PanIN-3 or high-grade PanINs.

They can be considered *carcinoma in situ,* and they represent the most advanced stage of PanIN progression.

This stage is characterized by the inactivation of essential tumor suppressor genes. Mothers against decapentaplegic homolog 4 or Deleted in Pancreatic Cancer 4 (SMAD4/DPC4) regulates cell cycle by transformant growth factor β (TGF β) signaling pathway; it activates the transcription of several cell cycle inhibitory factors. Thereby, its inactivation undergoes uncontrolled proliferation[19,20]. Tumor protein 53 (TP53) acts as a transcription factor that binds DNA to activate the transcription of genes involved in cell cycle and apoptosis. Thus, its loss brings on deregulation in cell division and cell death[21,22].

Independently of the classification of PanINs, they are noninvasive lesions and do not invade the basement membrane. Lately, PDAC acquires epithelial to

mesenchymal transition (EMT) characteristics and can invade; they disseminate through the blood vessels and metastasize[23].

In PDAC tumors, it has been shown that the stroma represents a high percentage of the tumor and makes less accessible chemotherapeutic agents or radiation to the inside tumor[24].

Tobacco or highly alcoholic drinks are associated with pancreatic cancer, and when decreased, in men, the incidence was also reduced[25,26]. Cholesterol and obesity are associated with an increase in incidence and mortality in pancreatic cancer patients. Some studies have shown a possible positive correlation between type I and II diabetes with the risk of suffering pancreatic cancer[27].

Chronic pancreatitis (CP) is a recurrent disease consisting of prolonged pancreatic inflammation. It is characterized by macro-morphologic and histologic changes that include fibrosis, atrophy of the gland, and ductal dilatation. Mass-forming chronic pancreatitis (MFCP) occurs when the pancreatic parenchyma enlarges, usually in the pancreatic head. It has been well studied the relation between CP and PDAC development; there is an accumulative risk of development PDAC along the time in patients with MFCP. MFCP characteristics in imaging diagnosis techniques are very similar to PDAC. In some circumstances, they can be confused; there is a need to improve PDAC diagnosis to discriminate patients with CP and MFCP[28,29].

PDAC symptoms in patients are not precise as other types of cancer; most common are abdominal and back pain, weight loss, loss of appetite, changes in bowel habits, or jaundice. These malignancies are not specific for PDAC detection, here remains the importance of pancreatic cancer diagnosis by imaging techniques[30].

PDAC symptoms in patients are not specific as in other types of cancer; most common are abdominal and back pain, weight loss, loss of appetite, changes in bowel habits, or jaundice. These symptoms are not specific for PDAC detection, here remains the importance of pancreatic cancer diagnosis by imaging techniques[31].

PDAC can be detected by computed tomography (CT), magnetic resonance imaging (MRI), or endoscopic ultrasound (EUS)[32,33]. These techniques are widely used in the clinic, but they have some limitations.

3. Diagnosis

PDAC diagnosis by imaging techniques is performed to look for the presence and stage of the tumor, the compromise of blood vessels by the tumor for a possible resection, and metastasis detection[34–36].

At present, several imaging techniques are effective in the detection of pancreatic and distant lesions. The most widely used are CT, MRI, or enhanced US (EUS). CT is the recommended technique for PDAC diagnosis[37–39].

Patients arrive with abdominal pain and fatigue corresponding to the most frequent symptoms; the first step in pancreatic tumor detection is abdominal EUS. Although EUS can detect PDAC, sensitivity only reaches 50-70%, CT with iodine contrast intravenously and/or MRI is the next step to confirm and detect tumor staging[40,41]. All imaging techniques can be used for PDAC detection, US, CT, MRI, and Positron Emission Tomography (PET). They are done specifically for the abdominal region to focus on the pancreas and surrounding structures. Still, all except US can be done in the whole body to look for metastasis, in example[42–44]. Unlike other neoplastic processes, there are no effective diagnostic screening methods for PDAC. The risk of development of the disease is low; consequently, population screening is not indicated. Only the at-risk population is monitored by MRI, EUS, and CT. EUS is used to detect small lesions, but overall, the probability of detecting precursor lesions using these techniques is low, no more than 20%[45].

PDAC can be misdiagnosed as MFCP; differentiating these two malignancies is a significant problem in the imaging detection of pancreatic cancers[46]. Pancreatic fibrosis or desmoplasia is found in CP and PDAC because both originate from PSCs[47,48]. It is essential to differentiate between CP and PDAC, some researches are needed to focus on the fibrotic stroma of PDAC, but targets should be exclusive for PDAC desmoplasia[49].

Metastasis is also one of the causes of the high mortality of cancer patients, and this usually means an advanced stage of the illness. It is crucial to detect these metastatic lesions early and remains a challenge in imaging detection[49,50].

Liquid biopsy (LB) is not an imaging technique for tumor detection, but it provides handy information about the presence of biomarkers related to the tumor[51,52]. LB is a novel method used for cancer diagnosis; it is obtained from body fluids such as blood, urine, saliva, and cerebrospinal fluid. Tumors and their metastases release biomarkers, circulating tumor cells (CTCs), cell-free nucleic acids (cfDNA and cfRNA), extracellular vesicles, tumor educated platelets (TEPs), can be detected and isolated by LB. Therefore, LB represents a minimally invasive technique for diagnosis and monitoring of patients[53].

Although LB seemed to be a promising diagnosis technique, it has low sensitivity and specificity in cancer detection. However, LB methods showed to be reliable prognosis biomarkers in PDAC patients in terms of overall survival (OS)[54]. Also, the variation of tumor biomarkers levels present in LB could predict the response to treatments several weeks before the treatment[55]. The implantation of LB in the clinics will reduce cost and time in detecting and monitoring patients. Still, there is a need to standardize protocols and improve biomarkers isolation from other body fluids different from blood.

I. Computed tomography (CT)

It refers to x-ray beams that come to a body, rotate around it, and produce signals creating cross-sectional images[56]. These images are called tomographic slices and contain more information than conventional x-rays. The computer collects the successive slices; they are digitally put together to form a three-dimensional image of the patient.

CT allows pancreas visualization and the whole abdominal part to detect organs and structures close around[57].

The standard CT protocol consists of the acquisition of 0.5-1 mm thick images with two phases. The parenchymal phase (40-50 s) allows the detection of pancreatic lesions and estimates the implication of adjacent arterial structures, and the venous phase (56-70 s) to determine the porto-mesenteric axis and

detect peritoneal and liver metastasis. Multiphase multi-detector row CT (MDCT) is a conventional CT with intravenous contrast administration; it is highly accurate in diagnosing primary tumors, locoregional extension, vascular invasion, distant metastasis, and resectability[58]. MDCT allows the reconstruction of images in different planes (axial, coronal, and sagittal) in both phases, which improves the visualization of adjacent structures[59].

In 86-89% of CT cases, PDAC may appear as low constricted masses with pancreatic duct dilatation with abrupt narrowing in both phases because they are hypovascular lesions with large desmoplastic content. In contrast, in 11-14% of the cases, the lesions appear isodense compared with the rest of the parenchyma, mainly in those smaller than 2.5 cm and may occasionally be missed[35]. Sometimes comes double duct sign, meaning that bile duct dilatation is combined with a dilated pancreatic duct in cases of pancreas head cancer[60]. When there is an irregular vessel wall, a high number of vessels in contact with the tumor, vascular caliber change, or peritumoral fat infiltration, vascular invasion is happening; this event is important for the diagnosis and treatment of PDAC[61,62].

In PDAC diagnosis, CT has a sensitivity of 89% and a specificity of 90%, similar to MRI, according to various meta-analyses[63]. With MCDT it has been an improvement of the sensitivity to up to 96%[64]. However, this sensitivity is reduced in small lesions detection, reaching 67-75% (Figure Intro. 4). CT also is used for the detection of distant metastasis in liver, lungs, or peritoneum[59].

II. Magnetic Resonance Imaging (MRI)

This technique employs strong magnetic fields forcing the alignment of protons in the body with the field. With a radiofrequency, protons are stimulated and exit the equilibrium state hitting the magnetic pull, and when the radiofrequency turns off, the sensor detects the energy released by the body protons[56]. MR cholangiopancreatography (MRCP) is a method that allows visualization and evaluation of biliary and pancreatic ducts[65], it is comparable to endoscopy in terms of diagnosis, but this approach is non-invase[66]. Additionally, diffusion-weighted images (DWI) are based on water molecules diffusion differences and

represented as apparent diffusion coefficient (ADC). Moreover, it is an excellent technique to follow cystic pancreatic tumor development[67]. ADC values have reported low numbers for PDAC compared to high values for pancreatitis, allowing the differentiation of these two diseases.

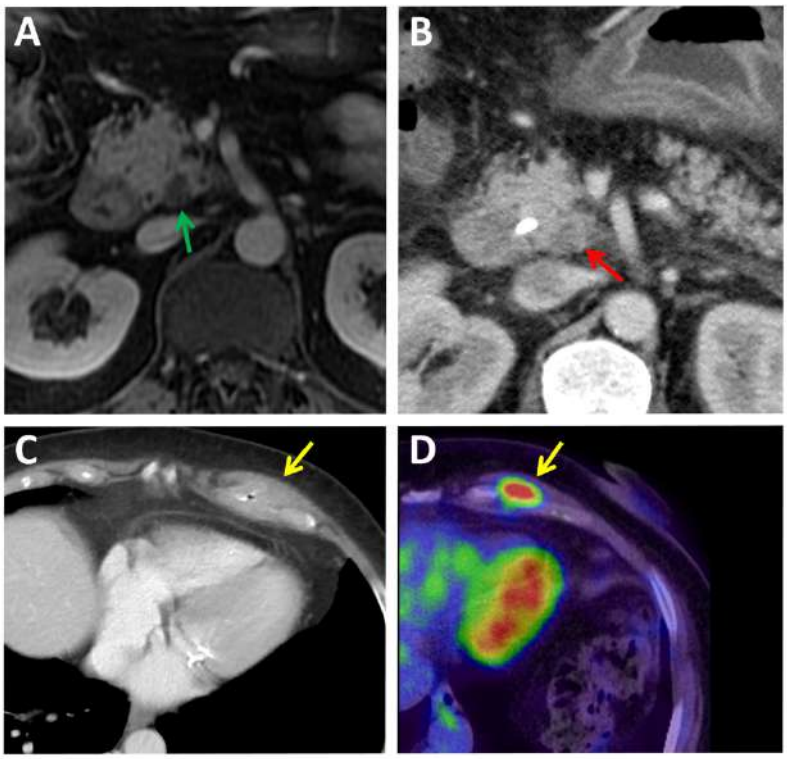

Figure Intro. 4. Infra-staged case of PDAC by MRI and CT. Imaging techniques diagnosed a T2 N0 PDAC, and histology was a locally advanced pT4 pN1 PDAC. (A) MRI shows a small cystic area in the pancreas uncinate process (green arrow), a bile duct structure, and no direct signs of malignancy. (B) CT showed a small hypodensity next to the superior mesenteric artery after the implantation of a bile stent (red arrow). Image taken from González-Gómez et al.[36] (C, D) A case of a false-positive diagnosis of metastatic tumor recurrence. (C) Some months after surgical excision of a PDAC stage pT2 pN0 M0 R0, an asymptomatic solid mass in the left costal wall (yellow arrow) was shown by a CT scan. (D) By [^{18}F]FDG PET-CT image, the patient was suspicious of a PDAC metastatic relapse. A tumor core biopsy found inflammatory and fibrotic tissue but no sign of malignant cells.

This approach has a high sensitivity in terms of PDAC detection and has several advantages against CT, like soft-tissue contrast resolution, and that it does not use ionizing radiation[68].

MRI is similar to CT in diagnosis and staging in terms of sensitivity and specificity, 89%. However, in lesions smaller than 2 cm, MRI is more valuable than CT, detecting up to 79% of the lesions that were not detected by CT[69]. Even detection of small tumors, even panINs < 5 mm, can be visualized on T2WI and MRCP[70].

III. Positron Emission Tomography (PET)

PET is a nuclear medicine technique used to measure blood flow, metabolism, neurotransmitters, and radiolabeled agents to determine physiological functions. A positron is emitted with some kinetic energy, and it is annihilated with an electron from the tissue. This new structure formed converts all its mass into energy and emits two photons in opposite directions, and finally, these photons are collected in the PET detectors. These photons detection give information about the concentration and spatial location in the patient (figure Intro. 5)[71].

This approach is quantitative and stable during a period. It is based on applying a radiotracer via intravenous and detecting the radioactivity emitted by the body[72].

It could be used without contrast, but tumor and its vasculature detection are limited[73]. At any rate, it is regularly employed with intravenous contrast, the most used radiocompound is 2-deoxy-[^{18}F] fluoro-D-glucose ([^{18}F] FDG), which is used in glycolytic pathways; consequently, cells with glucose transporters and/or with glycolytic enzymes will be positive in PET[74]. Normal pancreas has low glucose compared to PDAC tumors, making possible the detection of potential lesions and the prediction of aggressiveness and survival of patients[75]. However, there are some problems with [^{18}F] FDG in PET because glucose metabolism is not exclusive of cancer cells. Some tissues or inflammatory processes are positive to this technique and can be confusing, like pancreatitis and PDAC[76].

This technique is not routinely used in PDAC diagnosis; it is more useful in monitoring the response to treatment and tumor recurrence[78,79].

Combining two imaging diagnosis modalities has increased the specificity in terms of metastasis detection, [^{18}F] FDG PET/CT or MRI can be used to detect lymph node metastasis and identify distant metastasis[80].

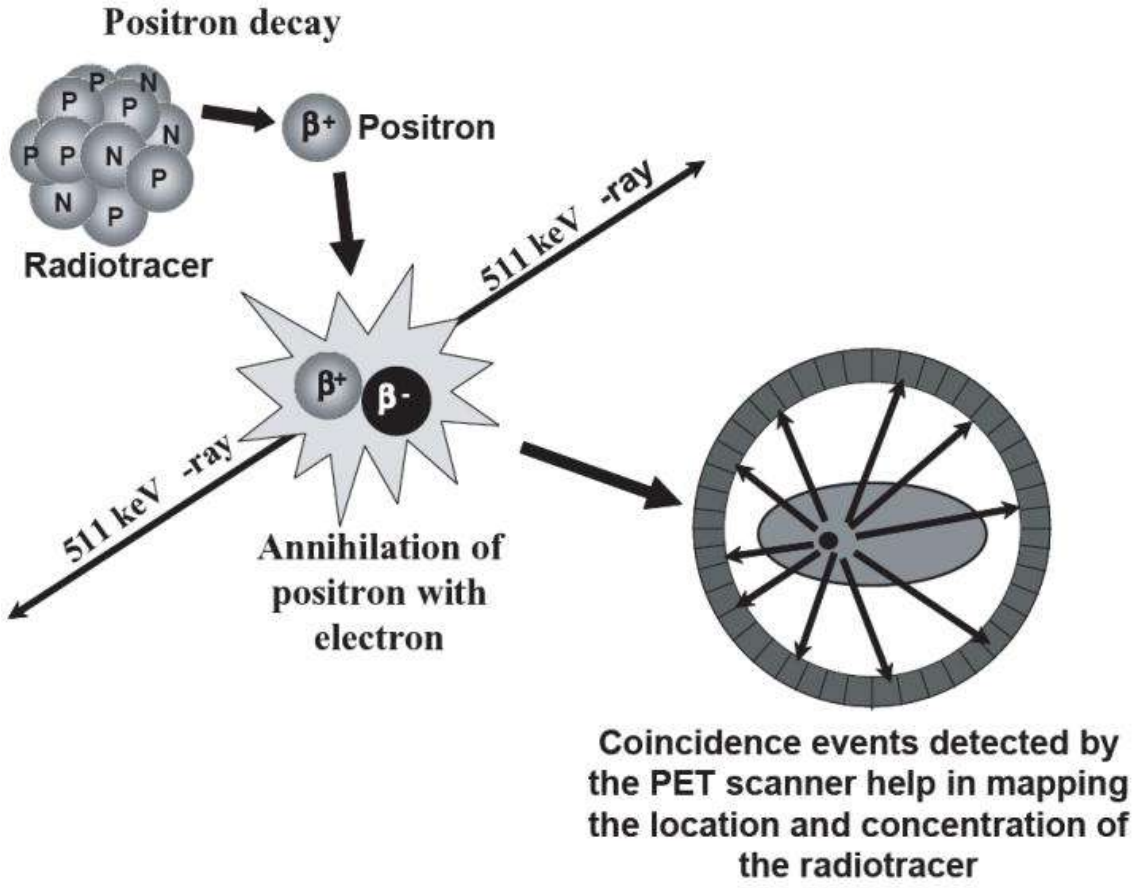

Figure Intro. 5. PET scan physic principle. Description of the PET scan process produced by the emission of positrons results in detecting gamma rays. Image taken from Cherry et al.[77]

IV. Immuno-positron emission tomography (immuno-PET).

This imaging technique takes advantage of PET and antibodies, increasing sensibility and selectivity, respectively. Besides being a diagnosis tool, it could be drawn on to predict therapeutic effect depending on the amount of target the antibody is directed[81]. During the last years, new biomarkers are being discovered; these targets are relevant for diagnosis and therapy in patients. These biomarkers can be used to be detected by antibodies and improve diagnosis.

Three main components of immuno-PET must be selected with the best characteristics for a representative image (figure Intro. 6):

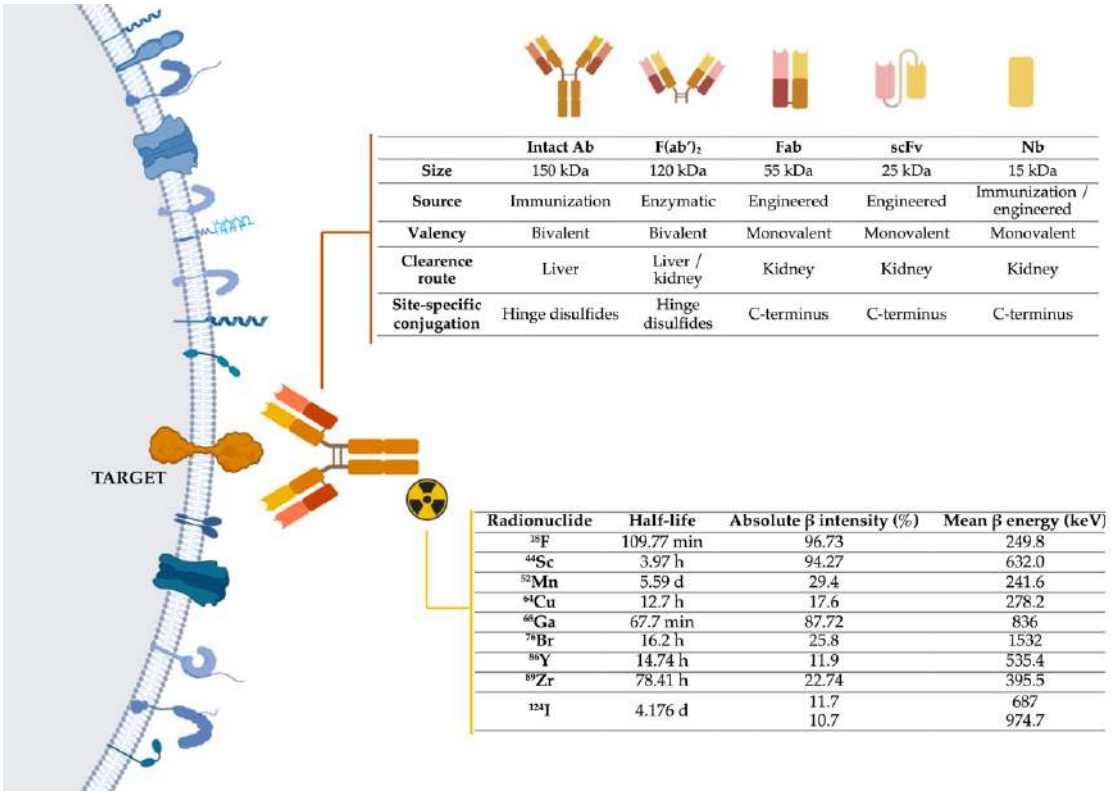

	Intact Ab	F(ab')$_2$	Fab	scFv	Nb
Size	150 kDa	120 kDa	55 kDa	25 kDa	15 kDa
Source	Immunization	Enzymatic	Engineered	Engineered	Immunization / engineered
Valency	Bivalent	Bivalent	Monovalent	Monovalent	Monovalent
Clearence route	Liver	Liver / kidney	Kidney	Kidney	Kidney
Site-specific conjugation	Hinge disulfides	Hinge disulfides	C-terminus	C-terminus	C-terminus

Radionuclide	Half-life	Absolute β intensity (%)	Mean β energy (keV)
^{18}F	109.77 min	96.73	249.8
^{44}Sc	3.97 h	94.27	632.0
^{52}Mn	5.59 d	29.4	241.6
^{64}Cu	12.7 h	17.6	278.2
^{68}Ga	67.7 min	87.72	836
^{76}Br	16.2 h	25.8	1532
^{86}Y	14.74 h	11.9	535.4
^{89}Zr	78.41 h	22.74	395.5
^{124}I	4.176 d	11.7 10.7	687 974.7

Figure Intro. 6. Representation of three main components of immune-PET. Abbreviations: Ab-antibody; Fab- Fragment antigen-binding; F(ab')$_2$- Fab dimer; scFv- single-chain variable fragment; Nb- nanobody; ^{18}F- fluorine; ^{44}Sc- scandium; ^{53}Mn- manganese; ^{64}Cu- copper; ^{68}Ga-galium; ^{76}Br- bromine; ^{86}Y- yttrium; ^{89}Zr- zirconium; ^{124}I-iodine[82,83]. Image taken from González-Gómez et al.[36]

a. Target.

Different cell components can be targets for antibodies recognition, proteins, saccharides, or lipids. The ideal epitope requires some characteristics: the target needs to be exposed on the cell surface or extracellular components for an easy recognition. Essential and functional components of tumors can be the target for immuno-PET, but also components from the tumor microenvironment (TME) such as extracellular matrix (ECM). TME regulates essential tumor survival, and it has been shown to be implicated in promoting tumor development and metastasis[84]; the detection of molecules of TME by immuno-PET would give additional and important information about the tumor.

It needs to be differentially expressed in the tumor compared to normal tissue. Additionally, some targets could predict prognosis and therapeutic response[85].

b. Antibodies.

An antibody or fragment-derived antibody is going to be used for target detection. Fragment-derived antibodies can be obtained by protein engineering or immunization. Antibody affinity for the target may be enough to be retained in the tumor, and unbound antigen should be quickly cleared to minimize background signal[86].

Different structures can be used to bind the target; the biggest one and the most commonly used are monoclonal antibodies (150 kDa); other smaller parts of the antibodies are recently being used as single chain-fragment variable-fragment crystalizable (scFv-Fc) (105 kDa), minibodies (80 kDa), diabodies (50 kDa), scFv (40 kDa) and nanobodies (15 kDa). All of these fragments derived from monoclonal antibodies remain the high affinity and specificity. Antibody fragments clearance differs depending on their size, charge, and hydrophobicity/hydrophilicity. Basically, there is a cutoff in 60 kDa; below this size, the clearance route is renal, and above 60 kDa, the clearance is hepatic. Depending on the size of the radiotracer, the clearance differs; consequently smallest tracers will be expulsed of the body quickly by kidneys[85,87,88].

c. Radionuclides.

The imaging modality and tracer selection depend on sensitivity, sensitivity, resolution, quantification, and multiplexing[89,90]. For immuno-PET techniques, the radionuclide will be a positron-emitting particle. It is important that the physical half-life of the radionuclide match with the biological half-life of the antibody. Typically, ^{89}Zr or ^{124}I with long half-lives are conjugated with monoclonal antibodies. Intermediates half-life isotopes as ^{64}Cu or ^{86}Y are normally labeled with intermediates antibody fragments as scFv-Fc or minibodies, and short half-lives as ^{18}F, ^{68}Ga, and ^{44}Sc are usually conjugated with diabodies, scFv, and nanobodies[91].

Short half-life isotopes will remain shorter time in the body of patients, but they have another significant advantage, ^{68}Ga and ^{44}Sc can be produced from a generator, a small and economic generator[92,93]. Although the use of ^{68}Ga is more frequent in PET, ^{44}Sc in ground state is a promising radionuclide for PET imaging.

The half-life of ^{44}Sc (3.97 h) is lower than ^{68}Ga; it is well suited for its use with small molecules or peptides due to their rapid biodistribution through the body[94].

Immuno-PET allows the detection of tumor biomarkers for an early diagnosis of PDAC as well as monitoring patients. Furthermore, these imaging techniques enable the quantification of the biomarkers in a non-invasive way; it can give similar information to immunohistochemistry data after a patient's biopsy but without any intervention.

4. Surgery

At the time of diagnosis, only around 25% of patients can undergo surgery. In 2006, the National Comprehensive Cancer Network (NCNN) introduced criteria to determine if a pancreatic tumor can be resectable or not. These criteria are based on the relationship between the tumor and the blood vessels, with arterial structures like celiac trunk (CT), hepatic artery (HA), and superior mesenteric artery (SMA); or with venous structures as portal vein (PV) and superior mesenteric vein (SMV)[95].

Table 1. Classification of PDAC tumors depending on their resectability. Definition criteria of resectability by NCCN v 1.2019. Modified table from González-Gómez et al.[36] and NCNN[96]. *Abbreviations: CT: celiac trunk; SMA: superior mesenteric artery; CHA: common hepatic artery; SMV: superior mesenteric vein; PV: portal vein; IVC: inferior vena cava.*

Resecability status	Location / Surgery	Arterial	Venous
Resectable	Located in the pancreas, completely removable by surgery	No tumoral contact with CT, SMA, or CHA	No tumoral contact with SMV, PV, or ≤*180º* without irregularity of the venous contour
Resecability Borderline (BR-PDAC)	There are possibilities that the tumor has reached the blood vessels; thus, it is unclear that the tumor can be resectable	<u>Head and uncinate process:</u> • Tumoral contact with CHA without CT extension or CHA bifurcation allowing safety and complete resection and reconstruction	<u>Head and uncinate process:</u> • Tumoral contact with IVC, PV >180º with venous contour irregularities or thrombosis, but with free proximal and distal portions that allows a suitable resection

		• Tumoral contact in SMA≤*180º.* • Tumoral contact with an anatomical variant of CHA	
		<u>Body-tail:</u> • Tumoral contact with CT≤*180º* • Tumoral contact with CT≥*180º* without aorta involvement, with gastroduodenal artery intact	
Locally advanced (LA-PDAC)	There is metastasis surrounding the pancreas, lymph nodes, and tissues and has involved blood vessels. Usually, surgery cannot eliminate the whole tumor	<u>Head and uncinate process:</u> • Tumoral contact with AMS>*180º* • Tumoral contact in CT>*180º*	<u>Head and uncinate process:</u> • SMV and PV irreconstructable by thrombosis or tumoral infiltration. • Contact with the sewer system in the 1st jejunal venous branch
		<u>Body-tail:</u> • Tumoral contact with AMS or CT>*180º* • Tumoral contact with CT and aorta	<u>Body-tail:</u> • SMV and PV irreconstructable by thrombosis or tumoral infiltration
Metastatic	Cancer has spread to other parts of the body and has gone through the vasculature system. The tumor cannot be removed by surgery		

Vascular invasion is relatively frequent, around 20 to 65%, being more frequent venous than arterial invasion. Basically, it is considered unresectable when there is a direct contact between the tumor and the vessel surface greater than 180º of its circumference (locally advanced and metastatic), and it can be considered

resectable when this contact is less than 180º (resectable and borderline resectable). Therefore, the tumor can be divided into four groups (Table 1).

The international group of pancreatic cancer expanded in 2017 the definition of BR-PDAC by including carbohydrate-antigen 19-9 (CA19-9) serum levels to determine preoperative conditions. Including these characteristics, BR-PDAC can be differentiated into BR-A for anatomical, BR-B for biological, and BR-C for conditional. BR-A is a margin-positive tumor in which the treatment consists of surgery followed by chemotherapy and/or radiotherapy; BR-B corresponds to tumors with probably nearby metastasis, and BR-C represents patients with a high risk of mortality due to host-related factors[97].

Ultimately, the biological evaluation of the tumor is performed, attending to the detection of lymph node metastasis and CA19-9 serum levels[98].

Specific signs can indicate vascular infiltration, such as contour irregularity, deformity, decreased caliber, or occupancy of the vascular lumen[99]. Nevertheless, tumor resectability consensus is being in constant actualization, and it is evolving with neoadjuvant therapy.

Normally, the number of tumors that can be resectable is very low; thereby, BR- and LA-PDAC are treated with chemotherapy or chemoradiotherapy before the surgery. After the treatment, the complete surgical resection can achieve 50% in BR-PDAC and 20% in LA-PDAC patients[100,101].

5. Treatment.

Pancreatic tumor cells have an uncontrolled capability to grow and metastasize due to their adaptive changes in signaling, adhesion, cellular metabolism, and immunoediting. Additionally, PDAC cells promote a dense functional stroma that facilitates tumor resistance to chemotherapy and radiation[102].

I. Standard of Care (SOC) in PDAC

In patients with resectable or BR-PDAC, the standard adjuvant treatment is a modified regimen of 5-fluorouracil/leucovorin, irinotecan, and oxaliplatin (mFOLFIRINOX)[103]. 5-Fluorouracil is a fluoropyrimidine antimetabolite drug that

inhibits the enzyme thymidylate synthase, impairing the synthesis of thymine. Leucovorin is also known as 5-formyltetrahydrofolic acid, it is a metabolite of folic acid and inhibits *de novo* synthesis of purines, pyrimidines, and methionine. Irinotecan is a camptothecin derivate that inhibits DNA topoisomerase I, leading to DNA breakage and cell death. And finally, oxaliplatin binds guanine and cytosine of DNA, producing a cross-linking of DNA, inhibiting DNA synthesis and transcription[104]. In PRODIGE 4/AACCORD 11 phase 3 trial, mFOLFIRINOX showed an increase of 4.3 months in overall survival (OS) compared to gemcitabine treatment in metastatic PDAC patients[105].

In the case of patients with LA-PDAC or metastatic disease, new combination therapies have shown a slight increase in the effectiveness of chemotherapy; gemcitabine + abraxane (GA) are the most used[106,107]. Gemcitabine (G) is a deoxycytidine (dCTP) analog; it inhibits ribonuclease reductase, preventing DNA synthesis and leading to cell death[104]. Abraxane (A) is an albumin-bound form of paclitaxel; paclitaxel hyper-stabilizes the structure of microtubules by binding to β subunit of tubulin, it impairs microtubules disassembly[108]. In MPACT phase 3 trial, GA combination demonstrated an OS of 8.5 vs 6.7 of G treatment[105]. Anyway, there is no significant difference between GA and mFOLFIRINOX treatments attending to toxicity and physics profiles; just some secondary effects like myelosuppression, fatigue, and alopecia are more frequent with mFOLFIRINOX treatment[109].

Despite the improvements in PDAC patients' treatments depending on the tumor stage, there is still a need to search and develop new drugs to prolong the OS of PDAC patients.

II. Targeted therapy

Precision or personalized medicine is a medical approach for treatment that considers individual variability in genes, environment, and lifestyle for each person. This laneway allows a more accurate prediction of treatment and prevention strategies that are better for a specific group of people.

During these last years, it has been an improvement in sequencing techniques; this data has allowed developing specific inhibitors against important targets

involved in the disease. It is essential to look for new targets that participate in PDAC appearance, progression, and metastasis despite this fact.

Several inhibitors have been generated and tested in clinical trials in PDAC patients.

a. KRAS mutations

Around 90% of PDAC mutations happen in K-RAS, the most common are G12D (36-38%), G12V (25-27%), and it is less common G12C (1-3%). Several inhibitors against mutated K-RAS have been effectively developed[110].

AMG510 is a $KRAS^{G12C}$ inhibitor (NCT03600883), it is well-tolerated, but it did not reduce tumor size[111]; MRTX849 is a potent $KRAS^{G12C}$ inhibitor, it reduced 33% of tumor size in two patients with metastatic PDAC[112], but certainly, this mutation is not frequent in PDAC tumors (2%) except in Asia (60%). There are no inhibitors against $KRAS^{G12D}$ effective in PDAC that represent the most frequent mutation. Still, a phase 1/2a trial with an RNA interference (RNAi) for this mutation called *siG12D-LODER™* (Silenseed Ltd.) showed an increased median OS combined with FOLFIRINOX treatment[113].

Other strategies have been under investigation, by way of downstream KRAS proteins, for instance, mitogen-activated kinase (MEK), extracellular signal-regulated kinase (ERK), and proteinase kinase b (PKB/AKT) inhibitors. Despite being very effective compounds *in vitro*, any MEK inhibitor showed an effect in PDAC remission, selumetinib nor primasertib, even in combination with SOCs[114]; as well as epidermal growth factor receptor (EGFR)[115] or AKT inhibitors did not show any effect[116]. On the contrary, trametinib, a MEK inhibitor, in combination with hydroxychloroquine, an autophagy inhibitor, could diminish tumor size in patients (NCT03825289)[117].

b. Tropomyosin receptor kinase (TRK), neuregulin-1 (NRG1), and Serine/threonine-protein kinase B-raf (BRAF)

Tropomyosin receptor kinase (TRK) is a transmembrane protein encoded by NTRK1, 2, and 3 genes, fusion of various of these genes activate the RAS-MEK

pathway constitutively. Larotrectinib showed a response in 75% of patients in NAVIGATE trial[118], and entrectinib was also approved by FDA for PDAC treatment with *NTRK* fusions[119].

Neuregulin-1 (NRG1) is an erbB-EGFR3 and erbB-EGFR4 receptor tyrosine kinase ligand. Patients with NGR1 fusions in PDAC tumors could benefit from the effect of afatinib as an EGFR-targeted therapy[119].

Serine/threonine-protein kinase B-raf (BRAF) mediates signal from RAS to MEK; $BRAF^{V600E}$ mutation makes the kinase constitutively active and promotes proliferation. Trametinib is a good treatment for PDAC patients harboring BRAF mutations[120].

c. DNA repair

After chemical and environmental damage to DNA, there is a biological repair process; these mechanisms are collectively called DNA-damage response (DDR); the cell can detect DNA lesions, signaling them and promoting their repair[121].

DDR defects are usually related to cancer; it favors proliferation by enhanced mutations and genome instability. In fact, DDR is commonly activated in early neoplastic lesions. As DDR is implicated in cancer initiation and development, several inhibitors have been developed to reduce malignant progression[122].

d. PARP inhibitors

Poly (ADP-ribose) polymerase (PARP) enzymes are implicated in DNA damage repair (DDR); it recognizes DNA breaks and recruits DDR proteins. Inhibition of PARP in tumor cells leads to cell death. Veliparib was very effective in patients with PDAC carrying BRCA1/2 (breast cancer 1/2) mutations[123], and olaparib increased in 4 months the OS in 2% of patients and stabilized the stage of the disease in 72% of patients in advanced stages of PDAC with BRCA1/2 mutations[124,125].

e. ATM/ATR inhibitors

Ataxia-telangiectasia mutated (ATM), and rad-3 related (ATR) are serine/threonine kinases that participate in the DDR pathway; both kinases induce cell cycle arrest and facilitate DNA repair[126]. In response to DNA double strain breaks (DSB), ATR is activated and coordinates a signaling pathway that stimulates DNA repair and limits cell progression by apoptotic or cytostatic mechanism; this response is known as DNA damage response (DDR)[127,128].

During DNA replication, there is a wide spectrum of abnormalities; it is named "replicative stress" (RS) what results in large and unprotected regions of DNA.

ATM deficiency promotes cell cycle progression and angiogenesis; this fact is present in 9-18% of PDAC patients. Both ATM and ATR inhibitors are in clinical development[129]. Several ATM inhibitors (AZD0156, KU60019, AZD1390) prevent ATM phosphorylation to sensitize tumor cells to DDR interfering strategies; its combination with olaparib showed promising partial responses in phase I clinical trials[130]. ATR inhibitor AZD6738 showed a synergistic effect with gemcitabine *in vitro* and *in vivo* experiments, suggesting an evaluation in clinical trials with patients with PDAC[131].

Both RS and improper ATR-response lead to excessive DNA damage. ATR has a dual role in cancer, then inhibitors of ATR and ATM could be effective in killing tumor cells with high levels of ROS, but its insufficient inhibition could promote tumor progression[132].

f. Metabolism

PDAC cells can reprogram metabolism for their energetic supply; it can be changed by oncogenes activation or by stromal communication[133]. PDAC tumors have a strong desmoplastic response and metabolic reprogramming; these lead to an increase in glucose, amino acid consumption, and lipid biosynthesis. PDAC patients can be differentiated depending on their metabolic tumor needs; they can be classified into glycolytic or lipogenic. Even more, the glycolytic subtype would be more aggressive and resistant to chemotherapy than the lipogenic one. This metabolic stratification correlates with molecular classifications previously described; by this stratification, tumors can be treated with specific treatments[134].

1. Tricarboxylic Acid Cycle (TCA)

The TCA cycle plays an essential role in the catabolism of organic fuel molecules, like sugars, fatty acids, and amino acids. These molecules need to be degraded into AcetylCoA (Acetyl coenzyme A), then it enters into TCA and is converted into carbon dioxide and energy[135]. TCA is one of the main ways to produce energy in tumoral cells via mitochondria.

Devimistat is a lipoate analog; it inhibits pyruvate dehydrogenase (PDH) and α-ketoglutarate dehydrogenase, decreasing mitochondrial metabolism and inducing apoptosis in pancreatic cancer tumors[136]. Even in combination with SOCs are showing promising results in PDAC patients with metastasis[137].

2. Autophagy

Autophagy collaborates in the catabolism of intracellular organelles and supports tumor growth in PDAC. Hydroxychloroquine is an autophagy inhibitor; by itself, it did not show any effect in patients with metastatic PDAC[138], but nowadays, it is being proved in combination with gemcitabine and nab-paclitaxel[139].

g. Extracellular matrix (ECM)

One of the reasons for the resistance of PDAC to chemotherapy and radiotherapy is the excessive growth of a fibrotic extracellular matrix stroma around the tumor cells, limiting the penetration into the tumor. The main components of ECM are collagen and hyaluronic acid. The ECM stroma generates high interstitial fluid pressures for vascular collapse; this limits the drug uptake[140].

1. Recombinant human hyaluronidase

Hyaluronic acid (HA) is overexpressed in the stroma of PDAC tumors; this consequently reduces tissue perfusion and difficult treatment. PEGPH20 (pegvorhyaluronidase-α) degrade HA, disrupting ECM and increasing drug delivery. It is actually working in clinical trials in combination with gemcitabine, nab-paclitaxel[141], and mFOLFIRINOX[142].

2. FAK/BKT inhibitors

Focal Adhesion Kinase (FAK) is a cytoplasmic tyrosine kinase that plays an important role in integrin-mediated signal transductions; it is involved in tumor invasion and metastasis.

Defactinib or GSK2256098 are potent FAK inhibitors in clinical trials that act in combination with SOCs.

Bruton tyrosine kinase (BTK) is a cytoplasmic tyrosine kinase important in B-lymphocyte development, differentiation, and signaling. Ibrutinib is a BTK inhibitor that reduces tumor growth in mice, but it did work in PDAC patients in combination with SOCs[143].

h. Immunotherapy

Pancreatic cancer evades immunological responses directly or inducing an immunosuppressive microenvironment. PDAC stroma is formed by cancer-associated fibroblasts (CAFs) that interact with tumor-associated macrophages and regulatory T cells. Immunotherapy has the potential to generate an immune response and mobilize it to the tumor to eliminate cancer cells. It can be an alternative to chemotherapy or a combination to increase effectiveness[144,145].

1. CD40

CD40 is part of the tumoral necrosis factor (TNF) receptor superfamily; it is expressed in immune cells and some tumor cells. Anti-CD40 antibody in combination with nab-paclitaxel resulted in the response of >50 % of PDAC patients[146]. The combination of CD40 antibody treatment demonstrated destruct tumor stroma by CD40-activated macrophages; the followed chemotherapy treatment resulted more efficient than normal treatment[147].

Table 2. Main therapies for PDAC treatments. Classification of PDAC treatments. Adapted from Nevala-Plagemann et al.

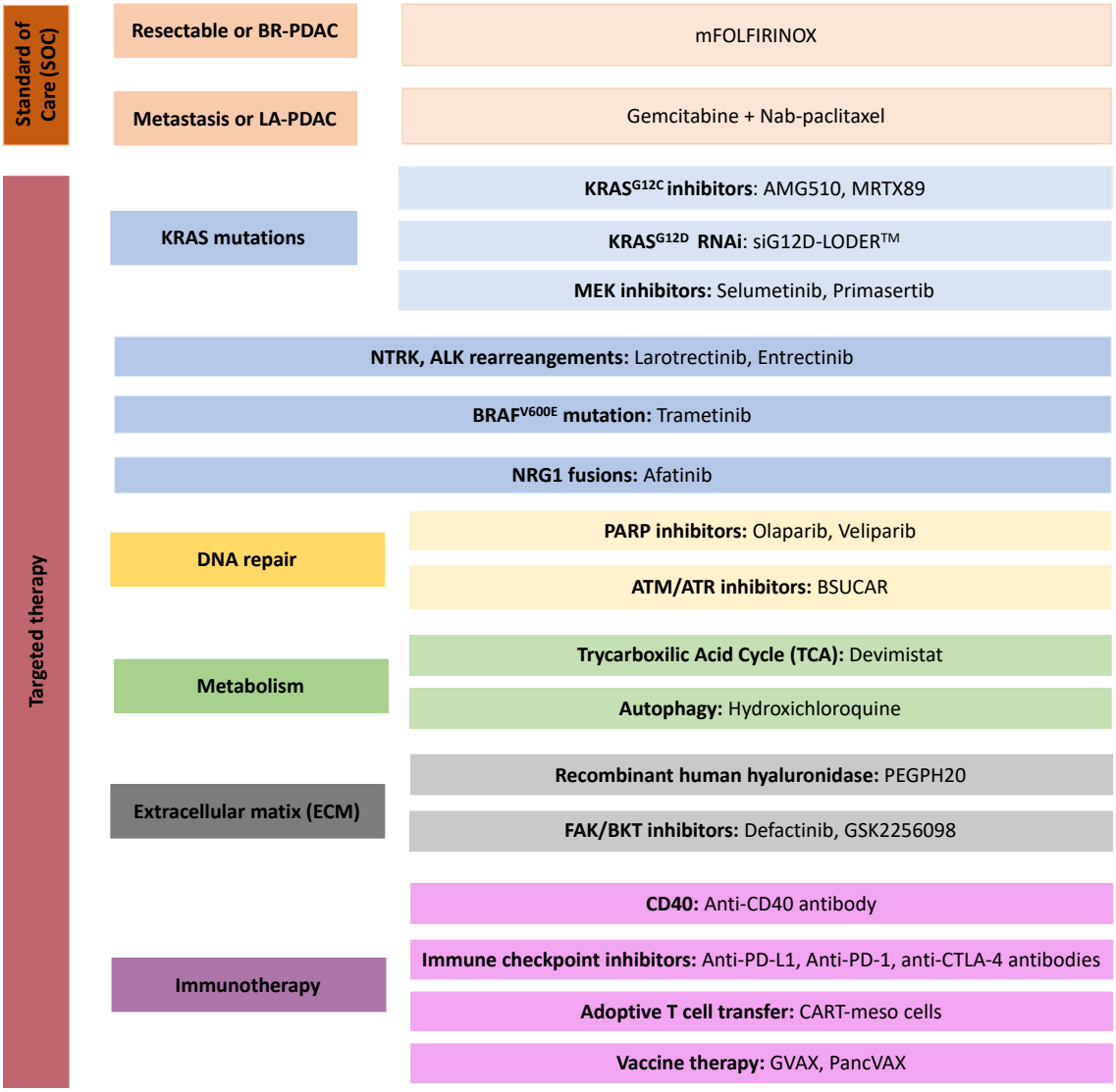

2. PD-1 and PDL-1.

The programmed death 1 (PD-1) is a surface protein present on B and T cells; it is responsible for the downregulation of the immune response. Their ligands, PD-L1 and PD-L2, are also crucial in the control of T cell activation[148]. Different antibodies against PD-1 and PD-L1 have been employed for immunotherapy in some cancer types with interesting and good results. In the case of PDAC treatment, it has not shown excellent results, but in combination with other immunotherapies or treatment, it could increase effectiveness[149].

3. CTL4

Cytotoxic T-lymphocyte-associated protein 4 (CTLA-4), also known as cluster differentiation 152 (CD152), is a protein receptor that downregulates immune response and serves as an immune checkpoint[150]. CTLA-1 is implicated in the priming phase (lymph node), while PD-1 and PD-L1 are involved in the effector phase (tumor). PDAC patients that have been treated with CTLA-4 antibodies alone or in combination with PD-1 antibodies have not worked; it could be due to the fibrotic stroma present in PDAC; in this way, antibodies were not able to enter into the tumor[151].

4. Adoptive T cell transfer

Chimeric Antigen Receptor (CAR) T cell therapy remains a challenge as a treatment for solid tumors. There are some clinical trials in PDAC patients where T cells expressing mesothelin-targeting CAR have been used, they have not been toxic, and tumor volume has been reduced in around 70% of patients[152].

5. Vaccine therapy

Several vaccines have been developed for PDAC. GVAX has been generated from a PDAC cell line that has been genetically modified to express granulocyte-macrophage colony-stimulating factor; unfortunately, it did not improve OS in PDAC patients[153].

6. PDAC Biomarkers

The early detection of PDAC in a non-invasive way remains a challenge; actually, differential diagnosis has several difficulties distinguishing between PDAC, CP, or benign lesions. It is important to discover specific biomarkers to improve the diagnosis and the treatment of PDAC patients[154]. Several studies and clinical trials identify cost-effective and non-invasive new biomarkers with high sensitivity and specificity for PDAC[155]. Several molecules can be used as biomarkers, like proteins, metabolites, cytokines, or non-codingRNAs (ncRNAs), among others.

Different techniques can also detect them, such as ELISA, liquid biopsies, or body fluids[154].

In general, biomarkers for PDAC can be classified as predictive, prognostic, and predictive.

I. CA 19-9

Carbohydrate antigen 19-9 (CA 19-9), also known as sialyl-Lewis^A, is a tetrasaccharide attached to O-glycans on the surface of the cells. It is implicated in cell-to-cell recognition processes[156]. CA 19-9 is a prognosis biomarker, it is the most used in clinics, and its levels are measured in serum by ELISA[157]. The serum marker used for PDAC detection is CA 19-9; elevated levels of CA 19-9 are interpreted as advanced PDAC and associated with poor prognosis[158]. CA 19-9 elevated levels after resection are typically related to hepatic- and peritoneal-based recurrence[159]. It is also established a cutoff of 100 U/ml of Ca 19-19 level; over these levels, there is a higher probability of recurrence after 6 months of surgery[160].

Nevertheless, high levels of CA 19-9 are also related to pancreatitis, cirrhosis, colorectal or gastric cancers[161]. It is also remarkable that only 65% of patients with resectable PDAC have elevated CA 19-9 serum levels[162]. Considering all these results, CA 19-9 is not recommended as a screening marker for PDAC patients[154], but its levels can predict the resection of the tumor as help for the surgery or can predict response to treatment[163].

II. microRNAs (miRNAs)

microRNAs (miRNA) are non-coding RNAs that regulate post-transcriptionally gene expression through their interaction with the 3' untranslated region (3'UTR) of mRNAs inducing its degradation[164]. miRNAs can be detected in different body fluids, such as serum, saliva, or urine, and some of them have been described recently as potential cancer biomarkers[165].

Several studies have discovered specific miRNAs with different expression levels in the normal pancreas, chronic pancreatitis, and PDAC. These miRNAs can be

used to classify patients depending on the cancer stage into stage I (miR-143, miR-223, and miR-30e expression), stage II-IV (miR-143, miR-223, and miR-204 at higher levels)[166]. Patients can be also be distributed into short-term survivors (<24 months) if they express miR-452, miR-105, miR-127, miR-518a-2. miR-187 and miR-30a-3p, or long-term survivors (>24 months) if they do not express these miRNAs or have lower expression levels[167]. It is also essential that some miRNAs can differentiate CP from PDAC; PDAC is characterized by higher levels of miR-21 and miR-155 and lower levels of miR-216 compared to CP or normal pancreas[168]. All these markers can be used as diagnostic and prognostic for PDAC patients in a non-invasive manner.

III. New possible biomarkers: ABC proteins

A large number of transmembrane proteins form ATP-binding cassette (ABC) transporters superfamily. These channels use ATP for the active transport of different molecules across the cell membrane[169].

An ABC transported comprises two identical halves; each has six transmembrane domains (TMDs) and a nucleotide-binding fold (NBF), which is located in the cytoplasm and transfers the energy to transport the substrate through the membrane. The NBFs contain 2 highly conserved and characteristic motifs, Walker A [G-(X)4-G-K-(T)-(X)6-I/V] and Walker B [R/K-(X)3-G-(X)-L-(hydrophobic)4-D] separated by 90-120 amino acids. And they also have an ABC signature upstream of the Walker B site [L-S-G-G-(X)3-R-hydrophobic-X-hydrophobic-A][170,171]. The TMD contains from 6 to 11 membrane-spanning α-helices; here remains the specificity of the substrate (figure Intro. 7)[172].

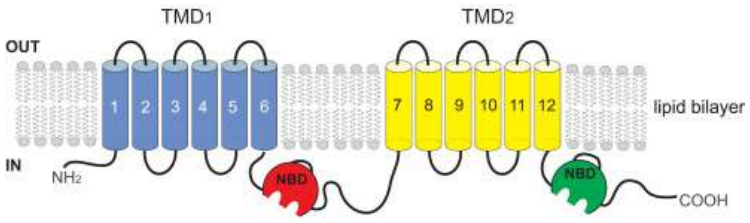

Figure Intro. 7. ABC protein's typical structure. Dermauw, W., Van Leeuwen, T. The ABC gene family in arthropods: comparative genomics and role in insecticide transport and resistance. *Insect Biochem Mol Biol* 45: 89-110

There are 48 ABC transporters in humans, and they can be divided into seven subfamilies from A to G by phylogenetic analysis[173].

The ABC transporters family is classified by their ATP-binding domains or nucleotide-binding folds (NBFs) sequence and organization. They can be classified into different clusters based on their topology. The majority of these proteins have a $[TMD_6\text{-}NBF]_2$ or $[NBF\text{-}TMD_6]_2$ conformation[174]. Multidrug resistance-related proteins (MRP) are ABC transporters with a TMD_n $[TMD_6\text{-}NBF]_2$ topologies. They present an additional transmembrane domain of 200 amino acids at the N-terminus domain; they also have a putative “Regulatory” (R) or “Connector” (C) domain located in the middle of the two homolog halves, it participates in the regulation of the protein[175]. ABC proteins are divided into 8 subfamilies in eukaryotes (ABCA to ABCI)[176].

ABC transporters require adenosine triphosphate (ATP) hydrolysis to transport substrates against a chemical gradient. Normally, ABC proteins act in a single direction, being efflux or influx pumps, but in some exceptional cases, they can be reversible[177,178]. The membrane domain switches, making accessible the binding of the substrate and Magnesium-ATP (MgATP), then happens the ATP hydrolysis and the substrate is released.

I. Alternating site. When one ATP site enters into the transition state conformation, the other cannot; then, the two sites may undergo ATP hydrolysis alternatively[179].

II. Switch. This model involves bidirectional communication between the NBDs and TMDs. ABC transporters are a class of ATPases that do not need phosphorylation of protein intermediate; consequently, the communication only involves noncovalent conformational changes. First, there is a switch between two principal conformations of the NBD; secondly, ATP molecules bind to the transporter, and a closed dimer is formed. Finally, after ATP hydrolysis derives in the dissociation and opening of the dimer for the release of phosphate (P) and adenosine diphosphate (ADP). The substrate crosses the membrane due to the conformational changes in the TMDs that are induced by the switching between the open and closed conformations. The two NBFs cooperate

and can be regulated by signals from the TMDs and enhance the kinetics of the switch[180].

III. Constant contact. This proposal suggests that NBDs dimerization is driven by ATP and NBDs dissociation by ADP, and although two molecules of ATP initiate dimerization, only one is undergoing hydrolysis[181].

The basic catalytic cycle of ABC transporters is very similar and consists of a series of steps:

1. Binding of the substrate-binding proteins for importers or the direct binding of substrates for exporters to the TMDs.
2. Binding of two molecules of ATP to the NBDs.
3. Dimerization of the NBDs.
4. Switching off the TMDs between the in- and outward or out-and inward-facing conformations.
5. ATP hydrolysis.
6. P, ADP, and substrate release.
7. NBD dissociation to reset the transporter.

Mutations in ABC transporters are associated with several diseases, defects in ABCA1 are related to Tangier disease, ABCA4 with Stargardt disease[182], ABCC7 involved in cystic fibrosis[183], ABCD1 in adrenoleukodystrophy[184], ABCB2/3 in immune deficiency[184], and a few ABCs in cancer, as some examples. The best-studied ABC transporters are ABCB1 or P-glycoprotein, ABCC1, and ABCG2. These proteins are highly expressed in the cell surface of tumor cells; it has been shown to be related with chemoresistance being possible targets for cancer treatment[184]. ABC transporters efflux drugs, decreasing the amount of drug inside the cell[184] consistently.

a. ABCC proteins

ABCC subfamily of proteins is also known as multidrug resistance-associated proteins (MRPs). 12 transporters with different functions form it; some of them are ion transport, cell surface receptor, or toxin secretion activities.

ABCC1, ABCC2, and ABCC3 transport drug conjugates of glutathione (GSH) and other organic anions. ABCC4, ABCC5, ABCC11, and ABCC12 channels are

smaller than the rest of the subfamily, they lack an amino-terminal domain, but it is not essential for transport function[185]. ABCC4 and ABCC5 develop resistance to nucleosides by transporting PMEA and purine analogs[186]. ABCC7 is a cystic fibrosis transmembrane conductance regulator (CFTR) protein; it has a role in exocrine secretions as a chloride ion channel; it has been shown that mutations in CFTR can cause cystic fibrosis[187]. ABCC8 and ABCC9 bind sulfonylurea and regulate potassium channels involved in modulating insulin secretion; it is known that mutations in ABCC8 underlie a genetic disorder called persistent hyperinsuline-mic hypoglycemia of infancy[188].

Table 3. Characteristics of ABCC subfamily proteins. GSH: glutathione; LTC_4: leukotriene; PGA: phosphoglyceric acid; GSSG: glutathione disulfide; $E_2$17ßG: 7ßestradiol 17-ß-D-glucuronide; cGMP: cyclic guanosine monophosphate; cAMP: cyclic adenosine monophosphate; DHEAS: *D*ehydroepiandrosterone; PMEA: p-Methoxyethylamphetamine

Protein	Expression	Function	Physiological substrates	Drug substrates	Inhibitors
ABCC1	Lung, testis, PBMC	Drug resistance	GSH, LTC_4, sulfated bile acids, bilirubin, PGA, GSSG, GSH-conjugate, $E_2$17ßG	Doxorubicin, vincristine, etoposide, MTX, camptothecin, CPT-11, SN-38, cyclophosphamide	Probenecid, sulfinpyrazone, indomethacin, verapamil, quercetin, genistein, cyclosporine, PAK-104P, steroid analogs, MK-571, ONO-1078, sulphonylurea, glibenclamide
ABCC2	Liver, kidney, intestine, brain	Organic anion efflux	LTC, GSH, GSSG, bilirubin-conjugates, LTD, LTE	Conjugates, cisplatin, etoposide, vinca alkaloids, anthracyclines, cam-tothecins, MTX, lopinavir, olmesartan	MK-571, furosemide
ABCC3	Lung, intestine, liver, placenta, adrenal gland	Drug resistance	LTC, cholate, glycocholate, taurocholate, $E_2$17ßG	Etoposide, teniposide, dinitrophenyl S-glutathione, acetaminophen	Etoposide, MTX

				glucuronide, vincristine, MTX	
ABCC4	Prostate, kidneys	Nucleoside transport	cGMP, cAMP, DHEAS, PGE, $E_2$17ßG, PMEA, purine analogs	MTX, 6-thioguanine, PMEA, 6-mercaptopurine, topotecan	MK-571, celecoxib, rofecoxib, diclofenac
ABCC5	Ubiquitous	Nucleoside transport	cGMP, cAMP, PMEA, purine analogs	6-Mercaptopurine, 6-thioguanine, PMEA, heavy metals, S-(2,4-dinitrophenyl)glutathione	Probenecid, sulfinpyrazone, benzbromarone, MK-571
ABCC6	Kidney, liver			LTC_4, N-ethylmaleimide S-glutathione, dinitrophenol glutathione, etoposide, doxorubicin, cisplatin, daunorubicin	Indomethacin, probenecid, benzbromarone
ABCC7	Exocrine tissue	Chloride ion channel	$E_2$17ßG		
ABCC8	Pancreas	Sulfonylurea receptor	Insulin		
ABCC9	Heart, muscle	Sulfonylurea receptor	Insulin		
ABCC10	Low in all tissues		$E_2$17ßG		
ABCC11	Breast, testis		cGMP, cAMP, LTC_4, DHEAS	5-FU, PMEA, MTX, bile acids	
ABCC12	Testis, brain, skeletal muscle, ovary				

1. ABCC3 (MRP3)

1,527 amino acids form ABCC3, which is the most similar to ABCC1, with 58% homology, and its topology resembles MRP1[189–191]. Even its similarity to ABCC1, substrates of these proteins are very different; ABCC3 is mainly implicated in the transport of bile acids and bile salt metabolism in normal conditions.

ABCC3 protein is expressed in liver, small intestine, and adrenal glands[192]. It is located in the basolateral membrane of polarized epithelial cells[193].

ABCC3 expression in the liver is highly inducible; it is upregulated during cholestasis and in the absence of ABCC2. It is induced when the canalicular route for the secretion of organic anions is blocked[194], and it could come via receptor-mediated pathways as nuclear receptors[195].

The induction of ABCC3 also happens in other organs like colon, in which is typical of bile salts[196].

ABCC3 has been related to chemotherapy resistance in different cancer types. ABCC3 expression levels are elevated in high-grade breast cancers and particularly after treatment in patients. Chemotherapeutical agents promote the expression of different ABCC transporters, and its downregulation leads to drug accumulation inside of the tumor cells and finally in cell death[197]. The role of these transporters seems to be drug efflux of compounds like paclitaxel, cisplatin, or doxorubicin[198].

Besides breast cancer, in lung cancer, has been seen an upregulation in ABCC3 transcription levels, and in normal conditions in lungs, there is no expression of ABCC3. Even more, its expression could confer malignant phenotypes in patients[199].

In PDAC patient samples also occurs the overexpression of ABCC3, and it is associated with lower survival. Some studies demonstrated the importance of ABCC3 in tumor progression[200] and its implication in multidrug resistance by secreting some drugs as 5-fluorouracil[201]. For these reasons, ABCC3 is an important biomarker for PDAC progression, prognosis, and treatment response in patients.

7. Animal models in cancer

New diagnostic and therapeutic methods are necessary to reduce cancer incidence and deaths. Positive experiments *in vitro* need to be extrapolated to animal models before starting clinical trials. Several animals have similar characteristics to humans; cancer research can help us look for genetic basis, mutations, and new diagnostic methods and test new compounds[202]. For diagnostic and therapeutic purposes, mouse models are the most used in cancer research.

I. Implantation models

By these models, different types of tumor can be implanted in mice, and we can distinguish into three types: allografts in which tumor cells are derived and implanted from the same species; xenografts when species are different, and the receptor is immunosuppressed; orthotopic when tumor cells are implanted into the same organ and heterotopic when it is implanted in the non-original site[203].

The advances in genetics modifications, like CRISPR/Cas9 technology, have permitted to modify tumor cells in different ways and see how they behave in mouse models. Especially, the case of gene knockouts (KO) has generated a wide window of explorations in diagnosis and treatments in cancer[204].

Patient-derived xenograft (PDX) models are also known as “avatar”; they show biological consistency with the original tumor. They are also phenotypically stable at the histological, genomic, transcriptomic, and genomic levels for several rounds of transplantation[205]. They are very used to predict drug responses due to their precedence from a human patient. Even PDX models lack natural stroma; it is replaced by murine stromal elements, mimicking original tumors in patients[206].

II. Genetically engineered models (GEMs)

Developments in GEM models have helped us understand the molecular pathways implicated in tumor initiation, progression, and metastasis, among others. GEM models should carry the same mutations that in human tumors, and

they have to be introduced in their endogenous loci. Genetic mutation should be silenced during embryonic and early postnatal development (except for inherited or pediatric tumors). They have to occur in a limited number of cells in target tissues or selected cell types. These models have helped to recreate human tumors and understand biological features about them[203].

8. Cancer Stem Cells (CSCs)

Cancer stem cells (CSCs) are a subpopulation of cancer cells that owns stem cells characteristics such as self-renewal, heterogenicity, and multi-lineage differentiation[207]. These cells have also been related to tumor initiation, progression, angiogenesis, and metastasis[208].

This concept was mentioned in the 19th century; some scientists such as Virchow, Cohnheim, or Müller described that tumor development was produced by some "embryonic rests" in the body and were the origin of cancer[209].

CSCs have been seen to be drivers of tumor establishment and growth and usually correlated to aggressiveness, heterogenicity, and therapy resistance (figure Intro. 8)[208]. As they can survive treatments, they can cause tumor relapses.

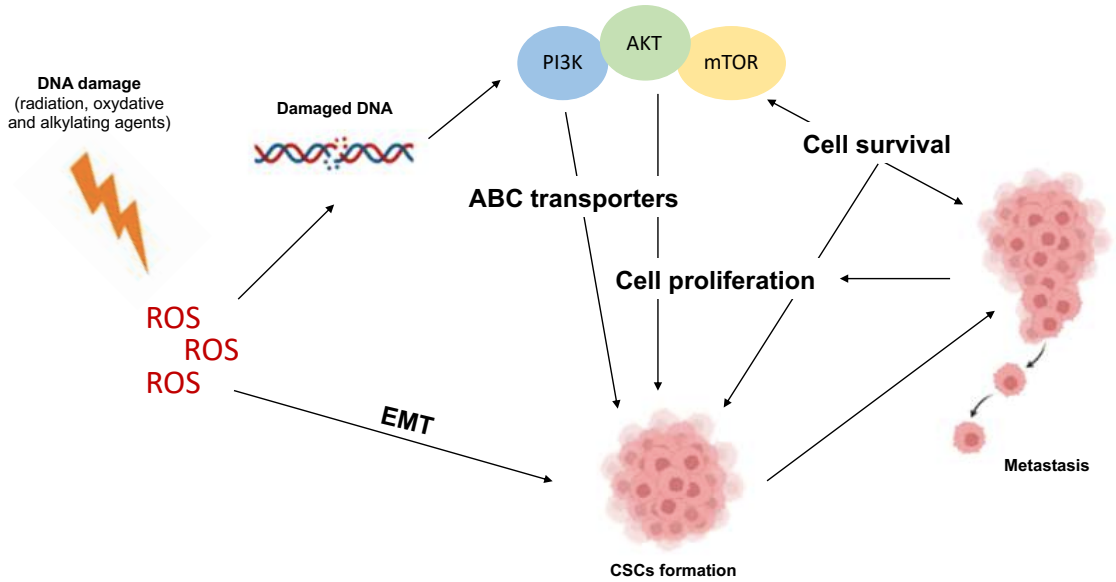

Figure Intro. 8. CSCs as potential target and biomarkers in cancer. *Adapted from Sudhalkar, N. et al.*[210]

I. CSCs implication in tumor initiation

Tumor initiation consists of several transformations; basically, cells lose their ability to control cell processes; this can be caused by accumulated mutations and leads to an increase in proliferation. Gene mutations consist in overexpression of oncogenes and inactivation of tumor suppressors, among others[211].

The CSC theory is based on the ability of a subset of cells with stem cell properties to initiate and progress cancer. This idea started in 1994 when the Dick group discovered that stem cells present in acute myeloid leukemia (AML) patients could induce AML after transplantation in mice[212]. From these studies, these stem cells have become called CSCs, and they have been found in other cancer types as colorectal, glioblastoma, breast, lung, or pancreas[208].

CSCs origination is hypothesized from normal stem cells or progenitor cells that under stimulus get out of their quiescent state and become activated to proliferate[213]. Isolated CSCs have the ability to repopulate parental tumors; this evidence supports the idea of the implication of CSCs in tumor initiation[214].

II. CSCs in tumor progression

There is an important crosstalk between CSCs located in the niche and the tumor microenvironment in tumor development. Because of the increasing size of the tumor, there are hypoxic areas, and new vasculature elements are needed to supply all tumor parts. To maintain CSCs characteristics, they communicate with tumor microenvironment to maintain an appropriate atmosphere for them, especially under stressful circumstances like during and after therapeutic treatment, which contributes to a heterogeneous phenotype of cells[215].

a. Drug resistance

Resistance to chemotherapy remains a challenge in most cancer types; here, CSCs play an important role. These cells do not respond to drugs and are enriched in stem cell properties, which leads to metastasis[216]. The communication and modification with tumor microenvironment contribute to this

CSCs resistance. Still, these cells are resistant themselves due to the high expression of anti-apoptotic proteins[217], enhanced aldehyde dehydrogenase (ALDH) activity[218], and ABC transporters[219,220].

All these properties of CSCs are significantly related to chemotherapy resistance; due to that, conventional cancer treatments are ineffective against CSCs by their innate resistance.

III. CSCs in metastasis

Metastasis is the process by which a secondary tumor grows in other organ tissue from the initial tumor; it involves several events grouped in local invasion, intravasation into the blood and lymphatic system, localization, and dissemination in the new site[15]. CSCs could start metastasis in the primary tumor, this cell population is called metastatic stem cells (MetSC), and they have a stem-like gene expression signature. However, the destination of the metastatic CSCs is still unknown as well as possible markers[221,222]. MetSCs are referred to disseminated tumor cells that are capable of reinitiating macroscopic tumor growth in a distant tissue. This definition does not depend on their phenotypic characteristics and is independent of other cell functional features. MetSCs are probably present in the initial tumor, and they are responsible for the metastatic process[223].

IV. CSCs biomarkers

Most markers used to identify CSCs are also found in resident stem cells, human embryonic stem cells (hESC), and adult tissues. Thus, it is important to combine the use of several biomarkers to identify and isolate CSCs.

a. CD44

CD44 is a transmembrane glycoprotein, also known as P-glycoprotein, that participates in cell-cell interaction, migration, and cell adhesion. It is highly expressed in several cancer types and promotes migration and invasion in the metastasis process by interacting with extracellular matrix ligands[224]. It is used

as a biomarker for CSCs in solid and hematological tumors; it is especially predictive and used in breast cancer[225]. Additionally, it could be applied as a diagnostic, therapeutic, and prognosis marker.

b. CD133

CD133 is a transmembrane glycoprotein, also known as prominin-1; it is localized in cellular protrusions ad its function is unclear; it is proposed to be organizing cell membrane topology[226]. This biomarker in normal conditions is only expressed in hESC and rarely in normal tissue cells[227]. It has been related to stemness as being implicated in tumorigenicity and its high ability to form spheroids[228]. CD133 is used as a biomarker in different cancer types, such as brain, lung, liver, ovarian, prostate, and pancreatic cancers[229].

c. EpCAM

Epithelial cell adhesion molecule (EpCAM) is a transmembrane glycoprotein involved in cell-cell adhesion. It is involved in cell signaling, migration, proliferation, and differentiation[230]. It is expressed on the basolateral side of epithelial cells in normal conditions, but in cancer cells, it is expressed all around the cell surface[231]. EpCAM is expressed in CSCs of most solid tumors, and it is related to worse prognosis[232].

d. SOX2

SOX2 is a transcription factor, also known as Sex-determining region Y (SRY)-related HMG-box 2, which function is the maintenance of undifferentiated phenotype in cells[233]. SOX2 is capable of inducing pluripotency in somatic cells with characteristics of embryonic stem cells[234]. SOX2 positive cell populations also express high CD133 levels and exhibit enhanced tumorigenicity, relating SOX2 to CSCs in colorectal, skin, and pancreatic cancer[235–237]. In CSCs, it confers chemotherapy resistance and favors the formation of tumor spheroids[238].

e. OCT-3/4 and NANOG

Octamer-binding transcription factor 3/4 (Oct3/4), also known as POU domain class 5 transcription factor 1 (POU5F1), is a transcription factor that regulates pluripotency in stem cells. This gene is upregulated in many cancers, especially lung cancer, and provides self-renewal, migration, resistance, and metastasis[239].

Nanog is a homeobox domain transcription factor that maintains pluripotency in hESCs[240]. It has been related to invasion, metastasis, and drug resistance in many cancer types. NANOG is a biomarker in liver and breast cancer[241].

V. CSCs metabolism

In normal conditions, cells obtain energy through the tricarboxylic cycle (TCA) coupled to oxidative phosphorylation (OXPHOS). Cancer cells (non-CSCs) have a higher proliferation.

They need to adapt their metabolism; thus, they produce ATP mainly by glycolysis, even in conditions with sufficient oxygen; this event is called Warburg effect or aerobic glycolysis[242]. They explode glycolysis because ATP is produced 100 times faster than by OXPHOS, even that ATP production rates are lower[243]. To be more productive, they overexpress glucose transporters and enzymes implicated in the cycle[244,245].

a. Increased glycolytic rates

Stem cells mostly use glycolysis to obtain ATP[246]; it has been demonstrated that CSCs have higher glycolytic rates than cancer cells[247]. Even more, glucose transporters, glucose uptakes, enzymes expression, lactate production, and ATP content are upregulated and increased in CSCs[248]. Then, CSCs switch from OXPHOS to glycolysis; this change has been linked to stemness characteristics in CSCs in cancers like breast, bladder, and hematological ones[249,250].

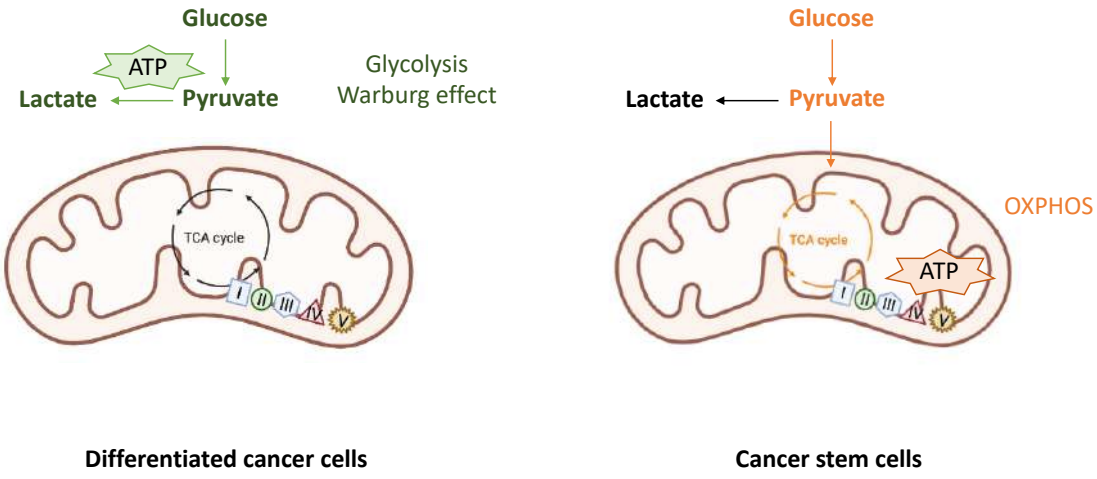

Figure Intro. 9. Cellular metabolism of CSCs and non-CSCs. Modified from *Sancho et al. 2015*

b. CSCs rely on OXPHOS to generate energy

On the contrary, CSC from other cancer types such as AML, glioblastoma, melanoma, and PDAC are supported by OXPHOS to obtain ATP[251,252]. Instead of glucose uptake, CSCs are sustained by mitochondrial fatty acid oxidation (FAO) to produce ATP and NADPH[253,254]. Fatty acids can be obtained by tumor cells by lipid uptake or de novo lipogenesis and activate intracellular lipolysis to mobilize FA stocks (figure Intro. 9)[134].

There are shreds of evidence that PDAC CSCs are mainly OXPHOS; it has been demonstrated that the mitochondrial biogenesis regulator and transcription coactivator peroxisome proliferator-activator 1 alpha (PPARGC1A; PCG-1α) is essential in CD133 positive CSCs population[251].

CSCs are located in the niche of tumors; this OXPHOS metabolism favors the cells in these extreme conditions; additionally, lactate secreted by non-CSCs cancer cells will serve to start mitochondrial metabolism[255]. Elevated lipid synthesis correlates with CSCs survival and characteristics.

Besides, mitochondria are involved in several pathways in apoptosis by releasing cytochrome C, metabolites production, and reactive oxygen species (ROS) secretion[256].

c. Metabolic plasticity of CSCs

Several CSCs populations with different metabolism are found; it is possible that CSCs can adapt their metabolism depending on the microenvironment conditions[242]. These changes could also help CSCs during tumor invasion, metastasis, and drug resistance[257]. In cases where OXPHOS is blocked, CSCs have been shown to be able to switch to a glycolytic metabolism[258]. Actually, hypoxic conditions and glucose concentration changes induce CSCs enrichment by increasing hypoxia-inducible factor 1 alpha (HIF1α)[259].

REFERENCES

1. Bauer GE. Islets of Langerhans. *Histology*. 1983:774-787. doi:10.1007/978-1-349-06859-3_22
2. de Oliveira RF, ChangetheRest change the, WHITE O, et al. Enhanced Reader.pdf. *Nature*. 2018;388:539-547.
3. Kulenović A, Sarač-Hadžihalilović A. Blood vessels distribution in body and tail of pancreas - A comparative study of age related variation. *Bosnian Journal of Basic Medical Sciences*. 2010;10(2):89-93. doi:10.17305/bjbms.2010.2700
4. Pancreas: Anatomy, functions, blood supply, innervation | Kenhub. https://www.kenhub.com/en/library/anatomy/the-pancreas. Accessed June 23, 2021.
5. Siegel RL, Miller KD, Jemal A. Cancer statistics, 2017. *CA: A Cancer Journal for Clinicians*. 2017;67(1):7-30. doi:10.3322/caac.21387
6. Bray F, Ferlay J, Soerjomataram I, Siegel RL, Torre LA, Jemal A. Global cancer statistics 2018: GLOBOCAN estimates of incidence and mortality worldwide for 36 cancers in 185 countries. *CA: A Cancer Journal for Clinicians*. 2018;68(6):394-424. doi:10.3322/caac.21492
7. Soweid AM. The borderline resectable and locally advanced pancreatic ductal adenocarcinoma: Definition. *Endoscopic Ultrasound*. 2017;6(9):S76-S78. doi:10.4103/eus.eus_66_17
8. Klöppel G. Neuroendocrine Neoplasms: Dichotomy, Origin and Classifications. *Visceral Medicine*. 2017;33(5):324-330. doi:10.1159/000481390
9. Hidalgo M, Cascinu S, Kleeff J, et al. Addressing the challenges of pancreatic cancer: Future directions for improving outcomes. *Pancreatology*. 2015;15(1):8-18. doi:10.1016/j.pan.2014.10.001
10. Li C, Morvaridi S, Lam G, et al. MSP-RON signaling is activated in the transition from pancreatic intraepithelial neoplasia (PanIn) to pancreatic ductal adenocarcinoma (PDAC). *Frontiers in Physiology*. 2019;10(FEB):1-8. doi:10.3389/fphys.2019.00147
11. Ferreira RMM, Sancho R, Messal HA, et al. Duct- and Acinar-Derived Pancreatic Ductal Adenocarcinomas Show Distinct Tumor Progression and Marker Expression. *Cell Reports*. 2017;21(4):966-978. doi:10.1016/j.celrep.2017.09.093
12. Shen R, Wang Q, Cheng S, et al. The biological features of PanIN initiated from oncogenic Kras mutation in genetically engineered mouse models. *Cancer Letters*. 2013;339(1):135-143. doi:10.1016/j.canlet.2013.07.010
13. Sipos B, Frank S, Gress T, Hahn S, Klöppel G. Pancreatic intraepithelial neoplasia revisited and updated. *Pancreatology*. 2009;9(1-2):45-54. doi:10.1159/000178874
14. Koorstra J-BM, Feldmann G, Habbe N, Maitra A. Morphogenesis of pancreatic cancer: role of pancreatic intraepithelial neoplasia (PanINs). *Langenbeck's Archives of Surgery 2008 393:4*. 2008;393(4):561-570. doi:10.1007/S00423-008-0282-X
15. Li F, Tiede B, Massagué J, Kang Y. Beyond tumorigenesis: Cancer stem cells in metastasis. *Cell Research*. 2007;17(1):3-14. doi:10.1038/sj.cr.7310118
16. Matsuda Y, Ishiwata T, Izumiyama-Shimomura N, et al. Gradual Telomere Shortening and Increasing Chromosomal Instability among PanIN Grades and Normal Ductal Epithelia with and without Cancer in the Pancreas. Lustig AJ, ed. *PLOS ONE*. 2015;10(2):e0117575. doi:10.1371/journal.pone.0117575
17. Caldas C, Hahn SA, Da-Costa LT, et al. Frequent somatic mutations and homozygous deletions of the p16 (MTS1) gene in pancreatic adenocarcinoma. *Nature Genetics*. 1994;8(1):27-32. doi:10.1038/ng0994-27
18. Yonezawa S, Higashi M, Yamada N, Goto M. Precursor Lesions of Pancreatic Cancer. *Gut and Liver*. 2008;2(3):137-154. doi:10.5009/gnl.2008.2.3.137
19. Schutte M, Hruban RH, Hedrick L, et al. DPC4 Gene in Various Tumor Types. *Cancer Research*. 1996;56(11).
20. Biankin A V., Biankin SA, Kench JG, et al. Aberrant p16INK4A and DPC4/Smad4 expression in intraductal papillary mucinous tumours of the pancreas is associated with invasive ductal adenocarcinoma. *Gut*. 2002;50(6):861-868. doi:10.1136/gut.50.6.861
21. Kern SE. p53: Tumor suppression through control of the cell cycle. *Gastroenterology*. 1994;106(6):1708-1711. doi:10.5555/uri:pii:0016508594904316
22. Yachida S, Lacobuzio-Donahue CA. The pathology and genetics of metastatic pancreatic cancer. *Archives of Pathology and Laboratory Medicine*. 2009;133(3):413-422. doi:10.5858/133.3.413

23. Dangi-Garimella S, Krantz SB, Shields MA, Grippo PJ, Munshi HG. *Epithelial-Mesenchymal Transition and Pancreatic Cancer Progression*. Transworld Research Network; 2012. http://www.ncbi.nlm.nih.gov/pubmed/22876384. Accessed October 27, 2021.
24. Hosein AN, Brekken RA, Maitra A. Pancreatic cancer stroma: an update on therapeutic targeting strategies. *Nature Reviews Gastroenterology and Hepatology*. 2020;17(8):487-505. doi:10.1038/s41575-020-0300-1
25. Lucenteforte E, La Vecchia C, Silverman D, et al. Alcohol consumption and pancreatic cancer: A pooled analysis in the International Pancreatic Cancer Case-Control Consortium (PanC4). *Annals of Oncology*. 2012;23(2):374-382. doi:10.1093/annonc/mdr120
26. Weiss W, Benarde MA. The temporal relation between cigarette smoking and pancreatic cancer. *American Journal of Public Health*. 1983;73(12):1403-1404. doi:10.2105/AJPH.73.12.1403
27. Berrington De Gonzalez A, Sweetland S, Spencer E. A meta-analysis of obesity and the risk of pancreatic cancer. *British Journal of Cancer*. 2003;89(3):519-523. doi:10.1038/sj.bjc.6601140
28. Kirkegård J, Mortensen FV, Cronin-Fenton D. Chronic Pancreatitis and Pancreatic Cancer Risk: A Systematic Review and Meta-analysis. *American Journal of Gastroenterology*. 2017;112(9):1366-1372. doi:10.1038/ajg.2017.218
29. Schima W, Böhm G, Rösch CS, Klaus A, Függer R, Kopf H. Mass-forming pancreatitis versus pancreatic ductal adenocarcinoma: CT and MR imaging for differentiation. *Cancer Imaging*. 2020;20(1):52. doi:10.1186/s40644-020-00324-z
30. Australian Sepsis Network. Signs and Symptoms of Sepsis. 2021:1-7. https://www.australiansepsisnetwork.net.au/community-awareness/signs-symptoms-sepsis.
31. Signs and symptoms of pancreatic cancer - Pancreatic Cancer UK. https://www.pancreaticcancer.org.uk/information/signs-and-symptoms-of-pancreatic-cancer/. Accessed March 8, 2021.
32. Toft J, Hadden WJ, Laurence JM, et al. Imaging modalities in the diagnosis of pancreatic adenocarcinoma: A systematic review and meta-analysis of sensitivity, specificity and diagnostic accuracy. *European journal of radiology*. 2017;92:17-23. doi:10.1016/j.ejrad.2017.04.009
33. Imaging diagnosis and staging of pancreatic ductal adenocarcinoma: a comprehensive review | Enhanced Reader. moz-extension://45f875a8-6053-bb49-8ae3-c81ebe7900d0/enhanced-reader.html?openApp&pdf=https%3A%2F%2Finsightsimaging.springeropen.com%2Ftrack%2Fpdf%2F10.1186%2Fs13244-020-00861-y.pdf. Accessed May 26, 2021.
34. Walters DM, Lapar DJ, De Lange EE, et al. Pancreas-protocol imaging at a high-volume center leads to improved preoperative staging of pancreatic ductal adenocarcinoma. *Annals of Surgical Oncology*. 2011;18(10):2764-2771. doi:10.1245/s10434-011-1693-4
35. Ishigami K, Yoshimitsu K, Irie H, et al. Diagnostic value of the delayed phase image for iso-attenuating pancreatic carcinomas in the pancreatic parenchymal phase on multidetector computed tomography. *European Journal of Radiology*. 2009;69(1):139-146. doi:10.1016/j.ejrad.2007.09.012
36. González-Gómez R, Pazo-Cid RA, Sarría L, Morcillo MÁ, Schuhmacher AJ. Diagnosis of Pancreatic Ductal Adenocarcinoma by Immuno-Positron Emission Tomography. *Journal of Clinical Medicine*. 2021;10(6):1151. doi:10.3390/jcm10061151
37. Brennan DDD, Zamboni GA, Raptopoulos VD, Kruskal JB. Comprehensive preoperative assessment of pancreatic adenocarcinoma with 64-section volumetric CT. *Radiographics*. 2007;27(6):1653-1666. doi:10.1148/rg.276075034
38. Shrikhande S V., Arya S, Barreto SG, et al. Borderline respectable pancreatic tumors: Is there a need for further refinement of this stage? *Hepatobiliary and Pancreatic Diseases International*. 2011;10(3):319-324. doi:10.1016/S1499-3872(11)60053-2
39. Al-Hawary MM, Francis IR, Chari ST, et al. Pancreatic ductal adenocarcinoma radiology reporting template: Consensus statement of the society of abdominal radiology and the American pancreatic association. *Gastroenterology*. 2014;146(1). doi:10.1053/j.gastro.2013.11.004
40. Therville N, Arcucci S, Vertut A, et al. Experimental pancreatic cancer develops in soft pancreas: Novel leads for an individualized diagnosis by ultrafast elasticity imaging. *Theranostics*. 2019;9(22):6369-6379. doi:10.7150/thno.34066

41. Miura F, Takada T, Amano H, Yoshida M, Furui S, Takeshita K. Diagnosis of pancreatic cancer. *HPB*. 2006;8(5):337-342. doi:10.1080/13651820500540949
42. Cherry SR, Jones T, Karp JS, Qi J, Moses WW, Badawi RD. Total-body PET: Maximizing sensitivity to create new opportunities for clinical research and patient care. *Journal of Nuclear Medicine*. 2018;59(1):3-12. doi:10.2967/jnumed.116.184028
43. Morone M, Bali MA, Tunariu N, et al. Whole-body MRI: Current applications in oncology. *American Journal of Roentgenology*. 2017;209(6):W336-W349. doi:10.2214/AJR.17.17984
44. Hickethier T, Mammadov K, Baeßler B, et al. Whole-body computed tomography in trauma patients: optimization of the patient scanning position significantly shortens examination time while maintaining diagnostic image quality. *Therapeutics and Clinical Risk Management*. 2018;Volume 14:849-859. doi:10.2147/TCRM.S162074
45. Canto MI, Harinck F, Hruban RH, et al. International cancer of the pancreas screening (CAPS) consortium summit on the management of patients with increased risk for familial pancreatic cancer. *Gut*. 2013;62(3):339-347. doi:10.1136/gutjnl-2012-303108
46. Elsherif SB, Virarkar M, Javadi S, Ibarra-Rovira JJ, Tamm EP, Bhosale PR. Pancreatitis and PDAC: association and differentiation. *Abdominal Radiology*. 2020;45(5):1324-1337. doi:10.1007/s00261-019-02292-w
47. Vonlaufen A, Joshi S, Qu C, et al. Pancreatic stellate cells: Partners in crime with pancreatic cancer cells. *Cancer Research*. 2008;68(7):2085-2093. doi:10.1158/0008-5472.CAN-07-2477
48. Vonlaufen A, Phillips PA, Xu Z, et al. Pancreatic stellate cells and pancreatic cancer cells: An unholy alliance. *Cancer Research*. 2008;68(19):7707-7710. doi:10.1158/0008-5472.CAN-08-1132
49. Erkan M, Hausmann S, Michalski CW, et al. How fibrosis influences imaging and surgical decisions in pancreatic cancer. *Frontiers in Physiology*. 2012;3 OCT(October):1-16. doi:10.3389/fphys.2012.00389
50. Jailkhani N, Ingram JR, Rashidian M, et al. Erratum: Noninvasive imaging of tumor progression, metastasis, and fibrosis using a nanobody targeting the extracellular matrix(Proceedings of the National Academy of Sciences of the United States of America(2019)116 (14181–14190) Doi:10.1073/pnas.1817442. *Proceedings of the National Academy of Sciences of the United States of America*. 2019;116(37):18745. doi:10.1073/pnas.1913962116
51. Best MG, Sol N, Kooi I, et al. RNA-Seq of Tumor-Educated Platelets Enables Blood-Based Pan-Cancer, Multiclass, and Molecular Pathway Cancer Diagnostics. *Cancer Cell*. 2015;28(5):666-676. doi:10.1016/j.ccell.2015.09.018
52. Adams DL, Martin SS, Alpaugh RK, et al. Circulating giant macrophages as a potential biomarker of solid tumors. *Proceedings of the National Academy of Sciences of the United States of America*. 2014;111(9):3514-3519. doi:10.1073/pnas.1320198111
53. Qi ZH, Xu HX, Zhang SR, et al. The significance of liquid biopsy in pancreatic cancer. *Journal of Cancer*. 2018;9(18):3417-3426. doi:10.7150/jca.24591
54. Sefrioui D, Blanchard F, Toure E, et al. Diagnostic value of CA19.9, circulating tumour DNA and circulating tumour cells in patients with solid pancreatic tumours. *British Journal of Cancer*. 2017;117(7):1017-1025. doi:10.1038/bjc.2017.250
55. Yin L, Pu N, Thompson E, Miao Y, Wolfgang C, Yu J. Improved assessment of response status in patients with pancreatic cancer treated with neoadjuvant therapy using somatic mutations and liquid biopsy analysis. *Clinical Cancer Research*. 2021;27(3):740-748. doi:10.1158/1078-0432.CCR-20-1746
56. National Institute of Biomedical Imaging and Bioengineering |. https://www.nibib.nih.gov/. Accessed June 17, 2021.
57. Hickethier T, Mammadov K, Baeßler B, et al. Whole-body computed tomography in trauma patients: Optimization of the patient scanning position significantly shortens examination time while maintaining diagnostic image quality. *Therapeutics and Clinical Risk Management*. 2018;14:849-859. doi:10.2147/TCRM.S162074
58. Kramer-Marek G, Gore J, Korc M. Molecular imaging in pancreatic cancer - A roadmap for therapeutic decisions. *Cancer Letters*. 2013;341(2):132-138. doi:10.1016/j.canlet.2013.08.008
59. Zhang L, Sanagapalli S, Stoita A. Challenges in diagnosis of pancreatic cancer. *World Journal of Gastroenterology*. 2018;24(19):2047-2060. doi:10.3748/wjg.v24.i19.2047
60. Ahn SS, Kim MJ, Choi JY, Hong HS, Chung YE, Lim JS. Indicative findings of pancreatic

cancer in prediagnostic CT. *European Radiology*. 2009;19(10):2448-2455. doi:10.1007/s00330-009-1422-6
61. Kim SS, Choi GC, Jou SS. Pancreas ductal adenocarcinoma and its mimics: Review of cross-sectional imaging findings for differential diagnosis. *Journal of the Belgian Society of Radiology*. 2018;102(1). doi:10.5334/JBSR.1644
62. Horton KM, Fishman EK. Multidetector CT angiography of pancreatic carcinoma: Part I, evaluation of arterial involvement. *American Journal of Roentgenology*. 2002;178(4):827-831. doi:10.2214/ajr.178.4.1780827
63. Treadwell JR, Zafar HM, Mitchell MD, Tipton K, Teitelbaum U, Jue J. Imaging Tests for the Diagnosis and Staging of Pancreatic Adenocarcinoma: A Meta-Analysis. *Pancreas*. 2016;45(6):789-795. doi:10.1097/MPA.0000000000000524
64. Raman SP, Horton KM, Fishman EK. Multimodality imaging of pancreatic cancer-computed tomography, magnetic resonance imaging, and positron emission tomography. *Cancer Journal (United States)*. 2012;18(6):511-522. doi:10.1097/PPO.0b013e318274a461
65. Sandrasegaran K, Lin C, Akisik FM, Tann M. State-of-the-art pancreatic MRI. *American Journal of Roentgenology*. 2010;195(1):42-53. doi:10.2214/AJR.10.4421
66. Adamek HE, Albert J, Breer H, Weitz M, Schilling D, Riemann JF. Pancreatic cancer detection with magnetic resonance cholangiopancreatography and endoscopic retrograde cholangiopancreatography: A prospective controlled study. *Lancet*. 2000;356(9225):190-193. doi:10.1016/S0140-6736(00)02479-X
67. Fattahi R, Balci NC, Perman WH, et al. Pancreatic diffusion-weighted imaging (DWI): Comparison between mass-forming focal pancreatitis (FP), pancreatic cancer (PC), and normal pancreas. *Journal of Magnetic Resonance Imaging*. 2009;29(2):350-356. doi:10.1002/jmri.21651
68. Tummers WS, Willmann JK, Bonsing BA, Vahrmeijer AL, Gambhir SS, Swijnenburg RJ. Advances in diagnostic and intraoperative molecular imaging of pancreatic cancer. *Pancreas*. 2018;47(6):675-689. doi:10.1097/MPA.0000000000001075
69. Lall CG, Howard TJ, Skandarajah A, DeWitt JM, Aisen AM, Sandrasegaran K. New Concepts in Staging and Treatment of Locally Advanced Pancreatic Head Cancer. *American Journal of Roentgenology*. 2007;189(5):1044-1050. doi:10.2214/AJR.07.2131
70. Kaissis G, Braren R. Pancreatic cancer detection and characterization—state of the art cross-sectional imaging and imaging data analysis. *Translational Gastroenterology and Hepatology*. 2019;4(May). doi:10.21037/tgh.2019.05.04
71. Berger A. Positron emission tomography. *British Medical Journal*. 2003;326(7404):1449. doi:10.1136/bmj.326.7404.1449
72. Shukla A, Kumar U. Positron emission tomography: An overview. *Journal of Medical Physics*. 2006;31(1):13-21. doi:10.4103/0971-6203.25665
73. Tamm EP, Balachandran A, Bhosale PR, et al. Imaging of Pancreatic Adenocarcinoma: Update on Staging/Resectability. *Radiologic Clinics of North America*. 2012;50(3):407-428. doi:10.1016/j.rcl.2012.03.008
74. Rijkers AP, Valkema R, Duivenvoorden HJ, Van Eijck CHJ. Usefulness of F-18-fluorodeoxyglucose positron emission tomography to confirm suspected pancreatic cancer: A meta-analysis. *European Journal of Surgical Oncology*. 2014;40(7):794-804. doi:10.1016/j.ejso.2014.03.016
75. Lee JW, Kang CM, Choi HJ, et al. Prognostic value of metabolic tumor volume and total lesion glycolysis on preoperative18f-fdg pet/ct in patients with pancreatic cancer. *Journal of Nuclear Medicine*. 2014;55(6):898-904. doi:10.2967/jnumed.113.131847
76. Yokoyama Y, Nagino M, Hiromatsu T, et al. Intense PET signal in the degenerative necrosis superimposed on chronic pancreatitis. *Pancreas*. 2005;31(2):192-194. doi:10.1097/01.mpa.0000168226.36085.58
77. Enhanced Reader. moz-extension://45f875a8-6053-bb49-8ae3-c81ebe7900d0/enhanced-reader.html?openApp&pdf=http%3A%2F%2Feknygos.lsmuni.lt%2Fspringer%2F360%2F1-117.pdf. Accessed October 18, 2021.
78. Lee JW, O JH, Choi M, Choi JY. Impact of F-18 Fluorodeoxyglucose PET/CT and PET/MRI on Initial Staging and Changes in Management of Pancreatic Ductal Adenocarcinoma: A Systemic Review and Meta-Analysis. *Diagnostics*. 2020;10(11):952. doi:10.3390/diagnostics10110952
79. Arnone A, Laudicella R, Caobelli F, et al. Clinical Impact of 18F-FDG PET/CT in the

Diagnostic Workup of Pancreatic Ductal Adenocarcinoma: A Systematic Review. *Diagnostics*. 2020;10(12):1042. doi:10.3390/diagnostics10121042
80. Eisenhauer EA, Therasse P, Bogaerts J, et al. New response evaluation criteria in solid tumours: Revised RECIST guideline (version 1.1). *European Journal of Cancer*. 2009;45(2):228-247. doi:10.1016/j.ejca.2008.10.026
81. van Dongen GAMS, Visser GWM, Lub-de Hooge MN, de Vries EG, Perk LR. Immuno-PET: A Navigator in Monoclonal Antibody Development and Applications. *The Oncologist*. 2007;12(12):1379-1389. doi:10.1634/theoncologist.12-12-1379
82. Romero E, Martínez A, Oteo M, Ibañez M, Santos M, Morcillo MÁ. Development and long-term evaluation of a new 68Ge/68Ga generator based on nano-SnO2 for PET imaging. *Scientific Reports*. 2020;10(1):12756. doi:10.1038/s41598-020-69659-8
83. Kerdjoudj R, Pniok M, Alliot C, et al. Scandium(III) complexes of monophosphorus acid DOTA analogues: A thermodynamic and radiolabelling study with 44Sc from cyclotron and from a 44Ti/44Sc generator. *Dalton Transactions*. 2016;45(4):1398-1409. doi:10.1039/c5dt04084a
84. Neophytou CM, Panagi M, Stylianopoulos T, Papageorgis P. The role of tumor microenvironment in cancer metastasis: Molecular mechanisms and therapeutic opportunities. *Cancers*. 2021;13(9). doi:10.3390/cancers13092053
85. Wu AM. Engineered antibodies for molecular imaging of cancer. *Methods*. 2014;65(1):139-147. doi:10.1016/j.ymeth.2013.09.015
86. Reddy S, Robinson MK. Immuno-Positron Emission Tomography in Cancer Models. *Seminars in Nuclear Medicine*. 2010;40(3):182-189. doi:10.1053/j.semnuclmed.2009.12.004
87. Designer genes: recombinant antibody fragments for biological imaging. https://www.researchgate.net/publication/12221651_Designer_genes_recombinant_antibody_fragments_for_biological_imaging. Accessed July 21, 2021.
88. Adams GP, Schier R, McCall AM, et al. Prolonged in vivo tumour retention of a human diabody targeting the extracellular domain of human HER2/neu. *British Journal of Cancer*. 1998;77(9):1405-1412. doi:10.1038/bjc.1998.233
89. Kircher MF, De La Zerda A, Jokerst J V., et al. A brain tumor molecular imaging strategy using a new triple-modality MRI-photoacoustic-Raman nanoparticle. *Nature Medicine*. 2012;18(5):829-834. doi:10.1038/nm.2721
90. Franc BL, Acton PD, Mari C, Hasegaway BH. Small-animal SPECT and SPECT/CT: Important tools for preclinical investigation. *Journal of Nuclear Medicine*. 2008;49(10):1651-1663. doi:10.2967/jnumed.108.055442
91. Smith DL, Breeman WAP, Sims-Mourtada J. The untapped potential of Gallium 68-PET: The next wave of 68Ga-agents. *Applied Radiation and Isotopes*. 2013;76:14-23. doi:10.1016/j.apradiso.2012.10.014
92. Romero E, Morcillo MA. Inorganic oxides with potential application in the preparation of a 68Ge/68Ga generator system. *Applied Radiation and Isotopes*. 2017;119:28-35. doi:10.1016/j.apradiso.2016.10.014
93. de Lucas AG, Schuhmacher AJ, Oteo M, et al. Targeting MT1-MMP as an ImmunoPET-Based Strategy for Imaging Gliomas. Ulasov I, ed. *PLOS ONE*. 2016;11(7):e0158634. doi:10.1371/journal.pone.0158634
94. Duchemin C, Guertin A, Haddad F, Michel N, Métivier V. Production of scandium-44m and scandium-44g with deuterons on calcium-44: cross section measurements and production yield calculations. *Physics in Medicine and Biology*. 2015;60(17):6847-6864. doi:10.1088/0031-9155/60/17/6847
95. Hackert T. Surgery for Pancreatic Cancer after neoadjuvant treatment. *Annals of Gastroenterological Surgery*. 2018;2(6):413-418. doi:10.1002/ags3.12203
96. *Available Online at NCCN.Org/Patients NCCN GUIDELINES FOR PATIENTS ® 2021*.
97. Isaji S, Mizuno S, Windsor JA, et al. International consensus on definition and criteria of borderline resectable pancreatic ductal adenocarcinoma 2017. *Pancreatology*. 2018;18(1):2-11. doi:10.1016/j.pan.2017.11.011
98. Anger F, Döring A, van Dam J, et al. Impact of Borderline Resectability in Pancreatic Head Cancer on Patient Survival: Biology Matters According to the New International Consensus Criteria. *Annals of Surgical Oncology*. 2021;28(4):2325-2336. doi:10.1245/s10434-020-09100-6
99. Lu DSK, Reber HA, Krasny RM, Kadell BM, Sayre J. Local staging of pancreatic cancer: Criteria for unresectability of major vessels as revealed by pancreatic-phase, thin-section

helical CT. *American Journal of Roentgenology*. 1997;168(6):1439-1443. doi:10.2214/ajr.168.6.9168704
100. Khorana AA, McKernin SE, Berlin J, et al. Potentially curable pancreatic adenocarcinoma: ASCO clinical practice guideline update. *Journal of Clinical Oncology*. 2019;37(23):2082-2088. doi:10.1200/JCO.19.00946
101. Khorana AA, Mangu PB, Berlin J, et al. Potentially curable pancreatic cancer: American society of clinical oncology clinical practice guideline. *Journal of Clinical Oncology*. 2016;34(21):2541-2556. doi:10.1200/JCO.2016.67.5553
102. Cid-Arregui A, Juarez V. Perspectives in the treatment of pancreatic adenocarcinoma. *World Journal of Gastroenterology*. 2015;21(31):9297-9316. doi:10.3748/wjg.v21.i31.9297
103. Conroy T, Hammel P, Hebbar M, et al. FOLFIRINOX or Gemcitabine as Adjuvant Therapy for Pancreatic Cancer. *New England Journal of Medicine*. 2018;379(25):2395-2406. doi:10.1056/NEJMoa1809775
104. Pereira NP, Corrêa JR. Pancreatic cancer: treatment approaches and trends. *Journal of Cancer Metastasis and Treatment*. 2018;4(6):30. doi:10.20517/2394-4722.2018.13
105. Singh RR, O'Reilly EM. New Treatment Strategies for Metastatic Pancreatic Ductal Adenocarcinoma. *Drugs*. 2020;80(7):647-669. doi:10.1007/s40265-020-01304-0
106. Von Hoff DD, Ervin T, Arena FP, et al. Increased Survival in Pancreatic Cancer with nab-Paclitaxel plus Gemcitabine. *New England Journal of Medicine*. 2013;369(18):1691-1703. doi:10.1056/NEJMoa1304369
107. Conroy T, Desseigne F, Ychou M, et al. FOLFIRINOX versus Gemcitabine for Metastatic Pancreatic Cancer. *New England Journal of Medicine*. 2011;364(19):1817-1825. doi:10.1056/NEJMoa1011923
108. Gaitanis A, Staal S. Liposomal doxorubicin and nab-paclitaxel: nanoparticle cancer chemotherapy in current clinical use. *Methods in molecular biology (Clifton, NJ)*. 2010;624:385-392. doi:10.1007/978-1-60761-609-2_26
109. Perri G, Prakash L, Qiao W, et al. Response and Survival Associated with First-line FOLFIRINOX vs Gemcitabine and nab-Paclitaxel Chemotherapy for Localized Pancreatic Ductal Adenocarcinoma. *JAMA Surgery*. 2020;155(9):832-839. doi:10.1001/jamasurg.2020.2286
110. Hendifar AE, Blais EM, Ng C, et al. Comprehensive analysis of KRAS variants in patients (pts) with pancreatic cancer (PDAC): Clinical/molecular correlations and real-world outcomes across standard therapies. *Journal of Clinical Oncology*. 2020;38(15_suppl):4641-4641. doi:10.1200/jco.2020.38.15_suppl.4641
111. Fakih M, O'Neil B, Price TJ, et al. Phase 1 study evaluating the safety, tolerability, pharmacokinetics (PK), and efficacy of AMG 510, a novel small molecule KRAS G12C inhibitor, in advanced solid tumors. . *Journal of Clinical Oncology*. 2019;37(15_suppl):3003-3003. doi:10.1200/jco.2019.37.15_suppl.3003
112. Hallin J, Engstrom LD, Hargi L, et al. The KRASG12C inhibitor MRTX849 provides insight toward therapeutic susceptibility of KRAS-mutant cancers in mouse models and patients. *Cancer Discovery*. 2020;10(1):54-71. doi:10.1158/2159-8290.CD-19-1167
113. Golan T, Khvalevsky EZ, Hubert A, et al. RNAi therapy targeting KRAS in combination with chemotherapy for locally advanced pancreatic cancer patients. *Oncotarget*. 2015;6(27):24560-24570. doi:10.18632/oncotarget.4183
114. Van Cutsem E, Hidalgo M, Canon JL, et al. Phase I/II trial of pimasertib plus gemcitabine in patients with metastatic pancreatic cancer. *International Journal of Cancer*. 2018;143(8):2053-2064. doi:10.1002/ijc.31603
115. Ko AH, Bekaii-Saab T, Van Ziffle J, et al. A multicenter, open-label phase II clinical trial of combined MEK plus EGFR inhibition for chemotherapy-refractory advanced pancreatic adenocarcinoma. *Clinical Cancer Research*. 2016;22(1):61-68. doi:10.1158/1078-0432.CCR-15-0979
116. Chung V, McDonough S, Philip PA, et al. Effect of selumetinib and MK-2206 vs oxaliplatin and fluorouracil in patients with metastatic pancreatic cancer after prior therapy: SWOG S1115 study randomized clinical trial. *JAMA Oncology*. 2017;3(4):516-522. doi:10.1001/jamaoncol.2016.5383
117. Kinsey CG, Camolotto SA, Boespflug AM, et al. Protective autophagy elicited by RAF→MEK→ERK inhibition suggests a treatment strategy for RAS-driven cancers. *Nature Medicine*. 2019;25(4):620-627. doi:10.1038/s41591-019-0367-9
118. Drilon A, Laetsch TW, Kummar S, et al. Efficacy of Larotrectinib in TRK Fusion–Positive

Cancers in Adults and Children . *New England Journal of Medicine*. 2018;378(8):731-739. doi:10.1056/nejmoa1714448
119. Russo M, Misale S, Wei G, et al. Acquired resistance to the TRK inhibitor entrectinib in colorectal cancer. *Cancer Discovery*. 2016;6(1):36-44. doi:10.1158/2159-8290.CD-15-0940
120. B Raf Kinase - an overview | ScienceDirect Topics. https://www.sciencedirect.com/topics/neuroscience/b-raf-kinase. Accessed July 7, 2021.
121. Jackson SP, Bartek J. The DNA-damage response in human biology and disease. *Nature*. 2009;461(7267):1071-1078. doi:10.1038/nature08467
122. Helleday T, Petermann E, Lundin C, Hodgson B, Sharma RA. DNA repair pathways as targets for cancer therapy. *Nature Reviews Cancer*. 2008;8(3):193-204. doi:10.1038/nrc2342
123. Lowery MA, Kelsen DP, Capanu M, et al. Phase II trial of veliparib in patients with previously treated BRCA-mutated pancreas ductal adenocarcinoma. *European Journal of Cancer*. 2018;89:19-26. doi:10.1016/j.ejca.2017.11.004
124. Kaufman B, Shapira-Frommer R, Schmutzler RK, et al. Olaparib monotherapy in patients with advanced cancer and a germline BRCA1/2 mutation. *Journal of Clinical Oncology*. 2015;33(3):244-250. doi:10.1200/JCO.2014.56.2728
125. Javle M, Shacham-Shmueli E, Xiao L, et al. Olaparib monotherapy for previously treated pancreatic cancer with DNA damage repair genetic alterations other than germline BRCA variants findings from 2 phase 2 nonrandomized clinical trials. *JAMA Oncology*. 2021;7(5):693-699. doi:10.1001/jamaoncol.2021.0006
126. Weber AM, Ryan AJ. ATM and ATR as therapeutic targets in cancer. *Pharmacology and Therapeutics*. 2015;149:124-138. doi:10.1016/j.pharmthera.2014.12.001
127. Huen MSY, Chen J. The DNA damage response pathways: At the crossroad of protein modifications. *Cell Research*. 2008;18(1):8-16. doi:10.1038/cr.2007.109
128. Harper JW, Elledge SJ. The DNA Damage Response: Ten Years After. *Molecular Cell*. 2007;28(5):739-745. doi:10.1016/j.molcel.2007.11.015
129. Russell R, Perkhofer L, Liebau S, et al. Loss of ATM accelerates pancreatic cancer formation and epithelial-mesenchymal transition. *Nature Communications*. 2015;6. doi:10.1038/ncomms8677
130. Abida W, Bang YJ, Carter L, et al. Abstract A094: Phase I modular study of AZD0156, a first-in-class oral selective inhibitor of ataxia telangiectasia mutated protein kinase (ATM), in combination with olaparib (AToM Study, Module 1). In: *Molecular Cancer Therapeutics*. Vol 17. American Association for Cancer Research (AACR); 2018:A094-A094. doi:10.1158/1535-7163.targ-17-a094
131. Wallez Y, Dunlop CR, Johnson TI, et al. The ATR inhibitor AZD6738 synergizes with gemcitabine in vitro and in vivo to induce pancreatic ductal adenocarcinoma regression. *Molecular Cancer Therapeutics*. 2018;17(8):1670-1682. doi:10.1158/1535-7163.MCT-18-0010
132. López-Contreras AJ, Fernandez-Capetillo O. The ATR barrier to replication-born DNA damage. *DNA Repair*. 2010;9(12):1249-1255. doi:10.1016/j.dnarep.2010.09.012
133. Li JT, Wang YP, Yin M, Lei QY. Metabolism remodeling in pancreatic ductal adenocarcinoma. *Cell Stress*. 2019;3(12):361-368. doi:10.15698/cst2019.12.205
134. Espiau-Romera P, Courtois S, Parejo-Alonso B, Sancho P. Molecular and Metabolic Subtypes Correspondence for Pancreatic Ductal Adenocarcinoma Classification. *Journal of Clinical Medicine*. 2020;9(12):4128. doi:10.3390/jcm9124128
135. Tricarboxylic acid cycle | biochemistry | Britannica. https://www.britannica.com/science/tricarboxylic-acid-cycle. Accessed September 7, 2021.
136. Devimistat (CPI-613) | ≥99%(HPLC) | Selleck | Dehydrogenase inhibitor. https://www.selleckchem.com/products/cpi-613.html. Accessed September 7, 2021.
137. Alistar A, Morris BB, Desnoyer R, et al. Safety and tolerability of the first-in-class agent CPI-613 in combination with modified FOLFIRINOX in patients with metastatic pancreatic cancer: a single-centre, open-label, dose-escalation, phase 1 trial. *The Lancet Oncology*. 2017;18(6):770-778. doi:10.1016/S1470-2045(17)30314-5
138. Yang A, Kimmelman AC. Inhibition of autophagy attenuates pancreatic cancer growth independent of TP53/TRP53 status. *Autophagy*. 2014;10(9):1683-1684. doi:10.1158/2159-8290.CD-14-0362
139. Zeh HJ, Bahary N, Boone BA, et al. A randomized phase II preoperative study of

autophagy inhibition with high-dose hydroxychloroquine and gemcitabine/nab-paclitaxel in pancreatic cancer patients. *Clinical Cancer Research*. 2020;26(13):3126-3134. doi:10.1158/1078-0432.CCR-19-4042

140. Zinger A, Koren L, Adir O, et al. Collagenase Nanoparticles Enhance the Penetration of Drugs into Pancreatic Tumors. *ACS Nano*. 2019;13(10):11008-11021. doi:10.1021/acsnano.9b02395
141. Hingorani SR, Zheng L, Bullock AJ, et al. HALO 202: Randomized phase II Study of PEGPH20 Plus Nab-Paclitaxel/Gemcitabine Versus Nab-Paclitaxel/Gemcitabine in Patients With Untreated, Metastatic Pancreatic Ductal Adenocarcinoma. In: *Journal of Clinical Oncology*. Vol 36. American Society of Clinical Oncology; 2018:359-366. doi:10.1200/JCO.2017.74.9564
142. Ramanathan RK, McDonough S, Philip PA, et al. A phase IB/II randomized study of mFOLFIRINOX (mFFOX) + pegylated recombinant human hyaluronidase (PEGPH20) versus mFFOX alone in patients with good performance status metastatic pancreatic adenocarcinoma (mPC): SWOG S1313 (NCT #01959139). *Journal of Clinical Oncology*. 2018;36(4_suppl):208-208. doi:10.1200/jco.2018.36.4_suppl.208
143. Tempero M, Oh D, Macarulla T, et al. Ibrutinib in combination with nab-paclitaxel and gemcitabine as first-line treatment for patients with metastatic pancreatic adenocarcinoma: results from the phase 3 RESOLVE study. *Annals of Oncology*. 2019;30:iv126. doi:10.1093/annonc/mdz154.001
144. Fan JQ, Wang MF, Chen HL, Shang D, Das JK, Song J. Current advances and outlooks in immunotherapy for pancreatic ductal adenocarcinoma. *Molecular Cancer*. 2020;19(1):1-22. doi:10.1186/s12943-020-01151-3
145. Panchal K, Sahoo RK, Gupta U, Chaurasiya A. Role of targeted immunotherapy for pancreatic ductal adenocarcinoma (PDAC) treatment: An overview. *International Immunopharmacology*. 2021;95. doi:10.1016/j.intimp.2021.107508
146. O'Hara MH, O'Reilly EM, Varadhachary G, et al. CD40 agonistic monoclonal antibody APX005M (sotigalimab) and chemotherapy, with or without nivolumab, for the treatment of metastatic pancreatic adenocarcinoma: an open-label, multicentre, phase 1b study. *The Lancet Oncology*. 2021;22(1):118-131. doi:10.1016/S1470-2045(20)30532-5
147. Vonderheide RH. CD40 Agonist Antibodies in Cancer Immunotherapy. *Annual Review of Medicine*. 2020;71:47-58. doi:10.1146/annurev-med-062518-045435
148. Inés Vargas-rojas M, Jiménez-álvarez L, Ramírez G, et al. *REVISTA DEL INSTITUTO NACIONAL DE ENFERMEDADES RESPIRATORIAS PD-1 y Sus Ligandos Como Reguladores de La Respuesta Inmune*. Vol 21.; 2008. www.iner.gob.mx272www.medigraphic.com. Accessed September 7, 2021.
149. Pu N, Lou W, Yu J. PD-1 immunotherapy in pancreatic cancer: current status. *Journal of Pancreatology*. 2019;2(1):6-10. doi:10.1097/JP9.0000000000000010
150. Fernández-Ponce C, David Hernández-Martínez J, Silvera-Redondo C. Ctla-4, una molécula que inhibe la activación de los linfocitos T. 2006;22(2).
151. Kabacaoglu D, Ciecielski KJ, Ruess DA, Algül H. Immune checkpoint inhibition for pancreatic ductal adenocarcinoma: Current limitations and future options. *Frontiers in Immunology*. 2018;9(AUG):1. doi:10.3389/fimmu.2018.01878
152. Beatty GL, O'Hara MH, Lacey SF, et al. Activity of Mesothelin-Specific Chimeric Antigen Receptor T Cells Against Pancreatic Carcinoma Metastases in a Phase 1 Trial. *Gastroenterology*. 2018;155(1):29-32. doi:10.1053/j.gastro.2018.03.029
153. Le DT, Picozzi VJ, Ko AH, et al. Results from a phase IIb, randomized, multicenter study of GVAX pancreas and CRS-207 compared with chemotherapy in adults with previously treated metastatic pancreatic adenocarcinoma (ECLIPSE study). *Clinical Cancer Research*. 2019;25(18):5493-5502. doi:10.1158/1078-0432.CCR-18-2992
154. Kunovsky L, Tesarikova P, Kala Z, et al. The Use of Biomarkers in Early Diagnostics of Pancreatic Cancer. *Canadian Journal of Gastroenterology and Hepatology*. 2018;2018. doi:10.1155/2018/5389820
155. Zhang WH, Wang WQ, Han X, et al. Advances on diagnostic biomarkers of pancreatic ductal adenocarcinoma: A systems biology perspective. *Computational and Structural Biotechnology Journal*. 2020;18:3606-3614. doi:10.1016/j.csbj.2020.11.018
156. Serum tumor markers - PubMed. https://pubmed.ncbi.nlm.nih.gov/14524394/. Accessed September 7, 2021.
157. Ray K. Erratum: Biomarkers for the early detection of PDAC. *Nature Reviews Gastroenterology and Hepatology*. 2017;14(9):505. doi:10.1038/nrgastro.2017.111

158. Goonetilleke KS, Siriwardena AK. Systematic review of carbohydrate antigen (CA 19-9) as a biochemical marker in the diagnosis of pancreatic cancer. *European Journal of Surgical Oncology*. 2007;33(3):266-270. doi:10.1016/j.ejso.2006.10.004
159. Hata S, Sakamoto Y, Yamamoto Y, et al. Prognostic impact of postoperative serum CA 19-9 levels in patients with resectable pancreatic cancer. *Annals of Surgical Oncology*. 2012;19(2):636-641. doi:10.1245/s10434-011-2020-9
160. Sugiura T, Uesaka K, Kanemoto H, et al. Serum CA19-9 is a significant predictor among preoperative parameters for early recurrence after resection of pancreatic adenocarcinoma. *Journal of Gastrointestinal Surgery*. 2012;16(5):977-985. doi:10.1007/s11605-012-1859-9
161. Kau SY, Shyr YM, Su CH, Wu CW, Lui WY. Diagnostic and prognostic values of CA 19-9 and CEA in periampullary cancers. *Journal of the American College of Surgeons*. 1999;188(4):415-420. doi:10.1016/S1072-7515(98)00326-3
162. Goggins M. Molecular markers of early pancreatic cancer. *Journal of Clinical Oncology*. 2005;23(20):4524-4531. doi:10.1200/JCO.2005.19.711
163. Swords DS, Firpo MA, Scaife CL, Mulvihill SJ. Biomarkers in pancreatic adenocarcinoma: Current perspectives. *OncoTargets and Therapy*. 2016;9:7459-7467. doi:10.2147/OTT.S100510
164. O'Brien J, Hayder H, Zayed Y, Peng C. Overview of microRNA biogenesis, mechanisms of actions, and circulation. *Frontiers in Endocrinology*. 2018;9(AUG):402. doi:10.3389/fendo.2018.00402
165. Lekchnov EA, Zaporozhchenko IA, Morozkin ES, Bryzgunova OE, Vlassov V V., Laktionov PP. Protocol for miRNA isolation from biofluids. *Analytical Biochemistry*. 2016;499:78-84. doi:10.1016/j.ab.2016.01.025
166. Noninvasive urinary miRNA biomarkers for early detection of pancreatic adenocarcinoma - PubMed. https://pubmed.ncbi.nlm.nih.gov/26807325/. Accessed September 8, 2021.
167. Bloomston M, Frankel WL, Petrocca F, et al. MicroRNA expression patterns to differentiate pancreatic adenocarcinoma from normal pancreas and chronic pancreatitis. *Journal of the American Medical Association*. 2007;297(17):1901-1908. doi:10.1001/jama.297.17.1901
168. Yang JY, Sun YW, Liu DJ, Zhang JF, Li J, Hua R. MicroRNAs in stool samples as potential screening biomarkers for pancreatic ductal adenocarcinoma cancer. *American Journal of Cancer Research*. 2014;4(6):663-673. /pmc/articles/PMC4266702/. Accessed September 8, 2021.
169. The MDR superfamily of genes and its biological implications - PubMed. https://pubmed.ncbi.nlm.nih.gov/7911445/. Accessed May 26, 2021.
170. Hyde SC, Emsley P, Hartshorn MJ, et al. Structural model of ATP-binding proteing associated with cystic fibrosis, multidrug resistance and bacterial transport. *Nature*. 1990;346(6282):362-365. doi:10.1038/346362a0
171. Bishop L, Agbayani R, Ambudkar S V., Maloney PC, Ferro-Luzzi Ames G. Reconstruction of a bacterial periplasmic permease in proteoliposomes and demonstration of ATP hydrolysis concomitant with transport. *Proceedings of the National Academy of Sciences of the United States of America*. 1989;86(18):6953-6957. doi:10.1073/pnas.86.18.6953
172. Dean M, Rzhetsky A, Allikmets R. The human ATP-binding cassette (ABC) transporter superfamily. *Genome Research*. 2001;11(7):1156-1166. doi:10.1101/gr.GR-1649R
173. Vasiliou V, Vasiliou K, Nebert DW. Human ATP-binding cassette (ABC) transporter family. *Human genomics*. 2009;3(3):281-290. doi:10.1186/1479-7364-3-3-281
174. Stergiopoulos I, Zwiers LH, De Waard MA. Secretion of natural and synthetic toxic compounds from filamentous fungi by membrane transporters of the ATP-binding cassette and major facilitator superfamily. In: *European Journal of Plant Pathology*. Vol 108. ; 2002:719-734. doi:10.1023/A:1020604716500
175. Tusnády GE, Bakos É, Váradi A, Sarkadi B. Membrane topology distinguishes a subfamily of the ATP-binding cassette (ABC) transporters. *FEBS Letters*. 1997;402(1):1-3. doi:10.1016/S0014-5793(96)01478-0
176. Dassa E. Natural history of ABC systems: Not only transporters. *Essays in Biochemistry*. 2011;50(1):19-42. doi:10.1042/BSE0500019
177. Wilkens S. Structure and mechanism of ABC transporters. 1000. doi:10.12703/P7-14
178. Balakrishnan L, Venter H, Shilling RA, Van Veen HW. Reversible transport by the ATP-binding cassette multidrug export pump LmrA: ATP synthesis at the expense of downhill ethidium uptake. *Journal of Biological Chemistry*. 2004;279(12):11273-11280. doi:10.1074/jbc.M308494200

179. Senior AE, Al-Shawi MK, Urbatsch IL. The catalytic cycle of P-glycoprotein. *FEBS Letters*. 1995;377(3):285-289. doi:10.1016/0014-5793(95)01345-8
180. Higgins CF, Linton KJ. The ATP switch model for ABC transporters. *Nature Structural and Molecular Biology*. 2004;11(10):918-926. doi:10.1038/nsmb836
181. Sauna ZE, Kim IW, Nandigama K, Kopp S, Chiba P, Ambudkar S V. Catalytic cycle of ATP hydrolysis by P-glycoprotein: Evidence for formation of the E·S reaction intermediate with ATP-γ-S, a nonhydrolyzable analogue of ATP. *Biochemistry*. 2007;46(48):13787-13799. doi:10.1021/bi701385t
182. Tarling EJ, Vallim TQ d. A, Edwards PA. Role of ABC transporters in lipid transport and human disease. *Trends in Endocrinology and Metabolism*. 2013;24(7):342-350. doi:10.1016/j.tem.2013.01.006
183. Cant N, Pollock N, Ford RC. CFTR structure and cystic fibrosis. *International Journal of Biochemistry and Cell Biology*. 2014;52:15-25. doi:10.1016/j.biocel.2014.02.004
184. Higgins CF. ABC Transporters: From microorganisms to man. *Annual Review of Cell Biology*. 1992;8:67-113. doi:10.1146/annurev.cb.08.110192.000435
185. Characterization of the amino-terminal regions in the human multidrug resistance protein (MRP1) - PubMed. https://pubmed.ncbi.nlm.nih.gov/11082039/. Accessed May 26, 2021.
186. Borst P, Evers R, Kool M, Wijnholds J. A family of drug transporters: The multidrug resistance-associated proteins. *Journal of the National Cancer Institute*. 2000;92(16):1295-1302. doi:10.1093/jnci/92.16.1295
187. Quinton PM. Physiological basis of cystic fibrosis: A historical perspective. *Physiological Reviews*. 1999;79(1 SUPPL. 1). doi:10.1152/physrev.1999.79.1.S3
188. Aguilar-Bryan L, Nichols CG, Wechsler SW, et al. Cloning of the β cell high-affinity sulfonylurea receptor: A regulator of insulin secretion. *Science*. 1995;268(5209):423-426. doi:10.1126/science.7716547
189. Belinsky MG, Bain LJ, Balsara BB, Testa JR, Kruh GD. Characterization of MOAT-C and MOAT-D, New Members of the MRP/cMOAT Subfamily of Transporter Proteins. *JNCI Journal of the National Cancer Institute*. 1998;90(22):1735-1741. doi:10.1093/jnci/90.22.1735
190. Kool M, Van Der Linden M, De Haas M, et al. MRP3, an organic anion transporter able to transport anti-cancer drugs. *Proceedings of the National Academy of Sciences of the United States of America*. 1999;96(12):6914-6919. doi:10.1073/pnas.96.12.6914
191. Kiuchi Y, Suzuki H, Hirohashi T, Tyson CA, Sugiyama Y. cDNA cloning and inducible expression of human multidrug resistance associated protein 3 (MRP3) [1]. *FEBS Letters*. 1998;433(1-2):149-152. doi:10.1016/S0014-5793(98)00899-0
192. König J, Rost D, Cui Y, Keppler D. Characterization of the human multidrug resistance protein isoform MRP3 localized to the basolateral hepatocyte membrane. *Hepatology*. 1999;29(4):1156-1163. doi:10.1002/hep.510290404
193. Scheffer GL, Kool M, de Haas M, et al. Tissue distribution and induction of human multidrug resistant protein 3. *Laboratory Investigation*. 2002;82(2):193-201. doi:10.1038/labinvest.3780411
194. Zollner G, Fickert P, Silbert D, et al. Adaptive changes in hepatobiliary transporter expression in primary biliary cirrhosis. *Journal of Hepatology*. 2003;38(6):717-727. doi:10.1016/S0168-8278(03)00096-5
195. Maher JM, Cheng X, Slitt AL, Dieter MZ, Klaassen CD. Induction of the multidrug resistance-associated protein family of transporters by chemical activators of receptor-mediated pathways in mouse liver. *Drug Metabolism and Disposition*. 2005;33(7):956-962. doi:10.1124/dmd.105.003798
196. Inokuchi A, Hinoshita E, Iwamoto Y, Kohno K, Kuwano M, Uchiumi T. Enhanced expression of the human multidrug resistance protein 3 by bile salt in human enterocytes: A transcriptional control of a plausible bile acid transporter. *Journal of Biological Chemistry*. 2001;276(50):46822-46829. doi:10.1074/jbc.M104612200
197. Balaji SA, Udupa N, Chamallamudi MR, Gupta V, Rangarajan A. Role of the drug transporter ABCC3 in breast cancer chemoresistance. *PLoS ONE*. 2016;11(5). doi:10.1371/journal.pone.0155013
198. O'Brien C, Cavet G, Pandita A, et al. Functional genomics identifies ABCC3 as a mediator of taxane resistance in HER2-amplified breast cancer. *Cancer Research*. 2008;68(13):5380-5389. doi:10.1158/0008-5472.CAN-08-0234
199. Zhao Y, Lu H, Yan A, et al. ABCC3 as a marker for multidrug resistance in non-small cell lung cancer. *Scientific Reports*. 2013;3(1):1-6. doi:10.1038/srep03120

200. Adamska A, Domenichini A, Capone E, et al. Pharmacological inhibition of ABCC3 slows tumour progression in animal models of pancreatic cancer. *Journal of Experimental and Clinical Cancer Research*. 2019;38(1):312. doi:10.1186/s13046-019-1308-7
201. Hagmann W, Jesnowski R, Faissner R, Guo C, Löhr JM. ATP-binding cassette C transporters in human pancreatic carcinoma cell lines. *Pancreatology*. 2009;9(1-2):136-144. doi:10.1159/000178884
202. Li Z, Zheng W, Wang H, et al. Application of animal models in cancer research: Recent progress and future prospects. *Cancer Management and Research*. 2021;13:2455-2475. doi:10.2147/CMAR.S302565
203. Schuhmacher AJ, Squatrito M. Animal Models in Glioblastoma: Use in Biology and Developing Therapeutic Strategies. *Current Cancer Research*. 2017:219-240. doi:10.1007/978-3-319-56820-1_9
204. Lambert LJ, Muzumdar MD, Rideout WM, Jacks T. Basic Mouse Methods for Clinician Researchers: Harnessing the Mouse for Biomedical Research. In: *Basic Science Methods for Clinical Researchers*. Elsevier Inc.; 2017:291-312. doi:10.1016/B978-0-12-803077-6.00014-X
205. Aparicio S, Hidalgo M, Kung AL. Examining the utility of patient-derived xenograft mouse models. *Nature Reviews Cancer*. 2015;15(5):311-316. doi:10.1038/nrc3944
206. Zhang X, Claerhout S, Prat A, et al. A renewable tissue resource of phenotypically stable, biologically and ethnically diverse, patient-derived human breast cancer xenograft models. *Cancer Research*. 2013;73(15):4885-4897. doi:10.1158/0008-5472.CAN-12-4081
207. Yu Z, Pestell TG, Lisanti MP, Pestell RG. Cancer stem cells. *International Journal of Biochemistry and Cell Biology*. 2012;44(12):2144-2151. doi:10.1016/j.biocel.2012.08.022
208. Walcher L, Kistenmacher AK, Suo H, et al. Cancer Stem Cells—Origins and Biomarkers: Perspectives for Targeted Personalized Therapies. *Frontiers in Immunology*. 2020;11:1280. doi:10.3389/fimmu.2020.01280
209. Capp JP. Cancer stem cells: From historical roots to a new perspective. *Journal of Oncology*. 2019;2019. doi:10.1155/2019/5189232
210. Yin J, Zhang J. Multidrug resistance-associated protein 1 (MRP1/ABCC1) polymorphism: From discovery to clinical application. *Journal of Central South University (Medical Sciences)*. 2011;36(10):927-938. doi:10.3969/j.issn.1672-7347.2011.10.002
211. Ayob AZ, Ramasamy TS. Cancer stem cells as key drivers of tumour progression. *Journal of Biomedical Science*. 2018;25(1):1-18. doi:10.1186/s12929-018-0426-4
212. Lapidot T, Sirard C, Vormoor J, et al. A cell initiating human acute myeloid leukaemia after transplantation into SCID mice. *Nature*. 1994;367(6464):645-648. doi:10.1038/367645a0
213. Sell S. On the stem cell origin of cancer. *American Journal of Pathology*. 2010;176(6):2584-2594. doi:10.2353/ajpath.2010.091064
214. Zhou BBS, Zhang H, Damelin M, Geles KG, Grindley JC, Dirks PB. Tumour-initiating cells: Challenges and opportunities for anticancer drug discovery. *Nature Reviews Drug Discovery*. 2009;8(10):806-823. doi:10.1038/nrd2137
215. Lau EYT, Ho NPY, Lee TKW. Cancer stem cells and their microenvironment: Biology and therapeutic implications. *Stem Cells International*. 2017;2017. doi:10.1155/2017/3714190
216. Chen X, Liao R, Li D, Sun J. Induced cancer stem cells generated by radiochemotherapy and their therapeutic implications. *Oncotarget*. 2017;8(10):17301-17312. doi:10.18632/oncotarget.14230
217. Wang Y, Scadden DT. Harnessing the apoptotic programs in cancer stem-like cells. *EMBO reports*. 2015;16(9):1084-1098. doi:10.15252/embr.201439675
218. Xu X, Chai S, Wang P, et al. Aldehyde dehydrogenases and cancer stem cells. *Cancer Letters*. 2015;369(1):50-57. doi:10.1016/j.canlet.2015.08.018
219. Xu F, Wang F, Yang T, Sheng Y, Zhong T, Chen Y. Differential drug resistance acquisition to doxorubicin and paclitaxel in breast cancer cells. *Cancer Cell International*. 2014;14(1):538. doi:10.1186/s12935-014-0142-4
220. Dean M. ABC transporters, drug resistance, and cancer stem cells. *Journal of Mammary Gland Biology and Neoplasia*. 2009;14(1):3-9. doi:10.1007/s10911-009-9109-9
221. Hermann PC, Huber SL, Herrler T, et al. Distinct Populations of Cancer Stem Cells Determine Tumor Growth and Metastatic Activity in Human Pancreatic Cancer. *Cell Stem Cell*. 2007;1(3):313-323. doi:10.1016/j.stem.2007.06.002
222. Hermann PC, Heeschen C. Metastatic cancer stem cells-Quo vadis? *Clinical Chemistry*. 2013;59(8):1268-1269. doi:10.1373/clinchem.2012.197830
223. Oskarsson T, Batlle E, Massagué J. Metastatic stem cells: Sources, niches, and vital

pathways. *Cell Stem Cell*. 2014;14(3):306-321. doi:10.1016/j.stem.2014.02.002
224. Senbanjo LT, Chellaiah MA. CD44: A multifunctional cell surface adhesion receptor is a regulator of progression and metastasis of cancer cells. *Frontiers in Cell and Developmental Biology*. 2017;5(MAR):18. doi:10.3389/fcell.2017.00018
225. Su J, Wu S, Wu H, Li L, Guo T. CD44 is functionally crucial for driving lung cancer stem cells metastasis through Wnt/β-catenin-FoxM1-Twist signaling. *Molecular Carcinogenesis*. 2016;55(12):1962-1973. doi:10.1002/mc.22443
226. Irollo E, Pirozzi G. CD133: To be or not to be, is this the real question? *American Journal of Translational Research*. 2013;5(6):563-581. www.ajtr.org. Accessed July 22, 2021.
227. Kim WT, Ryu CJ. Cancer stem cell surface markers on normal stem cells. *BMB Reports*. 2017;50(6):285-298. doi:10.5483/BMBRep.2017.50.6.039
228. Ren F, Sheng WQ, Du X. CD133: A cancer stem cells marker, is used in colorectal cancers. *World Journal of Gastroenterology*. 2013;19(17):2603-2611. doi:10.3748/wjg.v19.i17.2603
229. Glumac PM, LeBeau AM. The role of CD133 in cancer: a concise review. *Clinical and Translational Medicine*. 2018;7(1):18. doi:10.1186/s40169-018-0198-1
230. Huang L, Yang Y, Yang F, et al. Functions of EpCAM in physiological processes and diseases (Review). *International Journal of Molecular Medicine*. 2018;42(4):1771-1785. doi:10.3892/ijmm.2018.3764
231. Baizar M, Winter MJ, De Boer CJ, Litvinov S V. The biology of the 17-1A antigen (Ep-CAM). *Journal of Molecular Medicine*. 1999;77(10):699-712. doi:10.1007/s001099900038
232. Imrich S, Hachmeister M, Gires O. EpCAM and its potential role in tumor-initiating cells. *Cell Adhesion and Migration*. 2012;6(1):30-38. doi:10.4161/cam.18953
233. Takeda K, Mizushima T, Yokoyama Y, et al. Sox2 is associated with cancer stem-like properties in colorectal cancer. *Scientific Reports*. 2018;8(1). doi:10.1038/s41598-018-36251-0
234. Yu J, Vodyanik MA, Smuga-Otto K, et al. Induced pluripotent stem cell lines derived from human somatic cells. *Science*. 2007;318(5858):1917-1920. doi:10.1126/science.1151526
235. Herreros-Villanueva M, Zhang JS, Koenig A, et al. SOX2 promotes dedifferentiation and imparts stem cell-like features to pancreatic cancer cells. *Oncogenesis*. 2013;2(2):61. doi:10.1038/oncsis.2013.23
236. Takeda K, Mizushima T, Yokoyama Y, et al. Sox2 is associated with cancer stem-like properties in colorectal cancer. *Scientific Reports*. 2018;8(1). doi:10.1038/s41598-018-36251-0
237. Boumahdi S, Driessens G, Lapouge G, et al. SOX2 controls tumour initiation and cancer stem-cell functions in squamous-cell carcinoma. *Nature*. 2014;511(7508):246-250. doi:10.1038/nature13305
238. Lundberg I V., Edin S, Eklöf V, Öberg Å, Palmqvist R, Wikberg ML. SOX2 expression is associated with a cancer stem cell state and down-regulation of CDX2 in colorectal cancer. *BMC Cancer*. 2016;16(1). doi:10.1186/s12885-016-2509-5
239. Wang YJ, Herlyn M. The emerging roles of Oct4 in tumor-initiating cells. *American Journal of Physiology - Cell Physiology*. 2015;309(11):C709-C718. doi:10.1152/ajpcell.00212.2015
240. Heurtier V, Owens N, Gonzalez I, et al. The molecular logic of Nanog-induced self-renewal in mouse embryonic stem cells. *Nature Communications*. 2019;10(1):1-15. doi:10.1038/s41467-019-09041-z
241. Jeter CR, Yang T, Wang J, Chao HP, Tang DG. Concise Review: NANOG in Cancer Stem Cells and Tumor Development: An Update and Outstanding Questions. *Stem Cells*. 2015;33(8):2381-2390. doi:10.1002/stem.2007
242. Sancho P, Barneda D, Heeschen C. Hallmarks of cancer stem cell metabolism. *British Journal of Cancer*. 2016;114(12):1305-1312. doi:10.1038/bjc.2016.152
243. Martinez-Outschoorn UE, Peiris-Pagés M, Pestell RG, Sotgia F, Lisanti MP. Cancer metabolism: A therapeutic perspective. *Nature Reviews Clinical Oncology*. 2017;14(1):11-31. doi:10.1038/nrclinonc.2016.60
244. Garber K. Energy Deregulation: Licensing Tumors to Grow. *Science*. 2006;312(5777).
245. Barron CC, Bilan PJ, Tsakiridis T, Tsiani E. Facilitative glucose transporters: Implications for cancer detection, prognosis and treatment. *Metabolism: Clinical and Experimental*. 2016;65(2):124-139. doi:10.1016/j.metabol.2015.10.007
246. Jang H, Yang J, Lee E, Cheong JH. Metabolism in embryonic and cancer stemness. *Archives of Pharmacal Research*. 2015;38(3):381-388. doi:10.1007/s12272-015-0558-y

247. Ciavardelli D, Rossi C, Barcaroli D, et al. Breast cancer stem cells rely on fermentative glycolysis and are sensitive to 2-deoxyglucose treatment. *Cell Death and Disease*. 2014;5(7):e1336-e1336. doi:10.1038/cddis.2014.285
248. Liu PP, Liao J, Tang ZJ, et al. Metabolic regulation of cancer cell side population by glucose through activation of the Akt pathway. *Cell Death and Differentiation*. 2014;21(1):124-135. doi:10.1038/cdd.2013.131
249. Dong C, Yuan T, Wu Y, et al. Loss of FBP1 by snail-mediated repression provides metabolic advantages in basal-like breast cancer. *Cancer Cell*. 2013;23(3):316-331. doi:10.1016/j.ccr.2013.01.022
250. Semenza GL. Hypoxia-inducible factors: coupling glucose metabolism and redox regulation with induction of the breast cancer stem cell phenotype. *The EMBO Journal*. 2017;36(3):252-259. doi:10.15252/embj.201695204
251. Sancho P, Burgos-Ramos E, Tavera A, et al. MYC/PGC-1α balance determines the metabolic phenotype and plasticity of pancreatic cancer stem cells. *Cell Metabolism*. 2015;22(4):590-605. doi:10.1016/j.cmet.2015.08.015
252. Janiszewska M, Suvà ML, Riggi N, et al. Imp2 controls oxidative phosphorylation and is crucial for preservin glioblastoma cancer stem cells. *Genes and Development*. 2012;26(17):1926-1944. doi:10.1101/gad.188292.112
253. CAS Reference Linking. https://chemport.cas.org/cgi-bin/sdcgi?APP=ftslink&action=reflink&origin=npg&version=1.0&coi=1%3ACAS%3A528%3ADC%252BC3cXislWnug%253D%253D&md5=713230a9de6e021b27fb93f38b12d400. Accessed July 22, 2021.
254. Carracedo A, Weiss D, Leliaert AK, et al. A metabolic prosurvival role for PML in breast cancer. *Journal of Clinical Investigation*. 2012;122(9):3088-3100. doi:10.1172/JCI62129
255. Nakajima EC, Van Houten B. Metabolic symbiosis in cancer: Refocusing the Warburg lens. *Molecular Carcinogenesis*. 2013;52(5):329-337. doi:10.1002/mc.21863
256. Chandel NS. Mitochondria as signaling organelles. *BMC Biology*. 2014;12(1):34. doi:10.1186/1741-7007-12-34
257. Peiris-Pagès M, Martinez-Outschoorn UE, Pestell RG, Sotgia F, Lisanti MP, Warburg O. Cancer stem cell metabolism The cancer stem cell model: Omnis cellula e cellula. 2016. doi:10.1186/s13058-016-0712-6
258. Dong C, Yuan T, Wu Y, et al. Loss of FBP1 by snail-mediated repression provides metabolic advantages in basal-like breast cancer. *Cancer Cell*. 2013;23(3):316-331. doi:10.1016/j.ccr.2013.01.022
259. Conley SJ, Gheordunescu E, Kakarala P, et al. Antiangiogenic agents increase breast cancer stem cells via the generation of tumor hypoxia. *Proceedings of the National Academy of Sciences of the United States of America*. 2012;109(8):2784-2789. doi:10.1073/pnas.1018866109

HYPOTHESIS

HYPOTHESIS

PDAC is one of the tumors with higher mortality rates despite not being one of the most frequent. The patient survival rounds the five months in five years. The main problem of this cancer is the disease's diagnosis at late stages; normally, at these stages, the tumor has reached other organs and metastasized. The current diagnosis of PDAC is limited in detecting small lesions and metastasis; it also results in difficult to distinguish between benign and malignant tumors. Molecular imaging represents a novel approach in the specific detection of tumor biomarkers, besides constituting a non-invasive group of techniques. MRP proteins have been related to chemoresistance in different types of tumors, including PDAC.

ABCC3 has shown to be overexpressed in PDAC tumors and could constitute a new biomarker for PDAC diagnosis. As other members of MRP proteins, ABCC3 could be implicated in chemoresistance in PDAC tumors, being a prognostic biomarker. This transporter has also been related to stemness in other types of cancers; ABCC3 could be related to PDAC CSCs and play an important role in the chemoresistance of this stemness population. Immuno-PET is a non-invasive technique for cancer detection; it combines the specificity of Abs with the selectivity of the radionuclide. Nb-based probes conjugated with short-life radioisotopes could be used as a tool for molecular imaging by PET. This work aims to understand the role of ABCC3 in chemoresistance and stemness in PDAC and to generate and select Nbs that detect ABCC3 for its application in imaging and molecular therapy.

Hence, we have three main objectives for this work, structured in three chapters:

1. Study the role of ABCC3 in chemoresistance and stemness in PDAC tumors for the possible consideration of ABCC3 as a biomarker and prognostic marker for PDAC tumors.
2. Generation, selection, and validation *in vitro* of Nbs that target ABCC3.
3. Study possible applications of Nbs that target ABCC3 as imaging and therapeutic tools.

CHAPTER I / CAPÍTULO I

CHAPTER I.

ABCC3 as a biomarker of PDAC

INTRODUCTION

PDAC incidence is continuously increasing worldwide. Although the diagnosis techniques have been improved in selectivity and resolution, the mortality of patients is not decreasing. PDAC diagnosis and prognosis need to be improved, the patient symptoms are not specific of the disease, and the diagnosis occurs at late stages. And usually, around 50% of PDAC diagnosed patients present metastasis[1].

Once the tumor is diagnosed, the most efficient treatment is surgery. However, only less than 20% of patients have resectable tumors. Chemotherapy is not efficient in LA-PDAC patients due to heterogenicity and plasticity of tumor cells; there is a chemoresistance to actual treatments[2].

Tumor initiation, progression, and metastasis are associated with genetic alterations. These alterations in signaling pathways are related to increased proliferation, survival, chemoresistance, and invasion[3].

The identification of new biomarkers and targets for PDAC are needed for a better diagnosis and treatment. During the last years, the role of ABCC/MRP proteins has been investigated for their possible implication in the chemoresistance in PDAC tumors.

The most studied MRP transporters are ABCC1, which is nearly ubiquitously expressed, ABCC2 and ABCC3, mainly expressed in the liver. ABCC3 is homologous to ABCC1; they share around 60% of amino acid sequence[4].

ABCC proteins have been related to drug resistance in multiple cancer types, such as breast, bladder, lung, or brain tumors[5–7]. ABCC3 has been associated with tumor development in these tissues; in basal conditions, there is no expression of ABCC3 protein, and it is differentially expressed in that tumor cells[8,9]. Specifically, in PDAC, several ABCC proteins have been investigated to know the role of these transporters in the disease. ABCG2, ABCC1, ABCC3, ABCC4, and ABCC5 are present in PDAC samples from patients at mRNA levels. The expression of ABCG2, ABCC1, and ABCC4 do not correspond with tumor staging or grade. Meanwhile, ABCC3 and ABCC5 are overexpressed in pancreatic cancer tissues and correlate with tumor grading[10]. The differential expression of ABCC3 between healthy tissue and tumor point out ABCC3 as a

promising biomarker for PDAC diagnosis and could be targeted to increase chemotherapeutics effect.

Several substrates of ABCC3 have been described, including some anticancer drugs like vincristine, etoposide, cisplatin, or doxorubicin[11,12] but others as standard treatment in PDAC as gemcitabine or paclitaxel are still unknown.

In pancreatic tumors, ABCC1 has been shown to be implicated in gemcitabine resistance via SMAD2/3 and activating transcription factor 4 (ATF4)[13]. ABCC3 has been related to ATF4 in lung cancer[14], and due to its homology to ABCC1, it could be involved in the mechanism of gemcitabine resistance in PDAC.

ABCC3 has also been related to increased cell proliferation by signal transducer and activator of transcription 3 (STAT3) and HIF1-α pathway. Furthermore, the inhibition of ABCC3 decreases proliferation *in vitro* and *in vivo*, and stromal cells have been shown to overexpress ABCC3 protein in PDAC[15].

A small representation of PDAC tumors, around 1%, are cancer stem cells (CSCs). These cells are a specific type of stem cells; they are immortal tumor cells with self-renewal capacity and can differentiate into different lineages. More specifically, CSCs can be responsible for tumor growth (initiation, progression, and recurrence), metastasis, and chemoresistance[16]. CSCs are more resistant than non-CSCs to chemotherapy and radiotherapy treatments; it could be due to the higher expression of anti-apoptotic proteins, multidrug resistance genes, and ABC transporters[17,18]. Accurately, ABCC3 has been shown to be related to stemness genes in glioblastoma, breast cancer, and PDAC[19,20].

Cellular metabolism plays a key role in normal and tumor cells. The lack of vascularization characterizes PDAC tumors; it causes hypoxia and nutrient deprivation. In consequence, tumor cells suffer metabolic stress and reprogram their metabolism[21]. Hence, cancer cells explode anabolic pathways for nutrient acquisition, resulting in an increase of glycolytic, lipid, and amino acid biosynthesis and maintenance of redox homeostasis[22].

CSCs have different metabolic phenotypes compared to cancer cells. There are pieces of evidence that CSCs can dynamically change their metabolic state to favor glycolysis or mitochondrial metabolism[23].

OXPHOS supports PDAC CSCs to obtain ATP[24–26], instead of glucose uptake, they are sustained by mitochondrial fatty acid oxidation (FAO) to produce ATP and Nicotinamide adenine dinucleotide phosphate (NADPH)[27,28]. It has been demonstrated that the mitochondrial biogenesis regulator and transcription coactivator peroxisome proliferator-activator 1 alpha (PPARGC1A; PCG-1α) is essential in CD133 positive CSCs population[26].

CSCs have an increased metabolic rate, resulting in elevated reactive oxygen species (ROS) production; purposely, high levels of ROS are toxic for cells and can end in cell death. These ROS levels are neutralized or regulated by increased activity of antioxidant enzymes[29]. Thus, ROS levels have to be controlled inside the mitochondria in oxidative CSCs to maintain their stemness properties; this mechanism has been suggested to be done by antioxidant pathways.

Glutathione (L-γ-glutamyl-L-cysteinyl-glycine; GSH) is a well-known antioxidant cell component. Glutathione is synthesized in the cytosol, but it is transported to different organelles, such as mitochondria, and also to the extracellular space, especially under oxidative stress conditions. GSH concentrations in the cell are balanced between its synthesis and degradation. The main components of GSH secretion are MRP proteins; this ability to regulate GSH networks has been related to the stemness ability of CSCs[30,31].It has been pointed out that pancreatic CSCs have elevated glutathione content and that GSH inhibition decrease stemness ability, cell cycle arrest, and finally, induces apoptosis[32].

Gemcitabine treatment increases CSCs, but further induces ROS production and GSH accumulation; these results suggest that chemoresistance of CSCs depends on GSH content and oxidative metabolism[33]. Even more, CSCs population needs glutathione concentrations within the mitochondria for chemoresistance and self-renewal abilities[34].

We aim to understand the relation between ABCC3, chemoresistance, stemness, and metabolism. ABCC3 could be considered a new biomarker of PDAC, and even more, its expression could predict the response to chemotherapeutic agents.

OBJECTIVES

ABCC3 is differentially expressed in tumor cells compared to normal tissue and seems to be implicated in chemoresistance in PDAC.

The objective is to validate the role of ABCC3 as a biomarker and target for PDAC. By generating loss of function models in different established PDAC cell lines and patient-derived xenografts, we will study the role of ABCC3 in PDAC development, resistance to chemotherapy, and stemness.

Thus, the objectives of this chapter are:

1. Generation of ABCC3 loss of function models in different PDAC cell lines.
2. Determine the function of ABCC3 in chemoresistance to standard PDAC therapeutic agents.
3. Investigate the relation between stemness and ABCC3 in PDAC.
4. Explore CSCs metabolism and ABCC3 implication in PDAC.

MATERIAL AND METHODS

Mammalian cell culture

The human cell lines HEK-293T (GP2), CFPAC-1, IMIM-PC2, MIA PaCa-2, and Panc-1 were grown as monolayers in Dulbecco's modified Eagle's medium (DMEM, Sigma) supplemented with 10% Fetal Bovine Serum (FBS, Gibco) and 1% penicillin and streptomycin (P/S, Gibco) at 37ºC, 5% CO_2. AsPc-1 and BxPc-3 pancreatic cell lines were cultured in Roswell Park Memorial Institute medium (RPMI, Sigma) supplemented with 10% FBS and 1% P/S, at 37ºC, 5% CO_2. All cell lines were obtained from Mariano Barbacid's laboratory (CNIO). Patient-derived xenografts cell lines, PDX185, PDX354, PDX215, and PDX253, were a gift from Dr. Patricia Sancho and were cultured in RPMI supplemented with 10% FBS and 1% P/S.

CRISPR mediated ABCC3 knock-out

Loss of function models were generated by using CRISPR/Cas9 technology. The design of sgRNAs for ABCC3 and non-targeting (NT) as control was performed using Zhang Lab tools and cloned into pKLV-U6gRNA-EF(BbsI)-PGKpuro2ABFP. Plasmids used in this work are listed in table 2.

1 µg of sgRNAs forward and reverse were annealed by adding 1.25 µl of annealing buffer (Tris 0.5M pH 7.5/8; NaCl/MgCl 0.1M; in H_2O) followed by 10 min of incubation at 95ºC, 5 min at 65ºC and 15 min at 4ºC. Then, 5 µl of sgRNAs were phosphorylated with T4 Kinase (PNK, NZYTech) in PNK buffer (NZYTech) with 1mM ATP by 30 min incubation at 37ºC and 10 min at 70ºC for inactivation.

5 µg of pKLV-U6gRNA-EF(BbsI)-PGKpuro2ABFP were digested with BbsI (New England Biolabs, NEB) in 5 µl of 2.1 NEB buffer at 37ºC overnight (O/N). After the digestion, the linearized vector was dephosphorylated with Alkaline Phosphatase (Roche) for 15 min at 37ºC. The cut BbsI fragment was extracted from an agarose gel and purified with Qiagen Gel Extraction kit.

For the ligation of the vector and the insert, 50 ng of pKLV-U6gRNA-EF(BbsI)-PGKpuro2ABFP extracted from the gel, and 0.8 ng of phosphorylated and annealed sgRNAs were incubated with 1 µl of T4 DNA ligase (Roche) and 1X T4

DNA ligase buffer for 2 h at room temperature (RT). Then, the ligation was transformed into DH10B *E. coli* strain by heat shock. 5 µl of the ligation was added to 100 µl of DH10B competent bacteria. Then, cells were incubated for 5 min on ice, 150 s at 42ºC, and 2 min on ice. 900 µl of LB media was added, and bacteria were incubated for 1 h at 125 rpm at 37ºC. Finally, bacteria were plated in LB-Ampicillin plates. Individual colonies were grown in LB-Ampicillin, O/N at 37ºC and 150 rpm. DNA was extracted with Qiagen Plasmid DNA extraction kit and sequenced with U6-fw primer to corroborate the insertion of sgRNAs.

Table 1. Oligonucleotides

Oligonucleotides	Sequence (5'-3')	Reference
sgABCC3 #2 Forward	CACCGTACCTGCGGCACCATTGTCGGT	This work
sgABCC3 #2 Reverse	TAAAACCGACAATGGTGCCGCAGGTA	This work
sgRNA NT Forward	TTATGCCGATCGCGTCACATT	[35]
sgRNA NT Reverse	TGTGACGCGATCGGCATAATT	[35]
hABCC3 Forward	AGCTCGGCTCCAAGTTCTG	This work
hABCC3 Reverse	GACCCACAGGTAGATGCAGG	This work
U6-fw	GACTATCATATGCTTACCGT	Addgene

Table 2. Plasmids.

Plasmids	Genotypes and properties	Reference
pLentiCas9-Blast	(Ap^R), FUGW-H1 derivative; Cas9 expression	Addgene
pKLV-U6gRNA-EF(BbsI)-PGKpuro2ABFP	(Ap^R), pBluescript-derivative; gRNA expression	Addgene
pKLV-U6sgRNA$_{ABCC3\#2}$-EF(BbsI)-PGKpuro2ABFP	(Ap^R), pBluescript-derivative; sgRNAABCC3#2 expression	This work

pKLV-U6sgRNA$_{NT}$-EF(BbsI)-PGKpuro2ABFP	(Ap^R), pBluescript-derivative; sgRNAABCC3#2 expression	This work

Cell transfection and transductions

HEK-293T (GP2) cells at 80% of confluence were transfected using a final concentration of 9 µg/ml of poly(ethylenimine) (PEI, Polysciences), 3 µg of pMD2.G and 6 µg psPAX2 for viral production, 5 µg of pLentiCas9, and 500 µl optiMEM incubated for 15 min at RT and added dropwise to the cells. Media was changed after 16 h, viruses were collected 24 h later, and target cells were infected at a confluence of 60%. plentiCas9-Blast was transduced CFPAC-1, IMIM-PC2, and MIA PaCa-2, and cells were selected with 3, 6, and 7 µg/ml of blasticidin, respectively. pKLV-U6gRNA-EF(BbsI)-PGKpuro2ABFP with sgRNA for ABCC3 or NT were transduced into CFPAC-1-Cas9, IMIM-PC2-Cas9, and MIA PaCa-2-Cas9 and selected with 1, 1, and 2 µg/ml of puromycin, respectively.

Cells expressing Cas9 protein were corroborated by western blot with Cas9 (Santa Cruz) antibody and sgNT or sgABCC3 cells by flow cytometry with BFP or ABCC3 detection (MRP3-II9 clone).

pHIV-Luc-ZsGreen[36] was used to incorporate luciferase genes into the cell lines for their monitoring by luminescence signal. After the transduction, cells were sorted by FACS by detecting ZsGreen fluorescence.

Cell viability assay

Cells were seeded in 96-well plates (Corning) at a density of 1.5 x 10^3 cells per well in DMEM or RPMI. 24 hours later, compounds were added, gemcitabine from 300 nM and 1/3 dilutions; and abraxane from 100 µM and 1/10 dilutions. Compounds were left for 72 hours, and 10 µl of MTT1 was added (5 mg/ml thiazolyl blue tetrazolium bromide in PBS). 4 hours later, when crystals were formed, 100 µl of MTT2 (10%SDS-0.87%HCl) were added, and plates were read at 595nm and 750nm using a plate reader (Biotech, Beckman Coulter). Absorbance read was token at 0h and 72h. Population doubling was calculated

by normalizing to absorbance at 595nm at t=0h. The percentage of survival was calculated in comparison with control conditions of each cell line.

Flow cytometry assay

Cells were trypsinized, washed with PBS, and blocked with PBS-5%FBS for extracellular staining or PBS-5%FBS-0.1%Saponin for intracellular staining. Cells were resuspended in blocking buffer with the primary antibody (table 3) for 30 minutes at 4ºC. Samples were washed twice with PBS and incubated with the secondary antibody, when necessary, for 30 minutes at 4ºC. Cells were washed twice with PBS and incubated with molecular probes at 37 ºC for 30 minutes or 1 hour. Finally, samples were washed with PBS and resuspended in 500 µl of PBS-0.5mM ethylenediaminetetraacetic acid (EDTA) with Sytox as viability marker (Molecular probes, S11341) and analyzed in Gallios cytometer (Beckman Coulter).

Table 3. Flow cytometry antibodies list.

Antibody	Brand	Dilution	Incubation
ABCC3 (M3II9)	Invitrogen	1:150	30 min, 4ºC
CD133-PE (clone 7)	Biolegend	1:400	30 min, 4ºC
PE mouse igG1, K isotype	Biolegend	1:400	30 min, 4ºC
APC goat anti-mouse IgG	Biolegend	1:1500	30 min, 4ºC
Monochlorobimane (mClB)	Sigma-Aldrich	1:1000	1 hour, 37ºC
CellRox Deep Red	Invitrogen	1:1000	30 min, 37ºC
Annexin V-FITC	Immunostep	1:20	30 min, 4ºC

Sphere-formation assay

PDAC spheres were generated and expanded in DMEM-F12 (Gibco) supplemented with B-27 (A3582801, Gibco) and basic fibroblast growth factor (PeproTech EC). 10^5 cells/ml/well were seeded in ultra-low attachment 24-well plates (Nunc). For serial passaging, spheres were harvested at day 7 dissociated

into single cells with accutase, and then re-grown in the same conditions for 7 days. Sphere formation capacity was assessed 3-11 days after seeding, depending on the cell line. Spheres were defined as morphologically characteristic three-dimensional structures approximately >35 μm, containing an average of 50 cells.

Extreme Limiting Dilutions Assays (ELDA)

Different numbers of cells (1, 10, 10^2, 10^3, and 10^4) were seeded in ultra-low attachment 96-well plates (Nunc), and the number of spheres >35 μm was determined by using an inverted microscope (Leica IX81) using an x10 objective with phase contrast.

CSCs frequency and statistical values were calculated using ELDA software[37].

Bioluminescence imaging

Tumor growth in tumor-bearing mice was monitored by bioluminescence imaging using IVIS Lumina III (Beckman Coulter). For bioluminescence detection, 150 mg/kg of luciferin (Merck) was IP injected, and 10 minutes later, the signal was acquired at 1-2 s. Bioluminescence data was measured in radiants (p/sec/cm^2/sr).

***In vivo* models**

Mice were housed according to institutional guidelines, and all experimental procedures were performed in compliance with the institutional guidelines for the welfare of experimental animals approved by Research Ethics Committee of the Autonomous Community of Aragon (PI 56/20) and in accordance with the guidelines for Ethical Conduct in the Care and Use of Animals as stated in The International Guiding Principles for Biomedical Research involving Animals, developed by the Council for International Organizations of Medical Sciences (CIOMS). Briefly, mice were housed according to the following guidelines: a 12 h light/12 h dark cycle, with no access during the dark cycle, temperatures of 65-75 ºF (~18–23 °C) with 50-60% humidity; a standard diet with fat content ranging

from 4 to 11%; sterilized water was accessible at all times; for handling, mice were manipulated gently and as little as possible; noises, vibrations, and odors were minimized to prevent stress and decreased breeding performance; and enrichment was always used per the facility's guidelines to help alleviate stress and improve breeding.

Subcutaneous tumors: Male and female 6- to 10-week-old NU-Foxn1nu nude mice (Envigo) were subcutaneously injected with 10^6 IMIM-PC2 or CFPAC-1 cells expressing Cas9-Control sgRNA (NT) or Cas9 sgABCC3 diluted 1:1 in 50 µl of Matrigel (Corning) per injection.

Orthotopic PDAC tumors: Female 6- to 10-week-old NU-Foxn1nu nude mice (Envigo) were submitted to surgery anesthetized with 2.5%Isofluorane-1.5%O_2. A minimal incision was performed in the animal's skin and muscle. The spleen and pancreas were extracted carefully with tweezers from the body and orthotopically injected with 10^6 IMIM-PC2 cells expressing Cas9-control sgNT, or Cas9 sgABCC3 diluted 1:1 in 15 µl of Matrigel (Corning) per injection. After the injection, the spleen and pancreas were reintroduced into the animal body. The muscle was sutured, and the skin was stapled. Tumor growth was monitored bi-weekly for up to 2 months.

Mouse tumor growth was followed by bioluminescence by IVIS Lumina III (Beckman Coulter). For luminescence detection, 150 mg/kg of luciferin (Merck) was injected IP, and 10 minutes later, the signal was acquired at 1-2 s.

The chemotherapeutic treatment started when the tumor reached a bioluminescence value of 10^7 p/sec/cm^2/sr in orthotopic pancreatic tumors. 30 mg/kg of abraxane was administered intravenously (IV) twice a week, and 70 mg/kg of gemcitabine was administered intraperitoneally once a week for 3 weeks.

Tumors were collected and mechanically disaggregated with the help of a scalpel and treated with PBS-EDTA 10mM for 10 min, 3000 rpm at 37ºC. Samples were filtrated through a nylon 40 µm filter. The single-cell suspension was analyzed by flow cytometry as described above (table 3).

Bioinformatical analysis

Oncomine: The expression level of ABCC3 in PDAC and normal pancreas was analyzed using Ocomine Compendium of Expression Array Data[38]. Briefly, the P-value for statistical significance was set up as 0.05. The platforms used for this study were as follows: Pei Pancreas, Ishikawa Pancreas, Iacobuzio-Donahue Pancreas 2, Segara Pancreas, Grutzman Pancreas, and TCGA Pancreas.

Survival: Gene expression and PDAC patient survival data were obtained by TCGA Pancreas, RNA_Seq, cBioPortal, and Human Protein Atlas[39]. Data was analyzed and shown in Human Protein Atlas. Based on the FPKM value of ABCC3, patients were classified into two expression groups, and the correlation between expression level and patient survival was examined. The prognosis of each group of patients was estimated by Kaplan-Meier survival, and log-rank tests compared the survival outcomes of the two groups. Both median and maximally separated Kaplan-Meier plots are presented in the Human Protein Atlas, and genes with log-rank P values less than 0.001 in maximally separated Kaplan-Meier analysis were defined as prognostic genes. If the group of patients with high expression of a selected prognostic gene has a higher observed event than the expected event, it is an unfavorable prognostic gene; otherwise, it is a favorable prognostic gene. Genes with a median expression less than FPKM 1 were lowly expressed and classified as unprognostic in the database even if they exhibited a significant prognostic effect in survival analysis.

Pearson's product-moment correlation: Raw UMI counts per gene of 24 human PDAC from the study by Peng et al.[40], as well as sample annotations, were downloaded from the Chinese National Genomics Data Center (accession #CRA001160). Raw counts underwent denoising using the provided cluster annotation and the DCA Python software 11 and subsequent normalization using the scran R package12. Finally, the different populations were identified using the markers provided in Elyada et al.[41]. All bioinformatics analyses regarding Peng dataset were performed using RStudio v1.3

Statistical analysis

Log-rank and Wilcoxon tests have been applied for Kaplan Meyer survival curves. Pearson's product-moment was applied to determine gene correlations and test for association/correlation between paired samples. Tukey's Honest Significant Difference (HSD) was applied to compare *ABCC3* expression across tumor grades in pancreatic cancer vs. normal samples.

Flow cytometry gating was performed using Flowjo 8.8.6 software. Statistical significance was determined using a two-sided Student's t-test. Statistical analysis was obtained from Prism 6 (GraphPad) and Microsoft Excel (Microsoft) software. Mean values are shown (unless otherwise specified), and error bars represent SDs. *p*-values of the pairwise comparisons are indicated in the graphs as *** $p < 0.001$; ** $p < 0.01$; * $p < 0.05$; and n.s., not significant).

RESULTS

ABCC3 is overexpressed in PDAC tumors

Previous studies have shown that ABCC3 is overexpressed at mRNA levels in PDAC patient samples, and they correlate with tumor grading[10,42]. We analyzed several data from different databases, and we observed that at mRNA level, ABCC3 is overexpressed in PDAC compared to normal pancreas (figure 1A). Also, the expression of ABCC3 in tumor patients correlates with poor prognosis, having low survival probabilities (figure 1B). These data and bioinformatic analysis point to ABCC3 as a possible biomarker for PDAC.

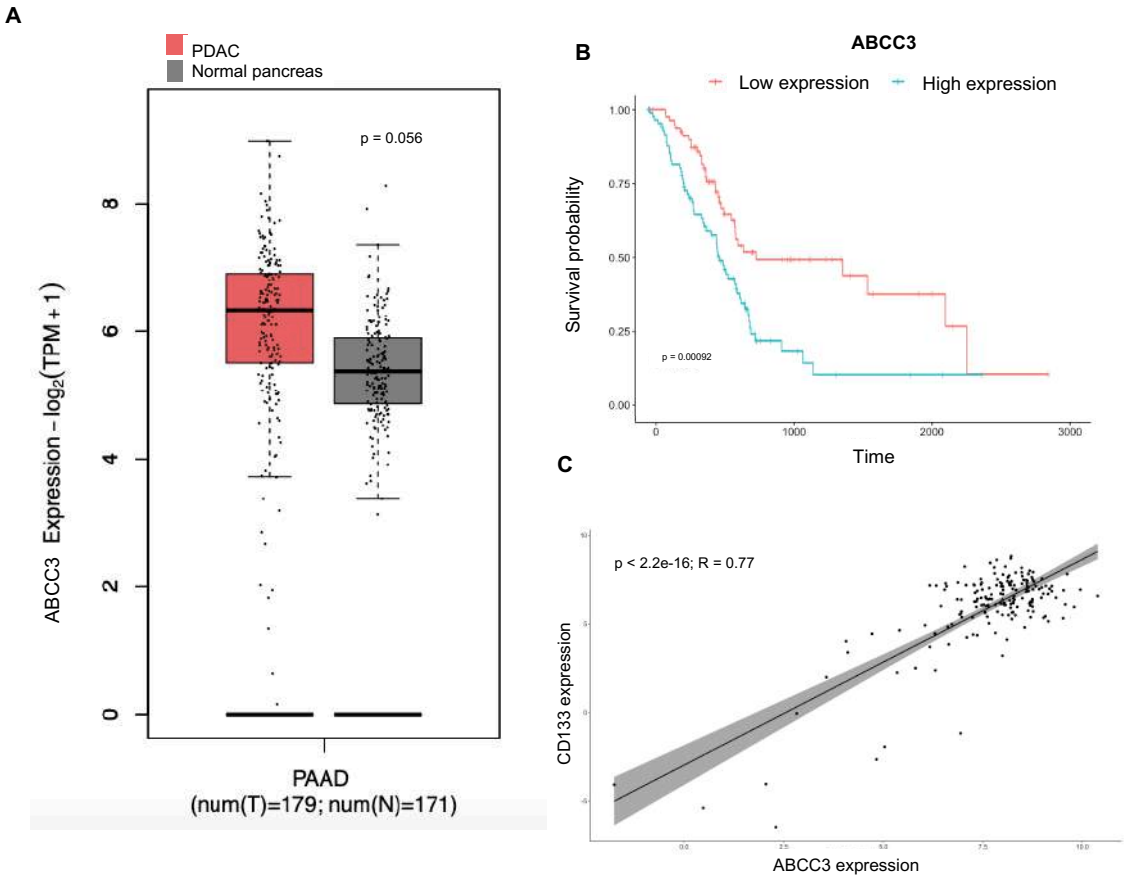

Figure 1. ABCC3 is overexpressed in PDAC tumors, and it is associated with a poor prognosis. A) *ABCC3* expression in PDAC patients (red) and normal pancreas (grey). Data generated with Oncomine[38]. Tukey's Honest Significant Difference (HSD). TCGA-PAAD dataset. The figure shows the difference between pairs, the 95% confidence interval, and the p-value of the pairwise comparisons**. B)** Kaplan-Meier curves for overall survival in the TCGA-PAAD dataset (RNA_Seq, cBioPortal) for ABCC3 in PDAC patients. Log-rank and Wilcoxon test for survival curves. Cut off top high vs. low. ***p<0.01; **C)** *ABCC3* and *CD133* expression in PDAC samples. TCGA-PAAD dataset (RNA_Seq, cBioPortal). Pearson's product-moment correlation. ***p<0.001

ABCC3 has been related to stemness in other types of cancers, such as melanoma[43] or breast[44] tumors. We looked for the relation with some stemness markers in PDAC, and we found that ABCC3 is positively related to CD133 expression, suggesting a possible link between ABCC3 and stemness in PDAC (figure 1C).

In order to study the role of ABCC3 in PDAC, we characterized *ABCC3* at the mRNA and protein levels. We observed a different range of *ABCC3* expression within a panel of established cell lines by qRT-PCR and flow cytometry (figure 2A and C). There is correlation between the expression of ABCC3 mRNA and protein levels. We also analyzed the ABCC3 expression in primary cultures of PDAC PDXs. These primary cultures presented lower levels of expression of *ABCC3* at the mRNA level compared to most of the established cell lines used in this work (figure 2B).

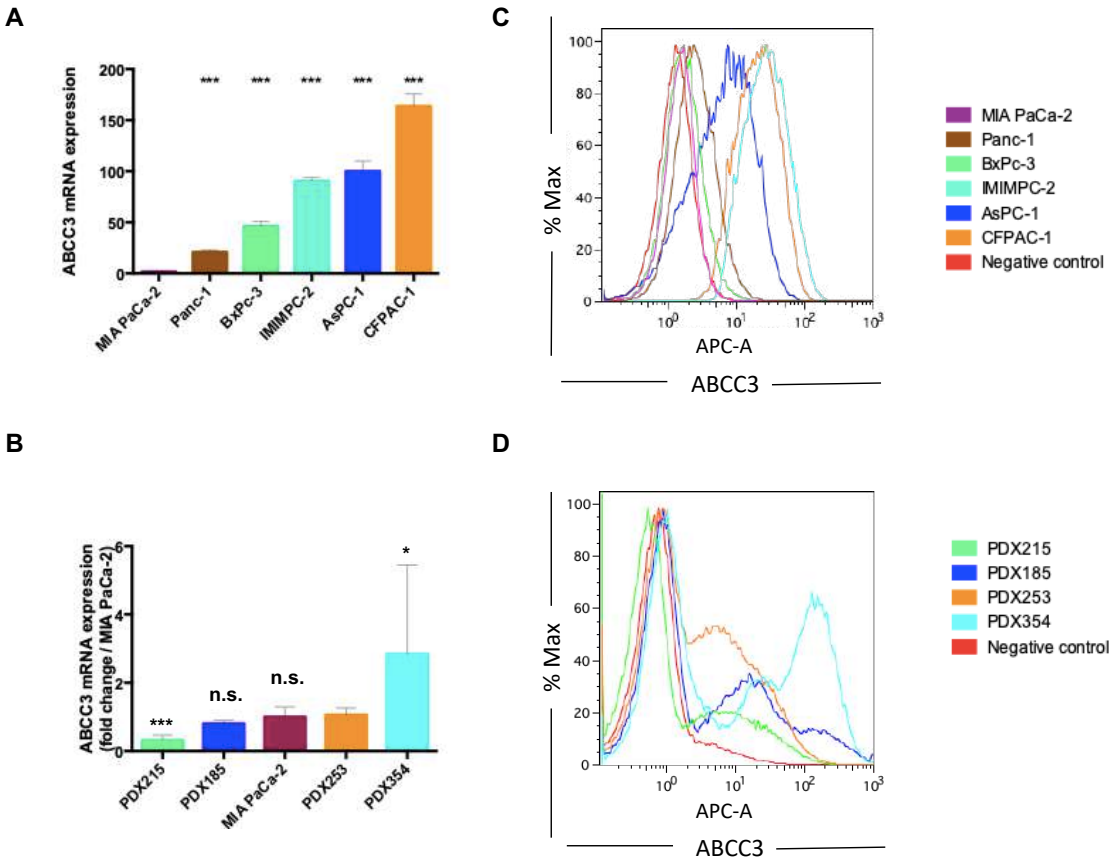

Figure 2. ABCC3 expression in PDAC cell lines and PDXs. ABCC3 mRNA expression levels in **A)** established cell lines and in **B)** PDXs. *Unpaired t-test was used (n.s. no significant, * p<0.05, ** p<0.01, *** p<0.001). Dark and light blue lines indicate the inhibition of 20 nM of gemcitabine in MIA PaCa-2-Cas9 sgNT and sgABCC3, respectively.* ABCC3 protein expression levels in **C)**

established cell lines and in **D)** PDX primary cell lines. *ABCC3 mRNA expression data are represented as fold change of MIA PaCa-2 cell line.*

However, we observed two different populations when analyzing ABCC3 expression in primary cultures of PDX by flow cytometry. The main population with neglected ABCC3 expression and a smaller percentage of cells with high expression levels (figure 2D). These two populations could have different characteristics and play different roles in the tumor.

ABCC3 is related to increased proliferation and stemness

CSCs are a subpopulation of cells implicated in tumor initiation, progression, and metastasis. CSCs have unique characteristics such as differentiation into different cell lineages, increased proliferation, and self-renewal. This subpopulation of cells has been shown to play a key role in cancer recurrence and chemotherapeutic resistance. CSCs chemoresistance is characterized by enhanced DNA damage repair, alterations of cellular metabolism, impaired apoptotic response, and increased activation of drug efflux pumps. There is a possible relationship between ABCC3 expression and CSCs that could mediate their chemotherapeutic acquired resistance.

We have observed two populations in PDXs cultures attending to ABCC3 expression. We thought that these two populations based on ABCC3 expression could be related to stemness; the ones with higher levels of ABCC3 could correspond to CSCs due to their ability to drug resistance.

PDXs maintain the tumor heterogenicity present in patients' tumors and have been well established as models to study stemness ability. Previous reports indicate that CSCs express ABC transporters in the membrane conferring resistance to chemotherapeutic agents[45,46].

Cancer cells behave differently when culturing in adherent or spheroids media. Cell culture in spheroids-enriched cultures is characterized by low cell adhesion and, in many cases, low oxygen and chemotherapy drug stimulation. This method is one of the most used for the isolation and characterization of CSCs. Hence, CSCs subpopulation would be enriched in spheroids cultures, allowing to study

the stemness ability of cells. PDAC CSCs are characterized by the expression of CD133[47], thus we looked for the expression of ABCC3 in CD133 positive population by flow cytometry assays.

In adherent conditions, CD133 positive ($CD133^+$) cells have higher levels of ABCC3 compared to CD133 negative ($CD133^-$) cells in the four PDX cells (figures 3A, B, and S1). Additionally, PDX cells were grown as spheroids, and we could observe an increase in ABCC3 and CD133 proteins (figure 3C), which corroborates the positive relation between ABCC3 and stemness.

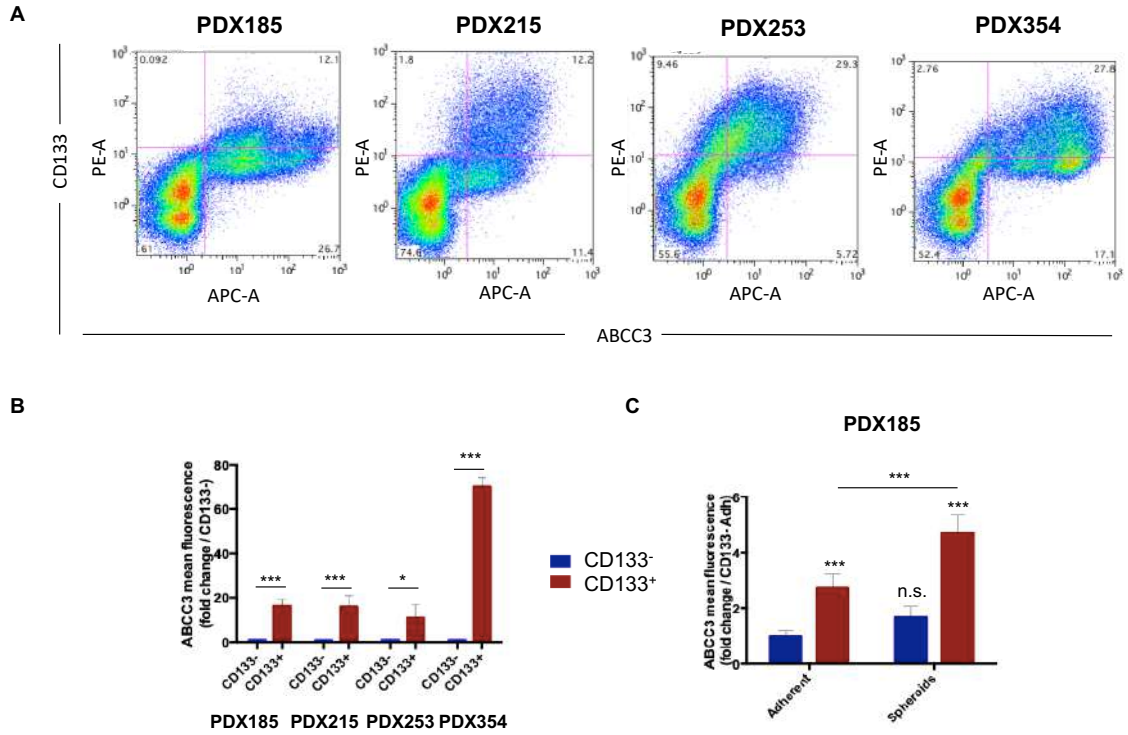

Figure 3. ABCC3 is related to stemness. A) Correlation between the expression of ABCC3 and CD133 in PDXs in flow cytometry assays**. B)** ABCC3 protein expression in CD133 populations. *ABCC3 fluorescence is represented as the fold change of $CD133^-$ population.* **C)** ABCC3 protein expression of PDX185 in adherent and spheroids conditions. *ABCC3 fluorescence is represented as the fold change of $CD133^-$ population in adherent conditions. Unpaired t-test was used (n.s, non-significant, * p<0.05; **. P<0.01; *** p<0.001, n=3).*

Since ABCC3 is more expressed in spheroids-enriched conditions, we wanted to study if it plays a functional role in stemness. To this end, we generated several ABCC3 deficient PDAC cell lines by CRISPR/Cas9 system, referred to as Cas9

sgABCC3 cells. Control cells using a non-targeting sgRNA were also generated, referred to as Cas9 sgNT (figure 4A)

It was previously demonstrated that the inhibition of ABCC3 decreased proliferation in PDAC cell lines and stopped PDAC tumor growth[15]. In agreement, ABCC3-deficient cells (sgABCC3) of two different PDAC cell lines (IMIM-PC2 and CFPAC-1) showed a reduced proliferation rate *in vitro* compared to ABCC3-expressing cells (sgNT) (figure 5A). Furthermore, ABCC3-deficient tumors presented a slower growth compared to ABCC3-expressing tumors (figure 5C). We corroborated previous results demonstrating the implication of ABCC3 in PDAC tumor growth[48].

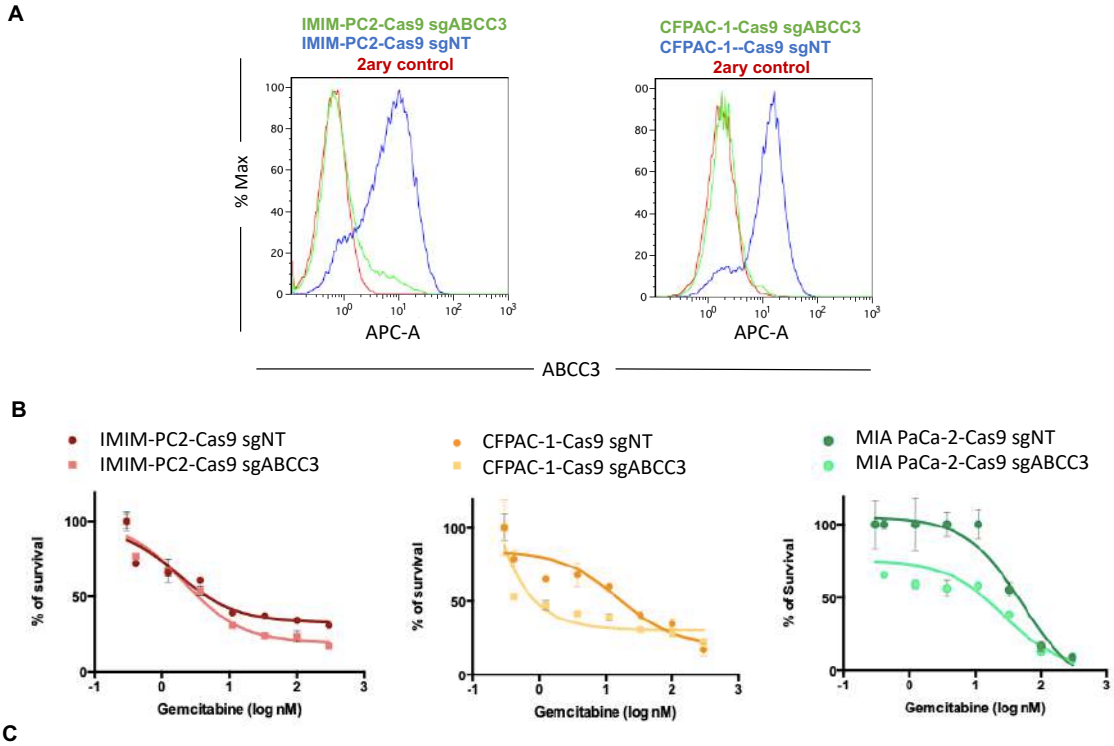

C

	IC_{50} Gemcitabine (nM)	
IMIM-PC2-Cas9 sgNT	10.47 ± 1.32	***
IMIM-PC2-Cas9 sgABCC3	4.27 ± 0.56	
CFPAC-1-Cas9 sgNT	15.85 ± 1.41	****
CFPAC-1-Cas9 sgABCC3	0.84 ± 0.03	
MIA PaCa-2-Cas9 sgNT	40.56 ± 1.81	****
MIA PaCa-2-Cas9 sgABCC3	11.23 ± 1.24	

Figure 4. ABCC3 is implicated resistance to gemcitabine. A) Flow cytometry chart of ABCC3 expression analysis in sgNT and sgABCC3 cells. **B)** Dose response to gemcitabine of sgNT and sgABCC3 PDAC cell lines for 72 h. **C)** IC_{50} values for gemcitabine treatment in sgNT and sgABCC3 PDAC cell lines after 72 h. *Data are represented as mean ± SD. Unpaired t-test was performed (n.s, no significant; * p<0.05; ** p<0.01; *** p<0.001; **** p<0.0001).*

ABCC3 genetic ablation impairs PDAC cell lines proliferation *in vitro* and *in vivo*. We have previously observed that ABCC3 is related to stemness. Given that CSCs have increased proliferation rates, we wanted to corroborate the relationship between ABCC3 and stemness in PDAC.

By seeding different cell numbers in extreme limiting dilution assays (ELDA), we could observe that ABCC3-expressing cells could form spheroids with a small number of cells, with more self-renewal characteristics (figure 5B and D). To test these abilities *in vivo,* different number of cells were inoculated subcutaneously in nude mice. ABCC3-expressing tumors presented a shorter latency for tumor formation, and tumor growth was faster than in ABCC3-deficient tumors (figures 5C and D).

A

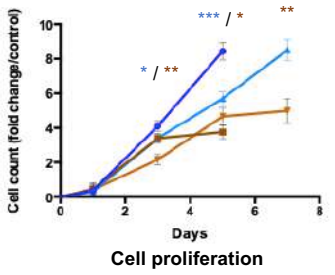

B

Number of cells	10^4	10^3	10^2	10	CSCs freq	p
IMIM-PC2-Cas9 sgNT	4/4	3/4	2/4	1/4	1/371	1.93e-08
IMIM-PC2-Cas9 sgABCC3	1/4	0/4	0/4	0/4	1/39228	
CFPAC-1-Cas9 sgNT	4/4	4/4	2/4	1/4	1/106	6.20e-08
CFPAC-1-Cas9 sgABCC3	2/4	1/4	0/4	0/4	1/10804	

C

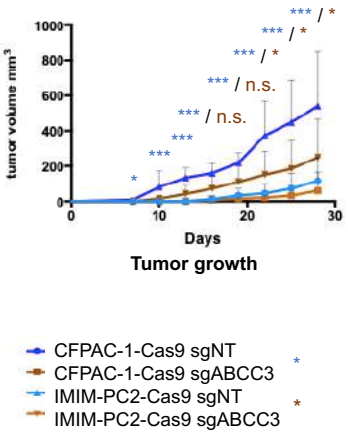

D

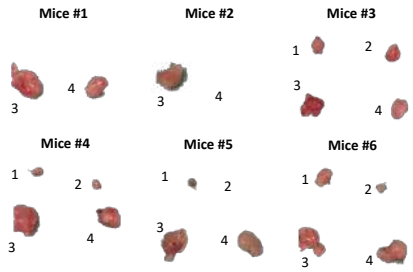

Number of cells	10^4	10^3	CSCs freq	p
1 - IMIM-PC2-Cas9 sgNT	5/7	4/7	1/4615	2.96e-03
2 - IMIM-PC2-Cas9 sgABCC3	1/7	1/7	1/35632	
3 - CFPAC-1-Cas9 sgNT	7/7	7/7	1	2.34e-06
4 - CFPAC-1-Cas9 sgABCC3	5/7	2/7	1/6386	

Figure 5. ABCC3 expression increase proliferation *in vitro* and *in vivo*. A) Cell proliferation in sgNT and sgABCC3 cells. *Data are represented as mean ± SD. Unpaired t-test was performed (n.s, no significant; * p<0.05; ** p<0.01; *** p<0.001; **** p<0.0001). blue * corresponds to t-test between CFPAC-1-Cas9 sgNT and sgABCC3; orange * corresponds to the t-test between IMIM-PC2-Cas9 sgNT and sgABCC3.* **B)** ELDA assays with spheroids cultures of sgNT and sgABCC3 cells. *Statistical data were analyzed using ELDA software*[37]. **C)** Subcutaneous tumor growth of sgNT and sgABCC3 cells. *Data are represented as mean ± SD. Unpaired t-test was performed*

*(n.s, no significant; * p<0.05; ** p<0.01; *** p<0.001; **** p<0.0001). blue * corresponds to t-test between CFPAC-1-Cas9 sgNT and sgABCC3; orange * corresponds to the t-test between IMIM-PC2-Cas9 sgNT and sgABCC3.* **D)** Tumorigenicity assay in subcutaneous tumors of sgNT and sgABCC3 cells. *Statistical data were analyzed using ELDA software*[37]*.*

ELDA assays, both *in vitro* and *in vivo*, allow the determination of the self-renewal abilities of cells in culture or tumors. These results indicated that ABCC3-expressing cells have self-renewal characteristics, suggesting the implication of ABCC3 expression in PDAC CSCs. Additionally, CSCs frequencies in both cases*, in vitro and in vivo*, were considerably higher in sgNT than sgABCC3 cells, confirming that ABCC3 plays an important role in stemness in PDAC.

To corroborate the relationship between ABCC3 and CD133 expression, we generated spheroids from PDAC ABCC3-expressing and ABCC3-deficient cells (Figure 6A). Interestingly, spheroids formed by ABCC3-deficient cells (sgABCC3) cells were smaller than ABCC3-expressing (sgNT) cells. ABCC3 expression in ABCC3-expressing cells was significantly increased in spheroids-enriched conditions in $CD133^+$ population (figure 6D). Even more, the $CD133^+$ population was not so enriched, compared to adherent culture, in ABCC3-deficient cells (figure 6B and C). We demonstrated the expression of ABCC3 transporters in CSCs, characterized by CD133 expression. Moreover, the expression of ABCC3 protein was significantly increased when cells were cultured in spheroids-enriched conditions.

To expand these findings, we analyzed PDX primary cultures in adherent and spheroids-enriched conditions. Importantly, ABCC3 expression was increased in $CD133^+$ compared to $CD133^-$ population. Thus, ABCC3 expression is shown in CSCs, increasing in stemness-enriched conditions (figure 3B and S1).

Altogether, these results indicate that ABCC3 plays a role in proliferation, self-renewal, and CSCs maintenance.

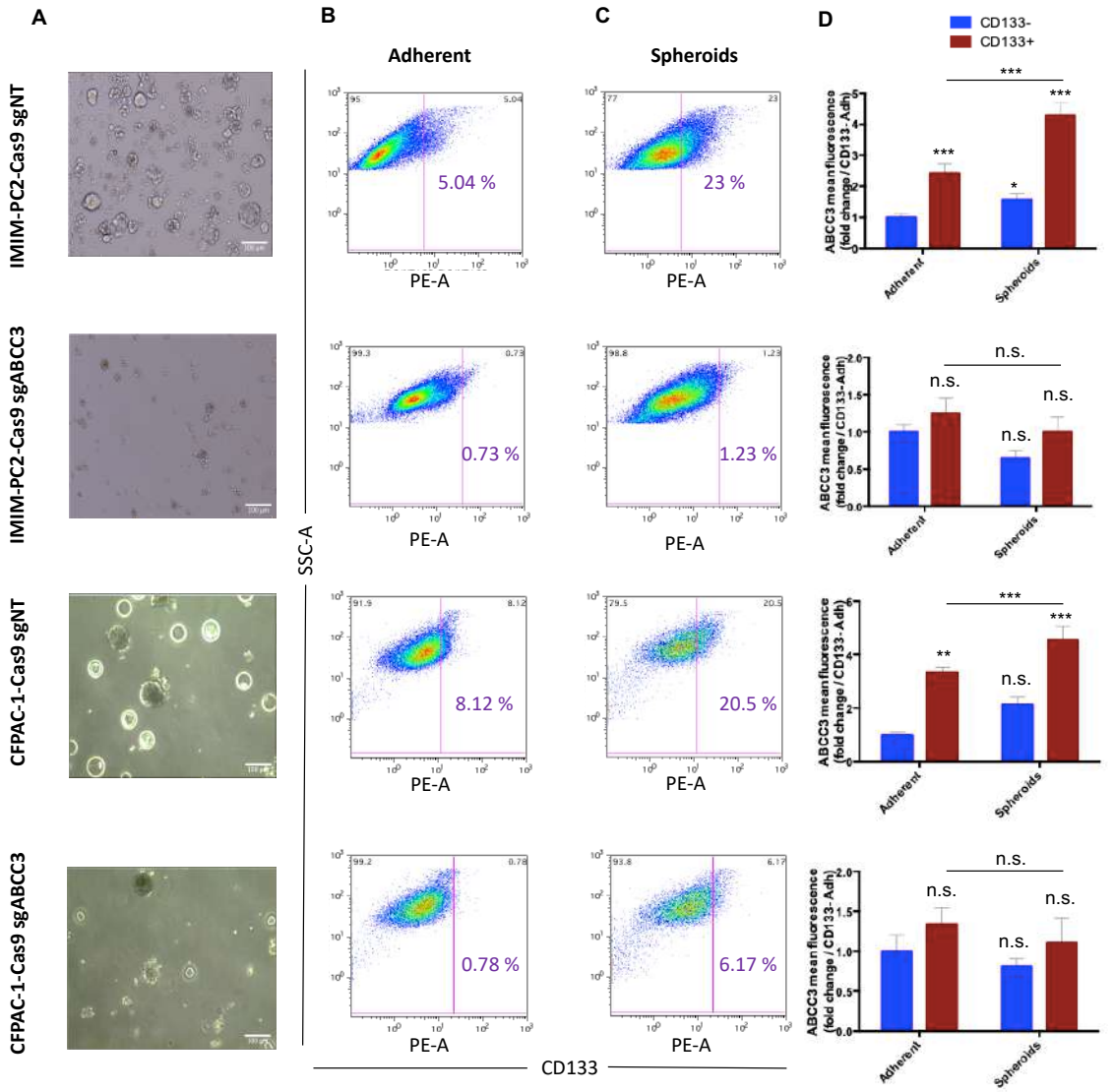

Figure 6. ABCC3 expression is increased in stemness-rich conditions, and ABCC3-deficient cell spheroids do not increase CD133 population. ABCC3 and CD133 expression analysis in IMIM-PC2-Cas9 sgNT and sgABCC3, and CFPAC-1-Cas9 sgNT and sgABCC3. **A)** Bright-field images of spheroids in stemness-rich conditions of sgNT and sgABCC3 cell lines. *Images were taken with Leica IX81 microscopy, scale 100 um.* CD133 expression in **B)** adherent cultures and in **C)** spheroids culture. **D)** ABCC3 protein expression in CD133 population in adherent vs. spheroids cultures. *ABCC3 mean fluorescence is represented as the fold change of CD133$^-$ population in adherent conditions, n=3. Data are represented as mean ± SD. Unpaired t-test was performed (n.s, no significant; * p<0.05; ** p<0.01; *** p<0.001; **** p<0.0001).*

ABCC3 is implicated in gemcitabine resistance in PDAC

ABCC proteins have been related to chemoresistance, one of the main features of CSCs, in different cancer types. In particular, ABCC3 has been shown to be

implicated in cisplatin resistance in lung, breast, and brain cancer[19,49,50]. Since gemcitabine is part of the standard treatment for PDAC patients, we interrogated the role of ABCC3 in the resistance to gemcitabine in this tumor. To this end, we treated with gemcitabine ABCC3-expressing (sgNT) and ABCC3-deficient (sgABCC3) of IMIM-PC2 and CFPAC-1. Both cell lines are the ones characterized in this work with the higher expression of ABCC3 in basal conditions.

ABCC3-deficient cells were more sensitive to gemcitabine treatment for 72 h in both cell lines (figure 4B and C). IMIM-PC2-Cas9 sgNT cells were more resistant to gemcitabine than IMIM-PC2-Cas9 sgABCC3 cells (IC_{50} of 10.47 and 4.27 nM, respectively). And the difference was even higher in CFPAC-1-Cas9 sgNT and CFPAC-1-Cas9 sgABCC3 cells, IC_{50} of 15.85 and 0.84 nM (figure 4B and C). The sensitivity between sgNT and sgABCC3 to gemcitabine was statistically significant in the tested PDAC cell lines, pointing to a role of ABCC3 in the resistance to gemcitabine treatment in PDAC.

We saw that ABCC3-expressing cells are more resistant to gemcitabine treatment, so we wanted to investigate if ABCC3 is responsible for this resistance to gemcitabine in PDAC. MIA PaCa-2 cells in basal conditions do not express ABCC3, but after gemcitabine treatment, there is an increase in the expression of ABCC3, and it is expressed in $CD133^+$ cells (figure 7A and C). MIA PaCa-2-Cas9 sgABCC3 cannot express ABCC3, but there is no enrichment in $CD133^+$ population after treatment (figure 7B and D).

The difference in gemcitabine resistance is very high in MIA PaCa-2-Cas9 sgNT and MIA PaCa-2-Cas9 sgABCC3 cells, IC_{50} of 40.56 and 11.23 nM, respectively (figure 4B and D).

In addition to this sensitivity in ABCC3-deficient cells, as it was observed in IMIM-PC2 and CFPAC-1 cell lines, it looks that cells with no basal expression of ABCC3 are more resistant to gemcitabine than cells with high basal expression of ABCC3. These results indicated the importance of the expression of ABCC3 in every tumor stage; it could predict the response to standard PDAC treatment.

Hence, we proposed that there is a direct relationship between gemcitabine resistance and ABCC3 expression in PDAC.

These results also showed that cells could adapt the expression of ABCC3 transporters depending on the conditions; in this case, under gemcitabine treatment, CSCs can induce the expression of ABCC3 transporters, possibly to eliminate drugs from the cells and avoid cell death.

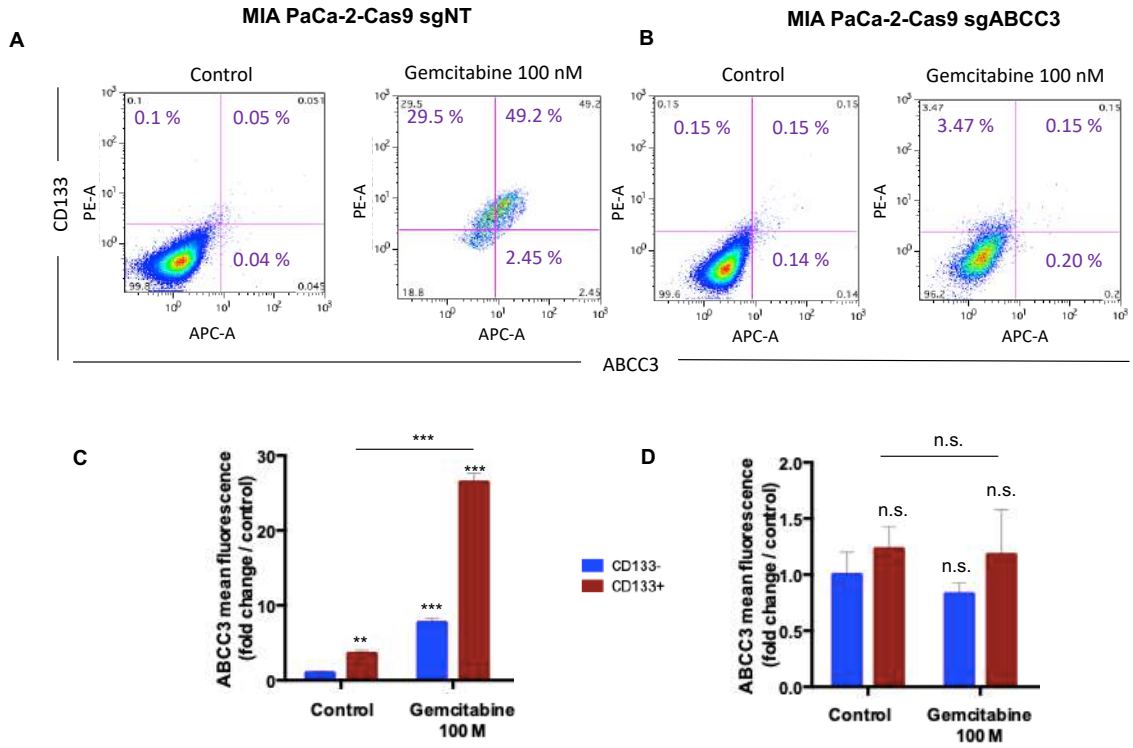

Figure 7. ABCC3 expression is increased in response to gemcitabine treatment. CD133 and ABCC3 expression in basal conditions and under gemcitabine treatment after 72 h in **A)** MIA PaCa-2-Cas9 sgNT and **B)** MIA PaCa-2-Cas9 sgABCC3 cells. ABCC3 expression in control, and gemcitabine 72 h treatment in **C)** MIA PaCa-2-Cas9 sgNT and **D)** MIA PaCa-2-Cas9 sgABCC3 cells. *ABCC3 mean fluorescence is represented as the fold change of CD133- control population. Data are represented as mean ± SD. Unpaired t-test was performed (n.s, no significant; * p<0.05; ** p<0.01; *** p<0.001; **** p<0.0001); n=3.*

ABCC3 transporter is not implicated in abraxane resistance in PDAC

ABCC3 has been shown to be implicated in gemcitabine resistance in PDAC cell lines. The current standard treatment of PDAC patients consists of the combination of gemcitabine and abraxane once a week for three weeks cycles. We showed that ABCC3-expressing tumors seemed to be more resistant to chemotherapeutic agents for PDAC treatment. Then we investigated if ABCC3 could also be implicated in the mechanism of resistance to abraxane.

Abraxane consists of NAB-paclitaxel albumin-bound particles. NAB-paclitaxel is an anti-microtubule agent that promotes the assembly of microtubules from tubulin dimers and stabilizes microtubules by preventing depolymerization. It has been shown to improve the effectiveness of gemcitabine treatment in metastatic-PDAC tumors in patients. The overall response of clinical trials combination of GA was 37%, and the OS was 10 months. Additionally, the median progression-free survival reached 6.7 months[51]. As observed, ABCC3 was implicated in the resistance to gemcitabine; this transporter could also be implicated in the transport of abraxane.

To evaluate the role of ABCC3 in response to abraxane, we performed dose-response curves for this treatment in ABCC3-expressing and ABCC3-deficient cells of CFPAC-1, IMIM-PC2, and MIA PaCa-2 cell lines. On the contrary to what we saw upon gemcitabine treatment, after abraxane treatment, there is no significant difference in the sensitivity of ABCC3-expressing and deficient cells (figure S2). These data suggest that ABCC3 is not implicated in the resistance to abraxane treatment.

To corroborate that, we performed flow cytometry experiments to study the expression of ABCC3 and CD133 under abraxane treatment.

We treated ABCC3-expressing and ABCC3-deficient cells of MIA PaCa-2 cells, the cell line that showed the ability to modulate the expression of ABCC3 under gemcitabine treatment. We could observe that there was not an increase of ABCC3 expression in MIA PaCa-2-Cas9 sgNT cells (figure 8C); then, ABCC3 might not be implicated in abraxane resistance. Additionally, we did not observe a major increase in $CD133^{+}$ population in ABCC3-expressing cells (figure 8A) or ABCC3-deficient cells (figure 8B).

In contrast to the role of ABCC3 in gemcitabine resistance in PDAC, we did not observe the involvement of ABCC3 in abraxane resistance. There is the possibility that other ABCC transporters, such as ABCC1, could be implicated in the chemotherapeutic resistance for this drug.

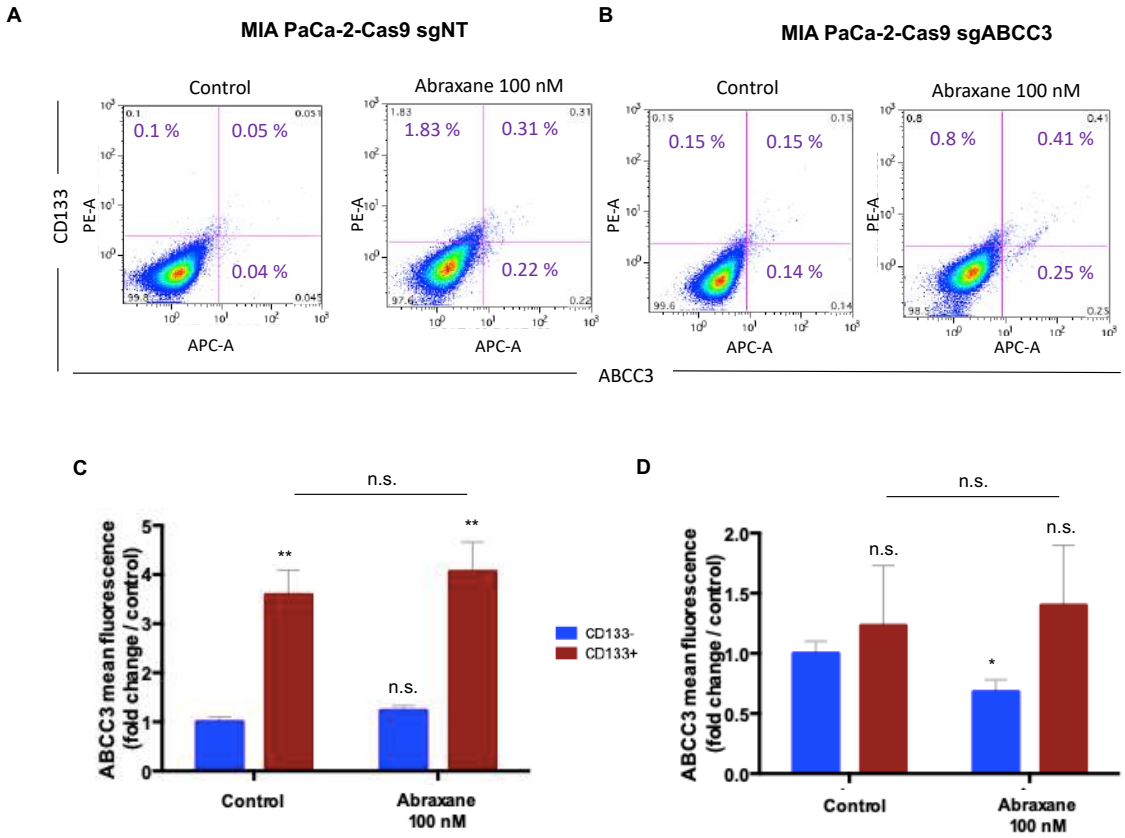

Figure 8. ABCC3 expression is not increased in response to abraxane treatment. CD133 and ABCC3 expression in basal conditions and under abraxane treatment after 72 h in **A)** MIA PaCa-2-Cas9 sgNT and **B)** MIA PaCa-2-Cas9 sgABCC3 cells. ABCC3 expression in control, and abraxane 72 h treatment in **C)** MIA PaCa-2-Cas9 sgNT and **D)** MIA PaCa-2-Cas9 sgABCC3 cells. *ABCC3 mean fluorescence is represented as the fold change of CD133- control population. Data are represented as mean ± SD. Unpaired t-test was performed (n.s, no significant; * p<0.05; ** p<0.01; *** p<0.001; **** p<0.0001); n=3.*

Gemcitabine and abraxane treatment is more effective in the absence of ABCC3 in preclinical models of PDAC

We observed that ABCC3-deficient (sgABCC3) cells are more sensitive to gemcitabine treatment *in vitro*. Since the current treatment for PDAC patients consists of the combination of gemcitabine and abraxane, we wanted to assess the role of ABCC3 in response to chemotherapeutic agents *in vivo*.

IMIM-PC2-Cas9 sgNT and sgABCC3 orthotopic PDAC tumor growth was monitored by IVIS bioluminescence until they reached a similar size and the tumor was palpable (1-2.5 x 10^7 photons/sec/cm^2/sr). Then, mice were subjected

to a three weeks chemotherapeutic regimen of gemcitabine and abraxane. At the end of the treatment, pancreas were collected and processed for ABCC3 and CD133 expression measurement by flow cytometry. We could observe an increase in CSCs population measured by CD133 in IMIM-PC2-Cas9 sgNT tumor cells (20-30% of $CD133^+$ cells, figure 10A) compared to IMIM-PC2-Cas9 sgABCC3 tumor cells that only presented a percentage of 2-5% of $CD133^+$ cells (figure 10B).

It is important to note that the expression of ABCC3 was mainly found in $CD133^+$ cells in IMIM-PC2-Cas9 sgNT tumors (figure 10C). ABCC3-expressing tumors were bigger when measured at the end of the treatment than those generated from ABCC3-deficient cells (sgABCC3). And more importantly, ABCC3-deficient tumors responded to gemcitabine and abraxane treatment and stopped the tumor growth (figure 9A and B).

These results suggest a specific role of ABCC3 in chemoresistance and stemness *in vivo* that could influence patient outcomes. ABCC3 expression can be induced upon gemcitabine treatment even in tumors with no basal expression of ABCC3, conferring a high resistance to treatments.

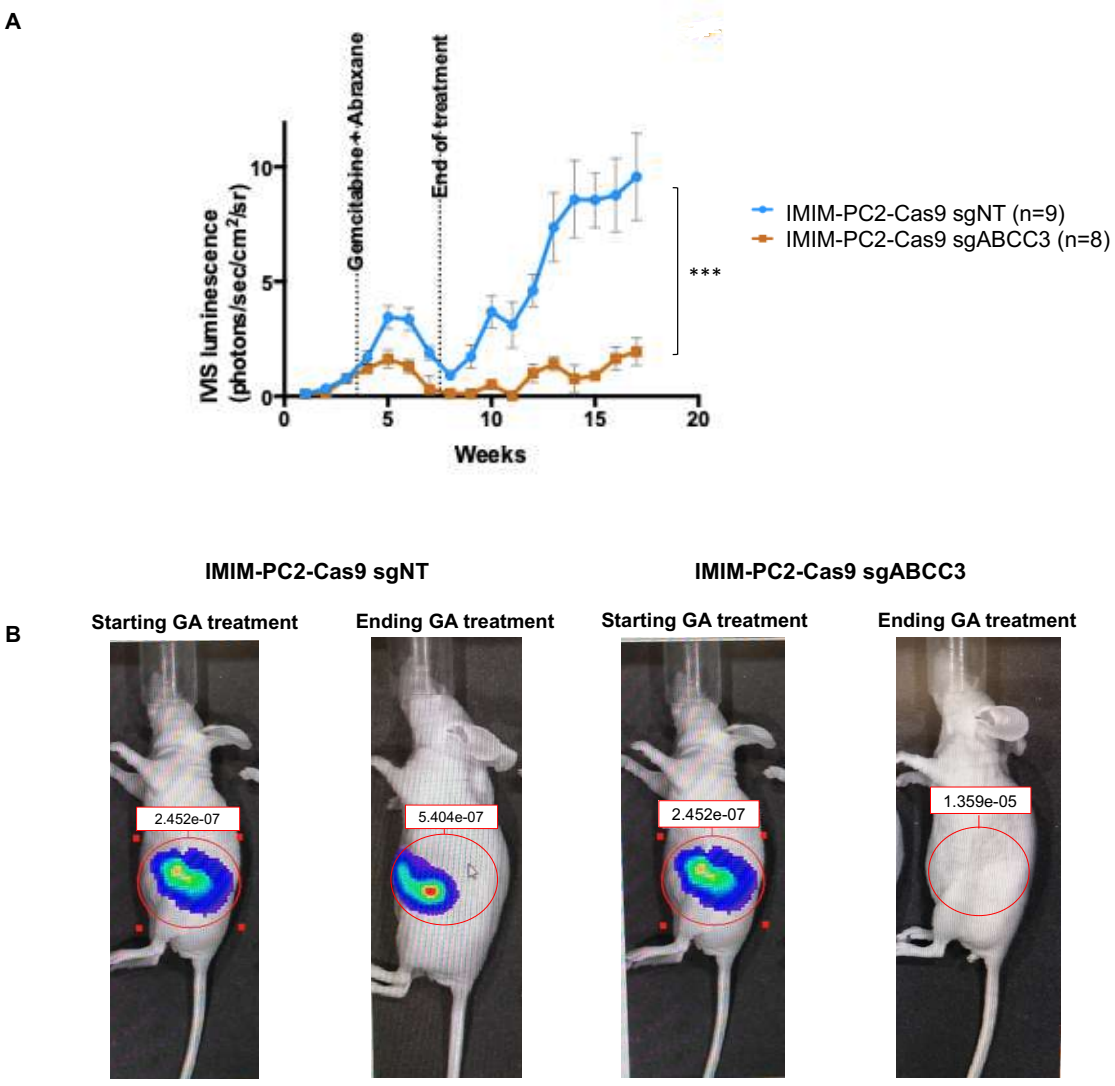

Figure 9. ABCC3 ablation stops PDAC tumor growth and improves GA treatment in PDAC mouse models. A) Tumor growth measurement by IVIS luminescence in IMIM-PC2-Cas9 sgNT and sgABCC3 orthotopic PDAC tumors under gemcitabine and abraxane treatment. *Data are represented as mean ± SD. Unpaired t-test was performed (n.s, no significant; * p<0.05; ** p<0.01; *** p<0.001; **** p<0.0001).* **B)** IVIS bioluminescence images of IMIM-PC2-Cas9 sgNT and sgABCC3 at the start and end of GA treatment.

It would be important to use ABCC3 as a prognostic marker for gemcitabine resistance in tumors. Still, it would be essential to determine ABCC3 levels along with the treatment for a possible increase in their expression. Additionally, ABCC3 inhibitors could serve as adjuvant therapy for current SOC treatment in PDAC.

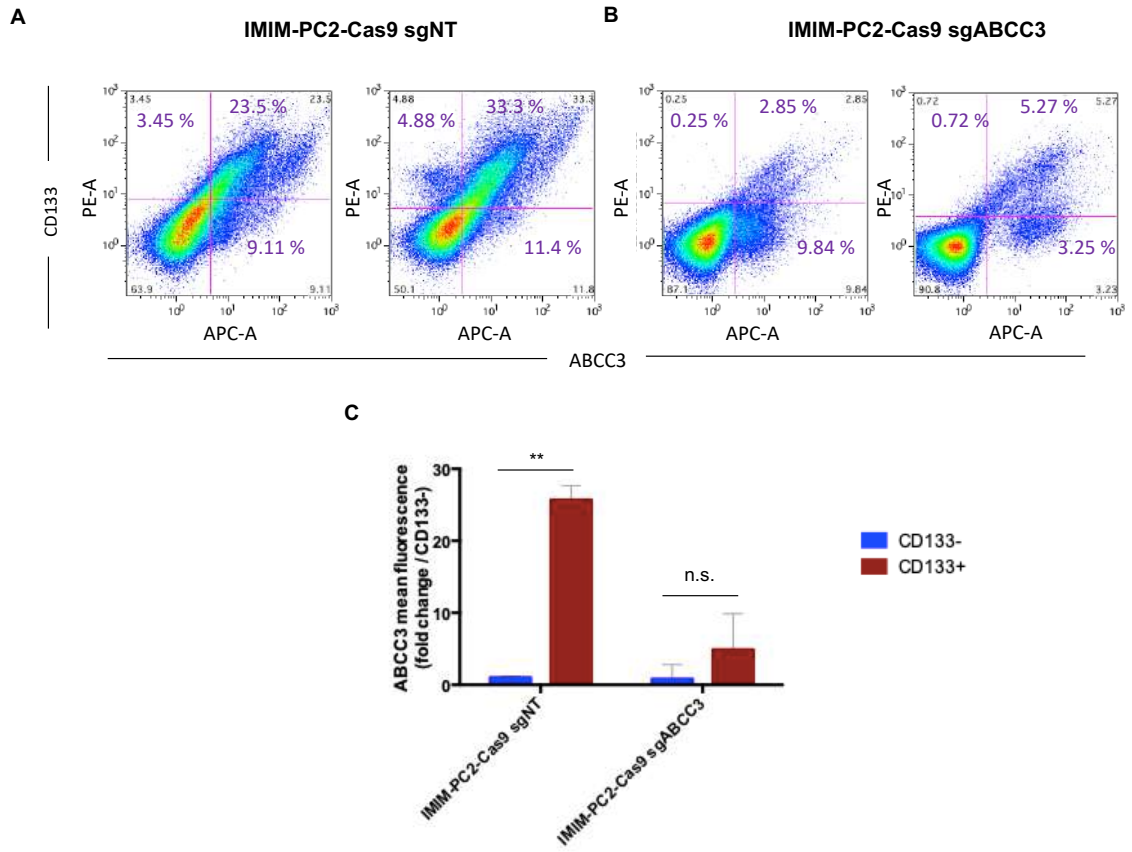

Figure 10. ABCC3 expression is implicated in the resistance to gemcitabine and abraxane in mouse models. A) CD133 and ABCC3 expression in mouse fresh tumor samples of IMIM-PC2-Cas9 sgNT and sgABCC3 cells from PDAC tumors. **B)** ABCC3 expression in IMIM-PC2-Cas9 sgNT and sgABCC3 fresh mouse samples. *ABCC3 fluorescence is represented as the fold change of IMIM-PC2-Cas9 sgNT CD133- cells. Unpaired t-test was performed (n.s, no significant; * p<0.05; ** p<0.01; *** p<0.001; **** p<0.0001); n=4.*

Mitochondrial metabolism is essential for ABCC3 activity

PDAC CSCs have an elevated rate of mitochondrial metabolism and consequently generate high levels of ROS[25]. To avoid cell death by ROS, the cells use different redox pathways that mediate antioxidants transport, including glutathione (GSH)[34]. Other ABCC proteins, as ABCC1 and ABCC2, are known GSH transporters[52], but it is not clear if ABCC3 could be participating in its transport.

As previously reported by Jagust et al., CSC-enriched spheroids showed an increase in different glutathione metabolism-related genes and enhanced GSH content, defining a relationship between GSH and stemness[34]. To address a

possible role of ABCC3 in the GSH transport in PDAC CSCs, we measured ROS production and GSH content in ABCC3-expressing (sgNT) and ABCC3-deficient (sgABCC3) PDAC cells.

We could observe higher levels of GSH and ROS in ABCC3-expressing cells in adherent conditions compared to ABCC3-deficient cells. Notably, these levels increased when these cells were cultured in spheroids enriched conditions (figure 11A and B). Importantly, in ABCC3-deficient cells, there is no increase in GSH or ROS content, even in spheroids-enriched conditions (figure 11A and B). We corroborated that CSCs have increased levels of ROS and found a possible role of ABCC3 in GSH transport.

ABC transporters need ATP for drug efflux; Giddings et al.[53] showed that ABC proteins use mitochondrial-derived ATP for doxorubicin secretion. These findings lead to the assertion that chemoresistant cells have an oxidative metabolism and elevated mitochondrial respiration. More interestingly, it was shown that ABC transporters use mitochondrial ATP for drug efflux[53].

To investigate if ABCC3 uses ATP from oxidative metabolism in PDAC CSCs, oligomycin was added before treatment to inhibit ATP synthase, and ROS levels were measured. The addition of oligomycin decreased ROS levels in ABCC3-expressing cells (CFPAC-1-Cas9 sgNT), but not in ABCC3-deficient cells (CFPAC-1- and MIA PaCa-2-Cas9 sgABCC3) nor MIA PaCa-2-Cas9 sgNT that in basal conditions do not express ABCC3 (figure 11C and D). Upon gemcitabine treatment, ROS levels were increased in ABCC3-expressing cells due to the enhanced mitochondrial metabolism.

Oligomycin blockade of ATP synthase prior to gemcitabine treatment significantly reduced ROS levels in both sgNT cells (figure 11C and D). The increase observed in ROS levels in ABCC3-deficient cells could be due to an increase in apoptosis (figure S3).

A possible role of ABCC3 in GSH transport could be occurring. To explore this possibility, we measured GSH content after adding oligomycin. In the case that ABCC3 is an influx transporter of GSH, the addition of oligomycin would impair ABCC3 transport, and GSH content will be diminished.

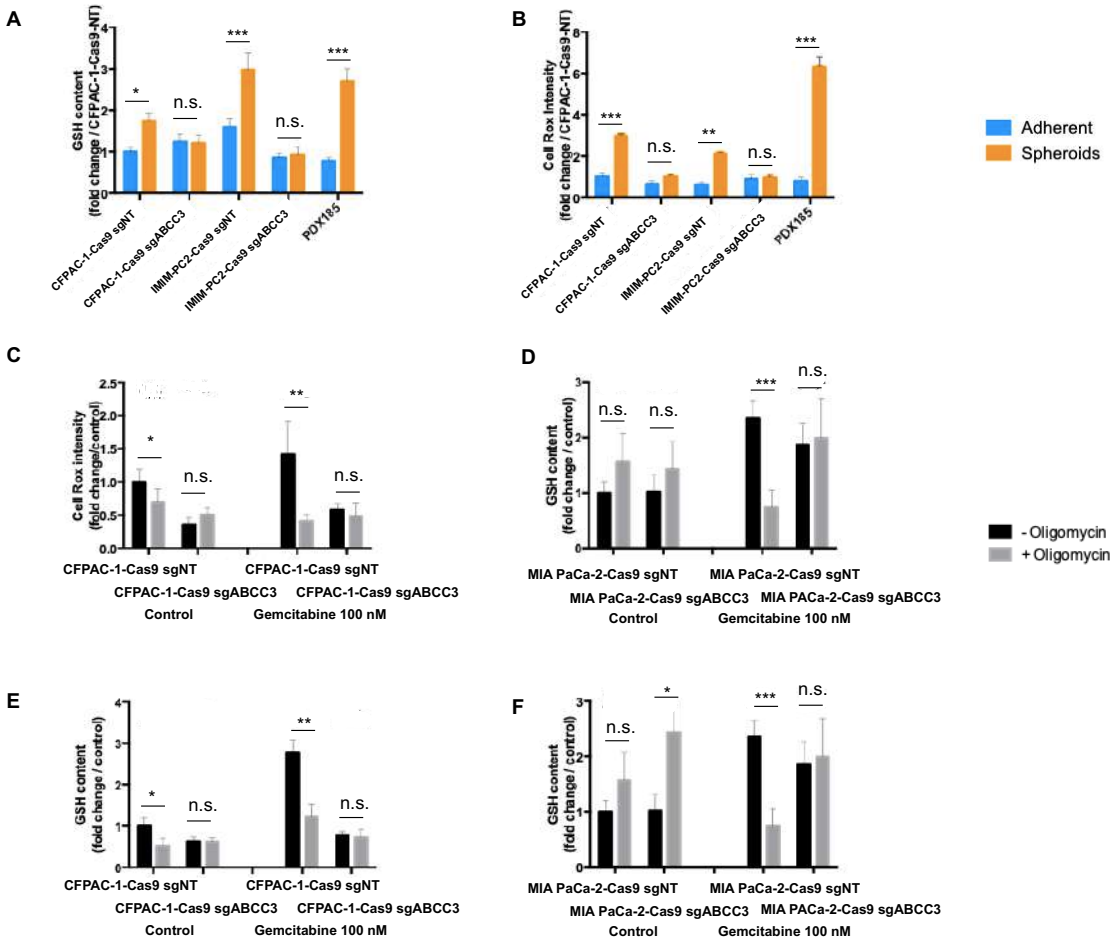

Figure 11. ABCC3 activity depends on mitochondrial metabolism. Representation of the GSH content and ROS measurement by flow cytometry. **A)** GSH content and **B)** ROS production in adherent and spheroid cultures of ABCC3-expressing (sgNT) and ABCC3-deficient (sgABCC3) PDAC cell lines. *Data is represented as the fold change of CFPAC-1-Cas9 sgNT in adherent conditions.* ROS measurement of $CD133^+$ population in **C)** CFPAC-1-Cas9 sgNT and sgABCC3 and in **D)** MIA PaCa-2-Cas9 sgNT and ABCC3) in basal conditions and after gemcitabine treatment upon oligomycin addition or not. *Data is represented as the fold change of control*. GSH content of $CD133^+$ population in **E)** CFPAC-1-Cas9 sgNT and sgABCC3 and in **F)** MIA PaCa-2-Cas9 sgNT and ABCC3) in control conditions and after gemcitabine treatment upon oligomycin addition or not. *Data is represented as the fold change of control*.

In basal conditions, the addition of oligomycin decreased GSH content in CFPAC-1-Cas9 sgNT but not in sgABCC3. These results correlate with ABCC3 expression and ROS production. This reduction does not occur in MIA PaCa-2-Cas9 sgNT and sgABCC3; it could be explained, at least in part, because these cells do not express ABCC3 in basal conditions. However, upon gemcitabine treatment, there was a 3-fold increase in the GSH content in sgNT cells that was

not observed in sgABCC3 cells. ABCC3-expressing cells presented lower levels of GSH when oligomycin was added prior to gemcitabine treatment. Importantly, this did not occur in ABCC3-deficient cells (11E and F). These results suggest that GSH could act as an antioxidant to reduce ROS levels and that GSH is transported into the cytoplasm, at least in part, by ABCC3.

ABCC1 is implicated in gemcitabine resistance in PDAC, but it is not related to stemness

ABCC1 is the most studied member of the MRP family. This transporter is almost ubiquitously expressed in the basolateral membrane of cells. ABCC1 has several known substrates such as hydrophobic and anionic molecules, glucuronide, and glutathione conjugates[54]. It is one of the transporters of the ABCC family that has been related to multidrug resistance in cancer[55]. Recently, it has been demonstrated in PDAC that ATF4 mediates gemcitabine resistance by binding to the ABCC1 promoter[56]. Different ABC transporters have been related to stemness in PDAC, such as ABCG2[57], and we also showed ABCC3.

As ABCC1 and ABCC3 share a high grade of homology, we interrogated if the lack of ABCC3 could be compensated by overexpressing ABCC1 in PDAC. As analyzed by flow cytometry, ABCC1 protein levels were not altered in ABCC3-deficient cells (figure 12A).

As previously described[58], ABCC1 expression is upregulated after gemcitabine treatment, but its expression is also increased upon abraxane treatment (figure 12B). Interestingly, contrary to what we found in ABCC3, the upregulation of ABCC1 induced by treatments was observed in the $CD133^-$ population (figure 12C).

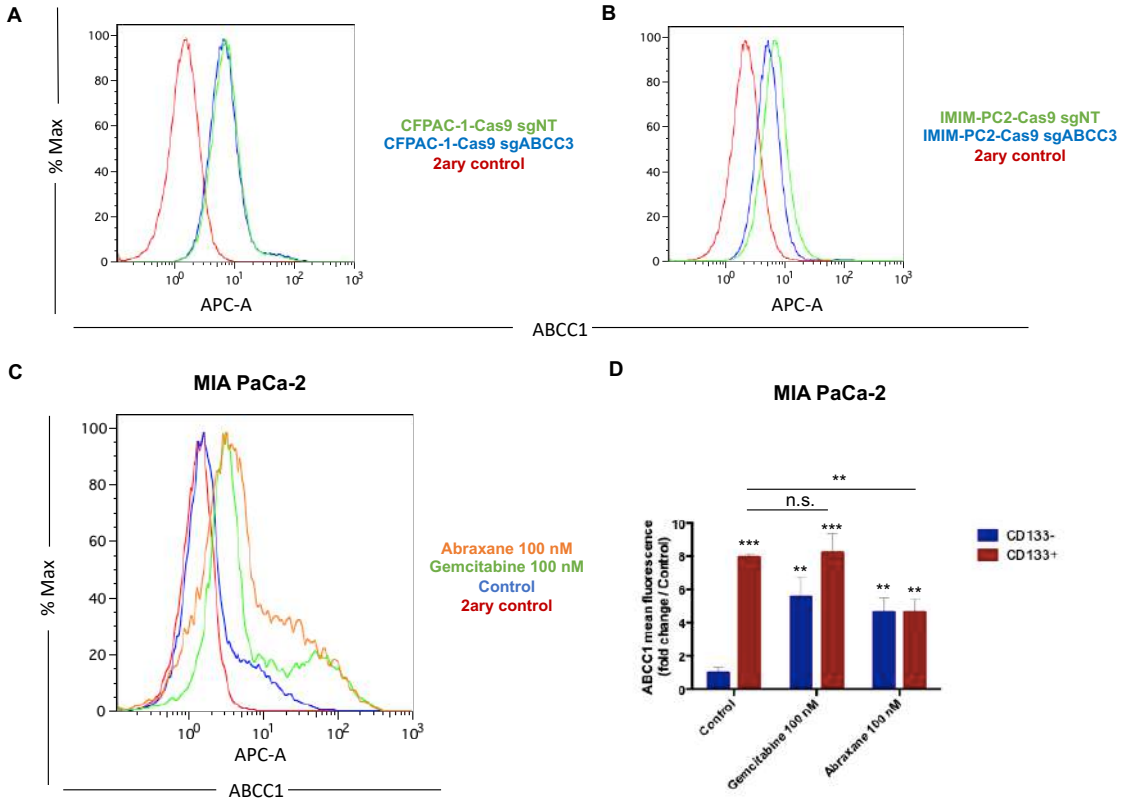

Figure 12. ABCC1 expression is increased in response to treatment in CD133$^-$ cells. ABCC1 expression in **A)** CFPAC-1-Cas9 sgNT and sgABCC3 cells and in **B)** IMIM-PC2-Cas sgNT and sgABCC3 cells. **C)** ABCC1 expression upon gemcitabine and abraxane treatment. Untreated cells were used as controls. **D)** ABCC1 expression in CD133 populations in control, gemcitabine, and abraxane treatment.

These results point to a specific role of ABCC3 and ABCC1 in CD133$^+$ and CD133$^-$ populations, respectively. On the one hand, ABCC3 is involved in the gemcitabine resistance in CSCs population. On the other hand, ABCC1 might play a role in gemcitabine and abraxane resistance in non-CSCs PDAC cells.

To corroborate that ABCC1 is not overexpressed in CSCs, we cultured a PDX185 primary cell line in spheroids enriched conditions. We confirmed that the increase of ABCC1 in response to the chemotherapeutic addition occurs mainly in CD133$^-$ population in spheroids-enriched conditions (figure 13A and B).

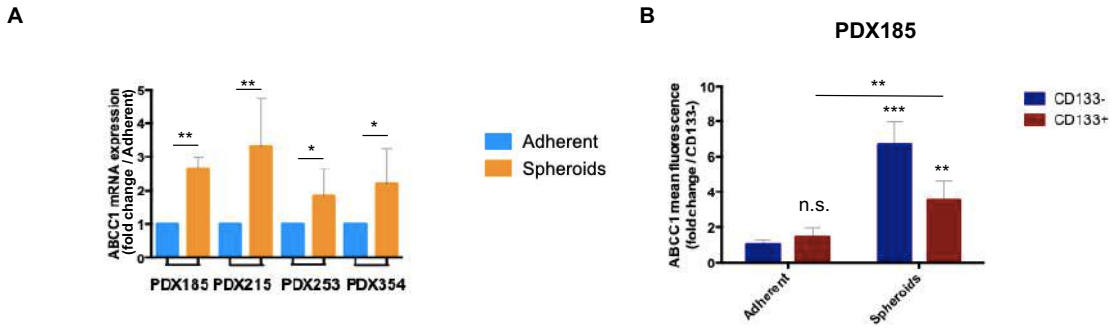

Figure 13. ABCC1 is not expressed in enriched stem cell populations. A) ABCC1 mRNA expression in PDX primary cultures. *Data is represented as the fold change of PDX in adherent conditions.* **B)** ABCC3 expression in adherent and spheroids conditions of PDX185 cultures. *Data is represented as the fold change of CD133- in adherent conditions.*

ABCC1, despite being homologous to ABCC3, seemed not to be overexpressed in CSCs after gemcitabine or abraxane treatment or spheroids-enriched conditions. On the contrary, it is upregulated in non-CSCs after standard chemotherapeutic PDAC treatment.

DISCUSSION

PDAC is an aggressive malignancy usually diagnosed at advanced stages of the disease. Additionally, tumor cells are highly chemoresistant, difficulting therapeutic options[1]. Despite drug resistance, adjuvant therapies have been demonstrated to improve effectiveness in resected-patients[59]. Considering the chemoresistance to standard drug treatment, there is a need to develop new specific inhibitors of PDAC biomarkers. ABCC / MRP transporters have been related to drug resistance in several cancers, and specifically, ABCC3 has been found to be overexpressed in PDAC compared to normal pancreas[60].

We have corroborated the overexpression of ABCC3 in PDAC and additionally its involvement in proliferation. The presence of ABCC3 in PDAC cells leads to increased proliferation *in vitro* and *in vivo* tumor growth.

Several MRP proteins have been related to drug resistance in PDAC. For example, upregulation of ABCC1 plays a role in gemcitabine resistance. It has been described that ATF4 binds to the promoter of ABCC1 to activate its transcription. In agreement, the downregulation of ATF4 inhibited proliferation, migration, and gemcitabine resistance[13].

We have found that ABCC3 is also implicated in the resistance to gemcitabine treatment in PDAC cells. ABCC3-deficient PDAC cells are more sensitive to gemcitabine, have lower self-renewal and sphere formation abilities. ABCC3 and ABCC1 could play a similar role in PDAC in terms of proliferation and chemoresistance. There have been some pieces of evidence that ATF4 is also related to ABCC3 in other types of cancers[61], so ATF4 could regulate both MRP transporters. Further studies on ATF4 and ABCC3 need to be performed.

On the contrary, ABCC3 does not seem to be implicated in abraxane resistance. Hence, abraxane is not secreted by ABCC3, and the genetic ablation of ABCC3 did not sensitize cells to this chemotherapeutic agent. The combination of abraxane, which affects cells independently of ABCC3 expression, with gemcitabine resulted efficient in reducing tumor growth in ABCC3-deficient tumors. Thus, ABCC3 inhibitors could improve the efficiency of standard chemotherapy for PDAC tumors.

It is well established that the inherent chemoresistance of this tumor is based, at least in part, on the presence of CSCs, a highly plastic and "stem"-like population of cells. CSCs have their own characteristics in terms of chemoresistance, invasiveness, autophagy, or metabolism. The current treatments for PDAC patients are ineffective, CSC subpopulation of cells resist treatments, and transient cells replenish CSCs[62]. New chemotherapeutic agents targeting CSCs have resulted in being effective in PDAC treatment. Metformin as an adjuvant with gemcitabine treatment in clinical trials has shown promising results in resectable PDAC tumors[63]. ABC transporters have been described to be present in the cell membrane of CSCs, contributing to the chemoresistance of these cells[64]. We investigated the involvement of ABCC3 transporter in the mechanism of resistance to gemcitabine and their possible expression in CSCs.

We could observe that ABCC3 is expressed in $CD133^+$ population, which indicated that ABCC3 is implicated in the chemoresistance capacity of CSCs in PDAC cells. Once we assessed the relationship between ABCC3 and stemness *in vitro*, we moved to orthotopic PDAC models to corroborate the implication of ABCC3 in gemcitabine resistance in CSCs. Interestingly, in treated mice, we observed that ABCC3-expressing tumors had an enriched CSC population and responded worse to the treatment. In contrast, ABCC3-deficient tumors had a low population of CSCs and decreased in size after the standard treatment. Altogether, these results indicate that targeting ABCC3 with specific inhibitors could be a new adjuvant drug that could improve standard chemotherapeutic treatments for PDAC.

ABCC1 was pointed out as a transporter implicated in gemcitabine resistance. Its overexpression is induced after gemcitabine treatment in PDAC. But interestingly, we described in this work that the expression of ABCC1 occurs in the $CD133^-$ population upon gemcitabine treatment, even on spheroids-enriched conditions. These data suggest that non-CSCs become chemoresistant by inducing ABCC1 expression, while ABCC3 is upregulated in CSCs. These results are relevant and suggest that inhibiting ABCC1 and ABCC3 could sensitize both CSCs, and non-CSCs populations might improve current PDAC treatments.

Cancer cells have an increased proliferation rate; thus, they have to adapt their metabolism. Cancer cells usually use glycolysis for the production of ATP and

building blocks (Warburg effect). CSCs have a different metabolic phenotype, and depending on the cancer type, they can explode glycolysis or OXPHOS. In any case, CSCs are dependent on mitochondrial functions. PDAC CSCs are characterized by an OXPHOS metabolism, in contrast to non-CSCs that rely on glycolytic pathways[65].

We bore out that PDAC CSCs obtain energy via mitochondrial activity. In basal conditions, CSC population had elevated ROS levels, and in response to gemcitabine treatment, they increased ROS production.

Recent reports about the activity of ABCC transporters demonstrated that these proteins use mitochondrial-derived ATP as a source of energy to efflux their substrates, including drugs[66].

We showed that by inhibiting mitochondrial ATP synthase with oligomycin, the production of ROS decreased in ABCC3-expressing cells more than in ABCC3-deficient cells, suggesting the relationship between mitochondrial ATP and ABCC3 activity. These data reinforce the relation between ABCC3 and CSCs, and their dependency on OXPHOS metabolism. Different inhibitors against mitochondrial metabolism, or ABCC3, or even the combination of both could lead to an increased effect of conventional treatment to reduce CSCs population to prevent relapses and chemoresistance in tumor patients.

Oxidative CSCs have elevated levels of ROS from cellular respiration that need to be counteracted. Enhanced GSH metabolism has been related to increased mitochondrial activity, protecting from death caused by ROS[67]. Glutathione peroxidases and transferases have been described to maintain OXPHOS and preserve mitochondrial function[68].

ABC transporters have been related to glutathione conjugates. The overexpression of both molecules in cells results in the efflux of cytotoxic agents leading to drug resistance[69]. ABCC1 and ABCC2 have been identified as glutathione-S-conjugate transporters in several cancer types. ABCC1 and 2 cotransport drugs with GSH for the secretion of both agents[70]. ABCC3 has been shown not to be implicated in the excretion of GSH, but it has been related to GSH transport, probably in infflux[71,72].

We demonstrated that ABCC3 is implicated in the internalization of GSH; ABCC3-deficient cells contain lower levels of glutathione compared to ABCC3-expressing cells. We also corroborated that CSCs have higher content of GSH compared to non-CSC population. We propose that with the inside transport of GSH by ABCC3, CSCs could counter and balance the presence of ROS produced by an elevated mitochondrial metabolism in response to treatments. Using different GSH metabolism inhibitors, CSCs could also be targeted as a strategy to improve current chemotherapeutic treatments (figure 14).

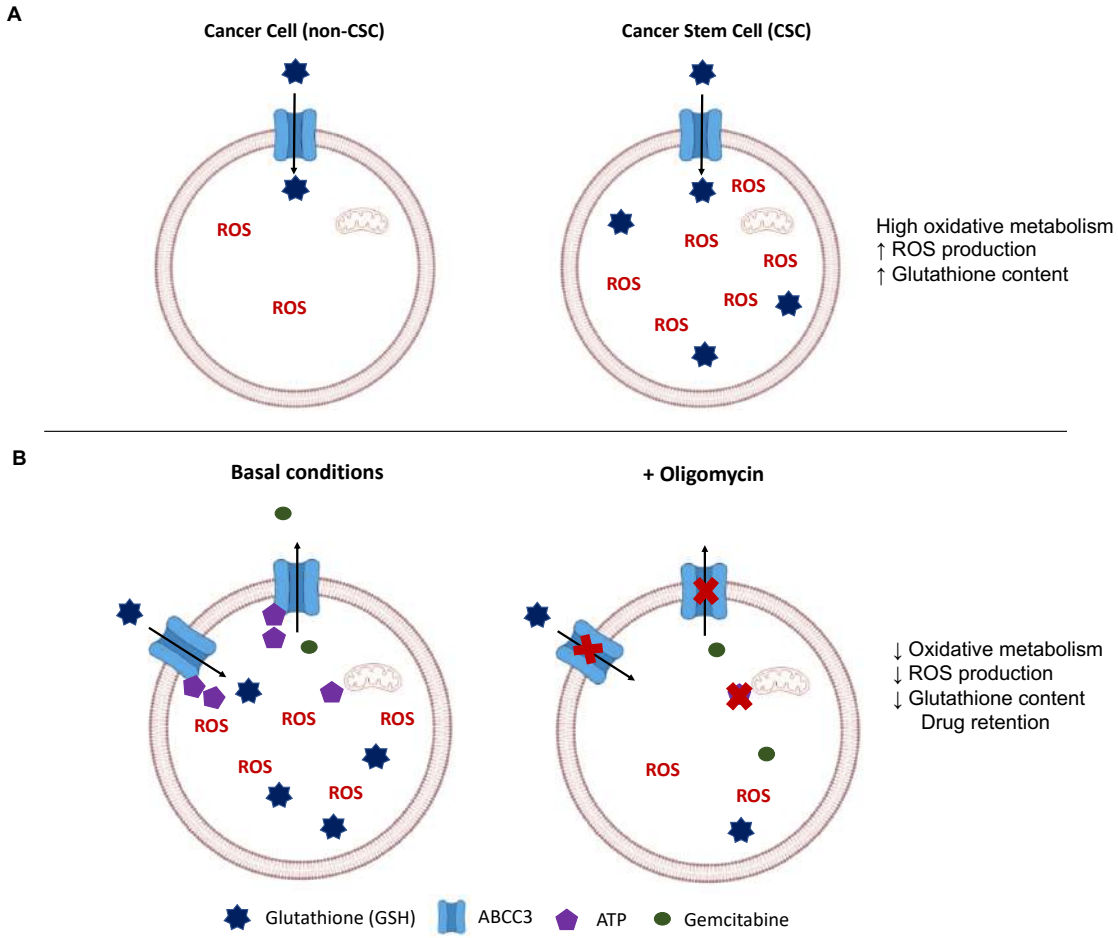

Figure 14. Graphical representation of the metabolism of non-CSCs and CSCs and the proposed implication of ABCC3. A) ROS production and GSH transport in non-CSCs and CSCs. **B)** ROS production, mitochondrial metabolism, and GSH transport in basal conditions and upon oligomycin treatment.

We can conclude that ABCC3 is expressed in the membrane of CSCs in PDAC tumors, which contributes to drug resistance. We observed that ABCC3 participates in gemcitabine resistance in PDAC cells and that its inhibition could

help to improve the effectiveness of conventional treatments. Our results support the oxidative metabolism of PDAC CSCs and their linkage with GSH metabolism to balance ROS levels. Also, ABCC3 was described as an import transporter of GSH in response to treatments.

The inhibition of ABCC3 could target CSCs sensitizing cells to chemotherapeutic agents. ABCC3 could be a predictive marker in ABCC3-expressing tumors. Additionally, its expression could also be monitored in initial ABCC3-deficient tumors. These tumors will overexpress ABCC3 after gemcitabine treatment, and its inhibition could be an adjuvant to improve patients' OS. In addition, ABCC1 inhibition would target non-CSCs to sensitize cancer cells to gemcitabine treatment. Both ABCC transporters inhibition would target CSCs of non-CSCs in PDAC tumors.

CONCLUSIONS

1. ABCC3 is overexpressed in PDAC tumors.
2. ABCC3 contributes to the increase in proliferation in PDAC cell lines in vitro and in vivo.
3. ABCC3 is implicated in the mechanism of chemoresistance to gemcitabine in established and PDXs cell lines in vitro.
4. ABCC3 is differentially expressed in CSCs.
5. ABCC3 uses mitochondrial-derived ATP for its activity in the transport of molecules.
6. ABCC3 is one of the influx transporters of GSH.

SUPPLEMENTAL FIGURES

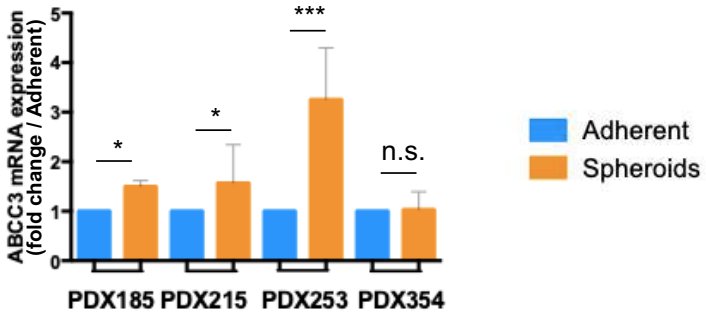

Figure S1. ABCC3 mRNA expression levels in PDXs in adherent and spheroids-enriched culture. *Data is represented as the fold change of PDX in adherent conditions.*

A

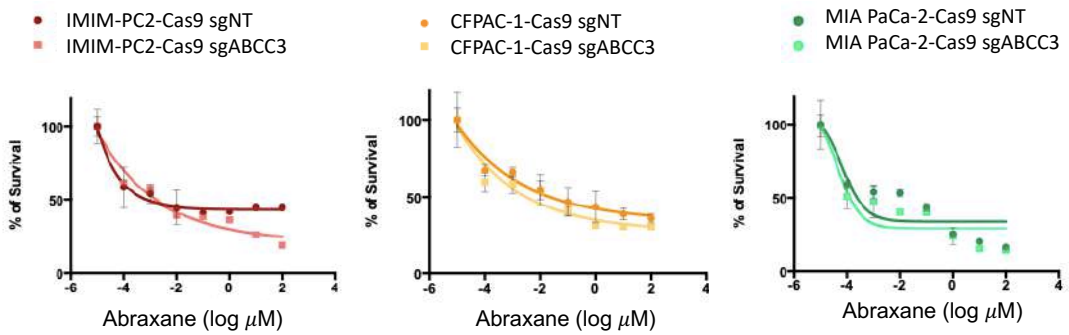

B

	IC_{50} Abraxane (nM)	
IMIM-PC2-Cas9 sgNT	5 ± 0.79	n.s.
IMIM-PC2-Cas9 sgABCC3	4 ± 0.81	
CFPAC-1-Cas9 sgNT	50 ± 7.92	n.s.
CFPAC-1-Cas9 sgABCC3	40 ± 5.24	
MIA PaCa-2-Cas9 sgNT	50 ± 6.85	n.s.
MIA PaCa-2-Cas9 sgABCC3	70 ± 11.37	

Figure S2. ABCC3 ablation did not sensitize PDAC cell lines to abraxane. A) Dose response to abraxane of sgNT and sgABCC3 PDAC cell lines for 72 h. **C)** IC_{50} values for abraxane treatment in sgNT and sgABCC3 PDAC cell lines after 72 h. *Data are represented as mean ± SD. Unpaired t-test was performed (n.s, no significant; * p<0.05; ** p<0.01; *** p<0.001; **** p<0.0001).*

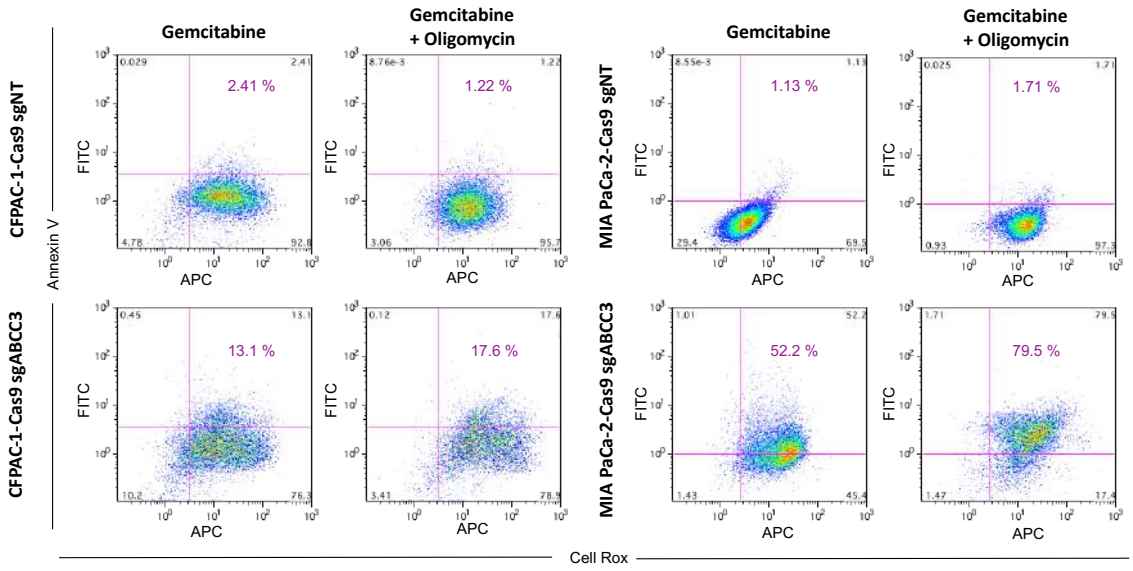

Figure S3. Annexin V and ROS measurement by flow cytometry. Annexin V expression and ROS levels measurement in ABCC3-expressing cells (CFPAC-1- and MIA PaCa-2-Cas9 sgNT) and ABCC3-deficient cells (CFPAC-1- and MIA PaCa-2-Cas9 sgABCC3) after gemcitabine treatments in the presence or absence of oligomycin.

REFERENCES

1. Adamska A, Domenichini A, Falasca M. Pancreatic ductal adenocarcinoma: Current and evolving therapies. *International Journal of Molecular Sciences*. 2017;18(7). doi:10.3390/ijms18071338

2. Satoi S, Yamamoto T, Matsui Y. Conversion surgery in patients with initially unresectable pancreatic ductal adenocarcinoma: where do we stand in 2018? *Journal of Pancreatology*. 2018;1(1):25-29. doi:10.1097/JP9.0000000000000001

3. Qian Y, Gong Y, Fan Z, et al. Molecular alterations and targeted therapy in pancreatic ductal adenocarcinoma. *Journal of Hematology and Oncology*. 2020;13(1):1-20. doi:10.1186/s13045-020-00958-3

4. Kool M, Van Der Linden M, De Haas M, et al. MRP3, an organic anion transporter able to transport anticancer drugs. *Proceedings of the National Academy of Sciences of the United States of America*. 1999;96(12):6914-6919. doi:10.1073/pnas.96.12.6914

5. Kuan CT, Wakiya K, Herndon JE, et al. MRP3: A molecular target for human glioblastoma multiforme immunotherapy. *BMC Cancer*. 2010;10(1):1-15. doi:10.1186/1471-2407-10-468

6. Chen ZS, Tiwari AK. Multidrug resistance proteins (MRPs/ABCCs) in cancer chemotherapy and genetic diseases. *FEBS Journal*. 2011;278(18):3226-3245. doi:10.1111/j.1742-4658.2011.08235.x

7. Multidrug Resistance Proteins MRP3, MRP1, and MRP2 in Lung Cancer | Clinical Cancer Research. https://clincancerres.aacrjournals.org/content/7/6/1798. Accessed June 9, 2021.

8. Liu X, Yao D, Liu C, et al. Overexpression of ABCC3 promotes cell proliferation, drug resistance, and aerobic glycolysis and is associated with poor prognosis in urinary bladder cancer patients. *Tumor Biology*. 2016;37(6):8367-8374. doi:10.1007/s13277-015-4703-5

9. Partanen L, Staaf J, Tanner M, Tuominen VJ, Borg Å, Isola J. Amplification and overexpression of the ABCC3 (MRP3) gene in primary breast cancer. *Genes Chromosomes and Cancer*. 2012;51(9):832-840. doi:10.1002/gcc.21967

10. König J, Hartel M, Nies AT, et al. Expression and localization of human multidrug resistance protein (ABCC) family members in pancreatic carcinoma. *International Journal of Cancer*. 2005;115(3):359-367. doi:10.1002/ijc.20831

11. Sparreboom A, Danesi R, Ando Y, Chan J, Figg WD. Pharmacogenomics of ABC transporters and its role in cancer chemotherapy. *Drug Resistance Updates*. 2003;6(2):71-84. doi:10.1016/S1368-7646(03)00005-0

12. Kool M, Van Der Linden M, De Haas M, et al. MRP3, an organic anion transporter able to transport anticancer drugs. *Proceedings of the National Academy of Sciences of the*

United States of America. 1999;96(12):6914-6919. doi:10.1073/pnas.96.12.6914

13. Wei L, Lin Q, Lu Y, et al. Cancer-associated fibroblasts-mediated ATF4 expression promotes malignancy and gemcitabine resistance in pancreatic cancer via the TGF-β1/SMAD2/3 pathway and ABCC1 transactivation. *Cell Death and Disease*. 2021;12(4):1-14. doi:10.1038/s41419-021-03574-2

14. Igarashi T, Izumi H, Uchiumi T, et al. Clock, and ATF4 transcription system regulates drug resistance in human cancer cell lines. *Oncogene*. 2007;26(33):4749-4760. doi:10.1038/sj.onc.1210289

15. Adamska A, Domenichini A, Capone E, et al. Pharmacological inhibition of ABCC3 slows tumour progression in animal models of pancreatic cancer. *Journal of Experimental and Clinical Cancer Research*. 2019;38(1). doi:10.1186/s13046-019-1308-7

16. Cancer Stem Cells: Implications for Cancer Therapy. https://www.cancernetwork.com/view/cancer-stem-cells-implications-cancer-therapy. Accessed June 9, 2021.

17. Australian Sepsis Network. Signs and Symptoms of Sepsis. 2021:1-7. https://www.australiansepsisnetwork.net.au/community-awareness/signs-symptoms-sepsis.

18. Quiñonero F, Mesas C, Doello K, et al. The challenge of drug resistance in pancreatic ductal adenocarcinoma: a current overview. *Cancer Biology and Medicine*. 2019;16(4):688-699. doi:10.20892/j.issn.2095-3941.2019.0252

19. Balaji SA, Udupa N, Chamallamudi MR, Gupta V, Rangarajan A. Role of the drug transporter ABCC3 in breast cancer chemoresistance. *PLoS ONE*. 2016;11(5). doi:10.1371/journal.pone.0155013

20. Al Mamun M, Mannoor K, Cao J, Qadri F, Song X. SOX2 in cancer stemness: Tumor malignancy and therapeutic potentials. *Journal of Molecular Cell Biology*. 2020;12(2):85-98. doi:10.1093/JMCB/MJY080

21. Veenstra V, Garcia-Garijo A, van Laarhoven H, Bijlsma M. Extracellular Influences: Molecular Subclasses and the Microenvironment in Pancreatic Cancer. *Cancers*. 2018;10(2):34. doi:10.3390/cancers10020034

22. Kamphorst JJ, Cross JR, Fan J, et al. Hypoxic and Ras-transformed cells support growth by scavenging unsaturated fatty acids from lysophospholipids. *Proceedings of the National Academy of Sciences of the United States of America*. 2013;110(22):8882-8887. doi:10.1073/pnas.1307237110

23. Zhu X, Chen HH, Gao CY, et al. Energy metabolism in cancer stem cells. *World Journal of Stem Cells*. 2020;12(6):448-461. doi:10.4252/WJSC.V12.I6.448

24. CAS Reference Linking. https://chemport.cas.org/cgi-

bin/sdcgi?APP=ftslink&action=reflink&origin=npg&version=1.0&coi=1%3ACAS%3A528%3ADC%252BC3cXislWnug%253D%253D&md5=713230a9de6e021b27fb93f38b12d400. Accessed July 22, 2021.

25. Sancho P, Burgos-Ramos E, Tavera A, et al. MYC/PGC-1α balance determines the metabolic phenotype and plasticity of pancreatic cancer stem cells. *Cell Metabolism*. 2015;22(4):590-605. doi:10.1016/j.cmet.2015.08.015

26. Janiszewska M, Suvà ML, Riggi N, et al. Imp2 controls oxidative phosphorylation and is crucial for preservin glioblastoma cancer stem cells. *Genes and Development*. 2012;26(17):1926-1944. doi:10.1101/gad.188292.112

27. Carracedo A, Weiss D, Leliaert AK, et al. A metabolic prosurvival role for PML in breast cancer. *Journal of Clinical Investigation*. 2012;122(9):3088-3100. doi:10.1172/JCI62129

28. Nakajima EC, Van Houten B. Metabolic symbiosis in cancer: Refocusing the Warburg lens. *Molecular Carcinogenesis*. 2013;52(5):329-337. doi:10.1002/mc.21863

29. Perillo B, Di Donato M, Pezone A, et al. ROS in cancer therapy: the bright side of the moon. *Experimental and Molecular Medicine*. 2020;52(2):192-203. doi:10.1038/s12276-020-0384-2

30. Homolya L, Váradi A, Sarkadi B. Multidrug resistance-associated proteins: Export pumps for conjugates with glutathione, glucuronate or sulfate. In: *BioFactors*. Vol 17. IOS Press; 2003:103-114. doi:10.1002/biof.5520170111

31. Ballatori N, Krance SM, Marchan R, Hammond CL. Plasma membrane glutathione transporters and their roles in cell physiology and pathophysiology. *Molecular Aspects of Medicine*. 2009;30(1-2):13-28. doi:10.1016/j.mam.2008.08.004

32. Jagust P, Alcalá S, Jr BS, Heeschen C, Sancho P. Glutathione metabolism is essential for self-renewal and chemoresistance of pancreatic cancer stem cells. *World Journal of Stem Cells*. 2020;12(11):1410-1428. doi:10.4252/wjsc.v12.i11.1410

33. Ju HQ, Gocho T, Aguilar M, et al. Mechanisms of overcoming intrinsic resistance to gemcitabine in pancreatic ductal adenocarcinoma through the redox modulation. *Molecular Cancer Therapeutics*. 2015;14(3):788-798. doi:10.1158/1535-7163.MCT-14-0420

34. Glutathione metabolism is essential for self-renewal and chemoresistance of pancreatic cancer stem cells | Enhanced Reader. moz-extension://45f875a8-6053-bb49-8ae3-c81ebe7900d0/enhanced-reader.html?openApp&pdf=https%3A%2F%2Fdigital.csic.es%2Fbitstream%2F10261%2F232323%2F1%2FGlutathione_Jagust_PV_Art2020.pdf. Accessed June 9, 2021.

35. Gallmeier E, Hermann PC, Mueller MT, et al. Inhibition of ataxia telangiectasia- and Rad3-related function abrogates the in vitro and in vivo tumorigenicity of human colon cancer cells through depletion of the CD133+ tumor-initiating cell fraction. *Stem Cells*.

2011;29(3):418-429. doi:10.1002/stem.595

36. Addgene: pHIV-Luc-ZsGreen. https://www.addgene.org/39196/. Accessed October 26, 2021.

37. Hu Y, Smyth GK. ELDA: Extreme limiting dilution analysis for comparing depleted and enriched populations in stem cell and other assays. *Journal of Immunological Methods*. 2009;347(1-2):70-78. doi:10.1016/j.jim.2009.06.008

38. Oncomine Login. https://www.oncomine.org/resource/login.html. Accessed November 4, 2021.

39. Assays and annotation - The Human Protein Atlas. https://www.proteinatlas.org/about/assays+annotation#tcga_survival. Accessed November 4, 2021.

40. Peng J, Sun BF, Chen CY, et al. Single-cell RNA-seq highlights intra-tumoral heterogeneity and malignant progression in pancreatic ductal adenocarcinoma. *Cell Research*. 2019;29(9):725-738. doi:10.1038/s41422-019-0195-y

41. Elyada E, Bolisetty M, Laise P, et al. Cross-species single-cell analysis of pancreatic ductal adenocarcinoma reveals antigen-presenting cancer-associated fibroblasts. *Cancer Discovery*. 2019;9(8):1102-1123. doi:10.1158/2159-8290.CD-19-0094

42. König J, Rost D, Cui Y, Keppler D. Characterization of the human multidrug resistance protein isoform MRP3 localized to the basolateral hepatocyte membrane. *Hepatology*. 1999;29(4):1156-1163. doi:10.1002/hep.510290404

43. Boumahdi S, Driessens G, Lapouge G, et al. SOX2 controls tumour initiation and cancer stem-cell functions in squamous-cell carcinoma. *Nature*. 2014;511(7508):246-250. doi:10.1038/nature13305

44. Walcher L, Kistenmacher AK, Suo H, et al. Cancer Stem Cells—Origins and Biomarkers: Perspectives for Targeted Personalized Therapies. *Frontiers in Immunology*. 2020;11:1280. doi:10.3389/fimmu.2020.01280

45. Zinzi L, Contino M, Cantore M, Capparelli E, Leopoldo M, Colabufo NA. ABC transporters in CSCs membranes as a novel target for treating tumor relapse. *Frontiers in Pharmacology*. 2014;5 JUL. doi:10.3389/fphar.2014.00163

46. Begicevic RR, Falasca M. ABC transporters in cancer stem cells: Beyond chemoresistance. *International Journal of Molecular Sciences*. 2017;18(11). doi:10.3390/ijms18112362

47. Glumac PM, LeBeau AM. The role of CD133 in cancer: a concise review. *Clinical and Translational Medicine*. 2018;7(1):18. doi:10.1186/s40169-018-0198-1

48. Adamska A, Domenichini A, Capone E, et al. Pharmacological inhibition of ABCC3 slows tumour progression in animal models of pancreatic cancer. *Journal of Experimental and*

Clinical Cancer Research. 2019;38(1):312. doi:10.1186/s13046-019-1308-7

49. Zhao Y, Lu H, Yan A, et al. ABCC3 as a marker for multidrug resistance in non-small cell lung cancer. *Scientific Reports*. 2013;3(1):1-6. doi:10.1038/srep03120

50. Pessina S, Cantini G, Kapetis D, et al. The multidrug-resistance transporter Abcc3 protects NK cells from chemotherapy in a murine model of malignant glioma. *OncoImmunology*. 2016;5(5). doi:10.1080/2162402X.2015.1108513

51. De Vita F, Ventriglia J, Febbraro A, et al. NAB-paclitaxel and gemcitabine in metastatic pancreatic ductal adenocarcinoma (PDAC): From clinical trials to clinical practice. *BMC Cancer*. 2016;16(1). doi:10.1186/s12885-016-2671-9

52. Nasr R, Lorendeau D, Khonkarn R, et al. Molecular analysis of the massive GSH transport mechanism mediated by the human Multidrug Resistant Protein 1/ABCC1. *Scientific Reports*. 2020;10(1):1-13. doi:10.1038/s41598-020-64400-x

53. Giddings EL, Champagne DP, Wu M-H, et al. Mitochondrial ATP fuels ABC transporter-mediated drug efflux in cancer chemoresistance. *Nature Communications*. 2021;12(1):1-19. doi:10.1038/s41467-021-23071-6

54. Cole SPC. Multidrug resistance protein 1 (mrp1, abcc1), a "multitasking" atp-binding cassette (abc,) transporter. *Journal of Biological Chemistry*. 2014;289(45):30880-30888. doi:10.1074/jbc.R114.609248

55. Yin J, Zhang J. Multidrug resistance-associated protein 1 (MRP1/ABCC1) polymorphism: From discovery to clinical application. *Journal of Central South University (Medical Sciences)*. 2011;36(10):927-938. doi:10.3969/j.issn.1672-7347.2011.10.002

56. Wei L, Lin Q, Lu Y, et al. Cancer-associated fibroblasts-mediated ATF4 expression promotes malignancy and gemcitabine resistance in pancreatic cancer via the TGF-β1/SMAD2/3 pathway and ABCC1 transactivation. *Cell Death and Disease*. 2021;12(4):1-14. doi:10.1038/s41419-021-03574-2

57. Skrypek N, Vasseur R, Vincent A, Duchêne B, Van Seuningen I, Jonckheere N. The oncogenic receptor ErbB2 modulates gemcitabine and irinotecan/SN-38 chemoresistance of human pancreatic cancer cells via hCNT1 transporter and multidrug-resistance associated protein MRP-2. *Oncotarget*. 2015;6(13):10853-10867. doi:10.18632/oncotarget.3414

58. Wei L, Lin Q, Lu Y, et al. Cancer-associated fibroblasts-mediated ATF4 expression promotes malignancy and gemcitabine resistance in pancreatic cancer via the TGF-β1/SMAD2/3 pathway and ABCC1 transactivation. *Cell Death and Disease*. 2021;12(4):1-14. doi:10.1038/s41419-021-03574-2

59. Oettle H, Post S, Neuhaus P, et al. Adjuvant chemotherapy with gemcitabine vs observation in patients undergoing curative-intent resection of pancreatic cancer: A randomized controlled trial. *Journal of the American Medical Association*.

2007;297(3):267-277. doi:10.1001/jama.297.3.267

60. Adamska A, Ferro R, Lattanzio R, et al. ABCC3 is a novel target for the treatment of pancreatic cancer. *Advances in Biological Regulation*. 2019;73. doi:10.1016/j.jbior.2019.04.004

61. Zhang Z, Yin J, Zhang C, et al. Activating transcription factor 4 increases chemotherapeutics resistance of human hepatocellular carcinoma. *Cancer Biology and Therapy*. 2012;13(6):435-442. doi:10.4161/cbt.19295

62. Hermann PC, Sainz B. Pancreatic cancer stem cells: A state or an entity? *Seminars in Cancer Biology*. 2018;53:223-231. doi:10.1016/j.semcancer.2018.08.007

63. Lonardo E, Cioffi M, Sancho P, et al. Metformin Targets the Metabolic Achilles Heel of Human Pancreatic Cancer Stem Cells. Hjelmeland AB, ed. *PLoS ONE*. 2013;8(10):e76518. doi:10.1371/journal.pone.0076518

64. Zinzi L, Contino M, Cantore M, Capparelli E, Leopoldo M, Colabufo NA. ABC transporters in CSCs membranes as a novel target for treating tumor relapse. *Frontiers in Pharmacology*. 2014;5 JUL. doi:10.3389/fphar.2014.00163

65. Sancho P, Barneda D, Heeschen C. Hallmarks of cancer stem cell metabolism. *British Journal of Cancer*. 2016;114(12):1305-1312. doi:10.1038/bjc.2016.152

66. Giddings EL, Champagne DP, Wu MH, et al. Mitochondrial ATP fuels ABC transporter-mediated drug efflux in cancer chemoresistance. *Nature Communications*. 2021;12(1):1-19. doi:10.1038/s41467-021-23071-6

67. Ribas V, García-Ruiz C, Fernández-Checa JC. Glutathione and mitochondria. *Frontiers in Pharmacology*. 2014;5 JUL. doi:10.3389/fphar.2014.00151

68. Cole-Ezea P, Swan D, Shanley D, Hesketh J. Glutathione peroxidase 4 has a major role in protecting mitochondria from oxidative damage and maintaining oxidative phosphorylation complexes in gut epithelial cells. *Free Radical Biology and Medicine*. 2012;53(3):488-497. doi:10.1016/j.freeradbiomed.2012.05.029

69. Gupta VK, Bhalla Y, Jaitak V. Impact of ABC transporters, glutathione conjugates in MDR and their modulation by flavonoids: An overview. *Medicinal Chemistry Research*. 2014;23(1):1-15. doi:10.1007/s00044-013-0612-6

70. Liu S, Yi Z, Ling M, Shi J, Qiu Y, Yang S. Predictive potential of ABCB1, ABCC3, and GSTP1 gene polymorphisms on osteosarcoma survival after chemotherapy. *Tumor Biology*. 2014;35(10):9897-9904. doi:10.1007/s13277-014-1917-x

71. Zelcer N, Saeki T, Reid G, Beijnen JH, Borst P. Characterization of Drug Transport by the Human Multidrug Resistance Protein 3 (ABCC3). *Journal of Biological Chemistry*. 2001;276(49):46400-46407. doi:10.1074/jbc.M107041200

72. ABCC3 - ABC-type glutathione-S-conjugate transporter - Callithrix jacchus (White-tufted-

ear marmoset) - ABCC3 gene & protein. https://www.uniprot.org/uniprot/F7I1G5. Accessed October 13, 2021.

CHAPTER II /CAPÍTULO II

CHAPTER II.

Generation of nanobodies that target ABCC3

INTRODUCTION

Antibodies (Abs) are proteins present in plasma and extracellular fluids. They are produced in response to foreign molecules and organisms as principal effectors of the adaptive immune system[1]. They can bind to an antigen with high affinity, selectivity, and specificity.

Conventional immunoglobulin G (IgG) Abs are glycoproteins produced and secreted by specialized B lymphocytes. They are also referred to as immunoglobulin, and four polypeptides form them. They are composed of two identical heavy (H; ~55 kDa) and two light (L; ~25 kDa) chains held together by disulfide and noncovalent bonds. The complete Ab's molecular weight is around 150 kDa, and they shape a Y structure. Each chain contains various constant (C) regions and one variable (V) joined by disulfide bonds[2]. Two parts can be distinguished (figure 1):

- **Antigen binding-domain (Fab).** They contain a binding site where they bind to the epitope.
- **Effector domain.** Consist of the fragment crystallizable region (Fc), they participate in biological functions as natural killer cell activation or phagocytosis.

Both parts of the Ab, Fab and Fc, are connected by the hinge, a region rich in proline, threonine, and serine. This component allows the movement of Fab domains to interact with the antigen[3,4].

Light and heavy chains are constituted by three hypervariable regions of 5 to 10 amino acids that form the epitope binding sites or complementarity-determining regions (CDRs), and some constant and conserved regions[1], known as framework regions (FRs).

The use of Abs has been increased since the last decades; due to their characteristics to recognize and bind different antigens, they have been used in several biomedical applications as well as in the diagnosis and treatment of different diseases[5].

By genetic modifications, different Ab-derived fragments can be obtained, such as $F(ab')_2$, Fab, single chain fragment variable (scFv), minibodies, and diabodies (Db). Those fragments have the same affinity and selectivity but different sizes[6].

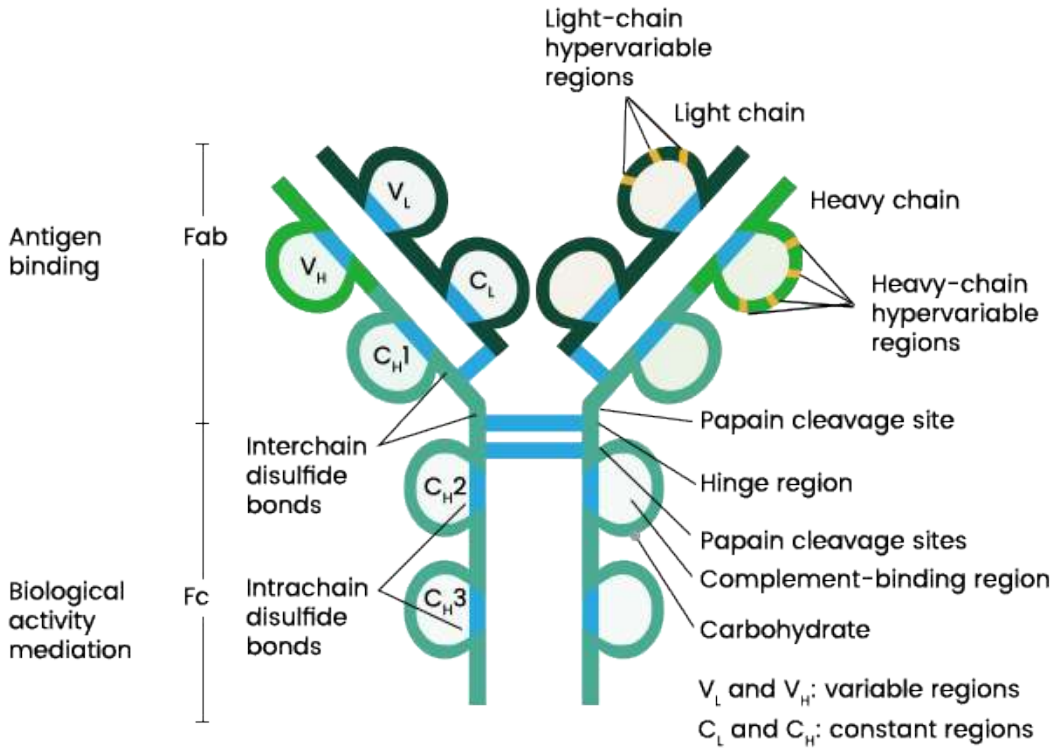

Figure 1. Ab structure. Description of the different parts of an Ab and the possible cutting sites to generate Ab-derived fragments. *Image taken from Janeway et al. 2021*

Nbs were discovered in 1993; although genetic engineering can generate them, they can also be generated by immunization in the Camelidae family[7].

Serum from Camelidae family contains heavy-chain antibodies (HCAbs) that lack the light chain[8]. The heavy chain of HCAbs is formed by three globular domains, the two CH2 and CH3 are highly homologous to the Fc domain of Abs, but CH1 is missing[9]. Thus, in the case of HCAbs, the Fab fragment is reduced to a single variable domain (VHH). Nbs obtained by Camelidae immunization correspond to the VHH regions.

VHH domain from HCAbs is functional when expressed independently; their amino acid length ranges from 120 to 150 amino acids. VHH structure is similar to human VH; it comprises 2 β-sheets, one with four and the other with five β-strands[10]. They share several properties with HCAbs, they are pretty resistant to extreme conditions (temperature, pressure, or proteases), and due to their small size, they can reach and bind to cavities or grooves of the antigens' surface[11].

Three CDRs form Nbs to bind to their antigens; FR connects CDR regions, also FRs act as scaffolds for CDRs. CDR fractions are variable to bind different antigens, but FR regions are sequentially and structurally conserved[10].

Amino acids' median length of Nbs is 123, being the minimal 109 and the maximal 137 amino acids. FR domains are highly conserved, and their amino acids length is 25 for FR1, 18 for FR2, and 37 for FR3[12]. There are some amino acid substitutions in FR2 sequence compared to VH sequences (F37, E44, R45, G47); these changes lead to increased hydrophilicity and solubility of VHHs[13]. The length of CDRs is diverse, especially in CDR3; amino acids values of CDR are 8 for CDR1, 8 for CDR2, and 16 for CDR3 (figure 2). Sequences of VHH are larger than human VH sequences[14].

In VHHs, there is an additional disulfide bond between CDR1 and CDR3, this bond is not necessary for Nbs function, but it has been demonstrated that it stabilizes the domain and rigidifies the long CDR3, forming a stronger interaction with the antigen[13]. The Cysteine (Cys) in CDR1 is conserved, and it is proposed to play a functional role in the disulfide bond for CDR loops stabilization.

VHH characteristics are the same as an intact Ab, but their molecular weight is only 15 kDa; even more, they have high stability, enhanced hydrophilicity, and protruding CDR3 regions that permit epitope interactions and improve tissue penetration[15].

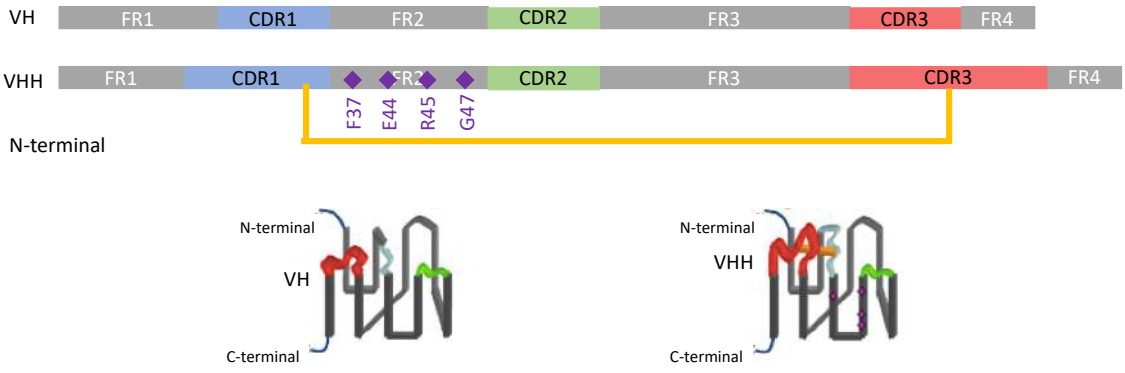

Figure 2. VH and VHH sequences and structures. Amino acid sequences of VH and VHH regions and their respective protein structures. FRs and CDRs are represented, as well as conserved aminoacids in VHH. *Image modified from Muyldermans et al. 2009.*

Nbs can be engineered and tailored for multiple applications and purposes. Due to their high selectivity and specificity, Nbs can recognize different conformations

of an antigen; this has been very useful for crystallization, protein-protein interactions, or inhibition of proteins[16]. Apart from laboratory research techniques, they have been used as diagnosis and therapeutic tools. For *in vitro* diagnosis, they result cheaply and easily for epitope detection. Moved to *in vivo* imaging, these agents are very useful due to their small size and, thus, their clearance route. Nbs present a fast clearance and reduced toxicity; they are an excellent tool for SPECT/CT or PET/CT[17] applications. As well as for its diagnosis use, they have also been tried in therapy; Nbs are good candidates for treatments due to their specificity and the ability to modify the structure of Nbs, i.e., humanization[16]. Recently, caplacizumab (ALX-0681), a bivalent Nb[18] for the treatment of patients suffering from thrombotic thrombocytopenic purpura, received approval from the European Medicines Agency (EMA) and the US Food and Drug Administration (FDA), giving domain Abs in the clinic and research a boost.

Owing to the characteristics of Nbs and their possible applications, their generation against a specific target can result in the improvement of the knowledge of molecules.

ABCC3 seems to be a candidate as a biomarker for PDAC in diagnosis and treatment, the generation of Nbs against ABCC3 can help us understand the role of ABCC3 in chemoresistance, and stemness can be used in the diagnosis of cancer by imaging tools as immuno-PET.

OBJECTIVES

We have demonstrated that ABCC3 correlates with stemness and chemoresistance in PDAC.

The goal for this chapter is the generation of Nbs against ABCC3 that could serve as diagnostic and therapeutic tools for PDAC. Nbs will be generated by camel immunization with ABCC3-overexpressing cells and selected using *Escherichia coli (E. coli)* display. Those Nbs will be validated and tested for the specific detection of ABCC3. Once selected and isolated, these Nbs will be validated and tested for the specific affinity to target ABCC3.

Therefore, the specific objectives of this chapter are:

1. Generation of a library of Nbs expressed on the surface of *E. coli.*
2. Selection of Nbs against ABCC3 by *E. coli* display.
3. Validation of the specificity of the selected Nbs against ABCC3 *in vitro*.

MATERIAL AND METHODS

Mammalian cell culture

The human cell lines CFPAC-1, IMIM-PC2, MIA PaCa-2, and A549 were grown as monolayers in Dulbecco's modified Eagle's medium (DMEM, Sigma) supplemented with 10% Fetal Bovine Serum (FBS, Gibco) and 1% penicillin and streptomycin (Gibco) at 37ºC, 5% CO_2. AsPc-1 and BxPc-3 pancreatic cell lines were cultured in Roswell Park Memorial Institute medium (RPMI, Sigma) supplemented with 10% Fetal Bovine Serum (FBS, Gibco) at 37ºC, 5% CO_2. All cell lines were obtained from Mariano Barbacid's laboratory (CNIO).

Camel immunization

Camel immunization was performed by Carlos Gutiérrez y Juan Alberto Corbera at University of Las Palmas de Gran Canaria.

Before the immunization, serum from the animal was collected and stored at -80ºC. 10^8 cells of T98G-CMV-ABCC3 (ABCC3-overexpressing cells) were resuspended in 2 ml of 4-(2-hydroxyethyl)-1-piperazineethanesulfonic acid

(HEPES). The injection was prepared by mixing the cells with the Gerbu adjuvant (Gerbu Biotechnick) and injected intramuscularly in multiple points the triceps. 6 immunizations were performed every 7 days. After the 6^{th} immunization, the serum from the animal was collected and stored at -80ºC. Also, 50 ml of blood was collected for lymphocytes isolation for VHH amplification and cloning of the library.

Bacterial strains, growth and induction conditions

E. coli strains used in this work are listed in Table 1. *E. coli* EcM1 bacteria carrying pNeae vector with VHH gene were grown at 30ºC in Luria Broth (LB) liquid medium with chloramphenicol (Cm) for plasmid selection in static conditions. LB plates and pre-inoculum media contained 2% (w/v) glucose for *lac* promoter repression. E. coli WK6 carrying pHEN6 vector with VHH gene were grown at 28ºC in LB medium with ampicillin (Amp) for plasmid expression in dynamic conditions.

Table 1. *E. coli* strains

Name	Genotype and properties	Reference	Use
***E. coli* K-12 strains**			
DH10B-T1^{R}	F^{-} *mcrA* Δ*mrr-hsdRMS-mcrBC φ80lacZDM15 ΔlacX74 recA1 endA1 araD139* Δ*(ara, leu)7697 galU galK rpsL (StrR) nupG tonA λ*$^{-}$	Invitrogen	Cloning
EcM1	MG1655Δ*fim*A-H	19,20	VHH display
WK6	*Δ*(*lac-proAB*), *galE*, *strA*, *nal*, F'[*lacI*^{q}*Z* ΔM15, *proAB*]	21	VHH production

Table 2. Plasmids.

Plasmids			
pNeae	(Cm$^{R)}$,pAK-Not-derivative; Intimin$_{EHEC}$ (1-654)-E-myc tag for cloning V_{HH}	19	VHH display
pNV$_{ABCC3(n)}$	pNeae-derivative; Display of V$_{ABCC3}$(n) clone in Intimin$_{EHEC}$ (1-654)-E-V$_{ABCC3(n)}$-myc	This work	VHH display
pHEN6	(Ap^{R}), pUC- and M13-ori, PelB, pIII; Periplasmic expression of Nbs with 6xHis-myc-tags	22	VHH periplasmic expression
pHEN6-V$_{ABCC3(n)}$	pHEN6-derivative; for periplasmic expression of Nb V $_{ABCC3(n)}$ with 6xHis-tag	This work	VHH periplasmic expression
pLentiCas9-Blast	(Ap^{R}), FUGW-H1 derivative; Cas9 expression	Addgene	Cas9 expression

pKLV-U6gRNA-EF(BbsI)-PGKpuro2ABFP	(Ap^R), pBluescript-derivative; gRNA expression	Addgene	gRNA expression
pKLV-U6sgRNA$_{ABCC3\#2}$-EF(BbsI)-PGKpuro2ABFP	(Ap^R), pBluescript-derivative; sgRNA$_{ABCC3\#2}$ expression	This work	sgRNA$_{ABCC3\#2}$ expression

Lymphocytes isolation

Blood samples were received, processed and lymphocytes isolates by Yago Margolles from Dr. Luis Ángel Fernandez laboratory from the Microbial biotechnology group at CNB, Madrid.

Blood samples from the camel were obtained after 42 days of immunization with cells. The whole blood sample was lysed using 1X Lysis buffer (0.15 M NH_4Cl, 1 mM $KHCO_3$, and 0.1 mM K_2EDTA, ratio 1:10) for 7 min at RT. Then, the reaction was stopped using 1X PBS. Subsequently, the sample was centrifuged at 1000 x g for 15 min at 4 ºC. The supernatant was discarded, containing red blood cells and lysates. Later, lymphocytes were washed with 1x PBS and further processed.

Total RNA from lymphocytes was extracted with the TRIzol kit (Life Technologies) according to the manufacturer's instructions. 1 µg of total RNA was used for cDNA synthesis with SuperScript II reverse transcriptase (Life Technologies) and random hexamers.

Plasmids and oligonucleotides

Plasmids used in this work are summarized in Table 2. The *E. coli* DH10B-$T1^R$ strain was employed for plasmid propagation and cloning experiments. DNA constructs were sequenced by the Sequencing Unit at the CNIO. PCR reactions for cloning were performed with Taq polymerase (NZYtech) using the indicated PCR programs for each purpose. Oligonucleotides are listed in table 3 and were commercially synthesized (Sigma).

pNeae and pHEN6 (figure S1) plasmids were digested with *SfiI* for 2 h at 50ºC and with *NotI, PstI,* or *BstEII* for 2 h at 37ºC.

The plasmid pNeae, present chloramphenicol resistance (Cm^R) and carries the *lacI* and *lac* promoter region, controlling a gene fusion between intimin residues 1–654 (from EHEC O157:H7 strain EDL933*stx*-) followed by the E-tag (GAPVPYPDLEPA) and a C-terminal myc-tag (EQKLISEED)[19].

pNeae plasmid and derivates were prepared from bacteria harvested from LB-Cm-glucose plates and electroporated into *E. coli* EcM1 strain for selections.

pHEN6 plasmid contains ampicillin resistance (Amp^R) and a tail of 6 Histidines (His Tag) that will be placed after the VHH for its purification with Nickel.

pHEN6 plasmid ad derivates were prepared from bacteria harvested from LB-Amp plates and electroporated into *E. coli* WK6 strain for VHH production.

Table 3. Oligonucleotides

Name	Sequence (5'-3')	Reference
sgABCC3 #2 Forward	CACCGTACCTGCGGCACCATTGTCGGT	This work
sgABCC3 #2 Reverse	TAAAACCGACAATGGTGCCGCAGGTA	This work
sgRNA NT Forward	UUAUGCCGAUCGCGUCACAUU	24
sgRNA NT Reverse	UGUGACGCGAUCGGCAUAAUU	24
VHH-SfiI	GTCCTCGCAACTGCGGCCCAGCCGGCCATGGCTCAGGTGCA GCTGGTGGA	25
VHH-NotI	GGACTAGTGCGGCCGCTGAGGACACGGTGACCTGGGT	25
pAK-direct	GTGACGCAGTAGCGGTAAACGGCAGAC	25
38	GGACTAGTGCGGCCGCTGGAGACGGTGACCTGGGT	26
A6E	GATGTGCAGCTGCAGGAGTCTGGAGGAGG	26
Forward Primer (FP)	CGCCAGGGTTTTCCCAGTCACGAC	26
Reverse Primer (RP)	TCACACAGGAAACAGCTATGAC	26

Library construction

The pool of amplified VHH was amplified from cDNA of lymphocytes by using VHH-SfiI and VHH-NotI following the next PCR program: 6 minutes at 95ºC, 32 cycles of 30 s at 94ºC, 30 s at 80ºC and 45 s at 72ºC, finally 10 min at 72ºC. For

library construction, the amplified VHHs were cloned into pNeae and electroporated in *E. coli* DH10B-T1^{R}; the library size was determined by colony-forming unit (CFU) counting. Electroporation was performed by mixing the ligation reaction with competent cells; in a cuvette of electroporation, a pulse of 2,5KV was applied for 3 s, then 1 ml of pre-warmed super optimal broth (SOC) was added, transferred to a tube, and incubated 1 h at 37ºC. Bacteria were plated in LB-Cm plates.

Nbs cloning for purification

Each selected individual clone was amplified, followed by the previous PCR program described, sequenced, excised from pNeae by *SfiI* or *PstI* and *BstEII,* and recloned into pHEN6 vector. Plasmid derivatives of pHEN6 with cloned VHH in *Sfi*I-*BstEII* or *PstI-BstEII* sites were employed for periplasmic expression of soluble Nbs into *E. coli* WK6 strain[21].

VHH amplificated products in pNeae were purified by using PCR purification kit (Qiagen) following the manufacturer's instructions. VHH purified products were digested with *SfiI* O/N at 50ºC followed by *PstI* or *BstEII* digestion O/N at 37ºC. The ligations were carried out by adding 3:1 ratio of insert:vector with T4 DNA ligase (NZYTech) for 3 h at RT. Bacterial transformation was performed by heat shock. 5 µl of the ligation was added to 100 µl of DH10B competent bacteria; then, cells were incubated 5 min on ice, 150 s at 42ºC, and 2 min on ice. 900 µl of LB media was added, and bacteria were incubated for 1 h at 125 rpm at 37ºC. Finally, bacteria were plated in LB-Ampicillin plates. Individual colonies were grown in LB-Ampicillin, O/N at 37ºC and 150 rpm. DNA extraction was performed by using QIAprep spin miniprep kit (Qiagen) following manufacturer instructions.

Nbs induction

For VHH induction in pNeae plasmid, bacteria were obtained from the pool of clones, in the case of libraries, or from individual colonies.

Bacteria were freshly grown and harvested from plates, diluted to an initial optical density $(OD)_{600}$ of 0.5, and grown in 50 ml of LB media with Cm and 1 mM isopropylthio-β-D-galactoside (ITPG) overnight (O/N) without shaking.

For over-expression of soluble VHH in the periplasm, *E. coli* WK6 cells with pHEN6 plasmid were grown to an OD_{600} of 0.6-0.8 in 660 ml of Terrific Broth with Amp and induced O/N at 28ºC, 180 rpm with 1mM IPTG.

Selection of *E. coli* display VHH libraries on cells

For the cell surface selection with *E. coli* display library, A549 and A549-Cas9 sgABCC3 were used for positive and negative selection, respectively.

A549 and A549-Cas9 sgABCC3 cell lines were grown as monolayers in 6-well culture plates (Nunc) containing culture media to a confluency of ∼60%, i.e., $\sim 10^6$ cells, and washed with Phosphate Buffer Saline (PBS, Sigma). Induced *E. coli* bacteria (equivalent to a final OD_{600} of 1) were harvested by centrifugation (4,000 x g, 5 min) and washed with 2 ml PBS. Washed bacteria (1 ml; $\sim 6 \times 10^7$ bacteria) were added to wells containing A549-Cas9 sgABCC3 #2 (negative selection) and incubated for 1 h at 37ºC. After incubation, the unbound bacteria were recovered and then added to wells containing A549 cells, incubated 30 min at 37ºC (for the first selection) or 15 min at 37ªC (other five selections). Next, A549 cells were washed 3 times with 1 ml PBS to remove any non-specifically bound bacteria and subsequently lysed with PBS supplemented with 0.5% Triton X-100 and 0.1% DNase. Serial dilutions of the cell lysate containing bacteria were plated to CFUs of bacterial recovered after the procedure, the rest of the culture was plated for recovering, and continued with the following selections. The process of selection consisted of 6 rounds for a specific method (figure 3).

Purification of Nbs from the periplasm of *E. coli*

Soluble Nbs with His Tag in their C-termini were induced in the periplasm of *E. coli* WK6 cells carrying pHEN6. Bacteria were harvested by centrifugation (4000 x g, 10 min, 14ºC) from 660 ml cultures, resuspended in 8 ml TES 4X buffer (Tris-EDTA-SDS), and incubated at 4ºC, 180 rpm for 1 h. 16 ml of TES 1X were added

and incubated at 4ºC, 180 rpm, 2 h. The periplasmic extract was obtained by adding 200 µl $MgCl_2$-hexahydrate 2M and centrifugation (10,000 x g, 30 min, 4ºC). And finally, the supernatant was dialyzed in 2 steps of 2h, and O/N at 4ºC against 5 L of PBS 1X. Dialyzed extract was loaded onto a Nickel-containing affinity resin (GE Healthcare), washed with PBS 1X, and bound protein eluted in 0.5M imidazole in PBS 1X using ÄKTA protein purification system (Sartorius). Fractions collected from purification were loaded onto an SDS-PAGE, and fractions corresponding to the monomeric Nbs (apparent molecular mass of 11-15 kDa) were collected. Eluted Nb was dialyzed against PBS 1X, in 2 steps of 2h, and O/N at 4ºC. Protein concentration was estimated using Bradford Reagent (Biorad) following manufacturer instructions. Briefly, 200 µl of Bradford reagent was added to several bovine serum albumin (BSA) dilutions, used as standards, and 2 µl of protein, after 10 minutes of incubation, the absorbance was read at 595 nm.

Analysis of Nbs specificity by flow cytometry.

Cells were washed with 1 ml PBS and collected with 10mM-EDTA in DPBS. 4 z 10^5 cells were blocked with 1% BSA in PBS and incubated with different amounts of the Nb (0.25, 0.5, 1, 2.5, 5, 10, and 20 µg) for 30 min, 4ºC. After incubation, the cells were washed once with 500 µl PBS and resuspended in 100 µl 1% BSA-PBS containing anti-His Tag Ab (Bio X-Cell, 1:1500). The cells were washed twice with 500 µl PBS and resuspended in 100 µl 1% BSA-PBS containing goat anti-mouse-APC Ab (Biolegend, 1:1500) and incubated 30 min at 4ºC. Then, cells were washed twice with 500 µl PBS, and the pellet was resuspended in 500 µl of 0.5 mM EDTA-PBS. For each experiment, at least 10^5 cells were analyzed in a Gallios flow cytometer (Beckman Coulter).

Immunofluorescence analysis of Nbs

Cells were seeded (~3 × 10^4 cells/well) and grown on sterile coverslips (13 mm diameter, VWR International) placed at the bottom of the wells in 24-well tissue culture plates for 24 h. The wells were washed with 1 ml PBS. Coverslips were blocked for 30 min with 500 µl 5% BSA in PBS and then incubated with Nb (10

µg) at 4ºC, O/N in a wet chamber. The coverslips were washed 3 times with 1 ml of PBS and incubated with anti-His Tag Alexa Fluor 647 (1:1500, Biolegend) at 4ºC for 30 minutes in a wet chamber. Next, coverslips were washed with PBS, water and mounted with Prolong (Invitrogen) on glass slides. The samples were visualized using widefield fluorescence microscopy (Leica AF6000).

The fixation step was skipped due to the inefficient binding of Nbs to ABCC3 epitopes in fixated cells. Immunofluorescence staining was performed in fresh samples.

Nbs binding imaging acquisition by Incucyte Sx5 system

Cells were seeded (~3 × 10^4 cells/well) in 96-well plates for 24 hours. 10 µg of Nb were incubated with anti-His Tag Alexa Fluor 647 (1:1500, Biolegend) for 30 minutes at 4ºC. Next, the mixture of Nb-His Tag-Alexa Fluor 647 was added to the cells. Phase contrast and near-infrared light images were acquired every 15 minutes for the first 2 hours and then every 2 hours in Incucyte SX5 (Sartorius) to determine Nbs binding to cells.

Protein extraction, SDS-PAGE, and Western Blot analysis

For protein isolation, cells were harvested in NP40 buffer (Sigma) supplemented with a protease inhibitor cocktail (Roche Applied Science).

Bacterial extracts were centrifugated (4,000 x g, 5 min, 4ºC), resuspended in 300 µl NP40 buffer, and sonicated by ultrasound (45 s at 65% power and 2 min reposing). Finally, the supernatant was taken from centrifugation (13,000 x g, 20 min, 4ºC).

50 µg of protein extracts were mixed with the same volume of SDS-sample buffer (Laemmli, 2X, Sigma), boiled fat 95ºC or 10 min, and loaded onto 12% SDS-PAGE gels and run using Running buffer (SDS-Glycine-Tris, Fisher Reagents). Proteins were either stained with Coomassie or transferred to a polyvinylidene difluoride (PVDF) membrane (Millipore).

Coomassie staining: Acrylamide gels were incubated with Staining buffer (0.1% (w/v) Coomassie blue R350 (v/v) methanol, 10% (v/v) acetic acid) for 30 min at RT with shaking. Then, gels were washed with De-staining buffer (50% (v/v) methanol, 10% (v/v) acetic acid in water) for 30 min and O/N at RT with shaking. Finally, gels were conserved in Storage solution (5% acetic acid in water).

Immunoblotting: Acrylamide gels were transferred to PVDF membranes O/N at 4ºC using Transfer Buffer (Glycine-Tris, Fisher Reagents). Membranes were sequentially blocked with 1X PBS containing 5% BSA; w/v and 0.1% Tween20 (v/v), incubated for specific detection of His-tagged proteins with Anti-His Tag Ab O/N, 4ºC (1:1000, Bio X-Cell), washed 3 times with 1X PBS containing 0.1% Tween20 (v/v), incubated with goat anti-mouse (1:15000, Licor), and washed again to remove unbound Ab. Bound Ab complexes were detected by using Odyssey (Licor Biosciences).

RESULTS

Immunization and construction of the *E. coli* display VHH library

We pointed out ABCC3 as a new possible biomarker of PDAC. Due to its involvement in drug resistance and stemness, we decided to generate Nbs against ABCC3 that could be used as a diagnosis and therapeutic tool.

For the generation of Nbs, we immunized camels with alive cells overexpressing ABCC3 (T98G-CMV-ABCC3).

Nbs were generated by camel immunization, serum from the animal was collected before the first injection of cells and stored at -80ºC (pre-immunization serum). The camel was immunized with 10^8 cells that overexpress ABCC3 once a week for 6 weeks, and the injections were administered intramuscularly in the triceps. Serum from the animal was collected 7 days after the last immunization and stored at -80ºC (post-immunization serum).

To check the immune response of the camel to the cells, we assayed the immunoreactivity of the pre-and post-immunization sera in cells expressing and not expressing ABCC3. The experiments were carried out by adding pre- or post-immunization serum to the cells. After the incubation with the serum, we added protein A conjugated to Alexa Fluor 647, which binds to Fc regions of Abs present in the serum.

First, we incubated sera with the cells used for the immunization, T98G-CMV-ABCC3. The incubation with the pre-immunization serum showed low fluorescence, corresponding to low binding of Abs present in the serum, corresponding to the basal levels of camel Abs. With the incubation with the post-immunization serum, protein A fluorescence was higher, demonstrating that the camel's immune system had generated Abs against the target cells (figure 1A).

Camel has produced a response against the cells that were used for the immunization. To determine if the camels specifically generated a response against ABCC3, we analyzed the pre-and post-immunization serum to A549 wild-type (WT), and ABCC3-deficient cells generated by CRISPR/Cas9 means A549-Cas9 sgABCC3 cells. A549 is a cell line derived from a lung carcinoma with one of the highest levels of ABCC3 described; it was used as positive control. We generated ABCC3 knock-out (KO) by CRISPR-Cas9 system as negative control

of ABCC3 expression. Abs from the serum were bound to A549 WT cells that express ABCC3 more than A549-Cas9 sgABCC3 cells, indicating that the camel generated Abs against ABCC3 (figure 1B).

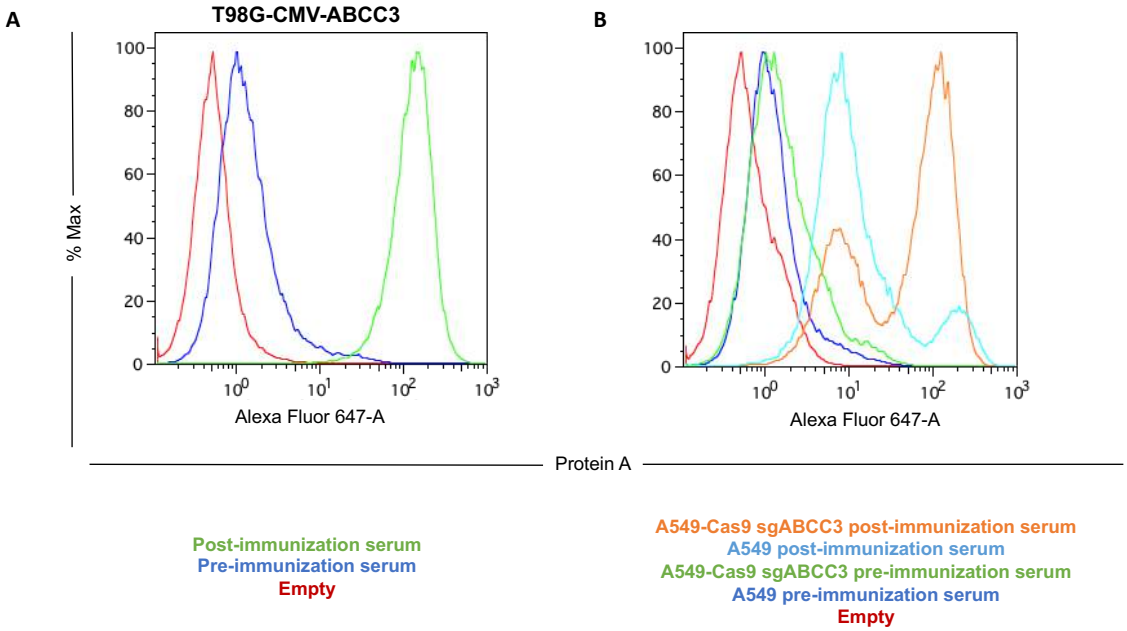

Figure 1. Evaluation of camel immunization by flow cytometry. Validation of camel serum bound to protein A in cells expressing and not expressing the antigen, ABCC3. **A)** Validation of sera in cells used for the immunization (T98G-CMV-ABCC3). **B)** ABCC3 specific validation of sera in WT and KO cells of ABCC3 in A549 cell line.

Once the serum was tested and validated, we started the generation of a Nbs library. 7 days after the 6th immunization in the camel, the serum was extracted, and serum lymphocytes were isolated by density gradient. RNA was isolated from these cells and retrotranscribed to cDNA. The pool of VHH gene segments was amplified from lymphocytes cDNA and cloned in a phagemid vector, generating a library size of 10^8 independent clones.

Once the library was generated for the E. coli display, the VHH regions had to be recloned in pNeae plasmid. The VHH gene segments were excised from the pool of phagemid DNA by the digestion with *SfiI* and *NotI* restriction enzymes; then, they were cloned into the same sites of *E. coli* display vector pNeae (Figure 1A, B, C, and D).

pNeae is a plasmid that fuses VHH sequences to the C-end of intimin polypeptide Neae[27]. NVHH fusion polypeptide includes 2 epitope tags flanking the VHH

domain for immunodetection, E and myc-tag (Figure 2F and G). Intimin is a virulence factor expressed on the outer membrane of some *E. coli* strains; by the fusion of intimin and VHH, the Nb can be expressed outside of the bacteria to recognize its antigen.

The selection of Nbs is going to be performed on the cell surface. For that purpose, bacteria need to reach the cells for the recognition of the antigens by Nbs, which are displayed in the *E. coli* surface by pNeae plasmid. Thus, the library with the pool of VHH regions was transformed in *E. coli* strain EcM1 (figure 1E). EcM1 strain has a deletion of the fimA-H operon encoding type 1 fimbriae, a natural adhesion involved in the recognition of mannosylated glycoproteins in epithelial cell surfaces. By losing fimbriae, the flagella are more motile, and the bacteria have an improved ability to move[28].

The final number of clones for this library was 2.7 x 10^8 independent clones. This size of the library is similar to the usual complexity of clones obtained by *E. coli* display; the usual range is 10^7 to 10^9 CFUs.

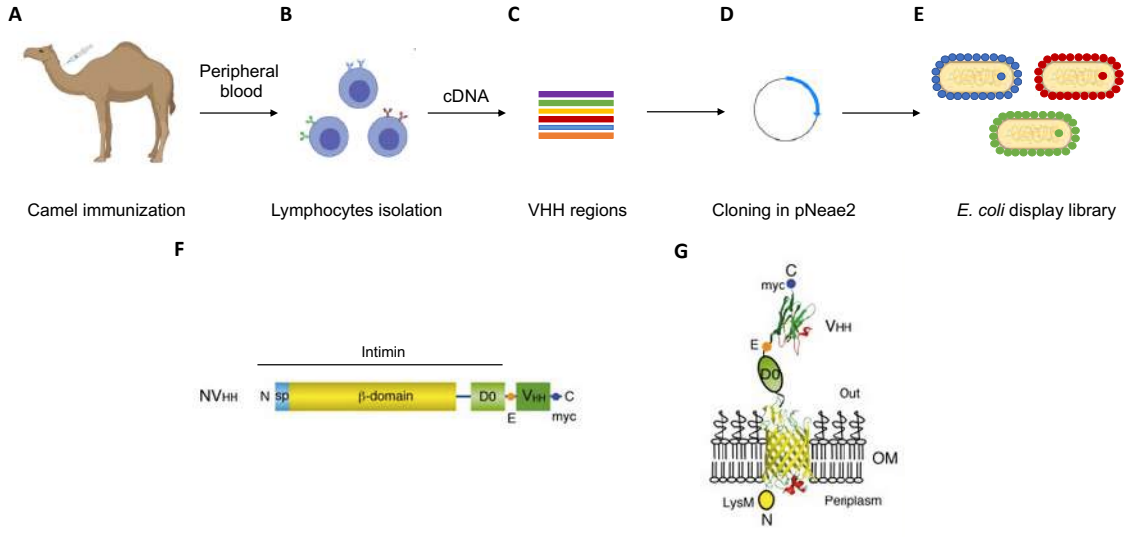

Figure 2. Generation of a Nb library in *E. coli* from camel immunization. Description of the steps to obtain the Nbs library in *E. coli.* **A)** Camel immunization with tumoral cells for 6 weeks. **B)** Lymphocytes isolation from camel blood. **C)** Amplification of cDNA of VHH regions from lymphocytes. **D)** Cloning of VHH regions into pNeae2 plasmid for Nbs expression. **E)** Expression of pNeae2 plasmid in the outer membrane of *E. coli.* **F)** Scheme of Intimin and VHH fusions, showing N-terminal secreted passenger (SP), LysM and β-domain, D0 Ig-like and VHH region. **G)** Model of VHH and intimin fusion in the outer membrane, with N-terminal LysM domain in the periplasm, β-barrel with linker in the outer membrane, and connecting with C-terminal D0 and

VHH domains exposed to the extracellular milieu. The E-tag and myc-tag epitopes flanking the VHH domain are indicated. *Image modified from Salema et al.*[28]

Selection of Nbs

The library contains around 10^8 clones with Nbs expressed in *E. coli* cells. While assesing Nbs library diversity still needs to be done, the pool of EcM1 bacteria expresses in the outer membrane different Nbs targeting diverse antigens. To isolate specific Nbs that recognize ABCC3, we performed a screening.

Typically, the selection of Nbs is performed using the target purified protein[28], in this case, ABCC3 is a very large transmembrane protein with no crystal structure available, and it is difficult to purify. For this reason, we performed the selection using ABCC3-overexpressing cells as previously described by Salema et al.[25].

The selection process on cell surface antigens consists of cycles of negative and positive, respectively. The negative selection consists of incubating bacteria with A549-Cas9-sgABCC3 cells that do not express ABCC3 for 1 hour at 37ºC. In this process, unspecific bacteria and those specific against other antigens will be bound to the cells and retained (figure 3A). After this incubation, the supernatant is collected and added on top of A549, which present high levels of ABCC3, for 15 minutes at 37ºC (figure 3B). In this selection, specific bacteria are going to bind to the cells. After 3 washes with PBS to remove all the unspecific bacteria, we collected bacteria by detaching cells with PBS-triton-DNase and plating them in LB-Cm-Glucose plates (figure 3C). Six rounds of selection followed this process.

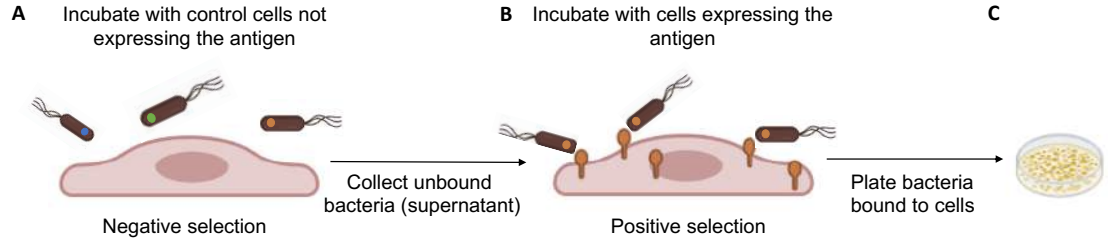

Figure 3. Nbs selection on cell surface antigens. A) Negative selection of bacteria with cells that do not express the antigen for 1 hour at 37ºC. **B)** Positive selection of bacteria collected from the supernatant from negative selection with antigen-expressing cells expressing the antigen for 30 minutes at 37ºC. **C)** Plating of bacteria bound to cells.

In parallel, we tested a new variation of this method to select Nbs. It consists of negative and positive selections, remaining the negative selection the same (figure 4A). However, for the positive selection, we put the supernatant in contact with a mixture of 90% of A549-Cas9 sgABCC3 cells and 10% of A549 cells for 15 minutes in a tube at 37ºC (figure 4B). With this step, we avoid the binding of the bacteria to the surface of the plate, and we add an extra selection with a high percentage of cells that do not express the antigen. After this time, we stained ABCC3 protein with an intracellular Ab (MRP3 Ab, clone M3II-9), and then we sorted positive cells by fluorescence-activated cell sorter (FACS). We generated a three-part structure; the first component is A549 cells, the second is the bacteria bound to ABCC3 on the cell surface, and the third is an intracellular ABCC3 Ab, by indirect fluorescence detection, bound inside A549 cells (figure 4B). By staining ABCC3 with the intracellular Ab, only the positive cells were selected by FACS. Sorted cells were covered mainly with bacteria expressing Nbs that recognize ABCC3. Finally, we plated positive ABCC3 cells with the specific bacteria bound. Six rounds of selection repeated this process.

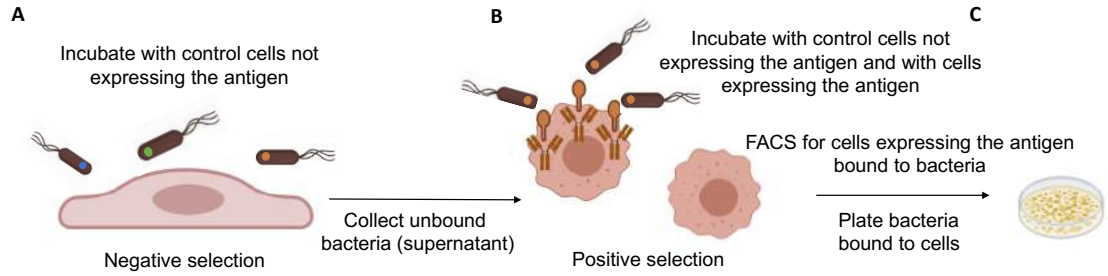

Figure 4. Nbs selection by FACS. A) Negative selection of bacteria with cells that do not express the antigen for 1 hour at 37ºC. **B)** Positive selection of bacteria collected from the supernatant of negative selection with a mix of cells that do express and cells that do not express the antigen (90:10 ratio) for 30 minutes at 37ºC. **C)** FACS for selecting cells that express the antigen with bacteria bound and plating bacteria bound to cells.

From the two methods of selection, different clones were obtained. Six rounds of selection were performed for each method. During the first rounds, the number of clones obtained has to be low, indicating that unspecific and non-ABCC3-targeting Nbs in bacteria are discarded, and our desired clones are selected and enriched. Around the 4th round of selection, the percentage of bacteria bound to

cells increases, suggesting an enrichment of the specific bacteria against our protein of interest.

While these experiments should be performed multiple times, including the selection of other antigens. Comparing the two selection methods, we can observe that the plating selection is irregular in terms of the number of bacteria bound to the cells, but we can observe that there is a selection in the first rounds of selections (11 % of bound bacteria) and an enrichment in the last ones (figure 5A-B). In the case of the selection by FACS, the first rounds of selections decreased the number of specific bacteria (0.01% of bound bacteria), and from the 4th selection, there is an enrichment of these positively selected clones (figure 5A-B).

We performed 6 rounds of selection. At this point, we obtained a pool of different clones; we validated those clones individually to look for the one that is more specific against ABCC3. The validation is performed by incubating 1 hour at 37ºC for each individual clone with negative cell lines (Cas9 sgABCC3) and positive cell lines (expressing ABCC3; figure 5C) after the incubation cells are observed by the microscope to determine if there was a binding of bacteria to the cells or not.

24 clones were picked to test either from plating or sorting selection. Only 4 plating clones were validated against negative and positive cell lines, and the 24 sorting clones were validated; all clones binding was tested ABCC3-expressing and ABCC3-deficient cells in A549 and A549-Cas9 sgABCC3 (selection cell line), T98G, and T98G-Cas9 sgABCC3 (immunization cell line), and IMIM-PC2 and IMIM-PC2-Cas9 sgABCC3 (PDAC cell line).

The modified selection method by FACS increased the specificity of the selection and gave better results in terms of the percentage of bound bacteria and specificity of individual clones.

A

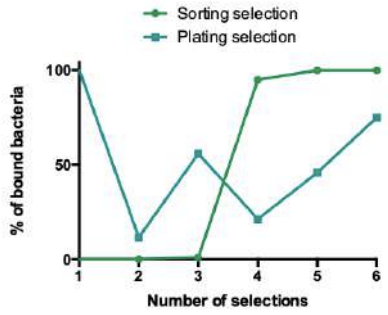

B

Round	Input bacteria to A549-Cas9 sgABCC3 #2 cells (CFU)	Bacteria bound to A549 cells (CFU)	%
Sorting round 1	60000000	6500	0.01
Sorting round 2	60000000	6100	0.01
Sorting round 3	60000000	565800	0.94
Sorting round 4	60000000	276250	0.46
Sorting round 5	60000000	57000000	95.00
Sorting round 6	60000000	90000000	150.00
Plating round 1	60000000	60000000	100.00
Plating round 2	60000000	6975000	11.63
Plating round 3	60000000	33500000	55.83
Plating round 4	60000000	12730000	21.22
Plating round 5	60000000	27500000	45.83
Plating round 6	60000000	45000000	75.00

C

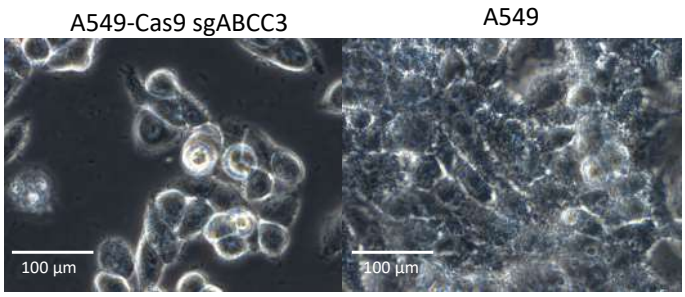

Figure 5. Validation of Nb individual clones. A) % of bacteria count in plating and sorting selection. **B)** % of bacterial binding from plating and sorting selections. **C)** Images of the validation of individual Nb clones in A549 and A549-Cas9 sgABCC3 cells.

Sequence of Nbs

Several Nbs against ABCC3 have been identified, selected, and validated. For testing Nbs in different cell lines, we needed to purify them. The purification is performed taking advance of a 6x histidine tail (His Tag) introduced at the Nb C-terminus by cloning the Nb into the pHEN6 plasmid. This tail favors its retention in a Niquel column. Depending on the restriction sites of the final sequences, the Nbs were amplified and digested either with *PstI/BstEII* or *SfiI/BstEII* and ligated (figure 6A-C).

Different clones were sequenced to corroborate the cloning and obtain each Nb sequence (figure 7A). FRs are conserved and differ in CDRs, which are characteristic of each Nb for epitope recognition.

The four plating Nb clones were sequenced, and they were different from each other. In the case of sorting selected Nbs, 24 clones were sequenced, 20 of 24 Nb clones had identical sequences. By the selection method, as it was mentioned before, the process consists of selecting the specific Nbs in the first rounds and

enriching the selected ones in the last rounds. This sequence results confirm that the FACS selection method worked better to obtain Nbs against ABCC3.

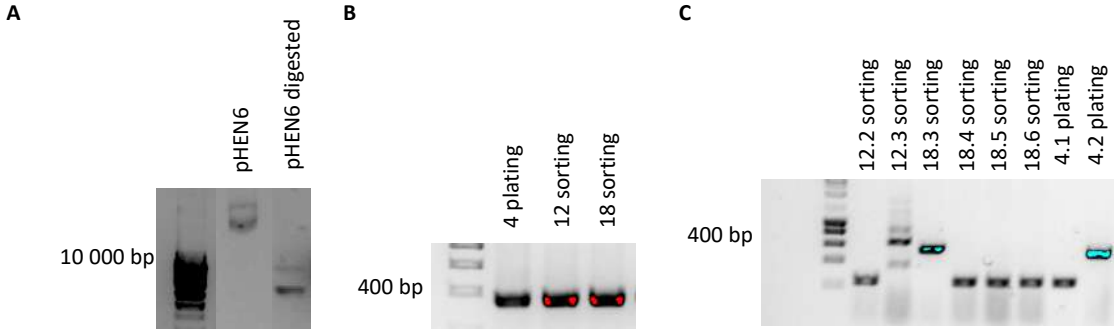

Figure 6. Cloning of Nbs from pNeae2 to pHEN6. A) Digestion of pHEN6 with SfiI and PstI. **B)** Amplification of Nbs in pNeae2 with *SfiI* or *PstI* and *BstEII*. **C)** Amplification by PCR of Nbs in pHEN6 with FP and RP primers.

Purification of Nbs

Nbs were cloned in pHEN6 to introduce a histidine tag and transformed into the WK6 *E. coli*, allowing the overexpression of soluble VHHs in the periplasm.

The process started with the growth of WK6 carrying pHEN6-VHH plasmid for 4 hours at 37ºC in agitation, then the expression of the VHH was induced with IPTG overnight (O/N) at 28ºC in agitation. The following day, the culture was centrifuged, and the pellet was resuspended in Tris-EDTA-Sucrose (TES) buffer, which disrupts the outer membrane of the cells. When cells were broken, they were centrifuged to separate the content of the periplasm from the rest of the cells. The supernatant is taken and passed through ÄKTA purification system (Cytiva) for VHH isolation. ÄKTA is a liquid chromatography system; the sample will move through the column, proteins with nickel affinity will be stacked in the column, and those that do not have nickel affinity will be cleared. Finally, by imidazole elution, we will obtain different fractions depending on the affinity to Nickel due to the concentration of imidazole by applying a gradient (figure 8A).

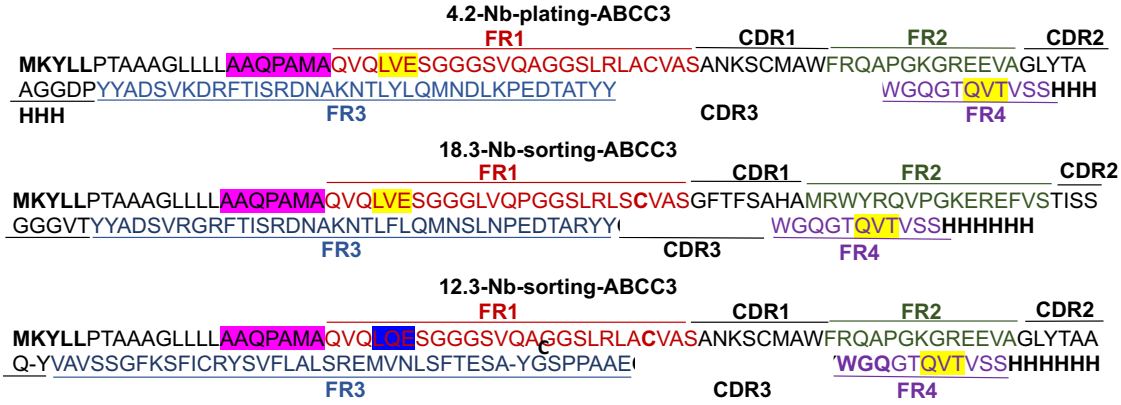

Figure 7. Sequences of Nbs clones. Different parts of Nbs are described and indicated, such as FRs and CDRs.

As observed in figure 8C by Coomassie staining and by immunoblotting of histidine in figure 8D, we can follow all the purification processes; in the pre-induction culture, there were not so many proteins in the periplasm, and with the IPTG induction, there is a considerable increase in proteins expressed on this bacterial space. A high amount of proteins remained in the pellet after the lysis and centrifugation, and we only have those present in the periplasm.

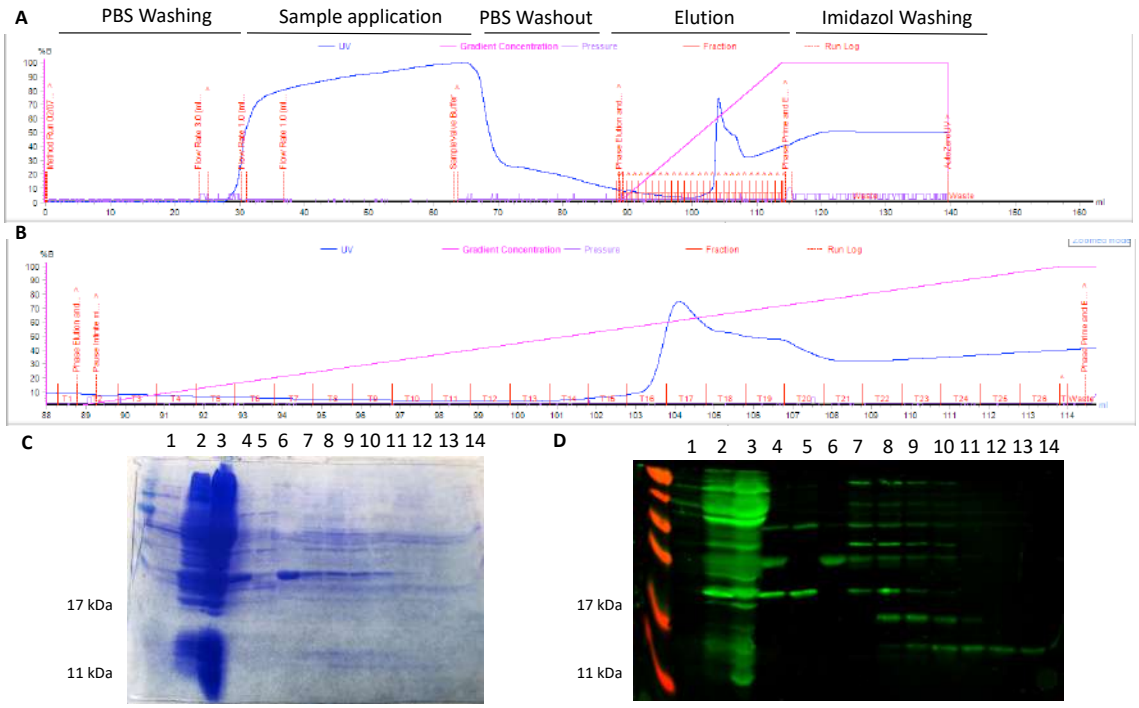

Figure 8. Purification of Nbs process. A) ÄKTA purification profile. **B)** Elution stage zoom. **C)** Coomassie staining and **C)** anti-Histidine staining of process fractions. *1: Pre-induction culture; 2: Post-induction culture; 3: Pellet ultracentrifuge; 4: Dialysis; 5: Sample application; 6: Washout;*

7: Fraction 16; 8: Fraction 17; 9: Fraction 18; 10: Fraction 19; 11: Fraction 20; 12: Fraction 21; 13: Fraction 22; 14: Elution imidazole 2M.

In the ÄKTA purification process, the Nickel column was washed with PBS to equilibrate; then, the sample was applied by flow. After this application, the column was washed with PBS to wash out those unspecifically bound proteins to the column. For the elution process, to displace the proteins bound to the nickel column, we generated an increasing imidazole gradient to separate proteins according to their affinity (figure S2). We collected several fractions, around 23 to 26, eluted by different concentrations of imidazole. In liquid chromatography systems, there is an ultraviolet (UV) laser that measures the absorption of the different components of the sample. In our case, attending to the fractions 1-16, the UV spectra did not show any signal, so no proteins were eluted at these concentrations. Around 60% of imidazole started appearing a peak in the UV; this peak corresponds to proteins bound to the column and comprises fractions 16 to 19. From fraction 20 to 26 there is still a signal in the UV laser until the imidazole concentration reaches 100%, which is 0.5M (figure 8B). As the UV laser did not return to 0, there still were proteins bound to the column; we increased the imidazole concentration to 2M and washed to elute every protein attached to the column.

Our Nbs have a 6x histidine tail. To check in what fractions we had our VHHs isolated, we ran an SDS-Page acrylamide gel for a Coomassie staining and for staining with an anti-His Tag Ab. Fractions 16-19 correspond to the UV peak eluted from 60% of imidazole-containing proteins of different sizes that present affinity to the nickel column that do not correspond to our Nbs. Moreover, for fractions 20-26 and elution with 0.5M imidazole, we could see proteins with histidine tail with a size of around 15 kDa, which may correspond to our Nbs (figure 8D).

In vitro validation of Nbs

Three different Nbs that recognize ABCC3 were purified from the two selection methods: 4.2-Nb-plating-ABCC3, 12.3-Nb-sorting-ABCC3, and 18.3-Nb-sorting-

ABCC3. The concentration of the Nbs was determined by Bradford protein assay and tested at different concentrations in cells. We took advantage of the 6x Histidine tail and used an anti-His Tag Ab to detect Nbs.

First of all, we tested different concentrations of Nbs in the selection cell lines, A549 and A549-Cas9 sgABCC3, in a range of 0.25 to 20 µg. The three Nbs have different sequences, their epitope recognition is unknown, and we want to test their affinity to ABCC3.

In some cases, by increasing the concentration of Nb, the fluorescent signal increased, as is the case of 4.2-Nb-plating-ABCC3 and 12.3-Nb-sorting-ABCC3. In other cases, by adding the lower amount of Nb, 0.25 µg, we obtained a high fluorescence peak, it is the case of 18.3-Nb-sorting-ABCC3 (figure 9A). Comparing the three Nb, we decide to test 12.3-Nb-sorting-ABCC3 and 18.3-Nb-sorting-ABCC3 because they look more specific against ABCC3 (figure 9B).

The selected Nbs were further evaluated in a panel of different cell lines with different ABCC3 expression levels.

Then, we tested the two sorting Nbs, 12.3 and 18.3, in different PDAC cell lines that express and do not express ABCC3. MIA PaCa-2 cell line does not express ABCC3 in normal conditions, and none of the Nbs detected any signal. In IMIM-PC2 and CFPAC-1 cell lines, we could discriminate between the Cas9 sgNT and the Cas9 sgABCC3 cells, validating our Nbs in the recognition in *vitro* of ABCC3 (figure 9C).

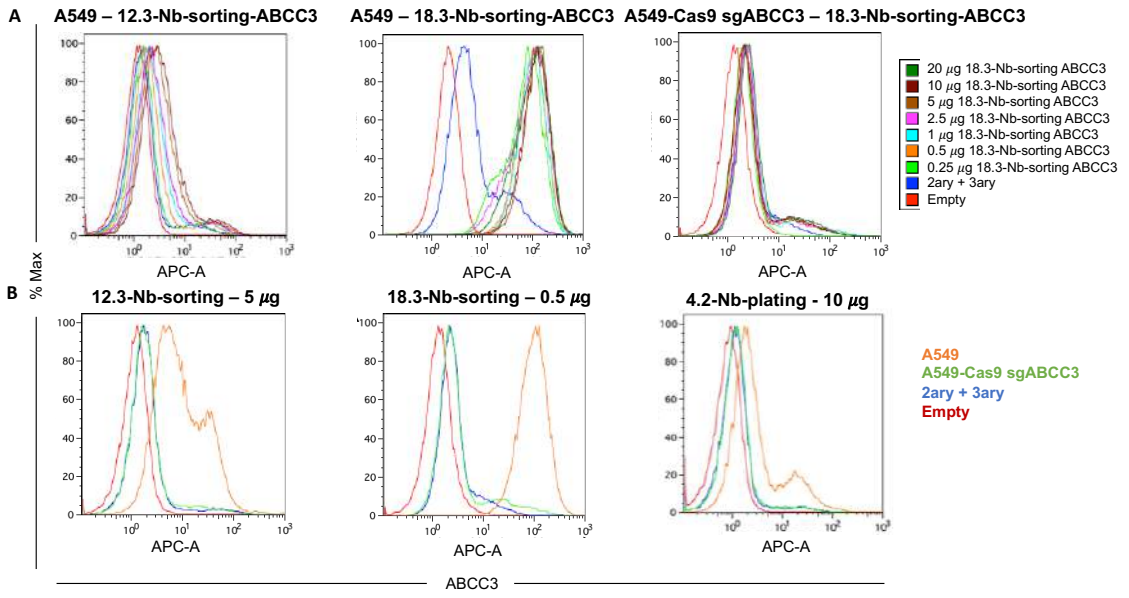

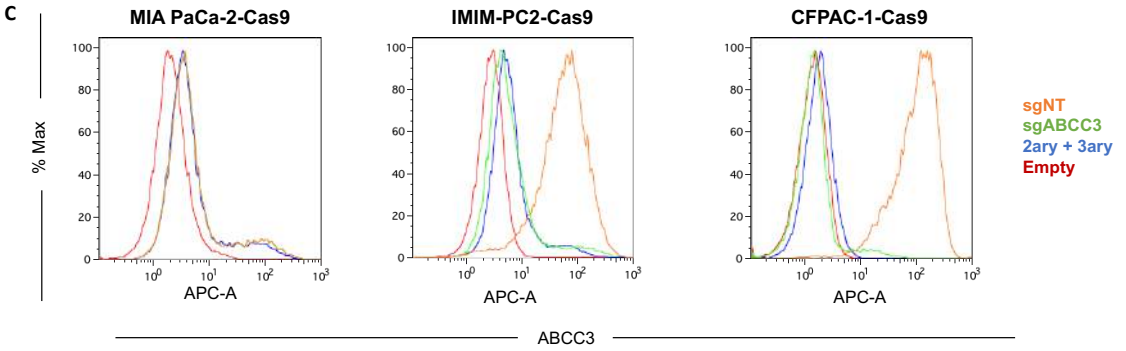

Figure 9. *In vitro* testing of Nbs by flow cytometry. A) Titration of Nbs in selection cell lines, A549 and A549-Cas9 sgABCC3. **B)** ABCC3 detection by Nbs in selection cell lines, A549 and A549-Cas9 sgABCC3. **C)** ABCC3 detection by Nbs in PDAC sgNT and sgABCC3 cells.

In the following steps, we tested Nbs in other techniques for ABCC3 detection, for example, immunofluorescence. The site of the Nbs recognition is unknown; to perform the experiment on cells, we detached them with trypsin, accutase, and PBS-EDTA. With the usage of trypsin or accutase, the Nbs could not recognize ABCC3 (figure S3), which means that these agents disrupt the epitope. After several attempts, we were able to perform immunofluorescence in fresh samples of cells, but the Nbs did not bind to fixed cells (figure 10A). Actually, the binding of the Nbs to intact cells could be an advantage for the *in vivo* recognition of the epitope.

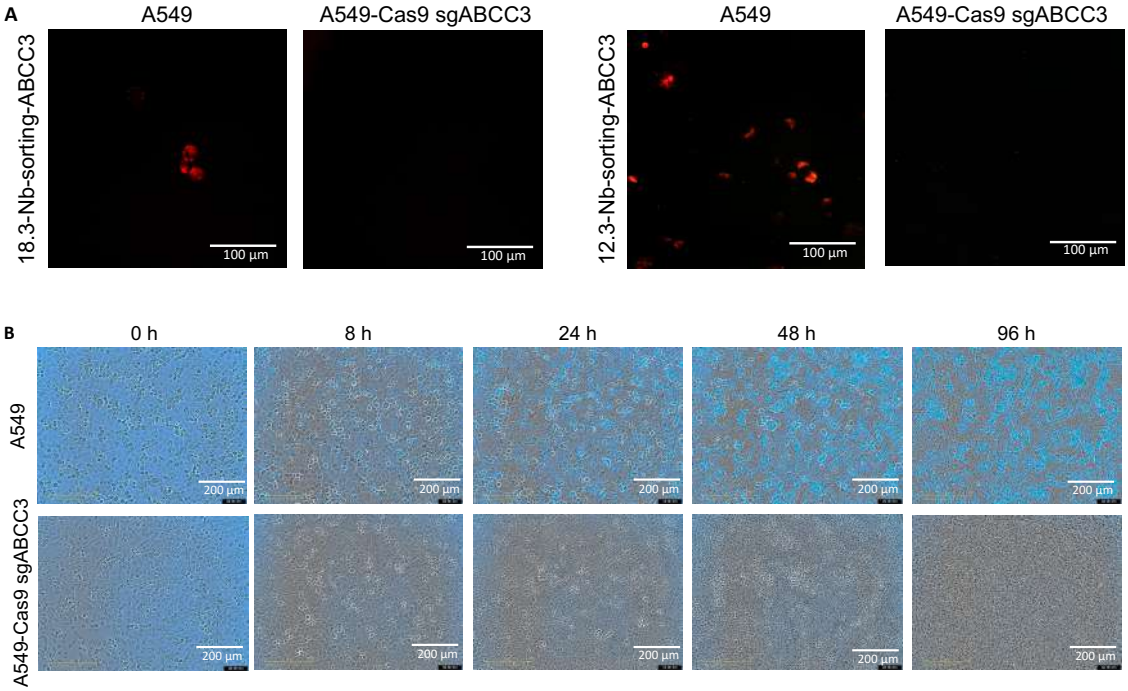

Figure 10. *In vitro* staining of Nbs by immunofluorescence. A) Immunostaining of Nbss in the selection cell lines, A549 and A549-Cas9 sgABCC3, detection with anti-His Tag-Alexa Fluor 647. Images taken with Leica AF6000 LX. **B)** Immunostaining of 18.3-Nb-sorting-ABCC3 Nb in the selection cell lines, A549 and A549-Cas9 sgABCC3, detection with anti-His Tag-Alexa Fluor 647. *Images taken with Incucyte (Sartorius), 20X.*

As last experiments in cell culture, we wanted to check at what times the Nb could bind to the antigen, how much time it is bound to it, and if the union is stable. For these experiments, we used Incucyte SX5 system to take images at different times. We added Nb, previously labeled to anti-His Tag-Alexa Fluor 647 Ab, to the cells. We could observe that during the first 8 hours, the Nb slowly binds to the positive cells; from 24 hours to 96 hours, almost all cells were labeled with Nb and lasted over 4 days. The Nb seemed to be very specific, and even being present in the media, it did not bind to the negative cells (figure 10B).

The Nb obtained following either a plating or sorting strategy for selection have been validated for ABCC3 detection *in vitro*. The Nbs obtained by FACS resulted more specific than plating Nb, and they were able to bind to ABCC3 expressing cell lines in flow cytometry and immunofluorescence. The Nbs can bind to the antigen in 30 minutes, but the binding can last for at least 96 hours in cells. As ABCC3 could be a promising biomarker for PDAC, 12.3-Nb-sorting-ABCC3 and 18.3-Nb-sorting-ABCC3 could be candidates for ABCC3 recognition for immunotargeted applications for the diagnosis and therapeutic treatment of PDAC.

DISCUSSION

Abs have been used during the last decades as diagnostic and therapeutic tools. Abs have high specificity, and even though their efficacy, their large size, and their immunogenicity constitute disadvantages in their use[29], but their immunogenicity can be minimized by genetic engineering[30]. Even more, the production of Abs is quite expensive, and they do not have a good cost-effectiveness ratio; there is also a lack in the efficiency of models of production[31]. These facts started the improvement of Abs; different fragments from the Abs have been generated by engineering, as Fabs or scFvs. Despite their reduced size, they maintain their specificity, but they have a shorter serum half-life[32].

The discovery of HCAbs in camelids began the new era of the use of Nbs. Nbs are formed by the antigen-binding region of the heavy chain of HCAbs. They are the smallest naturally derived antigen-binding fragments, and they have special characteristics[33].

The use of Nbs has been very diverse since their discovery; they have been employed in protein crystallization, immunoprecipitation, or biosensing. Nevertheless, especially, they have a high potential for diagnosis and therapy in diseases, and especially for cancer[29].

The most used method for Nbs selection is phage display. Phage display is a robust technology that consists of the display of Nbs (or other Ab fragments) on the surface of filamentous bacteriophages infecting *E. coli*[34]. VHH region is fused to phage coat protein 3 (pIII), to pelB that is the N-terminal signal peptide for its insertion in the inner membrane of *E. coli*, and finally, it is tagged with an epitope (HA, myc,…)[35,36]. The selection is performed with the purified protein coated in plates, and the phages are added to bind to the antigens[37].

Although this technique is the most commonly used for Nb selection, it has several limitations. There is much manipulation to produce phage stocks; bacteria have to be infected by helper phage and amplification of phages by re-infection[38]. There are also low levels of Nb displayed by plate conditions, limited protein coating, and the high binding of phages to plates, which makes selections unspecific against other antigens[39].

An alternative selection method for Nbs selection is yeast display. With this strategy, there is no need of high manipulation, and the background is reduced[40]. These problems solve phage display disadvantages, but it has other limitations. It is used for small library sizes due to the low efficiency of transforming yeast cells and their long time for growth[38].

The third selection method is *E. coli* display; in this case, the Nbs are expressed in the membrane for antigen recognition and yeast display. Because of the presence of two membranes and a periplasmic space in *E. coli* cells, there are possibilities of performing panning on cell surface for selection of Nbs. By using this bacteria, the manipulation is reduced, the growth is fast and simple, and even more, the transformation efficiency is high[38].

At least three types of selection can be performed for *E. coli* display. The first one is panning selection, which limits the number of bacteria added to the protein-coated. The second one is magnetic-activated cell sorting (MACS) selection with purified protein or target; in this case, the quantity of bacteria added is higher and the amount of protein. The last one is the selection on mammalian cell surface when there is no purified protein. Among this selection, the one that obtained better results in Nbs selection is MACS; this technique has higher efficiency than the other ones[27].

We started the generation of Nbs by immunizing camels with cells overexpressing ABCC3 and not the purified protein. Then, the camel would produce VHHs against different proteins and molecules, but with several selection rounds, we successfully isolated the specific Nbs targeting ABCC3. We isolate Nbs by two different selection methods based on the same "cell surface" principle. We could observe an enrichment in sorting selection compared to plating selection in which we obtained different candidates. Attending to the efficiency of selection, we could also see that sorting selection really decreased the number of bacteria bound to cells in the first rounds, and then there was an enrichment of these clones; in the plating selection, the decrease in bacterial binding was not as high as in the sorting one. The efficiency of FACS selection could be compared with MACS selection, but it can be performed in cases where the purified protein is unavailable. Instead of performing the FACS with the

specific Ab against our target protein, we can dye overexpressing cells and then perform the FACS for their sorting.

The Nbs were successfully validated in different cell lines with cells expressing and not expressing the antigen by different methods. So, we could use these Nbs as tools for ABCC3 detection because of the lack of Abs against this protein and the properties of Nbs. But more interestingly, they could be used for diagnosis by the detection of ABCC3, for example, in PDAC, and they can be tested for a possible application in therapy by the blockage of some essential parts of ABCC3 protein.

Further studies with these Nbs may be required for its complete validation for its use in diagnosis or therapy. Further assays could lead to selecting more clones with better characteristics due to the generation of the library. The isolated Nbs could be exploited for immunotargeted applications for the benefit of patients.

CONCLUSIONS

1. We have generated a nanobody library by immunization of camels.
2. We efficiently isolated Nbs targeting ABCC3 using E. coli display strategies based on cell surface selection.
3. 12.3 and 18.3-Nb-sorting-ABCC3 could specifically bind to ABCC3 in a panel of cell lines *in vitro*.
4. 18.3-Nb-sorting-ABCC3 remained bound to ABCC3-expressing cells for 96 h *in vitro*.

SUPPLEMENTAL FIGURES

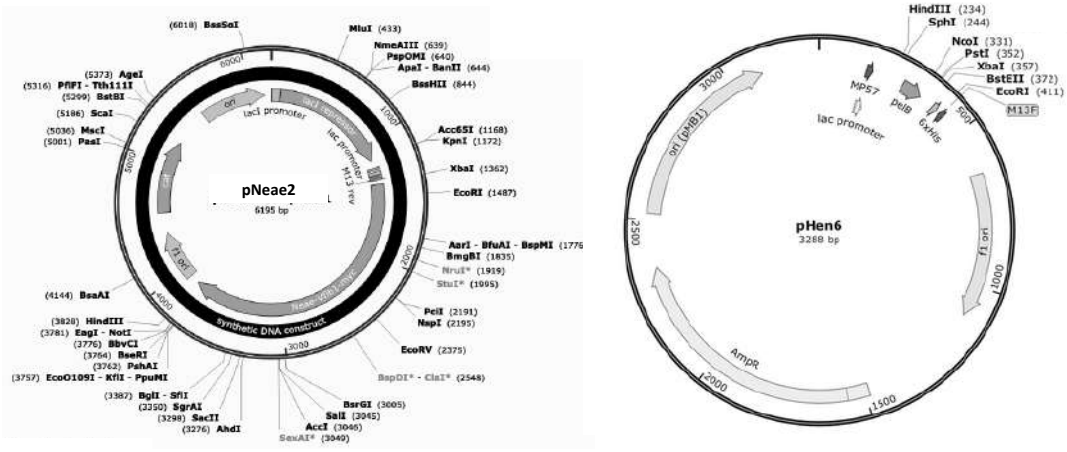

Figure S1. Plasmid description with restriction enzyme sites of pNeae2 and pHEN6.

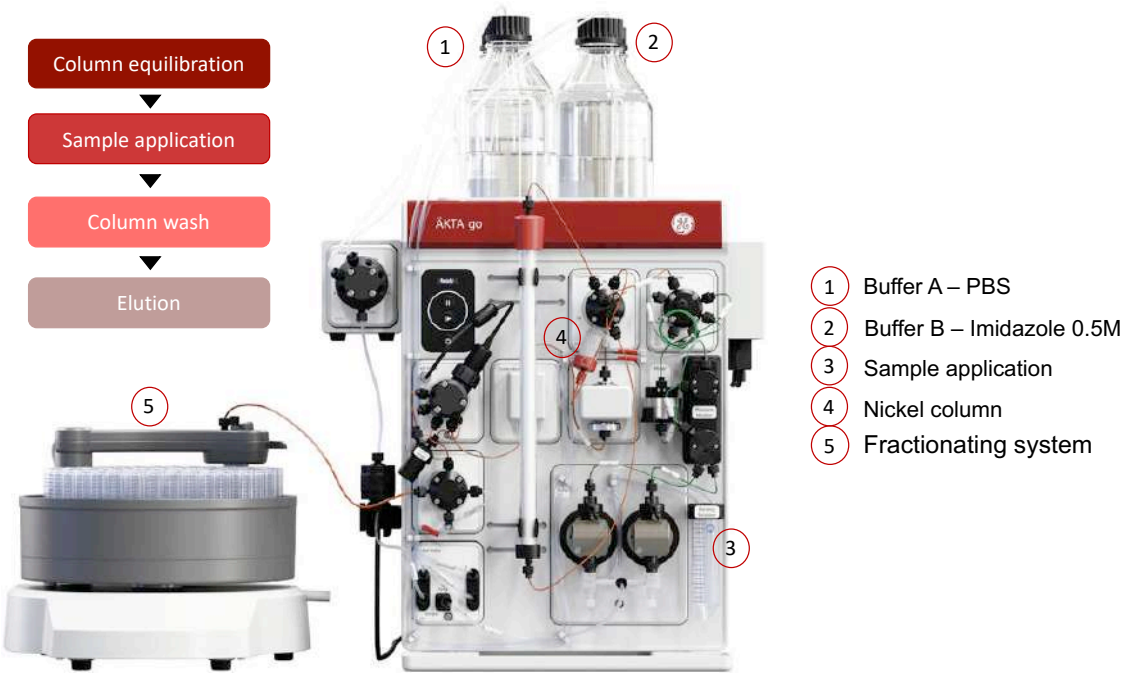

Figure S2. ÄKTA purification system process and components.

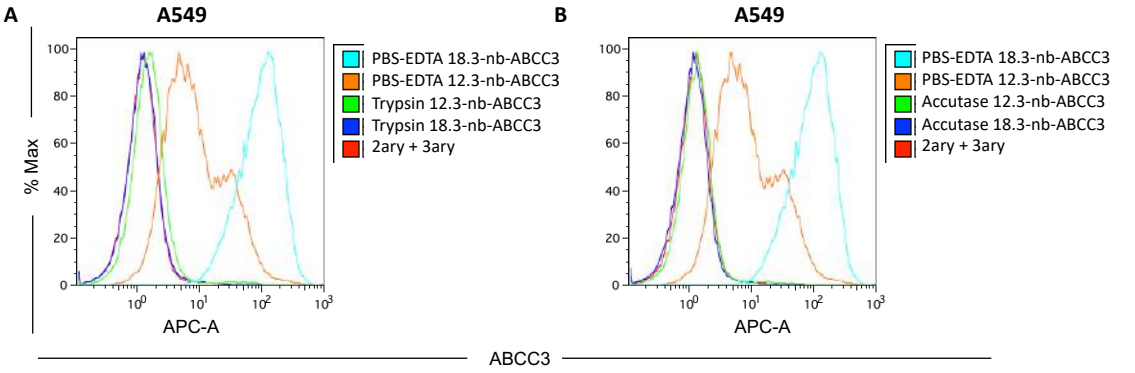

Figure S3. Recognition of ABCC3 by 12.3- and 18.3-Nb-sorting-ABCC3 with different methods for detaching cells. Nbs recognition by detaching cells with **A)** trypsin and **B)** accutase, compared with the efficient detaching with PBS-EDTA 10 mM.

REFERENCES

1. Lipman NS, Jackson LR, Trudel LJ, Weis-Garcia F. Monoclonal Versus Polyclonal Antibodies: Distinguishing Characteristics, Applications, and Information Resources. *ILAR Journal*. 2005;46(3):258-268. doi:10.1093/ilar.46.3.258
2. Vidarsson G, Dekkers G, Rispens T. IgG subclasses and allotypes: From structure to effector functions. *Frontiers in Immunology*. 2014;5(OCT):520. doi:10.3389/fimmu.2014.00520
3. NEZLIN R. General Characteristics of Immunoglobulin Molecules. In: *The Immunoglobulins*. Elsevier; 1998:3-73. doi:10.1016/b978-012517970-6/50001-1
4. Edmundson AB, Andersen KN. Immunoglobulin Structure. In: *Encyclopedia of Immunology*. Elsevier; 1998:1329-1334. doi:10.1006/rwei.1999.0340
5. Sci-Hub | | 10.2307/2876334. https://sci-hub.se/10.2307/2876334. Accessed July 27, 2021.
6. Wu AM. Engineered antibodies for molecular imaging of cancer. *Methods*. 2014;65(1):139-147. doi:10.1016/j.ymeth.2013.09.015
7. Antibody Structure and Function | Sino Biological. https://www.sinobiological.com/resource/antibody-technical/antibody-structure-function. Accessed July 27, 2021.
8. Hamers-Casterman C, Atarhouch T, Muyldermans S, et al. Naturally occurring antibodies devoid of light chains. *Nature*. 1993;363(6428):446-448. doi:10.1038/363446a0
9. Khong Nguyen V, Hamers R, Wyns L, Muyldermans S. Loss of splice consensus signal is responsible for the removal of the entire C(H)1 domain of the functional camel IGG2A heavy-chain antibodies. *Molecular Immunology*. 1999;36(8):515-524. doi:10.1016/S0161-5890(99)00067-X
10. Muyldermans S, Cambillau C, Wyns L. Recognition of antigens by single-domain antibody fragments: The superfluous luxury of paired domains. *Trends in Biochemical Sciences*. 2001;26(4):230-235. doi:10.1016/S0968-0004(01)01790-X
11. Van Der Linden R, De Geus B, Stok W, et al. Induction of immune responses and molecular cloning of the heavy chain antibody repertoire of Lama glama. *Journal of Immunological Methods*. 2000;240(1-2):185-195. doi:10.1016/S0022-1759(00)00188-5
12. Muyldermans S, Baral TN, Retamozzo VC, et al. Camelid immunoglobulins and nanobody technology. *Veterinary Immunology and Immunopathology*. 2009;128(1-3):178-183. doi:10.1016/j.vetimm.2008.10.299
13. Govaert J, Pellis M, Deschacht N, et al. Dual beneficial effect of interloop disulfide bond for single domain antibody fragments. *Journal of Biological Chemistry*. 2012;287(3):1970-1979. doi:10.1074/jbc.M111.242818

14. Melarkode Vattekatte A, Shinada NK, Narwani TJ, et al. Discrete analysis of camelid variable domains: sequences, structures, and in-silico structure prediction. doi:10.7717/peerj.8408

15. Bathula N V., Bommadevara H, Hayes JM. Nanobodies: The Future of Antibody-Based Immune Therapeutics. *Cancer Biotherapy and Radiopharmaceuticals*. 2021;36(2):109-122. doi:10.1089/cbr.2020.3941

16. Muyldermans S. A guide to: generation and design of nanobodies. *The FEBS Journal*. 2021;288(7):2084-2102. doi:10.1111/febs.15515

17. Sun S, Ding Z, Yang X, et al. Nanobody: A small antibody with big implications for tumor therapeutic strategy. *International Journal of Nanomedicine*. 2021;16:2337-2356. doi:10.2147/IJN.S297631

18. Scully M, Cataland SR, Peyvandi F, et al. Caplacizumab Treatment for Acquired Thrombotic Thrombocytopenic Purpura. *New England Journal of Medicine*. 2019;380(4):335-346. doi:10.1056/nejmoa1806311

19. Salema V, Marín E, Martínez-Arteaga R, et al. Selection of Single Domain Antibodies from Immune Libraries Displayed on the Surface of E. coli Cells with Two β-Domains of Opposite Topologies. *PLoS ONE*. 2013;8(9):1-18. doi:10.1371/journal.pone.0075126

20. Blomfield IC, McClain MS, Princ JA, Calie PJ, Eisenstein BI. Type 1 fimbriation and fimE mutants of Escherichia coli K-12. *Journal of Bacteriology*. 1991;173(17):5298-5307. doi:10.1128/jb.173.17.5298-5307.1991

21. Zell R, Fritz HJ. DNA mismatch-repair in Escherichia coli counteracting the hydrolytic deamination of 5-methyl-cytosine residues. *EMBO Journal*. 1987;6(6):1809-1815. doi:10.1002/j.1460-2075.1987.tb02435.x

22. Conrath KE, Lauwereys M, Galleni M, et al. β-Lactamase inhibitors derived from single-domain antibody fragments elicited in the Camelidae. *Antimicrobial Agents and Chemotherapy*. 2001;45(10):2807-2812. doi:10.1128/AAC.45.10.2807-2812.2001

23. Isolation of mononuclear cells and granulocytes from human blood. Isolation of monuclear cells by one centrifugation, and of granulocytes by combining centrifugation and sedimentation at 1 g - PubMed. https://pubmed.ncbi.nlm.nih.gov/4179068/. Accessed October 29, 2021.

24. Gallmeier E, Hermann PC, Mueller MT, et al. Inhibition of ataxia telangiectasia- and Rad3-related function abrogates the in vitro and in vivo tumorigenicity of human colon cancer cells through depletion of the CD133+ tumor-initiating cell fraction. *Stem Cells*. 2011;29(3):418-429. doi:10.1002/stem.595

25. Salema V, Mañas C, Cerdán L, et al. High affinity nanobodies against human epidermal growth factor receptor selected on cells by E. coli display. *mAbs*. 2016;8(7):1286-1301. doi:10.1080/19420862.2016.1216742

26. Crauwels M, Massa S, Martin C, et al. Site-specific radioactive labeling of nanobodies. In: *Methods in Molecular Biology*. Vol 1827. Humana Press Inc.; 2018:505-540. doi:10.1007/978-1-4939-8648-4_26

27. Salema V, Mañas C, Cerdán L, et al. High affinity nanobodies against human epidermal growth factor receptor selected on cells by E. coli display. *mAbs*. 2016;8(7):1286-1301. doi:10.1080/19420862.2016.1216742

28. Salema V, Marín E, Martínez-Arteaga R, et al. Selection of Single Domain Antibodies from Immune Libraries Displayed on the Surface of E. coli Cells with Two β-Domains of Opposite Topologies. *PLoS ONE*. 2013;8(9). doi:10.1371/journal.pone.0075126

29. Yang EY, Shah K. Nanobodies: Next Generation of Cancer Diagnostics and Therapeutics. *Frontiers in Oncology*. 2020;10:1182. doi:10.3389/fonc.2020.01182

30. Gonzales NR, De Pascalis R, Schlom J, Kashmiri SVS. Minimizing the immunogenicity of antibodies for clinical application. *Tumor Biology*. 2005;26(1):31-43. doi:10.1159/000084184

31. Liu JKH. The history of monoclonal antibody development - Progress, remaining challenges and future innovations. *Annals of Medicine and Surgery*. 2014;3(4):113-116. doi:10.1016/j.amsu.2014.09.001

32. Ewert S, Huber T, Honegger A, Plückthun A. Biophysical properties of human antibody variable domains. *Journal of Molecular Biology*. 2003;325(3):531-553. doi:10.1016/S0022-2836(02)01237-8

33. Hamers-Casterman C, Atarhouch T, Muyldermans S, et al. Naturally occurring antibodies devoid of light chains. *Nature*. 1993;363(6428):446-448. doi:10.1038/363446a0

34. Frenzel A, Schirrmann T, Hust M. Phage display-derived human antibodies in clinical development and therapy. *mAbs*. 2016;8(7):1177-1194. doi:10.1080/19420862.2016.1212149

35. Qi H, Lu H, Qiu HJ, Petrenko V, Liu A. Phagemid vectors for phage display: Properties, characteristics and construction. *Journal of Molecular Biology*. 2012;417(3):129-143. doi:10.1016/j.jmb.2012.01.038

36. Thie H, Schirrmann T, Paschke M, Dübel S, Hust M. SRP and Sec pathway leader peptides for antibody phage display and antibody fragment production in E. coli. *New Biotechnology*. 2008;25(1):49-54. doi:10.1016/j.nbt.2008.01.001

37. Hoogenboom HR. Overview of antibody phage-display technology and its applications. *Methods in molecular biology (Clifton, NJ)*. 2002;178:1-37. doi:10.1385/1-59259-240-6:001

38. Salema V, Fernández LÁ. *Escherichia* coli surface display for the selection of nanobodies. *Microbial Biotechnology*. 2017;10(6):1468-1484. doi:10.1111/1751-7915.12819

39. Even-Desrumeaux K, Nevoltris D, Lavaut MN, et al. Masked Selection: A Straightforward and Flexible Approach for the Selection of Binders Against Specific Epitopes and Differentially Expressed Proteins by Phage Display. *Molecular & cellular proteomics : MCP*. 2014;13(2):653-665. doi:10.1074/mcp.O112.025486

40. Gai SA, Wittrup KD. Yeast surface display for protein engineering and characterization. *Current Opinion in Structural Biology*. 2007;17(4):467-473. doi:10.1016/j.sbi.2007.08.012

CHAPTER III / CAPÍTULO III

CHAPTER III.

Applications of nanobodies: *in vivo* ABCC3 detection by nanobodies and their therapeutic potential

INTRODUCTION

Nbs are single-domain variable fragments that derive from camelid HcAbs. VHHs have several unique characteristics: reduced size (10-15 kDa), antigen specificity, stability, and solubility in aqueous solutions. The production of Nbs is highly efficient, easy, and affordable, which contributes to their use in biomedical implications. One of the most important properties of the Nbs is their high affinity and specificity in recognizing epitopes, even at low concentrations[1].

Non-invasive molecular imaging techniques use radiotracers labeled to Abs or fragment-derived Abs. Nbs have been used as a part of molecular probes for molecular imaging. VHHs are high/very stable, easy to label, present low immunogenicity and high specificity for the antigen/epitope. More importantly, their small size favors their use in imaging techniques due to their rapid clearance (0.5-1 h) via kidneys[2].

Nbs can also be employed as therapeutic agents; their activity relies on inhibiting molecules. The application of Nbs in pathologies focuses on the inhibition of several parts of molecules by competitive binding[1].

Altogether, Nbs present a high versatility for their use in multiple biomedical applications.

- **Diagnosis**

The diagnosis of PDAC tumors remains a challenge, although there have been improvements in detection techniques. There is a need for the development of diagnostic procedures for an early diagnosis of the disease.

As described in the introduction, there are various imaging techniques in diagnosing and staging local and distant pancreatic lesions. The most widely used are CT, MRI, or EUS. Although several international consensus guidelines recommend these techniques for suspected PDAC, they present some limitations in small lesions and metastasis detection[3,4].

One of the most used imaging techniques is [^{18}F]FDG PET, but it is limited in detecting PDAC[5]. Immuno-PET takes advantage of PET and Abs, increasing sensibility and selectivity, respectively. This molecular imaging PET could help in

tumor detection in a non-invasive way and by a whole-body visualization. Besides being a diagnostic tool, it could be drawn on to predict therapeutic effect depending on the target of the antibody is directed[6].

Immuno-PET is usually performed with mAbs, but other probes can be used as single-chain Abs and derivates such as Nbs. Nbs have characteristics that can improve immuno-PET imaging techniques, including faster pharmacokinetics and better noise-ratio signal[7]. Additionally, due to their small size, they have deeper tissue penetration and speedier clearance by kidneys. Furthermore, they have been reported to be poorly immunogenic and highly stable[8,9].

Immuno-PET imaging's goal is to obtain a fast and specific detection of a target. To this end, it is required a high specific tumor uptake and low retention in other tissues, including blood[10]. Importantly, immuno-PET allows the quantification of the biomarkers in a non-invasive manner.

The quantification of many molecular parameters in the tumor requires biopsies and a histopathological analysis involving patients' risk and might not capture the tumor heterogeneity.

As depicted in the introduction, there are different known PDAC biomarkers. Some of them have been used in immuno-PET as prognostic markers in preclinical settings[11].

The main components of the immuno-PET include the target, the antibody, and the radiotracer. The Ab or fragment-derivatives need to be labeled with radioisotopes to perform immuno-PET. Abs can be directly labeled with radioisotopes, but there are some limitations; they usually show long circulation times, which subsequently needs to increase the amount of probe to reach the tissues with the increase of radiation that it entails[12]. Several assays have demonstrated the instability of direct labeling compared to indirect labeling[13,14].

Several PET radioisotopes can be used for immuno-PET with different characteristics, including half-life radioactive decay and positron production system. Iodine-124 (^{124}I) is widely used as a PET radioisotope, and it is characterized by having a long half-life ($t_{1/2}$ = 4.2 days). ^{124}I emitted positrons are highly energetic (E_{max} of 1.5-2.1 MeV), and the intrinsic limit resolution is 2.3 mm[15]. Copper-64 (^{64}Cu) is a medium half-life radioisotope ($t_{1/2}$ = 12.7 hours), and

positron energy is lower than ^{124}I (E_{max} = 656 keV). Due to these characteristics, it is very versatile for PET, and it also has the benefit that it can be produced in a reactor or cyclotron, resulting easier and cheaper[16]. Fluorine-18 (^{18}F) is the most used in PET imaging, mainly due to the widespread use of [^{18}F]FDG. Attending to their characteristics, it is almost a pure positron emitter with positron energy similar to ^{64}Cu (E_{max} = 635 keV). ^{18}F facilitates high-resolution imaging, and it is widely used due to its short half-life ($t_{1/2}$ = 109.7 minutes)[17]. Another short-lived ($t_{1/2}$ = 68 minutes) radioisotope is Gallium-68 (^{68}Ga) with higher positron energy (E_{max} = 1.9 Mev). Therefore, ^{68}Ga has a larger positron spread and a similar resolution to ^{18}F. Even more, ^{68}Ga can be produced in a generator from a source of decaying germanium-68 (^{68}Ge), which is more affordable, does not require a specific installation as it occurs with reactors or cyclotrons[18].

Finally, it is essential that the half-life of the radioisotopes and the half-life of the antibodies need to march.

To complete the molecular probe for immuno-PET, both components, the Ab and radioisotope, need to be bound.

Usually, the two components of the immuno-PET probes are bioconjugation using chelating agents. These linkers are metal-chelating molecules. For an effective radiopharmaceutical agent, it is essential the formation of a kinetically inert metal chelate and the stable covalent attachment of the chelator moiety to the biomolecule. A wide variety of molecules are synthesized and studied; mainly, they can be classified in macrocyclic and acyclic chelators. While macrocyclic chelators present greater kinetic stability, acyclic chelators usually have faster rates of metal binding[19]. Leastways, the chelator has to be appropriately chosen to fit the selected radiometal, even though some chelators are more applicable (*e.g.,* 1,4,7,10-tetraazacyclododecane-1,4,7,10-tetraacetic acid, DOTA) than others (*e.g.,* DiamSar).

There are three main conjugation strategies to conjugate the chelator to the biomolecule: peptide, thiourea, and thioether bond. For their use *in vivo* and clinics, the linker should be stable under physiological conditions and without interfering with the specificity of the biomolecule. The first strategy is the peptide bond; it reacts with an activated carboxylic acid and a primary amine. The second one is the thiourea bond that happens via an isothiocyanate group and an amine.

The third one is the thioether bond formed by the reaction of a thiol group and a maleimide. Bioconjugation of the linker can be alternatively accomplished by a biorthogonal reaction, which is an extension of "click chemistry" [20]. Bioorthogonal reactions must produce a chemically and biologically inert linkage via a reaction that displays high selectivity between the two coupling partners; be kinetically fast and be biocompatible in terms of operating at physiological conditions. Additionally, some specific biorthogonal reactions can occur in vivo, allowing for a two-step pre-targeting strategy[19].

- **Theragnosis**

The radioisotopes used for diagnostic nuclear medicine are gamma-emitters with high permeability into the body. On the contrary, therapeutic nuclear medicine uses beta-emitter radionuclides with high radiation damage to the cells.

Gamma-rays used in conventional radiotherapy expose a limited body area to a high-energy X-ray beam for cell radiation. These rays cause breaks in the DNA strain, causing cell damage and death. An alternative for cancer irradiation is targeted radionuclide therapy (TRNT); this method applies radiation specifically to cancer cells, minimizing the exposure of healthy tissue. There are two different ways of TRNT. The first one is the natural accumulation of agents; some examples are Iodine-131 (^{131}I) for thyroid cancer, ^{131}I-MIBG in neuroblastoma, and Strontium-89 (^{89}Sr)-chloride in osteosarcomas. The second strategy is based on biomolecules that interact with tumor-associated antigens that are accessible by circulating agents on the cell surface. These labeled biomolecules can be used as treatment alone or in combination with current cancer treatments [21].

Abs and derivatives used for immuno-PET can be modified by changing the radioisotope for therapeutic and theragnostic purposes[22]. An example of labeled antibodies applied in PDAC is hPAM4; it is also known as clivatuzumab. It is a humanized form of an antibody against mucin 1 (MUC1). MUC1 has been described as a biomarker of early pancreatic adenocarcinoma[23]. ^{90}Y-Clivatuzumab is actually in phase II of clinical trials for PDAC patients, for an early diagnosis by SPECT/CT and radioimmunotherapy combined with gemcitabine[24].

There are other examples of molecular probes for theragnosis in PDAC; MVT - 5873 is a monoclonal antibody against CA19-9 epitope. It is understudies in phase I of clinical trials in patients with metastatic PDAC in combination with mFOLFIRINOX[25,26].

Nbs could be used as a diagnostic tool as well as therapeutic agents in PDAC patients. Specific Nbs against several PDAC biomarkers could help in the theragnostic field.

OBJECTIVES

We have isolated and validated Nbs that target ABCC3. This ABC transporter could be further studied as a biomarker for PDAC, and it could be used to predict the tumor sensitivity or resistance for some current treatments.

The main objective of this section is to test ABCC3 Nbs in mouse models and prove different linkers for chelator bonds to study further biomedical applications such as diagnosis and therapy. We also want to try Nbs as inhibitor molecules of ABCC3 to better respond to actual PDAC treatments.

Thus, the main objectives of this chapter are:

1. Evaluate the use, biodistribution, and toxicity of ABCC3 Nbs *in vivo* using PDAC mouse models.
2. Modify and evaluate the conjugation and labeling of the Nbs for their possible use in diagnostic and therapeutic applications.
3. Evaluate the use of ABCC3 Nbs as therapeutic tools in proliferation and in combination with chemotherapeutic treatments.

MATERIAL AND METHODS

Mammalian cell culture

The human cell lines IMIM-PC2, MIA PACa-2, and A549 were grown as monolayers in Dulbecco's modified Eagle's medium (DMEM, Sigma) supplemented with 10% Fetal Bovine Serum (FBS, Gibco) and 1% penicillin and streptomycin (Gibco) at 37ºC, 5% CO_2. All cell lines were obtained from Mariano Barbacid's Laboratory (CNIO).

Bacterial growth and Nbs purification

Bacteria were grown and inducted as indicated in M&M of chapter I.

Nbs purification was performed as described in M&M of chapter II.

Flow cytometry analysis of Nbs in *in vitro* cultured cells

Experiments were done accordingly to M&M of chapter II.

Cell viability assays

Assays were performed by following M&M in chapter I.

Bioluminescence imaging

Tumor growth in tumor-bearing mice was monitored by bioluminescence imaging using IVIS Lumina III (Beckman Coulter) when they reached a tumor volume of 350 mm^3 in subcutaneous or 10^7 p/sec/cm^2/sr of luminescence in orthotopic pancreatic tumors. For luminescence detection, 150 mg/kg of luciferin (Merck) was IP injected, and 10 minutes later, the signal was acquired at 1-2 s.

Detection of Nbs *in vivo* by flow cytometry assays in heterotopic and orthotopic mouse xenografts

A single dose of 150 µg of Nb-ABCC3 was administered intraperitoneally (IP) to tumor-bearing mice. 0.5, 1, 2, 24, and 48 h post- injections, animals were sacrificed, and tumors, pancreas, liver, kidneys, and blood were collected. Samples were then mechanically disaggregated using a scalpel and treated with PBS-EDTA 10 mM for 10 min at 3000 rpm at 37ºC. Tumors and organs were filtrated through a nylon 40 µm cell strainer and incubated with anti-His Tag 647 antibody (1:1500, Biolegend), 4ºC, 30 min. Samples were acquired by a cytometer (Gallios, Beckman Coulter), and data were analyzed. Data were gated to select singlets and green fluorescent protein (GFP) positive cells (Figure S1).

Conjugation and labeling of Nbs

All the experiments of conjugation and labeling of Nbs were performed by Dr. Miguel Ángel Morcillo from the group of radioisotopes in biomedicine at CIEMAT, Madrid.

The conjugation was based on the procedure described by Vosjan et al.[27]. All the calculations were performed, estimating the molecular weight of Nbs in 15000 g/mol. For the conjugation, 2 mg of 12.3-Nb were completed until 1 mL with PBS. The pH was adjusted to 8.9-9.1 with a Na_2CO_3 0.1 M solution. The 12.3-Nb was mixed 1:5 with p-SCN-Bn-NOTA chelating agent dissolved in 20 µl of DMSO. The mix was incubated for 90 min at 37ºC and 550 rpm. The mixture was purified to eliminate the unconjugated p-SCN-Bn-NOTA with a molecular exclusion column G25-Sephadex PD10 (GE Healthcare Life Sciences) by eluting with a 5 mg/ml solution of gentistic acid/0.25 M sodium acetate, obtaining a 2 ml fraction corresponding to the NOTA conjugated Nb.

The labeling was performed with ^{68}Ga radioisotope following the protocol described by García-Toraño et al..[28] The ^{68}Ga was obtained by the ^{68}Ge/^{68}Ga generator designed at the CIEMAT by Romero et al. [29]. The ^{68}Ga was obtained from the ^{68}Ge/^{68}Ga generator by the fractionated elution using HCl 1M as mobile phase at a 1 ml/min flow rate. A fraction of 1 ml was collected, containing 85% of the eluted ^{68}Ga. The ^{68}Ga fraction was neutralized using 0.2 g of HEPES

dissolved in water. 0.710 mg of 12.3-Nb-NOTA was added to the ^{68}Ga eluted and neutralized and incubated 30 min at 37ºC and 550 rpm. The mix was purified by an exclusion column G25-Sephadex PD10 using PBS as mobile phase. Finally, the quantification of ^{68}Ga activity of 12.3-Nb-NOTA-^{68}Ga eluted was measured by an activimeter (IBC, Veenstra Instruments) previously calibrated to this radionuclide. The efficiency of the reaction was calculated as the percentage of activity present in the collected fractions corresponding to the elution profile of Nb-NOTA compared to the total activity used in the synthesis.

All the steps performed were analyzed by liquid chromatography (HPLC) and compared to a commercial solution of known molecular weights (Calbiochem, Merck). Using an SRT-SEC-150, 5 µm, 7.8 x 300 mm (SEPAX), and a solution of sodium phosphate 0.05M/sodium chloride 0.15 M (pH 6.8) as mobile phase with a flow rate of 1 ml/min. Different aliquots were acquired and analyzed by HPLC under the described conditions to study the conjugation and labeling processes.

In vivo assays

Mice were housed as described in the Materials and methods section from chapter I.

Subcutaneous models: 6 to 10-week-old male and female NU-Foxn1nu nude mice (Envigo) were subcutaneously injected with 10^6 A549 cells expressing Cas9/Control sgRNA or Cas9/sgRNA-ABCC3 mixed 1:1 with 50 µl Matrigel (Corning) per injection. Tumor growth was monitored bi-weekly for up to 2 months or human endpoint.

Orthotopic models: 6 to 10-week-old NU-Foxn1nu nude female mice (Envigo) were submitted to surgery anesthetized with 2.5%Isofluorane-1.5%O_2. A minimal incision was performed in the animal's skin and muscle. The spleen and pancreas were extracted carefully with tweezers from the body and orthotopically injected in the pancreatic tail with 10^6 IMIM-PC2 cells expressing Cas9-control sgRNA (sgNT) or Cas9-sgABCC3 in 15 µl Matrigel (Corning) per injection. The muscle was sutured, and the skin was stapled. Tumor growth was monitored daily for a week and bi-weekly for up to 2 months.

Statistical analysis

Results were expressed as mean ± SD. Statistical tests were performed using Graphpad Prism 6. Unpaired Student's t-tests were used to compare the means of two groups.

RESULTS

ABCC3 Nbs target human ABCC3 *in vivo*

The target recognition of 12.3 and 18.3-Nb-sorting ABCC3 was validated *in vitro* using a panel of tumor cell lines and PDXs.

Once the target specificity was determined, we proceeded to determine the value of these ABCC3-Nbs detecting ABCC3 expressing cells *in vivo.* To this end, we tested the Nbs in subcutaneous and orthotopic PDAC tumors. Usually, the injection of Nbs in mice comprises a range between 100 and 300 µg; the dose we used was 150 µg; this concentration did not result in toxicity in other studies and exhibited good affinity of the epitope binding[30,31].

First, we tested the Nbs 12.3 and 18.3-Nb-sorting-ABCC3 in subcutaneous tumors, A549, and A549-Cas9 sgABCC3 cells were injected; the Nbs were administered IP, and after 1 h, tumors were processed to a single cell suspension. The Nb was detected, taking advantage of the His-Tag encoded in pHEN6 plasmid. The detection of 6xHis-Tag determined the binding of the Nbs to the tumors by flow cytometry assays. To identify inoculated tumor cells, A549 and A549-Cas9 sgABCC3, IMIM-PC2-Cas9 sgNT, and sgABCC3 expressed green fluorescent protein (GFP) as reporter marker. In the cell suspension proceeding from the tumor, we could find different types of cells by gating GFP positive cells in flow cytometry assays. Specifically, we detected the binding of Nbs in tumor cells.

In basal conditions, the pancreas and the brain present low levels of ABCC3 expression, and low levels of Nbs were detected in both organs. Renal clearance is the main route of secretion of Nbs due to their small size; despite being the main clearance route, it was expected that the Nbs pass through the kidneys, accordingly to what we thought, the Nb was cleared, and we did not find binding of the Nbs in kidney cells (figure 1A). Liver has ABCC3 basal expression levels, and we did not observe any binding of the Nbs (figure 1A); this absence of binding in the mouse liver indicated that the Nbs do not recognize mouse ABCC3.

As shown in figure 1B, the 12.3 and 18.3 Nbs could bind to the ABCC3 expressing cells (A549) but not to the ABCC3-deficient tumor (A549-Cas9 sgABCC3). Both 12.3 and 18.3 Nbs were able to detect specifically ABCC3 in subcutaneous

tumors. As it was mentioned before, Nbs did not detect mouse Abcc3, but they detected human ABCC3. Human *ABCC3* and mouse *Abcc3* sequences are highly homologous, some regions are conserved in both species, but they differ in others (figure S2). The recognition of human ABCC3 and not mouse ABCC3 by the Nbs could guide us through the region where the Nbs bind to the protein.

To recreate a more clinical setting of PDAC tumors, we generated orthotopic tumors of Cas9 sgNT and Cas9 sgABCC3 cells of IMIM-PC2 cell line in the pancreas. The Nb was also administered IP, and tumors and tissues were collected and processed 1 h after the injection of the Nb.

We could observe that the Nbs specifically detects ABCC3 in PDAC tumors in mouse models (figure 1B). In addition to the corroboration of the specificity of Nbs in the detection of ABCC3, we could demonstrate that by the IP injection of the Nbs, they can reach the subcutaneous, and even more, the PDAC tumors. We also observed that 1 hour is a sufficient time to detect bound Nbs to the target.

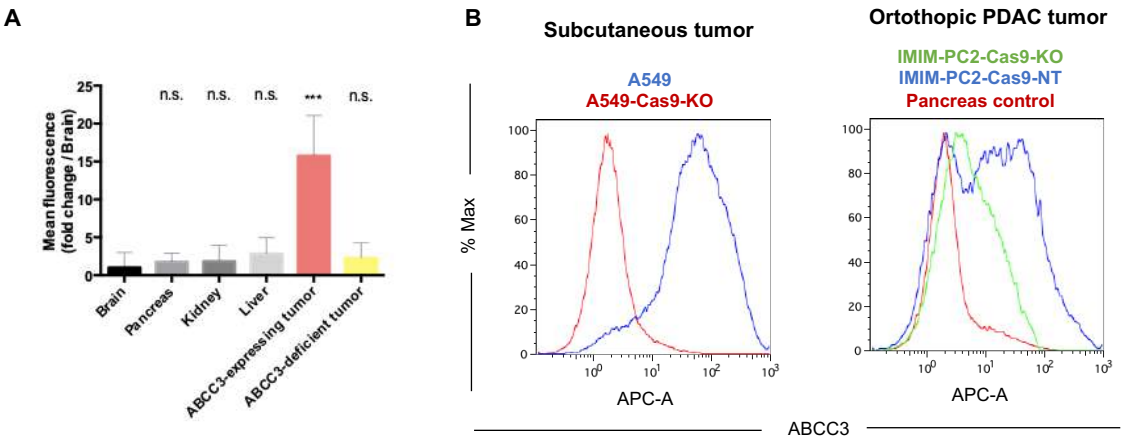

Figure 1. Nbs targeting ABCC3 specifically bind to ABCC3. A) ABCC3 detection by Nbs in mice by flow cytometry in healthy tissues. *Data are represented as the mean + SD fluorescence of Nb-His-Alexa647 normalized to brain tissue sample. Unpaired t-test was used (n.s, non-significant, *** p<0.001, n=5)*. **B)** ABCC3 detection in subcutaneous tumors of control cell lines, A549 and A549-Cas9 sgABCC3, and orthotopic PDAC tumor cell lines, IMIM-PC2-Cas9 sgNT and sgABCC3. **C)** H&E staining of orthotopic IMIM-PC2-Cas9 sgNT tumor embedded in paraffin.

Nb clearance is characterized by short times, 0.5-1 h, and it is advantageous for imaging techniques. However, we were interested in determining the remaining time of binding of the Nbs to the tumors for the use of other radioisotopes or possible further applications, such as "click chemistry". The Nb fluorescent signal

was measured at 0.5, 1, 2, 24- and 48-hours post-injection of the Nb. Nb was detected with a 6xHis-Tag antibody in the single-cell suspension of the tumors by flow cytometry. We could observe that the Nb is bound to ABCC3-expressing tumors at any time between 0.5 and 48 h post-injection. But according to the increasing time that the Nb remains in the body, the unspecific bound of the Nb is cleared, and the signal-noise ratio is improved (figure 2A). We also checked Nb detection in mouse organs; we did not observe specific detection of ABCC3 in the pancreas, liver, or kidneys. In healthy tissue, there is no expression of human ABCC3 (figure 2B).

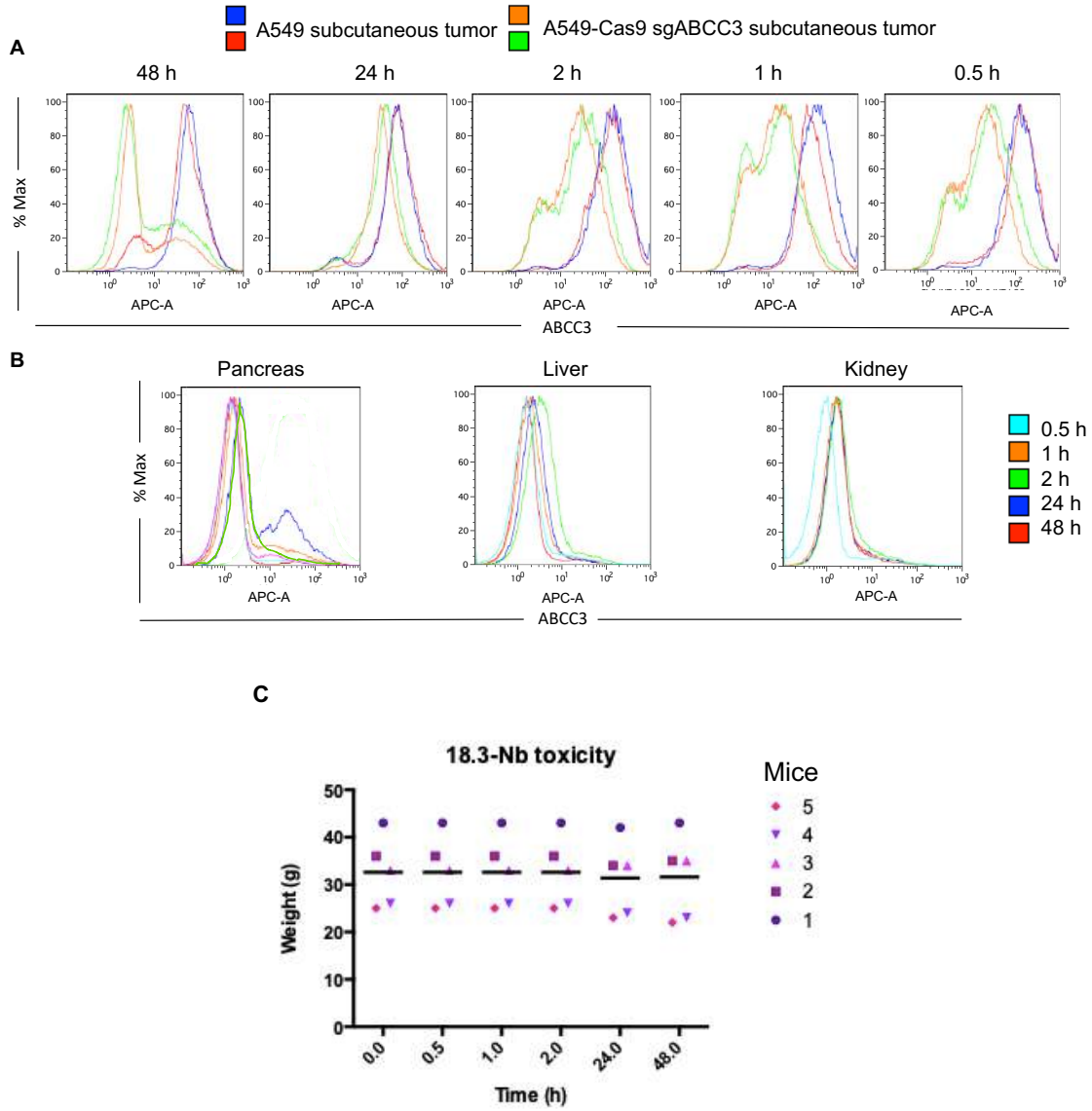

Figure 2. ABCC3 Nbs binding in mice over 48 hours detected by flow cytometry. A) ABCC3 detection by Nbs in subcutaneous A549 and A549-Cas9 sgABCC3 tumors. Representative data is shown; *n=3 for each time condition.* **B)** ABCC3 detection by Nbs in pancreas, liver, and kidney. **C)** Mouse weight of animals injected with Nbs for 48 h. *Mouse weight and mean are represented.*

Finally, we proved the toxicity of Nbs in mice for longer times than 1 hour; various behavior and conditions of the animals were observed to determine the healthy state of the mice, such as mouse movements, cleaning, and physical appearance, taking into account symptoms of subcutaneous tumors. Also, the weight of the animals was measured, and mice's weight did not decrease significantly; in the worst case, no more than 6% was lost after the injection of the Nb (figure 2C). Additionally, we did not observe any sign of pain in the animals following the mouse Grimace scale by the national center for the replacement, refinement, and reduction of animals in research (NC3R[2], figure S2). Hence, Nb did not result toxic for animals in a period of 48 h.

Conjugation and labeling of Nbs

Once anti-ABCC3 Nbs were tested in PDAC orthotopic mouse models and validated for detecting ABCC3 in an *in vivo* setting, further modifications are required to be used as an immuno-PET probe. The radionuclide can be directly or indirectly bound to the Ab. Still, the direct labeling consists of harsh processes that include high temperatures and non-aqueous solutions, resulting in incompatible with Nbs. On the contrary, the indirect labeling of Nbs is most efficient and common, although it requires longer times to synthesize and purifying[32].

First, radioisotope has to be linked to the Nb. To this end several chelator agents can be used including 1,4,7-triazacyclononane-1,4,7-triacetic acid (NOTA) and 1,4,7,10-tetraazacyclododecane-1,4,7,10-tetraacetic acid (DOTA).

Several antibody-based probes to be labeled with ^{68}Ga employ NOTA, which advantageously can maintain the structure and specificity of the antibodies and give a better signal than DOTA[33].

In collaboration with the group of Dr. Miguel Ángel Morcillo (CIEMAT), we conjugated the Nbs with p-SCN-bn-NOTA and marked them with ^{68}Ga as a radioisotope for the imaging.

Its half-life allows us to detect the signal, and the radiation will be lower due to the time it will be emitted in the body. Thus, we decided to conjugate the Nbs with NOTA and labeled them with ^{68}Ga.

A MW pattern solution was injected into the liquid chromatography to determine the retention time of known molecules (figure 3A and B).

12.3-Nb-sorting-ABCC3 showed different peaks with retention times of 10.02, 10.62, 10.94, and 11.96 min, corresponding to MW ranging 150 g/mol (figure 3C). NOTA conjugated 12.3-Nb-sorting ABCC3 exhibit diverse peaks that difficulted determining the peak that corresponds to the Nb. Still, a clear peak at 220 nm showed peaks with retention times at 10.14 and 10.71 min, corresponding to MW of 1300 g/mol (figure 3D).

Finally, 12.3-Nb-sorting-ABCC3-NOTA-^{68}Ga obtained a low activity of ^{68}Ga, with an efficiency of 2.17% (figure 3E), which may be due to a deficient conjugation with NOTA.

A

Protein	Molecular weight (g/mol)	Retention time (min)
Glutamate dehydrogenase	290000	5.390
Lactate dehydrogenase	142000	6.013
Enolasa	67000	6.480
Miokinasa	32000	7.367
Nanobody	15000	7.924*
Citocromo C, monómero	12400	8.080

* Expected retention time for Nbs calculated with the MW pattern

B

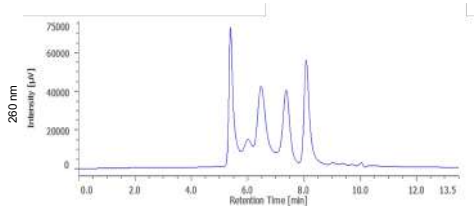

C

12.3-Nb-sorting-ABCC3

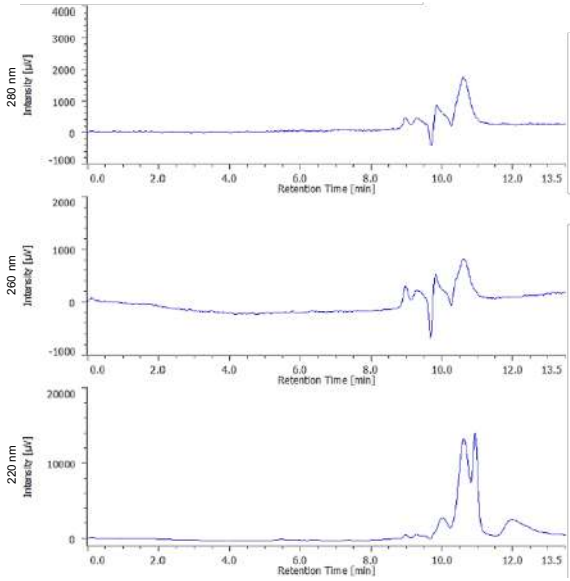

D

12.3-Nb-sorting-ABCC3-NOTA

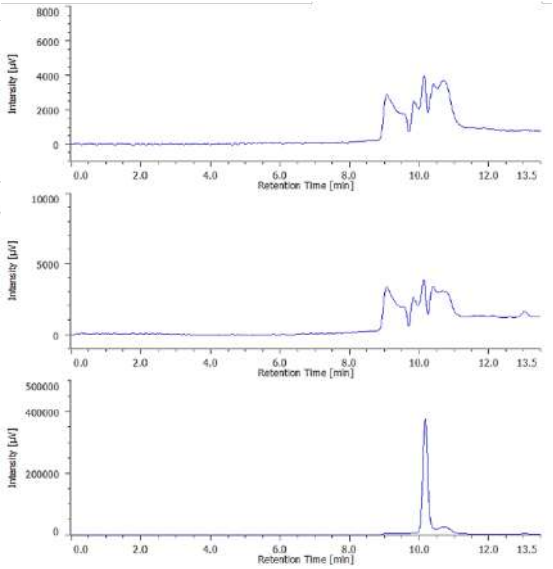

E

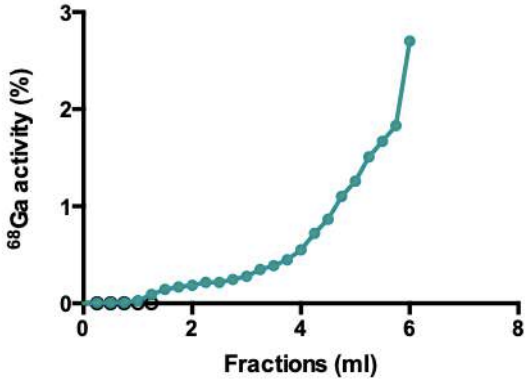

Figure 3. NOTA conjugation and ^{68}Ga label of 12.3-Nb-sorting-ABCC3 activity validation. **A)** MW and retention times table. **Retention time of the Nb was estimated using the molecular weight pattern.* **B)** Chromatogram of MW pattern solution at 260 nm. **C)** Chromatogram of 12.3-Nb-sorting-ABCC3 at 280, 260 and 220 nm. **D)** Chromatogram of 12.3-Nb-sorting-ABCC3-NOTA at 280, 260, and 220 nm. **E)** 12.3-Nb-sorting-ABCC3-NOTA-^{68}Ga elution profile.

Overall, the retention times obtained in all stages of the conjugation and labeling did not correspond to the MW of the Nb. This data is still preliminary and needs to be repeated. If we find similar results, other methods such as Coomassie staining blots could be used to exclude problems with the HPLC.

The conjugation and labeling of the Nb can interfere with the specificity of the epitope detection. To confirm that the immunoreactivity was not altered, we tested the affinity *in vitro* by flow cytometry assays, although the percentage of conjugation was low. We performed a flow cytometry assay for ABCC3 detection in A549 and A549-Cas9 sgABCC3 with the Nb to corroborate that. We did not observe any loss in the specificity of detection of ABCC3 at any concentration of the Nb, even with the VHH-conjugated (figure 4A) or with the VHH-conjugated and labeled (figure 4B).

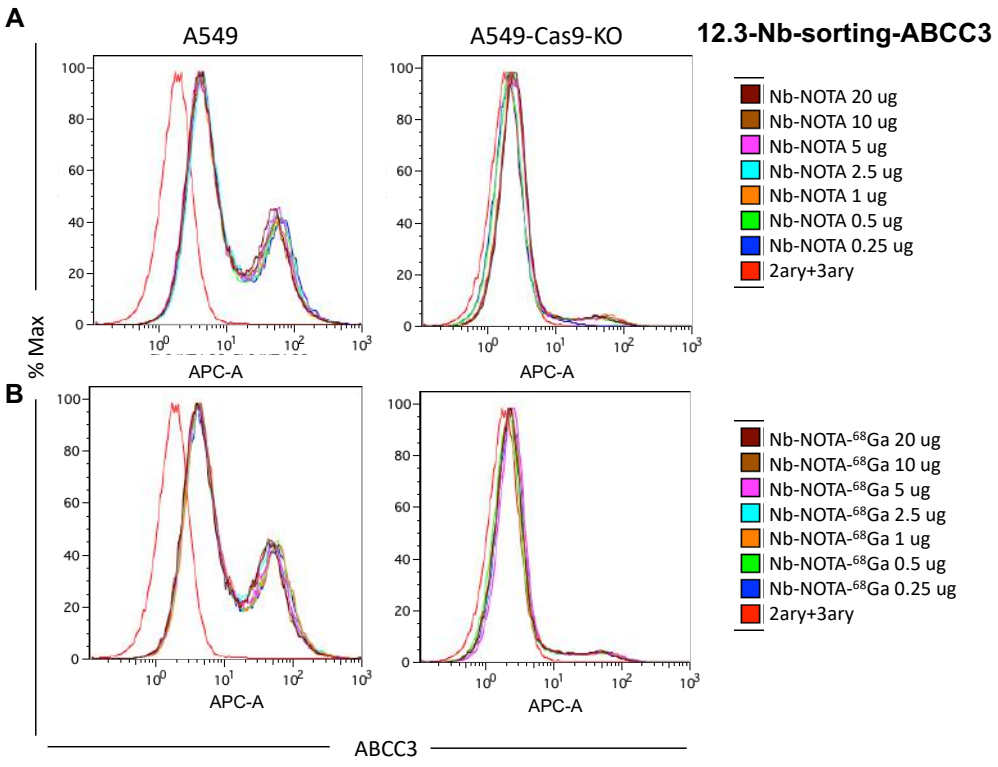

Figure 4. NOTA conjugation and ^{68}Ga of 12.3-Nb-sorting-ABCC3 Nb validation by flow cytometry. A) ABCC3 detection by 12.3-Nb-sorting-ABCC3 conjugated with NOTA. **B)** ABCC3 detection by 12.3-Nb-sorting-ABCC3 conjugated and labeled with NOTA-^{68}Ga.

These results showed that the specificity of 12.3-Nb-sorting-ABCC3 was not altered, probably corresponding to the unconjugated Nb; then, further studies with the Nb-NOTA conjugated need to be performed. Despite the low efficiency of conjugation and labeling, we could observe that the Nb is highly stable, given that the Nb was exposed to changes of pH and solutions in conjugation and labeling strategies.

Therapeutic effect of ABCC3 Nbs

We had seen that ABCC3 nanobodies could detect the transporter *in vitro* and *in vivo.* ABCC3 inhibition has been shown to implicate a reduction in proliferation in PDAC[18]. We corroborated the relation between ABCC3 expression and increased proliferation in Chapter I. Then, we wanted to check if the selected and validated nanobodies' binding to the extracellular domains of ABCC3 protein could impair proliferation or improve the response to gemcitabine treatment.

To this end, we added different amounts of nanobody to PDAC cell lines and determined their proliferation. The addition of 1, 5, and 10 µg of 18.3-Nb-sorting-ABCC3 showed a decrease in proliferation in IMIM-PC2-Cas9 sgNT compared with sgABCC3 cells (figure 5A). In the case of 12.3-Nb-sorting-ABCC3, the reduction in proliferation was bigger, being the inhibition of the proliferation higher than 50% (figure 5B). The binding of Nbs to ABCC3 then diminishes the proliferation of ABCC3-expressing cells (sgNT), being a possible option for treatment. Still, if we look at 12.3-Nb-sorting-ABCC3, it also inhibits the proliferation of sgABCC3 cells, suggesting that 12.3-Nb could inhibit additionally another target.

Once demonstrated that the Nbs reduce cell proliferation in ABCC3-expressing cells of PDAC, we investigated if these Nbs could also affect the response to gemcitabine. It could be used as a therapeutic agent.

As shown in Chapter I, ABCC3 overexpression confers resistance to gemcitabine; nanobodies could also be bound to the region implicated in gemcitabine efflux. These experiments were performed in MIA PaCa-2 cell line due to their ability to modulate ABCC3 expression under determined conditions. For example, as shown in Chapter I, in basal conditions, MIA PaCa-2 cells do not express ABCC3, and under gemcitabine treatment, MIA PaCa-2 cells overexpress ABCC3 to efflux the drug outside of the cell.

To determine if the 18.3-Nb can sensitize to gemcitabine in PDAC cells, we added a range of concentrations of Nb (0.1, 0.25, 0.5, 1, 2.5, 5, 10, and 20 µg) before the addition of gemcitabine.

The addition of different concentrations of 18.3-Nb did not affect the proliferation of ABCC3-expressing or deficient cells because they do not express ABCC3 (Data not shown). The dose of gemcitabine used was 20 nM; this concentration is around its IC_{50} in MIA PaCa-2-Cas9 sgABCC3 cells and inhibits a 20% in MIA PaCa-Cas9 sgNT cells.

It had no effect when 18.3-Nb-sorting-ABCC3 was added before gemcitabine in MIA PaCa-2-Cas9 sgABCC3 cells (Data not shown). Still, in sgNT cells, we could observe a decrease in the proliferation proportionally related to the amount of nanobody added (Data not shown). In conclusion, 18.3-Nb-sorting-ABCC3 may

have an inhibitory effect in the extracellular domain responsible for the resistance to gemcitabine, and its addition generated a similar effect to the genetic ablation of ABCC3.

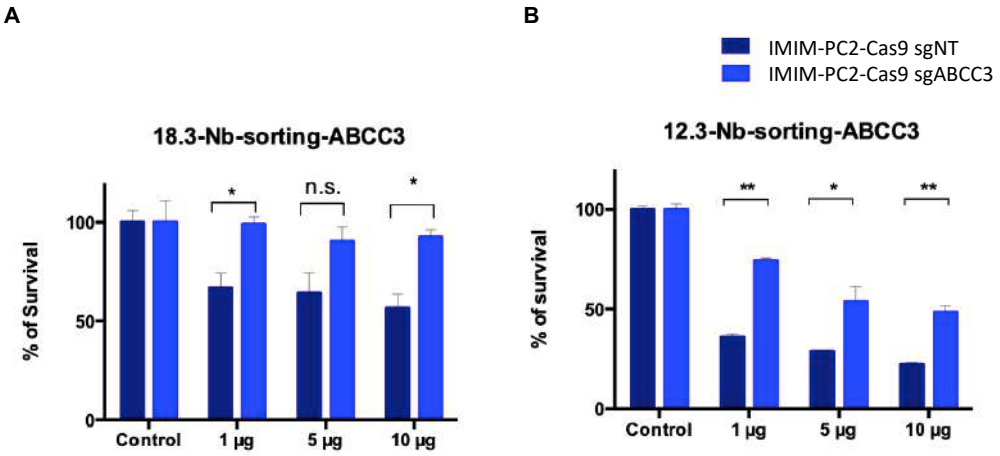

Figure 5. Nbs inhibit proliferation and decrease gemcitabine resistance in ABCC3-expressing cells. Determination of the growth inhibitory effect by viability assays in IMIM-PC2-Cas9 sgNT and sgABCC3 cell lines of **A)** 18.3-Nb-sorting-ABCC3 and of **B)** 12.3-Nb-sorting-ABCC3; *unpaired t-test was used (n.s. no significant, * p<0.05, ** p<0.01).*

12.3 and 18.3 Nbs could be employed as therapeutic agents due to the inhibition of proliferation. A more interestingly, 18.3-Nb can improve the sensitivity to gemcitabine treatment.

DISCUSSION

Current diagnosis of PDAC patients by imaging techniques, CT, MRI, PET, and EUS, is widely used and valuable for the clinic, but they present several limitations[4,34]. When PDAC is suspected, diagnostic imaging techniques have two main purposes: evaluating the relationship of the tumor with the mesenteric and portal vessels and the detection of metastatic disease[3,35].

Imaging techniques are not accurate in the detection of small lesions or metastasis. There are a lot of infra-staging tumors and false-positive diagnoses; these issues remain challenges in the diagnosis of PDAC patients for radiologists[10].

"Immunotargeted imaging" is an attractive and innovative method for the specific diagnosis of PDAC. Nbs have unique properties such as robust structure, stability, and solubility in aqueous solutions, reduced size, and reversible refolding[36]. By the specificity and selectivity of Nbs, they can be used as a tool to identify new biomarkers. More importantly, the expression of biomarkers can occur earlier than any changes in tumor size or tissue morphological changes[37]. Due to the diagnosis of PDAC at late stages of the disease, the detection of biomarkers before the morphological alterations could help diagnose the disease. With early treatments and resection, the survival of patients could be improved.

One of the techniques for detecting biomarkers in PDAC is biopsies and histological analyses; these techniques are not precise due to tumor heterogenicity. Thereby, immuno-PET allows the quantification of biomarkers in a non-invasive way and whole-body imaging[38].

Several targets are functionally important in PDAC and might have clinical potential as prognostic biomarkers in immuno-PET. Proteins and molecules present at the plasmatic membrane that are overexpressed on tumor or its microenvironment are potentially suitable for tumor-targeted imaging. Other components of the tumor microenvironment, such as extracellular matrix molecules, arise as promising candidates for developing immuno-PET probes for diagnosing and monitoring PDAC patients[39].

The different Nbs generated and validated against ABCC3 in our laboratory demonstrated to detect ABCC3 protein in subcutaneous and orthotopic PDAC tumors.

Our results, in agreement with previous reports[40], pointed ABCC3 as a new biomarker of PDAC. ABCC3 overexpression correlates with resistance to gemcitabine and stemness properties. Immuno-PET performed with these Nbs could help detect tumors, predict their response to chemotherapeutic agents, and monitor patients.

For immuno-PET probes, it is essential to match the Nb's half-life with the radioisotope's half-life. The renal clearance of Nbs is fast, around 0.5 and 1 h; We could use ^{68}Ga as radionuclide to avoid a long period of radioactivity exposure of patients[41]. For the linkage of the Nb with the radioisotope, the chelator needs to maintain the characteristics of both agents of the probe.

Different chelators can be conjugated to Abs or fragment-derived Abs depending on the radioisotope of choice[42]. DOTA is the chelator of choice for ^{90}Y and ^{177}Lu, and exceptionally for ^{64}Cu and ^{68}Ga due to their harsh labeling conditions for their stability *in vivo*[43]. NOTA resulted functional and stable in ^{86}Y and ^{177}Lu, but also with other radioisotopes such as ^{64}Cu and ^{68}Ga, and ^{44}Sc in an easier way, but also the efficiency of conjugation results higher[44].

The activity of ^{68}Ga in conjugated and labeled 12.3-NOTA-^{68}Ga resulted low (5%); these assays need to be repeated for an appropriate conjugation of the Nb.

By the conjugation and/or labeling, the epitope binding affinity can be altered, specifically, if the chelator addition occurs in CDR regions; however, there are several strategies to guide the conjugation and labeling processes.

One of the strategies for the improvement of the conjugation process could be sortase-mediated ligation. A site-specific sortase-mediated ligation is a powerful approach for the modification of molecules (figure S4). In this approach, the Nb is expressed with a C-terminal sequence corresponding to the sortase recognition domain (-LPXTG or -LPXTA). Sortase A enzyme cleaves the C-terminal residue, and a thioester Nb-sortase intermediate is formed. The intermediate is resolved by the nucleophilic attack of a short poly-glycine sequence of a protein or peptide conjugate[45]. By using sortase A strategy, we

could direct the conjugation of NOTA to the Nb, solving the limiting step of the conjugation. Additionally, this sortase A method can be applied to bind other agents, such as fluorophores or radioisotopes.

Besides the low efficiency of Nb labeling, we could observe the high stability of Nbs under conjugation and labeling processes. 12.3-Nb was stable after long incubation times at 37ºC and pH modifications, and the specificity against ABCC3 was not altered.

Nowadays, chemoresistance of cancer cells remains a problem, and also, standard treatments affect tumor and non-tumoral cells. Over the past years, a new generation of cancer treatments has been explored to solve this problem, targeted cancer therapies or TRNT. TRNT is based on interfering specific functional and essential targets; it focuses on specific molecular changes of each type of cancer[46]. The use of Abs or fragment-derived Abs in TRNT is one of the targeted radiotherapies that is emerging. Recently, Caplacizumab has been the first Nb approved by the FDA to treat thrombotic thrombocytopenic purpura[47]. The use of Nbs as TRNT can be performed in two different ways: by the inhibition potential of Nbs themselves; or by the labeling with gamma-emitters. Unlike radiotherapy, the radiation is not administered from outside of the body; the radiation is applied directly to the tumor. The cytotoxic radiation is delivered to cancer cells or their microenvironment due to antibodies binding to specific cancer biomarkers[48].

The Nbs developed against ABCC3 were selected by the specificity and selectivity in detecting epitopes for possible diagnosis use; the Nbs could also be used for therapy if the radioisotope is changed. Nbs can be used as therapeutic agents by labeling gamma-emitters; further studies to test their efficacy and potential as therapeutically agents after labeling could be performed.

Additionally, Nbs can have an inhibitory effect by themselves by binding to an important and necessary region for some processes, such as proliferation or drug resistance. There are shreds of evidence that the inhibition of ABCC3 leads to decreased proliferation, which could be related to HIF1α pathways[18]. Both 12.3 and 18.3 Nbs isolated for ABCC3 recognition resulted in having an inhibitory effect in the proliferation of PDAC cell lines. The administration of Nbs could stop the growth of the tumor and improve the patient's life. These Nbs might bind to

an extracellular domain of ABCC3 that in some way is implicated in proliferation pathways.

ABCC3 is also related to drug resistance. By impairing ABCC3, tumor cells could result in more sensitivity to gemcitabine treatment. In addition, as it was shown in Chapter I, ABCC3 is expressed in CSCs; with Nb therapy, we could target these resistant cells implicated in relapses.

Even more, 18.3-Nb-sorting-ABCC3 can increase the sensitivity to gemcitabine in PDAC cells that express ABCC3. Besides reducing proliferation by itself, the nanobody 18.3 can improve the effect of gemcitabine in these resistant cells. These therapies could have a high impact on the development of PDAC patients. Nbs could be used as imaging agents to detect the tumor, and by the blockage of ABCC3 transporters by the Nb, these cells could be more sensitive to chemotherapy. Also, the patient's disease could be monitored by several immuno-PET scanners with the Nb along with the treatment.

ABCC3 has been shown to be implicated in gemcitabine resistance, but it may look not to be involved in the resistance to abraxane, the other standard PDAC treatment.

The reduced size of Nbs is beneficial for specific applications, such as molecular imaging. However, therapeutic applications usually require slow clearance to avoid high doses and frequent administration. Despite the Nb clearance is fast, we could observe the binding of 18.3-Nb *in vivo* for at least 48 h; longer times have to be determined. As shown, some cells can modify the expression of ABCC3, then probably the half-life of the Nbs needs to be prolonged.

Different molecules can be linked to nanobodies to increase the size and maintain the specificity and selectivity to solve the time of clearance of the Nbs[49]. One strategy is the genetic fusion of the Nb with long serum half-life molecules, such as serum albumin[50]. Another method is the fusion of the Nb with the Fc region; this modification increases the size of the molecule extending its half-life[51]. Both strategies were demonstrated to be effective in extending Nbs serum half-lives, but they showed adverse effects on functionality, antigen recognition, or Nb production[52].

The potential of nanobodies is extensive; they can be used for many purposes and modified to adapt them to many applications. The generation of nanobodies libraries is a potential source of research; nanobodies against different molecules can be generated to improve our knowledge, diagnosis, or treatment of diseases and pathologies.

The demonstrated specific ABCC3 detection by 18.3-*Nb in vivo* could be used for the early diagnosis of PDAC in patients. Due to the relation between ABCC3, chemoresistance, and stemness would have an additional predictive value for the response to chemotherapeutic agents. 18.3-Nb also showed a therapeutic effect in diminishing the proliferation; in addition to the diagnosis of the tumor, the binding of the Nb to the ABCC3 epitope will stop or reduce the growth of the tumor. Even more, if the 18.3-Nb is given in combination with gemcitabine, cells that express ABCC3 will be sensitized to gemcitabine by the blockage of ABCC3 by the Nb. The synergistic effect of 18.3-Nb and gemcitabine will be effective in ABCC3-expressing cells. Still, in tumors that do not express ABCC3, after gemcitabine treatment, there is an induction of ABCC3 expression, and the 18.3-Nb would block these transporters, resulting in sensitizing cells. Along all the stages of the patient's disease, the state of the tumor and the expression of ABCC3 could be monitored by 18.3-Nb immuno-PET imaging.

CONCLUSIONS

1. 12.3 and 18.3-Nb-sorting-ABCC3 were able to detect ABCC3 in subcutaneous and orthotopic PDAC tumors.
2. 12.3-Nb resulted highly stable to changes in temperature, pH, and non-aqueous solutions.
3. 12.3 and 18.3 Nbs had an inhibitory effect in proliferation of ABCC3-expressing PDAC cells.
4. 18.3 Nb sensitized PDAC ABCC3-expressing cells to gemcitabine treatment, even in ABCC3-expressing cells in basal conditions or in cells that overexpress ABCC3 under gemcitabine treatment.

SUPPLEMENTAL FIGURES

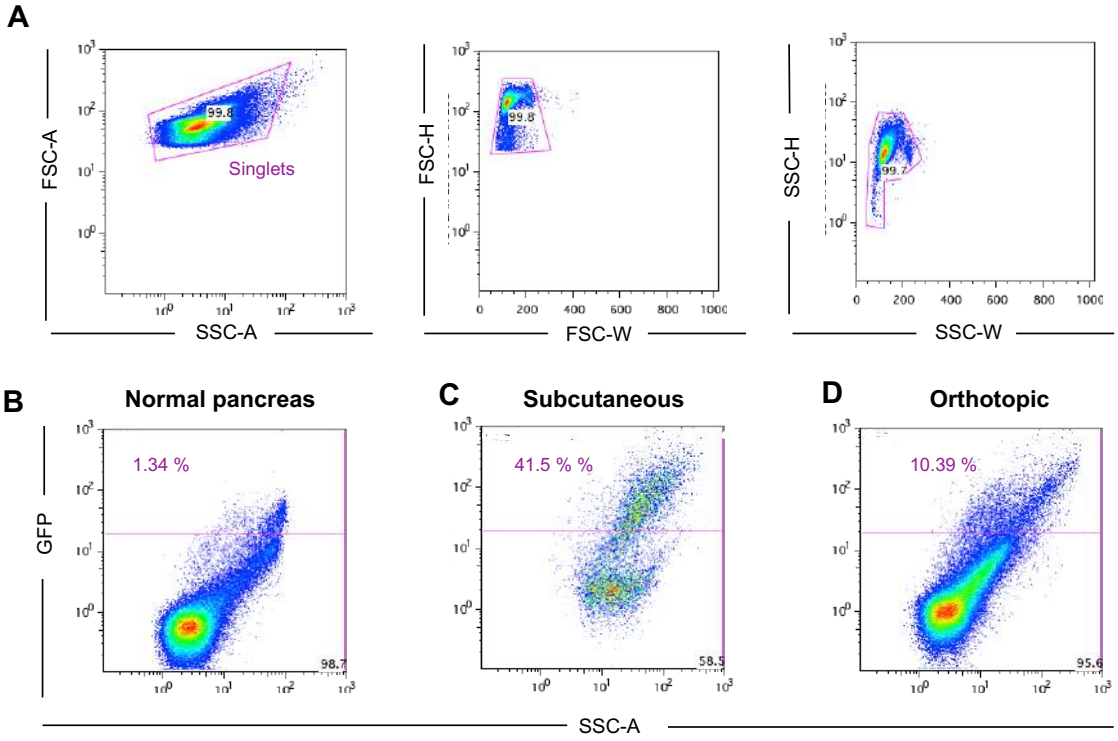

Figure S1. Gating of *in vivo* flow cytometry assays with Nbs. A) Gating workflow to eliminate singlets. GFP gating for non-GFP expressing cells, **B)** normal pancreas as negative control, **C)** subcutaneous, and **D)** orthotopic tumors.

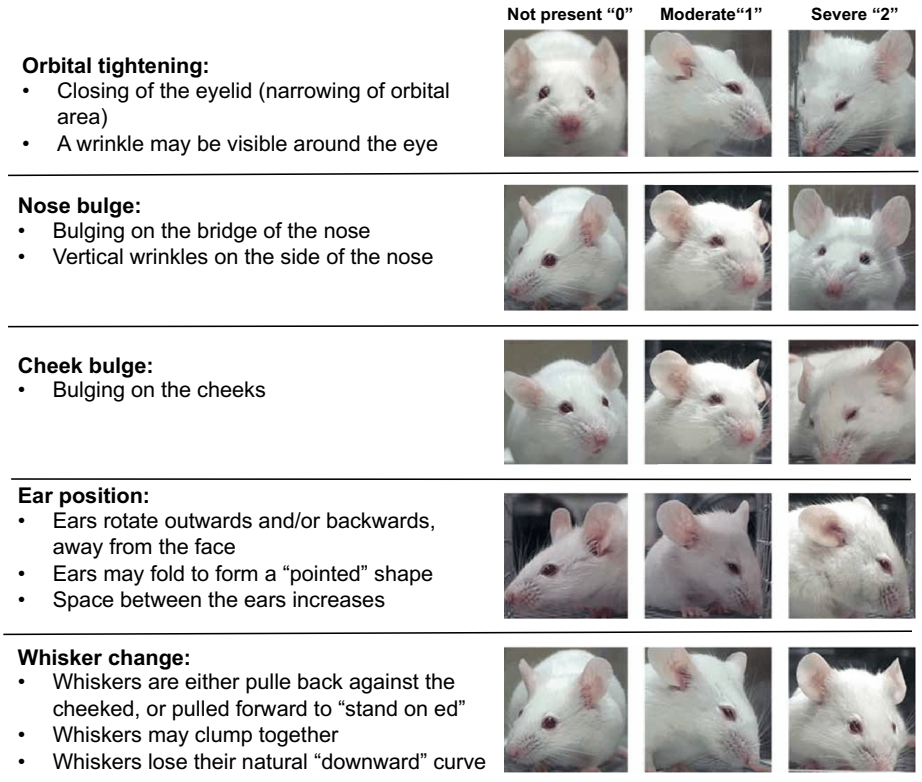

Figure S2. Mouse Grimace scale. Scale established to determine the grade of pain in rodents. *Image adapted from National center for the replacement, refinement, and reduction of animals in research (NC3R[2]).*

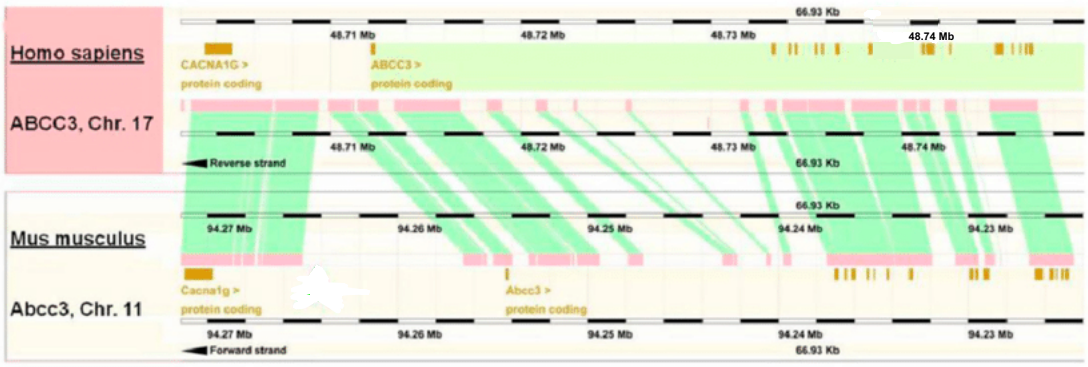

Figure S3. Human and mouse ABCC3 genes. Gene comparison between human (top) and mouse (bottom) ABCC3. Brown squares represent protein-coding regions, and pink represents conserved regions across both species. *Image modified from Canet et al.* [53].

REFERENCES

1. Hassanzadeh-Ghassabeh G, Devoogdt N, De Pauw P, Vincke C, Muyldermans S. Nanobodies and their potential applications. *Nanomedicine*. 2013;8(6):1013-1026. doi:10.2217/nnm.13.86

2. Harmand TJ, Islam A, Pishesha N, Ploegh HL. Nanobodies as: In vivo, non-invasive, imaging agents. *RSC Chemical Biology*. 2021;2(3):685-701. doi:10.1039/d1cb00023c

3. Walters DM, Lapar DJ, De Lange EE, et al. Pancreas-protocol imaging at a high-volume center leads to improved preoperative staging of pancreatic ductal adenocarcinoma. *Annals of Surgical Oncology*. 2011;18(10):2764-2771. doi:10.1245/s10434-011-1693-4

4. Al-Hawary MM, Francis IR, Chari ST, et al. Pancreatic ductal adenocarcinoma radiology reporting template: Consensus statement of the society of abdominal radiology and the American pancreatic association. *Gastroenterology*. 2014;146(1). doi:10.1053/j.gastro.2013.11.004

5. Zhu A, Lee D, Shim H. Metabolic positron emission tomography imaging in cancer detection and therapy response. *Seminars in Oncology*. 2011;38(1):55-69. doi:10.1053/j.seminoncol.2010.11.012

6. van Dongen GAMS, Visser GWM, Lub-de Hooge MN, de Vries EG, Perk LR. Immuno-PET: A Navigator in Monoclonal Antibody Development and Applications. *The Oncologist*. 2007;12(12):1379-1389. doi:10.1634/theoncologist.12-12-1379

7. Jovčevska I, Muyldermans S. The Therapeutic Potential of Nanobodies. *BioDrugs*. 2020;34(1):11-26. doi:10.1007/s40259-019-00392-z

8. Muyldermans S. Nanobodies: Natural Single-Domain Antibodies. *Annual Review of Biochemistry*. 2013;82(1):775-797. doi:10.1146/annurev-biochem-063011-092449

9. Muyldermans S. A guide to: generation and design of nanobodies. *The FEBS Journal*. 2021;288(7):2084-2102. doi:10.1111/febs.15515

10. González-Gómez R, Pazo-Cid RA, Sarría L, Morcillo MÁ, Schuhmacher AJ. Diagnosis of Pancreatic Ductal Adenocarcinoma by Immuno-Positron Emission Tomography. *Journal of Clinical Medicine*. 2021;10(6):1151. doi:10.3390/jcm10061151

11. Wang Y, Zhong X, Zhou L, et al. Prognostic Biomarkers for Pancreatic Ductal Adenocarcinoma: An Umbrella Review. *Frontiers in Oncology*. 2020;10:1466. doi:10.3389/fonc.2020.01466

12. Dewulf J, Adhikari K, Vangestel C, Van Den Wyngaert T, Elvas F. Development of antibody immuno-PET/SPECT radiopharmaceuticals for imaging of oncological disorders—an update. *Cancers*. 2020;12(7):1-29. doi:10.3390/cancers12071868

13. Sugiura G, Kühn H, Sauter M, Haberkorn U, Mier W. Radiolabeling strategies for tumor-targeting proteinaceous drugs. *Molecules*. 2014;19(2):2135-2165.

doi:10.3390/molecules19022135

14. Directly and indirectly technetium-99m-labeled antibodies--a comparison of in vitro and animal in vivo properties - PubMed. https://pubmed.ncbi.nlm.nih.gov/8418250/. Accessed October 31, 2021.

15. Friedman M, Ståhl S. Engineered affinity proteins for tumour-targeting applications. *Biotechnology and Applied Biochemistry*. 2009;53(1):1. doi:10.1042/ba20080287

16. Anderson CJ, Ferdani R. Copper-64 radiopharmaceuticals for PET imaging of cancer: Advances in preclinical and clinical research. *Cancer Biotherapy and Radiopharmaceuticals*. 2009;24(4):379-393. doi:10.1089/cbr.2009.0674

17. García-Toraño E, Medina VP, Ibarra MR. The half-life of 18F. *Applied Radiation and Isotopes*. 2010;68(7-8):1561-1565. doi:10.1016/j.apradiso.2009.11.052

18. Adamska A, Domenichini A, Capone E, et al. Pharmacological inhibition of ABCC3 slows tumour progression in animal models of pancreatic cancer. *Journal of Experimental and Clinical Cancer Research*. 2019;38(1). doi:10.1186/s13046-019-1308-7

19. Zeglis BM, Lewis JS. A practical guide to the construction of radiometallated bioconjugates for positron emission tomography. *Dalton Transactions*. 2011;40(23):6168-6195. doi:10.1039/c0dt01595d

20. Agarwal P, Bertozzi CR. Site-specific antibody-drug conjugates: The nexus of bioorthogonal chemistry, protein engineering, and drug development. *Bioconjugate Chemistry*. 2015;26(2):176-192. doi:10.1021/bc5004982

21. D'Huyvetter M, Xavier C, Caveliers V, Lahoutte T, Muyldermans S, Devoogdt N. Radiolabeled nanobodies as theranostic tools in targeted radionuclide therapy of cancer. *Expert Opinion on Drug Delivery*. 2014;11(12):1939-1954. doi:10.1517/17425247.2014.941803

22. Saji H. Application of radioisotopes for theranostics, a combination of diagnostics and therapy. *Yakugaku Zasshi*. 2015;135(4):551-556. doi:10.1248/yakushi.14-00227-2

23. Gold D V., Karanjawala Z, Modrak DE, Goldenberg DM, Hruban RH. PAM4-reactive MUC1 is a biomarker for early pancreatic adenocarcinoma. *Clinical Cancer Research*. 2007;13(24):7380-7387. doi:10.1158/1078-0432.CCR-07-1488

24. Gold D V., Newsome G, Liu D, Goldenberg DM. Mapping PAM4 (clivatuzumab), a monoclonal antibody in clinical trials for early detection and therapy of pancreatic ductal adenocarcinoma, to MUC5AC mucin. *Molecular Cancer*. 2013;12(1):143. doi:10.1186/1476-4598-12-143

25. Study of HuMab-5B1 (MVT-5873) in Subjects With Pancreatic Cancer or Other Cancer Antigen 19-9 (CA19-9) Positive Malignancies - Full Text View - ClinicalTrials.gov. https://clinicaltrials.gov/ct2/show/NCT02672917. Accessed September 22, 2021.

26. Phase 1 Imaging Study of 89Zr-DFO-HuMab-5B1 With HuMab-5B1 - Full Text View - ClinicalTrials.gov. https://clinicaltrials.gov/ct2/show/NCT02687230. Accessed January 14, 2021.

27. Vosjan M. *Nanobody Constructs, Targeting Growth Factors and Their Receptors, for PET Imaging and Cancer Therapy*.; 2012.

28. García-Toraño E, Peyrés Medina V, Romero E, Roteta M. Measurement of the half-life of 68Ga. *Applied Radiation and Isotopes*. 2014;87:122-125. doi:10.1016/j.apradiso.2013.11.082

29. Romero E, Martínez A, Oteo M, Ibañez M, Santos M, Morcillo MÁ. Development and long-term evaluation of a new 68Ge/68Ga generator based on nano-SnO2 for PET imaging. *Scientific Reports*. 2020;10(1):12756. doi:10.1038/s41598-020-69659-8

30. Pruszynski M, D'Huyvetter M, Bruchertseifer F, Morgenstern A, Lahoutte T. Evaluation of an Anti-HER2 Nanobody Labeled with 225 Ac for Targeted α-Particle Therapy of Cancer. *Molecular Pharmaceutics*. 2018;15(4):1457-1466. doi:10.1021/acs.molpharmaceut.7b00985

31. McMurphy T, Xiao R, Magee D, et al. The Anti-Tumor Activity of a Neutralizing Nanobody Targeting Leptin Receptor in a Mouse Model of Melanoma. Facchiano A, ed. *PLoS ONE*. 2014;9(2):e89895. doi:10.1371/journal.pone.0089895

32. Küppers J, Kürpig S, Bundschuh RA, Essler M, Lütje S. Radiolabeling strategies of nanobodies for imaging applications. *Diagnostics*. 2021;11(9):1530. doi:10.3390/diagnostics11091530

33. Moon SH, Hong MK, Kim YJ, et al. Development of a Ga-68 labeled PET tracer with short linker for prostate-specific membrane antigen (PSMA) targeting. *Bioorganic and Medicinal Chemistry*. 2018;26(9):2501-2507. doi:10.1016/j.bmc.2018.04.014

34. Shrikhande S V., Arya S, Barreto SG, et al. Borderline respectable pancreatic tumors: Is there a need for further refinement of this stage? *Hepatobiliary and Pancreatic Diseases International*. 2011;10(3):319-324. doi:10.1016/S1499-3872(11)60053-2

35. Ishigami K, Yoshimitsu K, Irie H, et al. Diagnostic value of the delayed phase image for iso-attenuating pancreatic carcinomas in the pancreatic parenchymal phase on multidetector computed tomography. *European Journal of Radiology*. 2009;69(1):139-146. doi:10.1016/j.ejrad.2007.09.012

36. Schrankel CS, Gökirmak T, Lee CW, Chang G, Hamdoun A. Generation, expression and utilization of single-domain antibodies for in vivo protein localization and manipulation in sea urchin embryos. In: *Methods in Cell Biology*. Vol 151. Academic Press Inc.; 2019:353-376. doi:10.1016/bs.mcb.2018.11.005

37. Cornelissen B, Knight JC, Mukherjee S, et al. Translational molecular imaging in exocrine pancreatic cancer. *European Journal of Nuclear Medicine and Molecular Imaging*.

2018;45(13):2442-2455. doi:10.1007/s00259-018-4146-5

38. Wei W, Rosenkrans ZT, Liu J, Huang G, Luo QY, Cai W. ImmunoPET: Concept, Design, and Applications. *Chemical Reviews*. 2020;120(8):3787-3851. doi:10.1021/acs.chemrev.9b00738

39. McCabe KE, Wu AM. Positive Progress in ImmunoPET—Not Just a Coincidence. *Cancer Biotherapy and Radiopharmaceuticals*. 2010;25(3):253-261. doi:10.1089/cbr.2010.0776

40. Adamska A, Ferro R, Lattanzio R, et al. ABCC3 is a novel target for the treatment of pancreatic cancer. *Advances in Biological Regulation*. 2019;73. doi:10.1016/j.jbior.2019.04.004

41. Knowles SM, Wu AM. Advances in immuno-positron emission tomography: Antibodies for molecular imaging in oncology. *Journal of Clinical Oncology*. 2012;30(31):3884-3892. doi:10.1200/JCO.2012.42.4887

42. Cooper MS, Ma MT, Sunassee K, et al. Comparison of 64cu-complexing bifunctional chelators for radioimmunoconjugation: Labeling efficiency, specific activity, and in vitro / in vivo stability. *Bioconjugate Chemistry*. 2012;23(5):1029-1039. doi:10.1021/bc300037w

43. Radiopharmaceutical Chemistry between Imaging and Endoradiotherapy - Google Libros. https://books.google.es/books?id=LS9xDwAAQBAJ&pg=PA93&lpg=PA93&dq=dota+and+nota+conjugation+of+ab&source=bl&ots=RIUp-bVin2&sig=ACfU3U3hSEADWJHEZdlobPlPJ2EWudrXeQ&hl=es&sa=X&ved=2ahUKEwitlNWR3-3zAhULAWMBHf__CfoQ6AF6BAgZEAM#v=onepage&q=dota and nota conjugation of abnota&f=false. Accessed October 28, 2021.

44. Gansow OA, Brechbiel MW, Mirzadeh S, Colcher D, Roselli M. Chelates and antibodies: current methods and new directions. *Cancer treatment and research*. 1990;51:153-171. doi:10.1007/978-1-4613-1497-4_7

45. Gonzalez-Sapienza G, Rossotti MA, Tabares-da Rosa S. Single-domain antibodies as versatile affinity reagents for analytical and diagnostic applications. *Frontiers in Immunology*. 2017;8(AUG). doi:10.3389/fimmu.2017.00977

46. Baudino T. Targeted Cancer Therapy: The Next Generation of Cancer Treatment. *Current Drug Discovery Technologies*. 2015;12(1):3-20. doi:10.2174/1570163812666150602144310

47. Morrison C. Nanobody approval gives domain antibodies a boost. *Nature reviews Drug discovery*. 2019;18(7):485-487. doi:10.1038/d41573-019-00104-w

48. Sgouros G, Bodei L, McDevitt MR, Nedrow JR. Radiopharmaceutical therapy in cancer: clinical advances and challenges. *Nature Reviews Drug Discovery*. 2020;19(9):589-608. doi:10.1038/s41573-020-0073-9

49. Bannas P, Hambach J, Koch-Nolte F. Nanobodies and nanobody-based human heavy

chain antibodies as antitumor therapeutics. *Frontiers in Immunology*. 2017;8(NOV):1603. doi:10.3389/fimmu.2017.01603

50. Kontermann RE. Strategies for extended serum half-life of protein therapeutics. *Current Opinion in Biotechnology*. 2011;22(6):868-876. doi:10.1016/j.copbio.2011.06.012

51. Iqbal U, Trojahn U, Albaghdadi H, et al. Kinetic analysis of novel mono- and multivalent VHH-fragments and their application for molecular imaging of brain tumours. *British Journal of Pharmacology*. 2010;160(4):1016-1028. doi:10.1111/j.1476-5381.2010.00742.x

52. Kubetzko S, Sarkar CA, Plückthun A. Protein PEGylation decreases observed target association rates via a dual blocking mechanism. *Molecular Pharmacology*. 2005;68(5):1439-1454. doi:10.1124/mol.105.014910

53. Canet MJ, Merrell MD, Harder BG, et al. Identification of a functional antioxidant response element within the eighth intron of the human ABCC3 gene. *Drug Metabolism and Disposition*. 2015;43(1):93-99. doi:10.1124/dmd.114.060103